WYDZIAŁ BIOLOGII
i OCHRONY ŚRODOWISKA
Uniwersytet Łódzki

Stacjonarne Studia Doktoranckie
Ekologii i Ochrony Środowiska

Aleksandra Jakiel

Diversity and distribution of deep-sea Pseudotanaidae (Tanaidacea, Peracarida)

Różnorodność i rozmieszczenie głębokowodnych Pseudotanaidae (Tanaidacea, Peracarida)

Praca doktorska

wykonana w Katedrze Zoologii
Bezkręgowców i Hydrobiologii
Instytutu Ekologii i Ochrony Środowiska

pod kierunkiem :

- Prof. dr hab. Magdaleny Błażewicz

Łódź, 2020

Contents

Acknowledgements

I would like to express my special gratitude to my Supervisor Professor Magdalena Błażewicz for invaluable support at every stage of writing the dissertation. I am grateful for showing me the secrets of the deep sea as well as fascinating tanaids. I would like to thank for her patience, all the valuable hints and the time given to me.
Special thanks go to Dr Ferran Palero, who shared his knowledge with me and always gave me a piece of advice.
I also thank Dr Mark O'Loughlin who sent me words of encouragements from the Southern hemisphere.
I would like to thank all members of the Department of Invertebrate Zoology and Hydrobiology of the University of Lodz, especially to Dr Inma Frutos for warm words and great support through that time. Many thanks to Marta Gellert and Dr Anna Stępień, for all their help.
Special thanks go to my mother, who has always supported me..

Chapter 1. Introduction

Introduction

Deep-sea, understood as the ocean regions deeper than 200 m and below the area where penetration of sunlight maintains photosynthesis, is the biggest ecosystem on Earth (Ramirez-Llodra *et al.* 2010). Pragmatically, the ocean is divided on three depth ranges namely, (i) bathyal (continental slope) that extends from 200 m to 3000 m, (ii) abyssal (oceanic floor) extending from 3000 to 6000 m and (iii) hadal (oceanic trenches) which are deeper than 6000 m. Bathyal and hadal regions cover just a relatively small surface of the deep sea (around 10%), while the abyssal –oceanic floor – represents the largest (88%) marine ecosystem (Ramirez-Llodra *et al.* 2010). The abyssal has been considered a homogeneous environment for decades (Gage & Tyler 1991) compared with the conspicuous and striking physical barriers on land. The concept of the deep-sea as a vast and uniform ecosystem inhabited by organisms with unlimited dispersion potential was widely accepted (Rex & Etter 2010). The use of state-of-the-art technologies for mapping habitats has proved that abyssal environments are much more diverse than originally thought (Wefer 2003).

Barriers in the deep sea and their role in limiting dispersal

The thermohaline circulation is a circumglobal oceanic current that links the most distant parts of the ocean, making it the biggest ecosystem on Earth. It is assumed that this large oceanic current has a pivotal role in the distribution of propagules and larval or juvenile stages for many marine organisms. Numerous studies on ephemeral hydrothermal-vents demonstrate that sessile Siboglinidae or Bivalvia can produce pelagic larvae living much longer in the water column than similar organisms from non-hydrothermal habitats (Ramirez-Llodra *et al.* 2007).

It is generally assumed that species with planktonic larvae, large size and fast swimming behaviour have wider distributions than those without planktonic larval stages, small sizes and sessile. Life style (sessile, benthic, pelagic) and breeding behaviour of organisms (Brandt *et al.* 2012) are important factors influencing the dispersal and distribution of marine fauna, and large scavenging amphipods (>15 mm length) are definitely highly mobile organisms (Ingram & Hessler 1987). It is estimated that deep-sea species have greater dispersal potential than their shallow water counterparts (Baco *et al.* 2016), but mechanism behind this pattern are still

hardly understood (Astthorsson *et al.* 2007; Brix & Svavarsson 2010; Havermans *et al.* 2013; Rex & Etter 2010; Schnurr *et al.* 2014).

The seafloor presents various topographic features such as (i) mid-oceanic ridges, (ii) underwater mountain chains or (iii) oceanic trenches. The influence of those structures on the direction and character of oceanic currents is apparent. Deep-sea organisms, which use oceanographic currents as their main dispersal vectors, indirectly influence the distribution of marine organisms.

Oceanic ridges

Oceanic Ridges are geological structures on the sea bottom, where the plates separate and move apart (spreading seafloor). The gap between the plates is filled up with hot and soft rock, which form a new oceanic crust. This zone is usually not wider than a few km and the mountain chains formed during this volcanic process can rise up to 2000 m above sea floor (Wefer 2003). Oceanic ridges in Pacific, Indian and Atlantic oceans make the largest mountain chain in the world, spanning over 75000 km (Van Dover 2000) (Fig. 1.1).

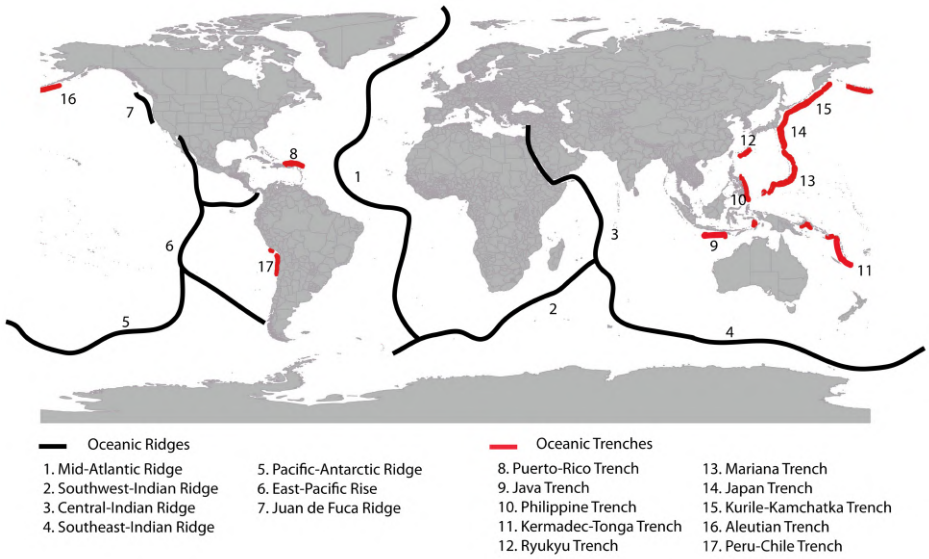

Fig 1.1. Major oceanic ridges and trenches.

Oceanic Ridges play a fundamental role in the distribution of water masses, as well as in the distribution of benthic organisms (Brix & Svavarsson 2010; Schnurr *et al.* 2014), although their isolating effect is less for mobile fauna than for sessile taxa

(Havermans *et al.* 2013; Riehl *et al.* 2018). The Greenland-Scotland-Ridge (GIR), located on Northern Atlantic waters (Fig. 1.2), successfully hampers mixing water masses originally coming from the south and north Atlantic (Logemann 2013). Mixing of two distinct water masses with different thermal, oxygenation and salinity parameters results in an area with high hydrological complexity (Jochumsen *et al.* 2016; Logemann 2013). The marine environment off Iceland is thus exceptionally diverse and unlikely to be occupied by the same species.

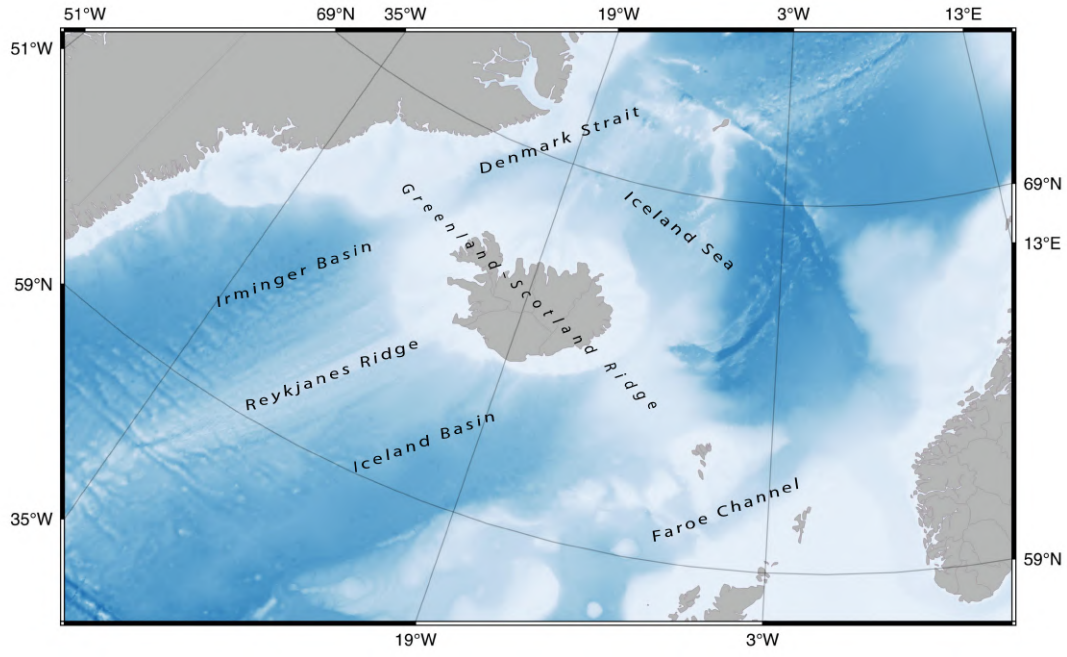

Fig 1.2. Localisation of Greenland-Scotland-Ridge (GIR).

Benthic assemblages of peracarid crustaceans on both sides of the ridge are distinct (Astthorsson *et al.* 2007). Diversified hydrological conditions influence calliopiids (amphipods) (Weisshappel 2001) and anthurideans (Negoescu & Svavarsson 1997), while distribution is also affected by depth in oecidiobranchids or munnopsids (Jennings *et al.* 2018; Schnurr *et al.* 2018).

Mid-Atlantic Ridge is considered a potential barrier separating abyssal species, although its effect clearly depends on species mobility. The good swimming abilities of munnopsids and some large amphipod scavengers (Bober *et al.* 2018a; Havermans *et al.* 2013; Malyutina *et al.* 2018b) make the ridge to be a week or

inefficient barrier, and populations on both sides are well-connected. On the contrary, weakly mobile isopods (e.g. Macrostylidae, Desmosomatidae and Nannoniscidae) are apparently well separated by the ridge. The Greenland-Iceland-Scotland Ridge (GIS-Ridge) is considered a prominent geographic barrier that influences the distribution of benthic fauna (Brix & Svavarsson 2010; Jennings *et al.* 2018; Negoescu & Svavarsson 1997; Schnurr *et al.* 2014, 2018; Stransky & Svavarsson 2010; Weisshappel 2000, 2001). GIS-Ridge has been demonstrated to be an effective barrier affecting the occurrence and dispersion of peracarid crustaceans. These results were confirmed for both bathyal as well as several abyssal species, which were recorded from both sides of the ridge. Isopods living off North Iceland are affected by environmental conditions. Temperature was pointed as a limiting factor reducing dispersion of anthuroideans (Negoescu & Svavarsson 1997), while oecidiobranchids isopods are clearly affected by depth (Jennings *et al.* 2018). Finally, the distribution model of munnopsids is complicated and affected by other parameters such as geographical and bathymetric gradients (Bober *et al.* 2018a)

Oceanic trenches include the deepest and least accessible parts of the ocean, hardly accessible for human and biologically almost unrecognized, but representing important hot spots of deep-sea biodiversity (Jamieson *et al.* 2010; Rex & Etter 2010). They are oceanic V-shape valleys formed along continental edges during subduction of the heavy oceanic crust (3 g/mm2) below the lighter continental crust (2.7 g/mm2). Trenches are characterized by specific environmental condition such as extremely high pressure. The deepest oceanic trench extends down to almost 11000 meters. Variation in food supply, low temperature and high hydrostatic pressure shape the unique character of hadal communities (Jamieson *et al.* 2010). Irregular pulses of particulate organic matter delivered from land or produced in autotrophic parts of the ocean are the main sources of food for the hadal fauna (Danovaro *et al.* 2002; Jamieson *et al.* 2010; Tittensor *et al.* 2011). Moreover, the V-shaped topography of trenches are considered as ‘traps’ for organic matter resulting in high biomass, density and diversity of benthic fauna (Danovaro *et al.* 2002; Jumars & Hessler 1976; Shirayama 1984).

Trenches are usually elongated and narrow geological structures which, similar to valleys on land, disrupt abyssal floor. They are considered as geographic

barriers disrupting gene connectivity (Etter *et al.* 2011). Bober et al. (2018b) proved that the Kurile-Kamchatka Trench (KKT) can reduce gene flow, although it is not acting as a barrier for every species. It was demonstrated that the macrostylid isopod *Macrostylis sabinae* Bober, Riehl, Henne & Brandt, 2018 was present on both sides of KKT, with genetic intraspecific variation being larger between samples collected from both sides of the KKT, than on the same side. Therefore, the isolating effect of KKT cannot be rejected.

Factors and Processes Shaping Deep Sea Diversity Patterns

The deep-sea has long been considered an azoic ecosystem (Koslow 2007). High pressure, low temperature, nutrient-poor, and entire darkness, make the deepest part of the ocean the most hostile environment. This paradigm, established by XIX-century naturalists, was questioned by the results obtained during the firsts deep-sea expeditions (e.g. HMS *Lightning* and HMS *Challenger*) which proved that the deep-sea is a biologically diverse part of the ocean (Gage & Tyler 1991). The recognition of the diversity in the deep sea resulted from the implementation of the dredges supported with fine mesh size nets for collecting deep-sea macroinvertebrates (Hessler & Sanders 1967). Use of improved scientific devices for collecting marine fauna and precisely defined sampling protocols have brought new high-quality data, proving that diversity in this homogenous and energy-poor environment is higher than previously assumed (Hessler & Sanders 1967). The deep sea hides an immense diversity, comparable with those levels observed in shallow-water ecosystems.

Although numerous efforts have been carried out since the discovery of life in the abyssal plains, the deep sea still stays as the least recognized ecosystem of the Earth. A high economic cost of deep-sea operations, including time-consuming and logistically difficult procedures, make the deep sea far from being satisfactorily explored (Van Dover 2000; Koslow 2007; Rex & Etter 2010). Numerous deep-sea expeditions have collected material on the continental slope (Brandt *et al.* 2010; McCallum *et al.* 2015; Poore *et al.* 2015), on abyssal (e.g. IceAGE (Brix *et al.* 2012, 2013); DIVA (Brandt *et al.* 2005; Martinez Arbizu & Schminke 2005); Vema-Transit (Brandt *et al.* 2018; Devey *et al.* 2018); SoJabio (Brandt *et al.* 2010); Sokhobio (Malyutina *et al.* 2018a); JPIO (Martinez Arbizu & Haeckel 2015); KuramBio I (Brandt & Malyutina, 2015) or in oceanic trenches KuramBio II (Brandt *et al.* 2016),

and they have brought numerous and diverse collections of invertebrates, most of which represent new species for science.

The mechanisms behind high biological diversity and unique evolutionary processes in the deep sea are still hardly understood. So far, a few hypotheses were proposed to explain that phenomenon. *Stability-time* hypothesis was the first explanation for deep-sea diversity (Sanders, 1968). It assumes that a high level of coexistence in a very stable environment will allow numerous micro-niches and trigger higher speciation rates. This paradigm is partially out of the date for the moment, as it is known that deep-sea ecosystems experience periods of dramatically changing temperatures, nutrient input, position of the thermohaline circulation, as well as mass extinction (Tyler *et al.* 2003). The *habitat heterogeneity* hypothesis suggests that heterogeneity and spatial complexity of habitats are positively correlated with diversity and may be a key factor favouring speciation. The impact of habitat heterogeneity on species diversity has been considered an important element for a long time and it is still generating many new discussions in high-class scientific journals (Allouche, Kalyuzhny, Moreno-Rueda, Pizarro, & Kadmon, 2012: Proceedings of the National Academy of Sciences of the United States of America; Leung, 2015: Scientific Reports). High habitat heterogeneity and complexity provide shelter for invertebrates and decrease the influence of mechanical stress (Koehl 1999). Predators impact and competition might be reduced in more heterogeneous areas (Almany 2004; Corkum & Cronin 2004; Hereu *et al.* 2005) whereas the number of potential ecological niches is essentially higher (Tews *et al.* 2004). Most studies concerning the impact of habitat heterogeneity on benthic marine fauna have dealt with shallow shelf areas (Almany 2004; Leung 2015; Włodarska-Kowalczuk *et al.* 2009); whereas heterogeneity of deep sea habitats at different spatial scales, and its impact on macrobenthic fauna distribution are basically unknown. Studies dedicated to benthic meiofauna showed that polymetallic nodule fields in Central Pacific might enable the co-existence of a large number of taxa with different life styles (Vanreusel *et al.* 2010), but further macrofaunal studies are needed.

Connectivity between deep-sea organisms separated by long geographic distances is one of the most appealing questions in marine biology. Rex & Etter (2010) stated that decreasing gene flow is expected when significant distances separate populations and can result in *isolation-by-distance* (IBD). Under this model,

contiguous populations should be more genetically close to each other than with geographically distant samples (Wright 1943). IBD may well explain the high diversity observed in the abyss. Sparsely distributed and rare populations spanning the vast dimensions of the deep-sea definitely hamper gene flow among populations and promote speciation (Danovaro *et al.* 2017). For example, morphologically identical species with distinct genetic characteristic have been detected for several invertebrates groups in North Atlantic (Brix *et al.* 2011; Faurby *et al.* 2011). Two species of *Eurycope* (Isopoda) separated by the Greenland – Scotland Ridge topographic barrier have been recorded along wide bathymetric ranges. Given that GSR is known to hamper gene flow, the presence of the same species on both sides of the ridge is questioned. Following a conservative interpretation, each of this widely distributed species can be considered as complexes of cryptic species namely: *Eurycope producta* and *E. inermis* complexes. Further molecular analysis prove that both groups are formed by six and four distinct species, respectively (Schnurr *et al.* 2018).

The availability of nutrients has a great impact on biological diversity patterns (Clarke & Gaston 2006; Danovaro *et al.* 2002; Evans *et al.* 2005; Jumars 1976). The main source of food in the deep sea comes from land or the euphotic zones of the ocean (Levin & Gage 1998; McCallum et al. 2015; Wolff, 1977; Woolley et al., 2016). Nevertheless, it was calculated that only 1% of primary production from the euphotic zone reaches the ocean floor (Rex & Etter 2010). This means that deep-sea ecosystems situated far away from land are expected to be less productive than those situated closer to continental margins. The *species-energy principle* hypothesis concerns the impact of the amount of particulate organic matter (POM) available on diversity levels in the abyss. POM produced in the process of photosynthesis in the euphotic zone (<200m) is considered as the main factor determining diversity (Clarke & Gaston 2006; Evans *et al.* 2005; McCallum *et al.* 2015; Woolley *et al.* 2016). It is an important source of energy for deep-sea organisms, delivered to the oceanic floor in a regular quantity or in irregular pulses (McClain & Hardy 2010; Smith 1985; Smith *et al.* 2006b; West *et al.* 2011). POM also includes corpses of large animals, plankton debris (detritic rain, faecal pellets, feathers), sea snow, dissolved organic matter, as well as phytodetritic aggregates, wood or terrigenous and subtidal materials (Beaulieu 2002; McClain & Hardy 2010; Smith 1985; Smith *et al.* 2006a). Terrigenous matter can come from two sources: the first, as regular inflows as a result

of erosion processes on the coast; the second, results from episodic impacts of hurricanes and tsunamis (West *et al.* 2011). The amount of POM that reaches the seabed decreases with depth and diminishes along a distance gradient from the coast (Tittensor *et al.* 2011) The positive relationship between POM availability and diversity confirms the principle of *the species energy principle* hypothesis (Danovaro *et al.* 2002; Jumars 1976) and was confirmed for macrofauna diversity on the continental slope (Levin & Gage 1998; McCallum *et al.* 2015) and in the abyss (Wolff 1977; Woolley *et al.* 2016).

Deep-sea mining and its potential impact on benthic organisms

Economically valuable minerals such as polymetallic or cobalt-rich ferromanganese sulphides and polymetallic nodules are present in the underwater ridge with inactive hydrothermal vents, as well as some abyssal areas. Their high economical value and the huge demand for some metals (i.e. cobalt, nickel, manganese) make the deep sea an economic target for numerous countries. The Clarion-Clipperton Zone (CCZ) covers 6 million km^2 (=1.4% of oceanic floor) and it is located between the Clarion and Clipperton Fracture Zones in the Central Pacific area (Fig. 1.3) (Glover *et al.* 2016). This area is well known to international commercial consortia as a main deep-sea mining region. Since 1994, deep sea economic activities are regulated by International Seabed Authority (ISA; https://www.isa.org.jm/) operating under United Nation Convention on the Law of the Sea. Besides the well-defined Licensed areas, ISA has established nine non-mining areas, known as Areas of Particular Environmental Interest (APEIs) (Fig. 1.3). The immense economical value and ineluctable exploration for polymetallic nodules brings numerous concerns about the resilience and natural recovery of the abyssal communities. ISA's writ is to ensure effective protection for the zone from harmful impacts in vulnerable deep-sea ecosystems. The principal obstacle for conservation and management strategies is a dearth of even the most basic knowledge about deep sea fauna in the area. Discovering new taxa in a sample taken from any arbitrary chosen spot in abyssal plains is a common outcome of deep sea expeditions (Brandt *et al.* 2015). The marginal understanding of the deep-sea ecosystems utterly impede an assessment of potential impact of deep-sea mining operations on the marine environment.

Clarion-Clipperton Fracture Zone of the Central Pacific is a geologically diverse fragment of the oceanic floor where sea-mountain chains and geological fractures structure the environment (Kaiser *et al.* 2017; Wedding *et al.* 2013, 2015). Not fully identified bottom-currents may generate a variety of environmental conditions (Simon-Lledó *et al.* 2019) and promote diversification on the abyssal floor (Taboada *et al.* 2018). Furthermore, polymetallic nodules unevenly distributed on the sea floor diversify the area at small scales (De Smet *et al.* 2017). Generally, nodules increase heterogeneity of the habitat, but not always reflecting heterogeneity of all taxa. Nematodes collected in nodule-rich and nodule-free areas differed slightly, although there are species significantly associated with the nodules (Pape *et al.* 2013; Singh *et al.* 2016). A detailed assessment of deep sea environments and fauna is essential for understanding the resilience of the benthic community and design of marine protected areas in regions facing anthropogenic pressure (Taboada *et al.* 2018).

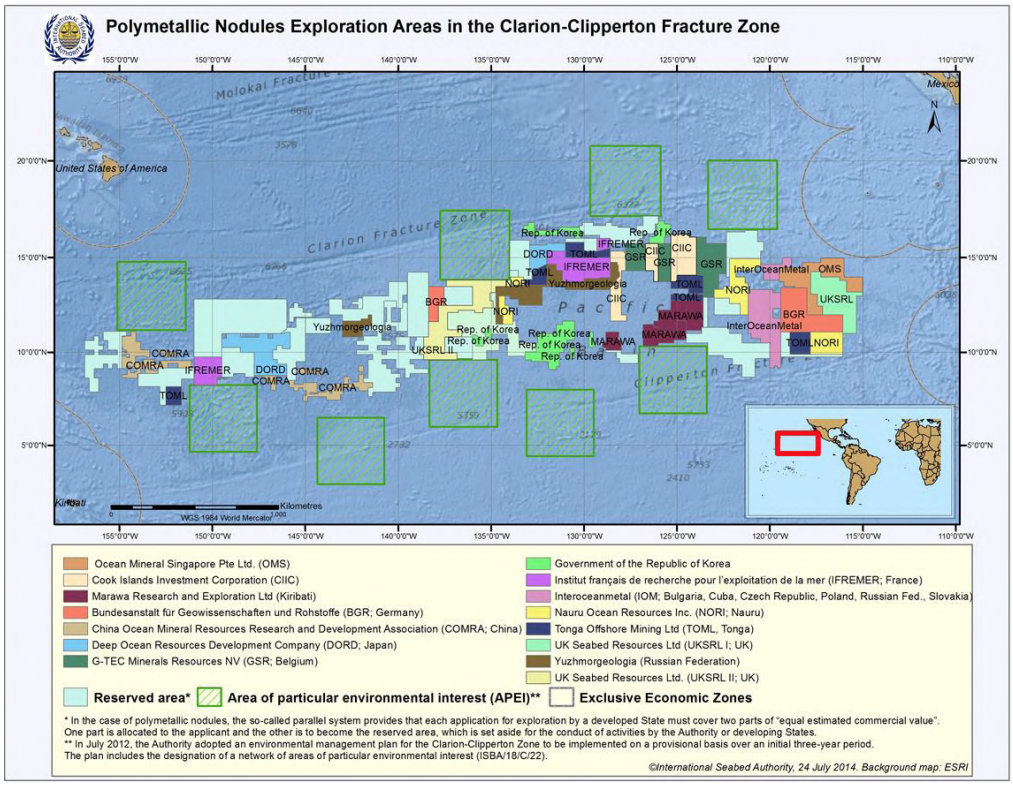

Fig 1.3. Licensed areas and Areas of Particular Environmental Interest (APEI) in polymetallic Nodules Area in Clarion-Clipperton Fracture Zone.
https://www.isa.org.jm/contractors/exploration-area.

Tanaidacea – scientific object

Tanaidacea is an order of crustaceans that belongs to the class Malacostraca and can be found occupying marine ecosystems in full latitudinal gradient from the Arctic to the Antarctic (Błażewicz-Paszkowycz *et al.* 2012). Tanaidacea are found throughout the entire depth gradient (Błażewicz-Paszkowycz *et al.* 2012; Gutu 2006; Jóźwiak & Błażewicz-Paszkowycz 2011) and are commonly recorded from tropical and deep-sea coral reefs (Jakiel *et al.* 2015; Stępień *et al.* 2019), mangrove swamps (Larsen *et al.* 2013), trenches (Kudinova-Pasternak, 1966), polymetallic nodules (Błażewicz *et al.* 2019), caves (García-Herrero *et al.* 2019), hydrothermal vents (Błażewicz-Paszkowycz *et al.* 2011a; Esquete & Cunha 2018; Larsen *et al.* 2006) or recent stromatolites (Rishworth *et al.* 2019). Most of them are truly marine crustaceans; however, a few representatives are known from brackish waters: *Longiflagrum amphibium* Stępień & Błażewicz-Paszkowycz, 2009 (West Australia) or *Heterotanais oerstedii* Krőyer, 1842 (Baltic Sea).

Tanaidacea are small crustaceans. Their usually elongated body is no longer than few millimeters. For this reason, Tanaidacea are considered the smallest bentic malacostracans. They are known to burry in fine bottom sediments composed of sand and mud or live inside of self-constructed tubes. Most tanaids are detritivores which collect the fine detritus from the surface of the sediment (Błażewicz-Paszkowycz & Ligowski 2002), but some are known to feed on algae or probably digest the wood (Błażewicz-Paszkowycz & Ligowski 2002; Johnson & Attramadal 1982a; Kudinova-Pasternak 1991). Feeding on the sediment makes tanaidaceans opportunistic predators that could prey on a variety of meiofauna taxa, and they have been reported as predators on echinoid larvae (Highsmith 1982, 1985), polychaetes (Oliver & Slattery 1985) nematodes and harpacticoid copepods (Feller 1980). One of the species, *Exspina typica* was observed to prey on holothurians (Alvaro *et al.* 2011), while the piercing mandible molar of some Pseudotanaidae or Leptognathiidae also suggests an active predatory behavior. The reduced molars and modified setation of some Anarthruridae (Bird 2004; Gellert & Błażewicz 2018) suggest they could feed on soft tissue-organisms. Tanaidacea is an important element of macrobenthic assemblages. In specific environmental condition, they can dominate in the benthic communities being present in thousands of individuals (Delille *et al.* 1985). Nevertheless,

tanaidaceans are often less abundant elements of the benthos, although often very diverse. In the shallow waters tanaids usually back down to the bigger invertebrates like polychaetes, amphipods or isopods, but in the deeper part of the oceans they are definitely one of the most important element that, together with polychaetes and isopods, shape the benthic assemblages (McCallum *et al.* 2015). So far, more than 1200 species (WoRMS, 2020) have been described, but it is expected that this number represent only a fraction (2–3%) of their real number (Appeltans *et al.* 2012; Błażewicz-Paszkowycz *et al.* 2012). It is emphasized that an unstudied area of the deep-sea floor, could host even several thousands of undescribed species of crustacea. Tanaidacea are Peracarida crustaceans and, like most peracarids, their females develop a marsupium (brood pouch) for caring the eggs and early developmental life stages. It is composed of oostegites, which grow up from the coxa of the pereopods to carry fertilized eggs and the first pre-juveniles stage. Six developmental stages can be mentioned among Tanaidacea. The first stage is manca I, that hatches from an egg but stay still in the female marsupium. The sixth pereonite and pleon is indistinct in this stadium. The second type is called manca II, it leaves marsupium, but stay in females tube. Pereonite-6 is visually separated and as long as pleonites. Manca II is lacking pereopod–6 and all pleopods. The third stage is called manca III, with pereopod–6 and pleopods buds. The fourth stage (neutrum) has full-developed appendages but without visible sexual features. The last two stages are preparatory female and male, and depending on the tanaidaceans, different types of sexual dimorphism are noted.

The order Tanaidacea is divided in two suborders: Apseudomorpha and Tanaidomorpha (WoRMS, 2020). Apseudomorpha are represented by 10 families and 345 species, while Tanaidomorpha includes 31 families and 953 species (Fig. 1.4).

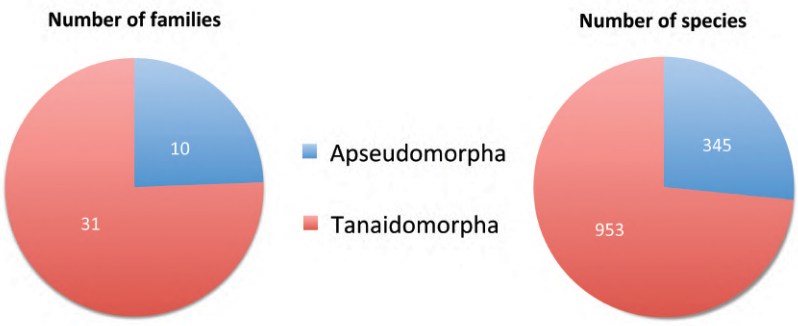

Figure 1.4. Diversity of families and species of Apseudomorpha and Tanaidomorpha, based on information from World Register of Marine Species (http://www.marinespecies.org/).

Both suborders have been established based on a series of morphological characters listed in Table 1.

Table 1. Morphological differences between Apseudomorpha and Tanaidomorpha.

Character	**Apseudomorpha**	**Tanaidomorpha**
body	dorso-ventrally flattened	cylindrical
rostrum	present	absent
antenna	biramous	uniramous
antenna	flagella multiarticulated	2-7 articles
mandibles	with palp (exc. Sphyrapodinae)	without palp
maxillule	with two endites (inner and outer); biarticulated palp	with one endite; palp present or absent
maxilla	well developed	well developed (Neotanaoida) or reduced (Paratanaoida)
maxillipedes	basis with endite	basis with or without endite
epignath	wide (kidney-shaped)	elongated, well developed with two lobes or elongated, poorly developed
cheliped exopod	present	absent
pereopod-1 exopod	present	absent
pereopod-1	often wide, setose	slender
pereopods type	swimming, burrowing, climbing	walking, equipped with glands to build tubes (only P1)
uropod endopod	often multiarticled	endopod with less than 8 articles

Most Tanaidomorpha and some Apseudomorpha (e.g. Kalliapseudidiae: Kakui & Hiruta, 2014) build tubes using secretions of 'spinning' glands located at the pereonites' junction to the cephalothorax (Siewing 1953). The secretion comes out through the canal that opens at the tip of the dactylus of the first pereopods (Johnson & Attramadal 1982b). Tubes can be transparent and elastic (Gellert & Błażewicz 2018) or incrusted with sediment particles such as detritus particles, sand grains, silt, foraminifera shells, spicules of sponges, debris or faecal pellets (Hassack & Holdich 1987). The tube gives a shelter from predators, but also plays a role in mating and breeding (Bückle Ramírez 1965; Johnson & Attramadal 1982b). It is a place for developing the first developmental stages (manca 2 and 3) and a shelter for moulting. Tanaidomorphs are characterized by strong sexual dimorphism; additionally, at least four types of males are present (Błażewicz-Paszkowycz *et al.* 2014; Larsen 2001). The first type of male (Tanaidae, Dana, 1849) shares morphological characters with females, but has bigger chelipeds, better-developed pleopods and more aesthetascs on antennule. The second type of male, called '*terminal'* (Larsen 2001), is characterized by an enlarged chela and non-functional (reduced) mouthparts. It is common in shallow-water families (e.g. Tanaissuidae Bird & Larsen, 2009, Nototanaidae Sieg, 1976 Sieg, 1976, and Leptocheliidae Lang, 1973). These chelae distinguish males from females, but they often share numerous morphological characters (e.g. leg setation). The third type of males, called '*preparatory*', are morphologically similar to females, and they are sexually mature (Bird & Holdich 1988) . '*Preparatory*' males have thicker antennules than females and better-developed pleopods. This type was described in Agathotanaidae Lang, 1971; Anarthruridae Lang, 1971b, Colletteidae Larsen and Wilson, 2002 or Tanaellidae Larsen and Wilson, 2002. The fourth type of male is called '*swimming*' or '*natatory*'. These males are morphologically very different from females. They have well-developed pleopods and a highly hydrodynamic body shape, providing unique swimming abilities. The mouthparts of swimming males are fully reduced which suggests a short lifespan (Typhlotanaidae Sieg, 1984, Leptognathiidae Sieg, 1976, Akanthophoreidae (Sieg 1986) and Pseudotanaidae Sieg, 1976.

Pseudotanaidae

Pseudotanaidae is a diverse and quite abundant family of Tanaidomorpha. The family, after including the data presented in this dissertation, is represented by 74 species and five genera (WoRMS, 2020): *Aknthinotanais* Sieg, 1977 (12 sp.), *Beksitanais* Jakiel, Palero & Błażewicz, 2019 (1 sp.), *Mystriocentrus* Bird & Holdich, 1989 (3 sp.), *Parapseudotanais* Bird & Holdich, 1989 (1 sp.), *Pseudotanais* Sieg, 1977 (57 sp.) (Fig. 1.5A). They inhabit shallow waters (<200 m) as well as the deep sea (>200 m) and are represented by 24 to 50 formally-described species, respectively (Figure 1.5B; Appendix 1). Pseudotanaidae are usually less abundant in shallow waters, but they are a relevant element of many benthic assemblages (Sieg 1980). They are abundant in polar zones and deep-sea ecosystems (Pabis *et al.* 2015), but their presence in tropical areas is not well studied.

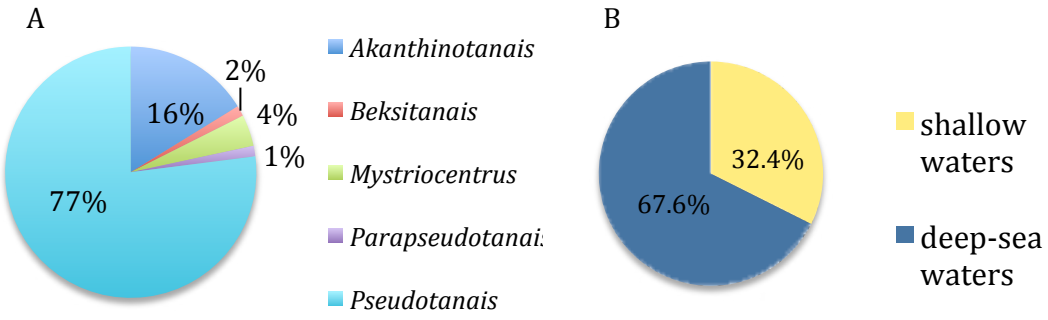

Figure 1.5. Pie charts: A) species composition of Pseudotanaidae by genera; B) diversity of Pseudotanaidae in shallow (<200 m) and deep-sea waters (>200 m) (see Appendix).

Sieg erected the family in 1976, even though the genus Pseudotanais was the first time mentioned by Sars in 1882 in the description of *Pseudotanais lilljeborgi*. Pseudotanaidae studies were initiated by early explorations in the North Atlantic Ocean. The first member of the family was described from shallow waters by Lilljeborg, *Pseudotanias forcipatus* (Lilljeborg 1864). In his pioneering research of Norway costal fauna, Sars (1882) described three Pseudotanaidae species. The list of shallow-water tanaids in the North Atlantic was completed by the description of four other taxa (*P. jonesi*, *P. mortenseni*, *P. similis*, and *P unicus*) by Sieg (1977). The first

deep-water *Pseudotanais* were discovered by Hansen based on material collected during the *Ingolf* Expediton (Hansen 1913) on North Atlantic waters. The list of deep-sea tanaids was only modified 76 years later with eleven species described by Bird & Holdich (1989). Extensive research on the temperate northern Atlantic resulted in 38 Pseudotanaidae species belonging to 4 genera, with 29 species distributed along northern European seas, four species formally described from Mediterranean waters and one species from the Black Sea. The list of Atlantic pseudotanaids from the Northern Hemisphere is completed with two species formally described from the Gulf of Mexico, one from the Barbados trench, one from Azores (Macaronesia) and one from a mud volcano on the Saharan Upwelling province. The family has been much less studied in the Southern Hemisphere, with two species known from the SE Atlantic, one from the West African Transition province and another from the Gulf of Guinea Upwelling. A single pseudotanaid species has been reported from SW Atlantic deep sea waters so far (*P. nordenskioldi* Sieg, 1977 in Kudinova-Pasternak, 1975). Pseudotanaids from North and Central Pacific Oceans are much less studied and only 28 species are known in the area (Dojiri & Sieg 1997; Sieg 1977). Finally, four species have been described from the Southern Ocean (Sieg 1977), and only one from the Indian Ocean (Fig. 1.6, Appendix 1). The lack of pseudotanaids in Southern Pacific or Atlantic waters and the Indian Ocean is most likely due to the small number of peracarid-centred sampling campaigns and research efforts (Błażewicz, pers comm).

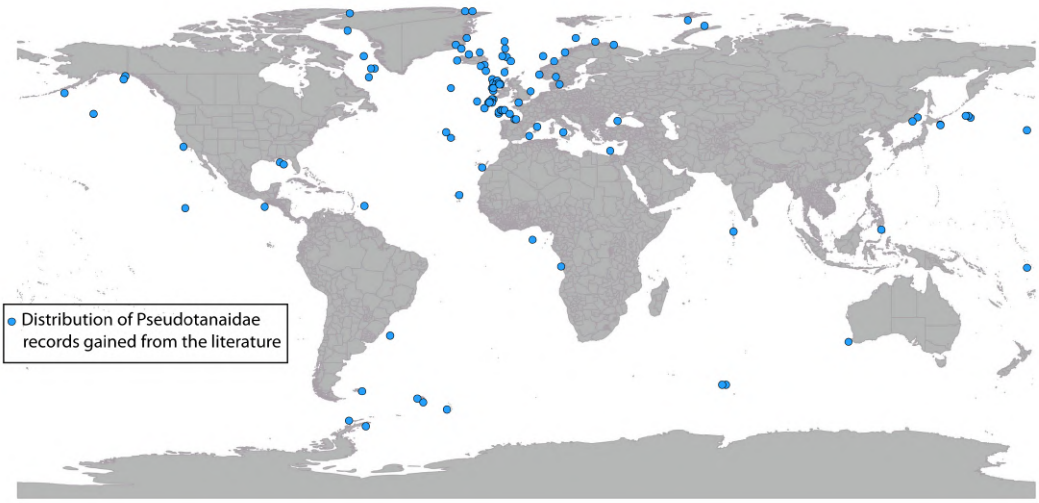

Figure 1.6. Distribution of the Pseudotanaidae records based on a literature data:(Băcescu 1960; Bamber 2005; Bamber *et al.* 2009; Bird & Holdich 1989c; b; Błażewicz-Paszkowycz *et al.* 2011a, 2013; Błażewicz-Paszkowycz & Bamber 2011; Bruce *et al.* 1963; [Dahl] in Sieg, 1977; [Debouttéville (1960), Debouttéville et al. (1954)] in Sieg

(1983); [Fee, Hatch] in Sieg (1977); (Dojiri & Sieg 1997; Greve 1965b; c; a; Holdich & Jones 1983; Jakiel *et al.* 2015; Just 1970) Kruuse, Ryder, Wandel in Hansen (1913); (Kudinova-Pasternak 1966b, 1973, 1975, 1978; Larsen 2012) Kudinova-Paseternak (1978); Lilljeborg (1864;); [McLelland] in Larsen and (Eds, 2007); (García-Herrero *et al.* 2019; Larsen & Shimomura 2007; Sars 1882, 1886; Shino & Shiino 1978; Sieg 1973, 1977; Sieg & Heard 1988; Stephensen 1937; VanHöffen 1914, 1907); [Vanhöffen, Kruuse, Ryder, Horring, Sars] in Hansen (1913); [Vanhöffen, R. Horring, H.J. Hansen, Sars, A.M. Norman, Stappers, Th. Scott] in Hansen (1913).

Morphology

Pseudotanaidae are small tanaidomorphs characterised by weakly calcified cuticles and often-narrow first or two first pereonites (Fig. 1.7, 1.8), although some members of *Pseudotanais* are an exception here (e.g. *P. baresnauti*, Bird, 1999; *P. colonus* Bird & Holdich, 1989). Many Pseudotanaids have elongated pereopods, which in case of *Beksitanais*, *Mystriocentrus*, *Parapseudotanais* and *Pseudotanais* have carpus bearing a specific spine named blade-like spine (Fig. 1.11F–H). These kinds of spines are absent in *Akantinotanais.* Furthermore, females of the Pseudotanaidae have a marsupium composed of only one pair of oostegites growing from the fourth pereonites.

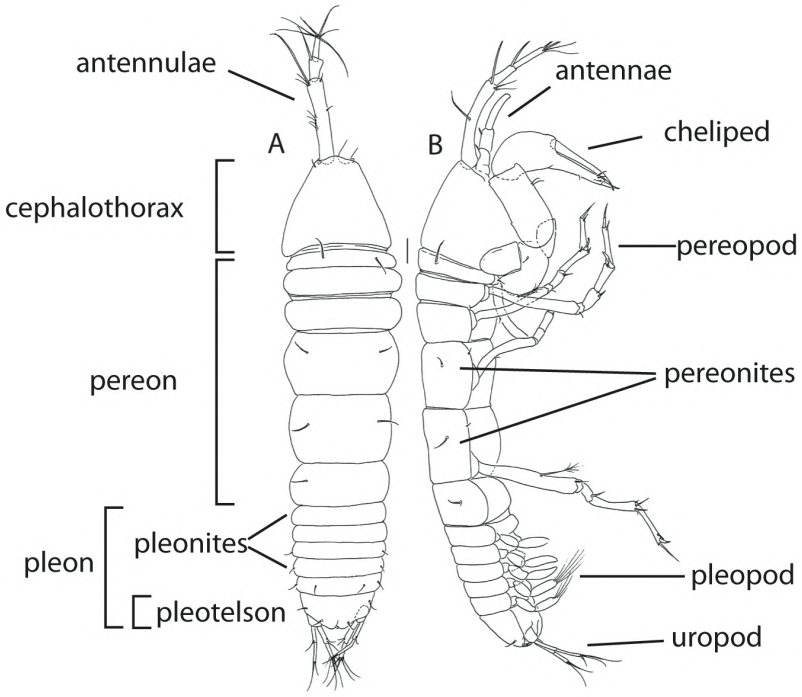

Figure 1.7. General pseudotanaid morphology based on *Pseudotanais oloughlini* Jakiel, Palero & Błażewicz, 2019. A) dorsal view; B) lateral view.

Figure 1.8. Confocal laser scanning microscope (CLSM) image of Pseudotanaidae specimen.

As in other malacostracans, the pseudotanaid head is composed of five segments and an *acron*, the thorax consists of eight segments and the pleon with five segments ending with a pleotelson. The two first thoracic segments are fused with the head forming a cephalothorax that is covered by a calcified carapace. In this way, the pereon in Pseudotanaidae is composed of six free segments (pereonites) (Fig. 1.7). The following pairs of appendages can be found in the head: antennulae (Fig. 1.9A) and antennae (Fig. 1.9B), mandibles (left (Fig. 1.9C) and right (Fig. 1.9D)), maxillules (Fig. 1.9E) and maxilla (Fig. 1.9F). The labrum and labium (Fig. 1.9G) are expansions of the cephalothorax which limit the mouth anteriorly and posteriorly, respectively. The first thoracic segment, merged with the head, is equipped with the maxilliped (Fig. 1.9H) and its epignath, while on the second thoracic segment supports the chelipedes. Each pereonite is equipped with a pair of pereopods. The free pleonites can bear a pair of appendages named pleopods (Fig. 1.10G). Each pleopod is composed of a basis, endopod and exopod, with both endopod and exopod bearing long setae. Pleotelson is tipped by a pair of biramous uropods (Fig. 1.10H). Both, uropodal exopod and endopod can be one or two articulated.

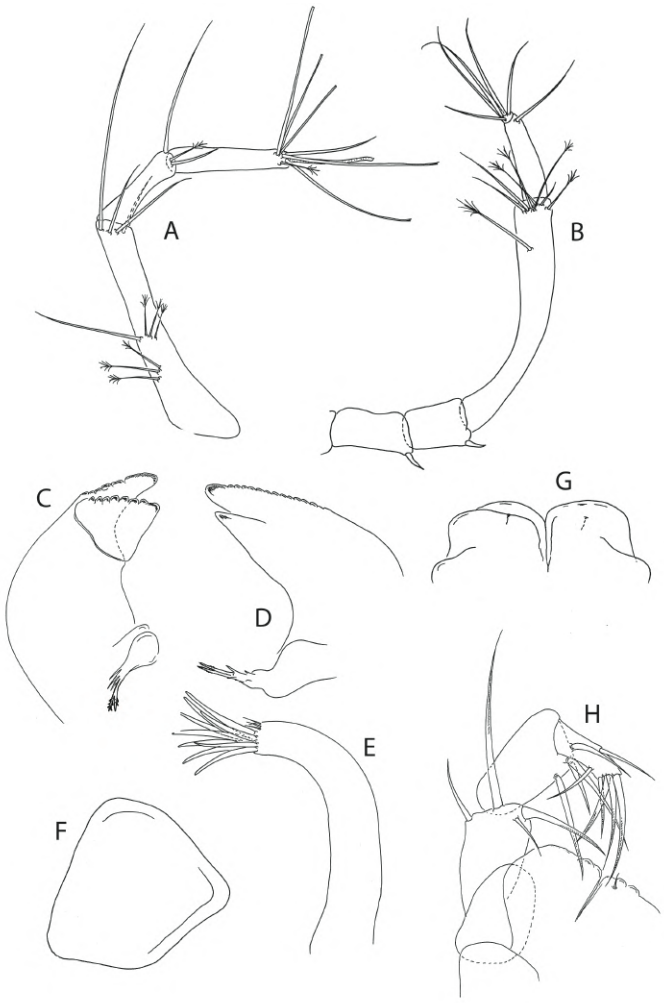

Figure 1.9. *Pseudotanais oloughlini* Jakiel, Palero & Błażewicz, 2019. A) antennule; B) antenna; C) left mandible; D) right mandible; E) maxillule; F) maxilla; G) labium; H) maxilliped.

Antennule and antenna of Pseudotanaidae are always uniramous. The antennule is composed of three articles and the terminal one is equipped with bifurcated setae, simple setae and one aesthetasc (Fig. 1.9A) The antenna is composed of six articles, and it is usually shorter than the antennule (Fig. 1.7). Antenna articles 2 and 3 bear a robust spine or a seta (Fig 1.11B, C) and article–4 is the longest.

Mouthparts. The labrum of Pseudotanaidae is wide and hood-shaped with distal margin naked or setose. The mandibles are often large and well-calcified, with the *lacinia mobilis* of left mandible well-developed and distally serrate, almost as large as incisor. Distal margin of left mandible is smooth but it is well serrate in the right mandible, which has a bifurcate incisor. Pseudotanaid mandibles have at least two types of molar; acuminate or coronal (Fig. 1.11D, E). The maxillule palp is distally bent and supported with seven to 11 distal spines, and the maxillule endite has two

setae. The maxilla is a relatively large and oval simple plate. The maxilliped endites are fully or partially fused, with a groove in mid-length or smooth. The maxilliped palp, composed of four articles, has three inner serrate setae and one outer seta in article-2, four setae in article-3, and six distal or subdistal setae in article–4 (Fig. 1.9H).

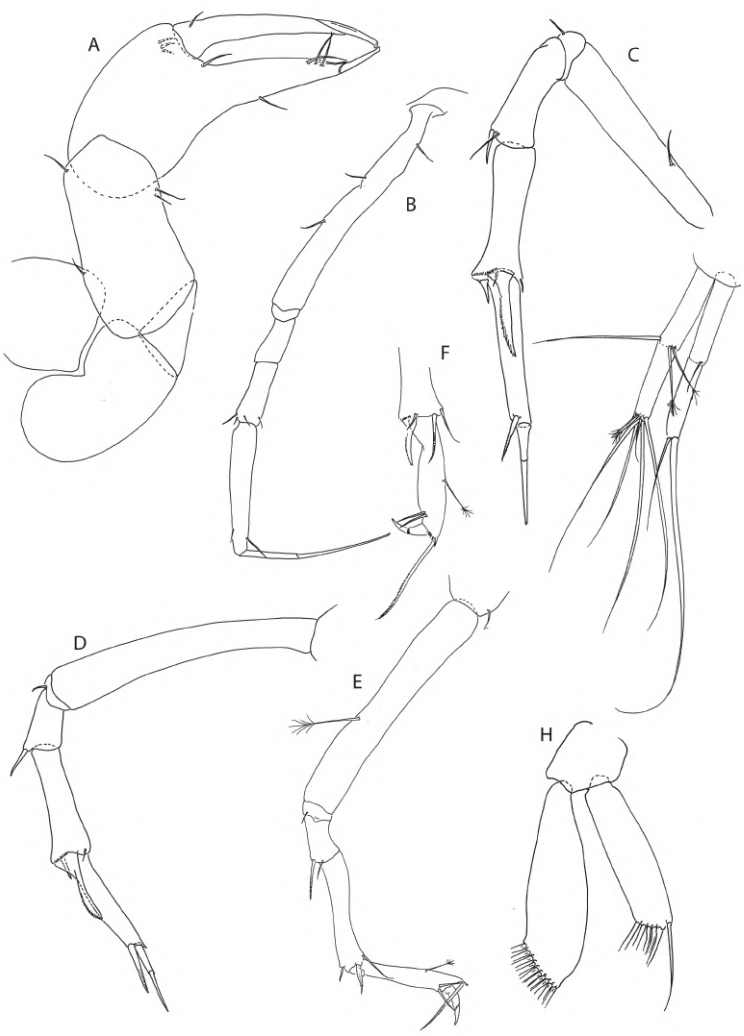

Figure 1.10. *Pseudotanais oloughlini* Jakiel, Palero & Błażewicz, 2019. A) cheliped; B) pereopod-1; C) pereopod-2; D) pereopod-3; E) pereopod-4; F) pereopod-5; G) pleopod; H) uropod.

The cheliped is composed by the following articles (Fig. 1.10): basis, merus, carpus, propodus, dactylus and fixed finger. Pereopod-1 (Fig. 1.10B) is usually longer than the following ones and has an internal canal for the transport of mucus specialized for tube production. Pereopod–2 is similar to pereopod–3. In the Pseudotanaidae family (except for *Akanthinotanais*) there is a characteristic blade-like spine (Fig. 1.11F, G, H) on the carpus pereopods 2–3 (Fig. 1.10C, D). Pereopods 4–6 (Fig. 1.10E

[pereopod–4], F [pereopod–5]). are similar to each other. These pereopods also carry the characteristic blade-like spine on carpus (except in *Akanthinotanais* and *Parapseudotanais*).

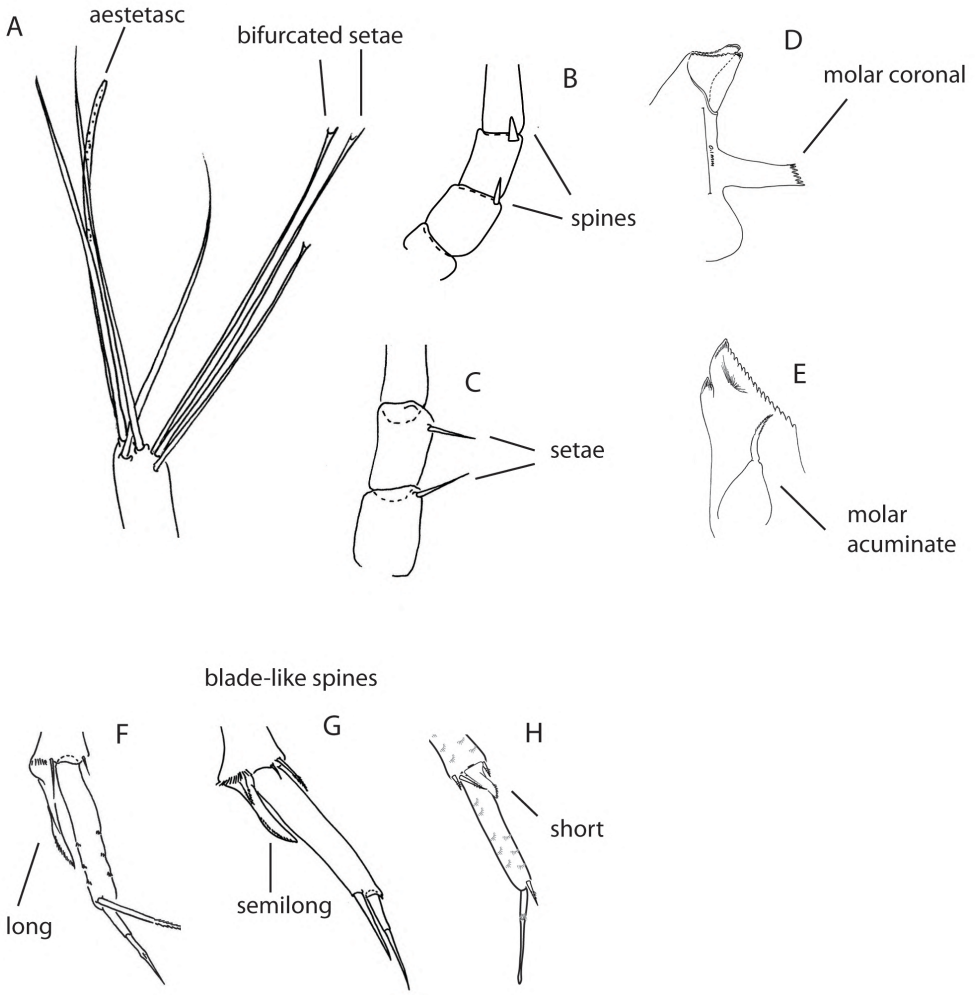

Figure 1.11. Detailed morphology of Pseudotanaidae. A) last article of antennulae with setation; B,C) second and third article of antennae; D,E) mandibles with molar; F,G,H) pereopods-3 with different length of blade-like spines.

Material and methods

The material studied in the present dissertation was obtained during three international scientific programs: Icelandic marine Animals: Genetics and Ecology (IceAGE); Kuril-Kamchatka Biodiversity Studies (KuramBIO); The European Joint Project Initiative – Oceans (JPI-O) (Table 2). Materials were collected using epibenthic sledge (EBS), Shipek grab (SG), Van Veen grab (VV) and box corers (GKG) (Fig. 1.12). EBS (Hessler & Sanders 1967) is a steel frame with two sliders, which allow shifting on the seabed. A 0.3 mm mesh net, where all samples will fall during the sliding, is associated to the frame. Epibenthic sled is a device used to obtain non-quantitative samples. The gear is pulled on the sea bottom collecting macrobenthic organisms from the seabed surface as well as from the thin layer of sediments (Thistle 2003).

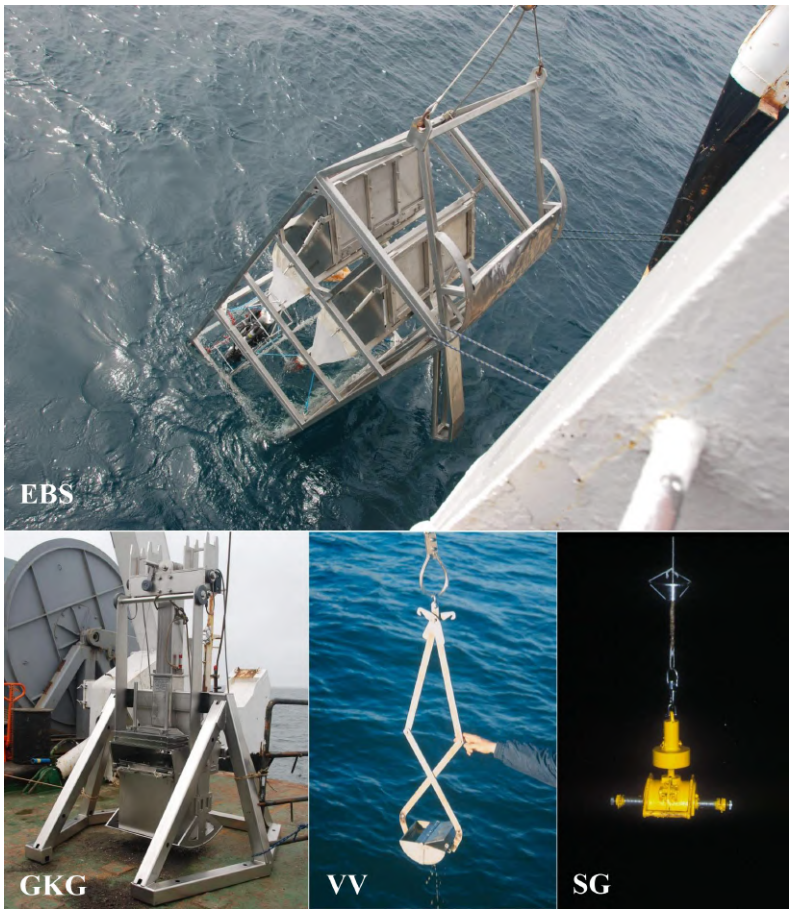

Figure 1.12. Different devices used for collecting the Pseudotanaidae studied in the current dissertation. EBS: Epibenthic sledge, GKG: Box-corer, VV: Van Veen grab, SG: Shipek grab. (Photos: I. Frutos).

The Box corer (Hessler & Jumars 1974) is a device for collecting quantitative samples of deep-sea macrofauna. It is built with a 50x50 cm box that is penetrating the sea bottom for 50 cm depth when the GKG reaches the seabed, a special mechanism closes it and it is hauled on board. This gear allows collecting meiofauna and microbiota samples also (Thistle 2003).
The Van Veen Grab Sampler is a device for collecting surface samples of bottom sediments, used in oceanographic studies. It allows for physical and chemical analyses of the sediments. It is a jaw sampler with ratchet lock, actuated when it touched the bottom. Up to 20 cm sediments layer can be extracted with this instrument.
Shipek grab is a device mostly used for geophysical analysis. SG contains two steel clamshells when the device reach the bottom powerful spring acting brought together both shovels (Audibert & Huang 2005).

On deck, the samples were sieved using 300 µm mesh size and immediately transferred into pre-cooled 96% ethanol (DNA studies) and kept in -20°C or transferred into 4% formalin (Brandt & Malyutina 2012). Specific methods applied are given in the methodology section of Chapters 2–4. Traditional taxonomy based on morphology is presented in chapters 2, 3 and 4; morphometric methods are presented in chapters 2 (page 38) and molecular methodology is described in chapters 3 and 4 (pages 118 and 124, respectively).

Table 2. Summary of Pseudotanaidae research material collected during international, deep-sea scientific expeditions: Icelandic marine Animals: Genetics and Ecology (IceAGE); Kuril-Kamchatka Biodiversity Studies (KuramBIO); The European Joint Project Initiative – Oceans (JPI-O).

Expedition	**Area**	**Depth (m)**	**Number of individuals (n)**
IceAGE I and II	North Atlantic: off Iceland	213–2750	323
JPIO	Central Pacific: Clarion-Clipperton Fracture Zone (CCZ)	4093–5030	67
KuramBIO I	North-west Pacific: Kurile-Kamchatka Trench adjusted area	4830–5780	273

Aims and hypotheses

This dissertation is aimed at improving our knowledge on the diversity and distribution of the Pseudotanaidae from three areas of the deep sea namely, North Atlantic (off Iceland), Central Pacific (Clarion-Clipperton Fracture Zone) and North-west Pacific (Kurile-Kamchatka Trench and adjacent abyssal plain). Each of these areas is characterized by unique topographies making them ideal scientific polygons for describing and testing the impact of physical barriers on the population connectivity and distribution of deep sea benthic peracarids. Three main hypotheses were formulated in relation with the expected connectivity patterns:

OCEANIC RIDGES AND TRENCHES INFLUENCE DEEP SEA SPECIES DISTRIBUTION

HYPOTHESIS 1: The Mid-Atlantic Ridge is acting as a barrier hampering the dispersion of Pseudotanaidae.

HYPOTHESIS 2: The Kurile-Kamchatka Trench is a barrier hampering dispersion of Pseudotanaidae.

PHYSICAL DISTANCE INFLUENCES POPULATION CONNECTIVITY OF SPECIES WITH RESTRICTED DISPERSAL ABILITY

HYPOTHESIS 3: Pseudotanaidae in five areas of Clarion-Clipperton Fracture Zone separated by hundreds of kilometres are represented by unique and distinct set of species.

Summary

A large collection of Pseudotanaidae was obtained during three international expeditions. Samples were taken from shelf areas down to the slope (213−2750 m) and from the abyss (4093–5780 m). In North Atlantic waters, six areas off Iceland (Irminger Basin, Iceland Basin, Norwegian Sea, Denmark Strait, Iceland-Faroe Ridge, and Norwegian Channel) were investigated. In this sampling collection, Pseudotanaidae was the most numerous Tanaidacea family. Morphological identification revealed five species, for which the descriptions are given in Chapter 2. A large group of indistinguishable specimens, from a wide depth range and different areas was discriminated using morphometric methods. This allowed me to distinguish variation within one species (*P. svavarssoni* and complex cryptic species of *P. svavarssoni*). Another 13 new species were described from Central Pacific waters (Chapter 3). All the new taxa present restricted distributions and where found on a few closest stations. The high heterogeneity in the area reduced the spatial distribution of each taxa, but an increasing number of available niches has triggered diversity levels. The integrative taxonomy approach applied on the third studied area, the abyss of the Kurile-Kamchatka Trench, has allowed us to identify six new species. The homogeneity of the abyss in KKT provides a wide distribution of pseudotanaids, and the examined taxa of the KKT did not show limited distributions.

Streszczenie

Podczas trzech międzynarodowych ekspedycji naukowych zgromadzono obszerną kolekcję skorupiaków z rodziny Pseudotanaidae. Próby pobierano ze stoku kontynentalnego (213–2750 m) i równiny abysalnej (4093–5780 m). W północnym Atlantyku zbadano sześć obszarów w pobliżu Islandii (Irminger Basin, Iceland Basin, Norwegian Sea, Danish Strait, Iceland and Faroe Ridge oraz Norwegian Channel). W niniejszej kolekcji Pseudotanaidae były najliczniejszą rodziną spośród wszystkich Tanaidacea. Na podstawie analizy morfologicznej zidentyfikowano cztery nowe dla nauki gatunki, a ich opis podano w rozdziale 2. W badanym materiale dużą grupę stanowiły morofologicznie identyczne osobniki, występujące w szerokim zakresie głębokości i pochodzące z różnych basenów wokół Islandii. Do ich oznaczenia użyto metod morfometrycznych. Dzięki temu możliwe było wyróżnienie nowego gatunku (*P. svavarssoni* oraz grupy gatunków kryptycznych opisanych jako *P. svavarssoni* complex).

Ze środkowego Pacyfiku opisano jeden nowy rodzaj (Beksitanais) oraz 13 nowych gatunków (rozdział 3). Wszystkie nowe taksony prezentują wąskie rozmieszczenie, ograniczone jedynie do sąsiadujących ze sobą stacji. Wysokie zróżnicowanie przestrzenne tego obszaru może zmniejszać dyspersję organizmów, ale rosnąca liczba dostępnych nisz powoduje wzrost różnorodności.

Trzecim badanym obszarem była równina abysalna rowu Kurylsko-Kamczackiego. Dzięki użyciu zintegrowanej taksonomii udało się zidentyfikować i opisać sześć nowych gatunków. Równina abysalna KKT jest mało urozmaicona pod względem topograficznym dzięki czemu Pseudotanaidae z badanego obszaru były szeroko rozprzestrzenione.

References

Allouche, O., Kalyuzhny, M., Moreno-Rueda, G., Pizarro, M. & Kadmon, R. (2012) Area-heterogeneity tradeoff and the diversity of ecological communities. *Proceedings of the National Academy of Sciences of the United States of America* 109, 17495–17500.

Almany, G.R. (2004) Differential effects of habitat complexity, predators and competitors on abundance of juvenile and adult coral reef fishes. *Oecologia* 141, 105–113.

Alvaro, M.C., Błażewicz-Paszkowycz, M., Davey, N. & Schiaparelli, S. (2011) Skin-digging tanaids: The unusual parasitic behaviour of Exspina typica in Antarctic waters and worldwide deep basins. *Antarctic Science* 23, 343–348.

Appeltans, W., Ahyong, S.T., Anderson, G., Angel, M. V., Artois, T., Bailly, N., Bamber, R.N., Barber, A., Bartsch, I., Berta, A., Błażewicz-Paszkowycz, M., Bock, P., Boxshall, G.H., Boyko, C.B., Brandão, S.N., Bray, R.A., Bruce, N.L., Cairns, S.D., Chan, T.Y., Cheng, L., Collins, A.G., Cribb, T., Curini-Galletti, M., Dahdouh-Guebas, F., Davie, P.J.F., Dawson, M.N., De Clerck, O., Decock, W., De Grave, S., De Voogd, N.J., Domning, D.P., Emig, C.C., Erséus, C., Eschmeyer, W., Fauchald, K., Fautin, D.G., Feist, S.W., Fransen, C.H.J.M., Furuya, H., Garcia-Alvarez, O., Gerken, S., Gibson, D., Gittenberger, A., Gofas, S., Gómez-Daglio, L., Gordon, D.P., Guiry, M.D., Hernandez, F., Hoeksema, B.W., Hopcroft, R.R., Jaume, D., Kirk, P., Koedam, N., Koenemann, S., Kolb, J.B., Kristensen, R.M., Kroh, A., Lambert, G., Lazarus, D.B., Lemaitre, R., Longshaw, M., Lowry, J., MacPherson, E., Madin, L.P., Mah, C., Mapstone, G., McLaughlin, P.A., Mees, J., Meland, K., Messing, C.G., Mills, C.E., Molodtsova, T.N., Mooi, R., Neuhaus, B., Ng, P.K.L., Nielsen, C., Norenburg, J., Opresko, D.M., Osawa, M., Paulay, G., Perrin, W., Pilger, J.F., Poore, G.C.B., Pugh, P., Read, G.B., Reimer, J.D., Rius, M., Rocha, R.M., Saiz-Salinas, J.I., Scarabino, V., Schierwater, B., Schmidt-Rhaesa, A., Schnabel, K.E., Schotte, M., Schuchert, P., Schwabe, E., Segers, H., Self-Sullivan, C., Shenkar, N., Siegel, V., Sterrer, W., Stöhr, S., Swalla, B., Tasker, M.L., Thuesen, E. V., Timm, T., Todaro, M.A., Turon, X., Tyler, S., Uetz, P., Van Der Land, J., Vanhoorne, B., Van Ofwegen, L.P., Van Soest, R.W.M., Vanaverbeke, J., Walker-Smith, G., Walter, T.C., Warren, A., Williams, G.C. & Wilson, S.P. (2012) The magnitude of global marine species diversity. *Current Biology* 22, 2189–2202.

Astthorsson, O.S., Gislason, A. & Jonsson, S. (2007) Climate variability and the Icelandic marine ecosystem. *Deep-Sea Research Part II: Topical*

Studies in Oceanography 54, 2456–2477.

Audibert, J.M. & Huang, J. (2005) Geophysical and Geotechnical Design. In: *Handbook of Offshore Engineering*. Elsevier, pp. 1145–1268.

Băcescu, M. (1960) Bacescu (1960) Citeva animale, Marea Negra, Malacostracei.

Baco, A.R., Etter, R.J., Ribeiro, P.A., von der Heyden, S., Beerli, P. & Kinlan, B.P. (2016) A synthesis of genetic connectivity in deep-sea fauna and implications for marine reserve design. *Molecular Ecology* 25, 3276–3298.

Bamber, R.N. (2005) The tanaidaceans (Arthropoda: Crustacea: Peracarida: Tanaidacea) of Esperance, Western Australia, Australia. *In: F.E. Wells, D.I. Walker and G.A. Kendrick (eds) 2005. The Marine Flora and Fauna of Esperance, Western Australia. Western Australian Museum, Perth* 1963, 613–728.

Bamber, R.N., Bird, G.J. & Błażewicz-Paszkowycz, M. (2009) Tanaidaceans (Crustacea: Malacostraca: Peracarida) From Soft-Sediment Habitats Off Israel, Eastern Mediterranean Historical ecology of Lessepsian migration View project. *Zootaxa* 2109, 1–44.

Bamber, R.N. & Błażewicz-Paszkowycz, M. (2013) Another inordinate fondness†: Diversity of the tanaidacean fauna of Australia, with description of three new taxa. *Journal of Natural History* 47, 1767–1789.

Beaulieu, S. (2002) Accumulation and Fate of Phytodetritus on the Sea Floor. In: , pp. 171–232.

Bird, G.J. (1999) A new species of Pseudotanais (Crustacea, Tanaidacea) from cold seeps in the deep Caribbean, collected by the French submersible Nautile. *Zoosystema* 21, 445–451.

Bird, G.J. (2004) Tanaidacea (Crustacea) of the Northeast Atlantic: non-filiform species of Anarthruridae Lang from the Atlantic Margin. *Zootaxa* 471, 1–44.

Bird, G.J. & Holdich, D.M. (1988) Deep-sea tanaidacea (Crustacea) of the North-East Atlantic: The tribe Agathotanaini. *Journal of Natural History* 22, 1591–1621.

Bird, G.J. & Holdich, D.M. (1989a) Deep-sea tanaidacea (Crustacea) of the North-East Atlantic: The genus Paranarthrura hansen. *Journal of Natural*

History 23, 137–167.

Bird, G.J. & Holdich, D.M. (1989b) Recolonisation of artificial sediments in the deep bay of biscay by tanaidaceans (crustacea: Peracarida), with a description of a new species of pseudotanais. *Journal of the Marine Biological Association of the United Kingdom* 69, 307–317.

Bird, G.J. & Holdich, D.M. (1989c) Tanaidacea (Crustacea) of the north−east Atlantic: the subfamily Pseudotanainae (Pseudotanaidae) and the family Nototanaidae. *Zoological Journal of the Linnean Society* 97, 233–298.

Bird, G.J. & Larsen, K. (2009) Tanaidacean phylogeny–the second step: the basal paratanaoidean families (Crustacea: Malacostraca). *Arthropod Systematics & Phylogeny* 67, 137–158.

Błażewicz-Paszkowycz, M. & Bamber, R.N. (2011) Tanaidomorph tanaidacea (crustacea: Peracarida) from mud-volcano and seep sites on the Norwegian Margin. *Zootaxa* 3061, 1–35.

Błażewicz-Paszkowycz, M., Bamber, R.N. & Anderson, G. (2012) Diversity of tanaidacea (crustacea: Peracarida) in the world's oceans - how far have we come? *PLoS ONE* 7.

Błażewicz-Paszkowycz, M., Bamber, R.N. & Cunha, M.R. (2011a) Apseudomorph tanaidaceans (Crustacea: Peracarida) from mud-volcanoes in the Gulf of Cadiz (North-east Atlantic). *Zootaxa* 2919, 1–36.

Błażewicz-Paszkowycz, M., Bamber, R.N. & Cunha, M.R. (2011b) New tanaidomorph tanaidacea (Crustacea: Peracarida) from submarine mud-volcanoes in the Gulf of Cadiz (North-east Atlantic). *Zootaxa* 2769, 1–53.

Błażewicz-Paszkowycz, M., Bamber, R.N. & Jóźwiak, P. (2013) Tanaidaceans (Crustacea: Peracarida) from the SoJaBio joint expedition in slope and deeper waters in the Sea ofJapan. *Deep-Sea Research Part II: Topical Studies in Oceanography* 86–87, 181–213.

Błażewicz-Paszkowycz, M., Jennings, R.M., Jeskulke, K. & Brix, S. (2014) Discovery of swimming males of Paratanaoidea (Tanaidacea). *Polish Polar Research* 35, 415–453.

Błażewicz-Paszkowycz, M. & Ligowski, R. (2002) Diatoms as food source indicator for some Antarctic Cumacea and Tanaidacea (Crustacea). *Antarctic Science* 14, 11–15.

Błażewicz, M., Jóźwiak, P., Jennings, R.M., Studzian, M. & Frutos, I. (2019) Integrative systematics and ecology of a new deep-sea family of tanaidacean crustaceans. *Scientific Reports* 9, 18720.

Bober, J., Brandt, A., Frutos, I. & Schwentner, M. (2019) Diversity and distribution of Ischnomesidae (Crustacea: Isopoda: Asellota) along the Kuril-Kamchatka Trench – A genetic perspective. *Progress in Oceanography* 178.

Bober, S., Brix, S., Riehl, T., Schwentner, M. & Brandt, A. (2018a) Does the Mid-Atlantic Ridge affect the distribution of abyssal benthic crustaceans across the Atlantic Ocean? *Deep-Sea Research Part II: Topical Studies in Oceanography* 148, 91–104.

Bober, S., Riehl, T., Henne, S. & Brandt, A. (2018b) New Macrostylidae (Isopoda) from the Northwest Pacific Basin described by means of integrative taxonomy with reference to geographical barriers in the abyss. *Zoological Journal of the Linnean Society* 182, 549–603.

Bogorov, V.G. (1973) Fauna of the Kurile–Kamchatka Trench and its environment. *Academy of sciences of the USSR. Proc. Inst. Oceanol* 86.

Brandt, A., Arbizu, P.M., Malyutina, M. V & Alalykina, I.L. (2016) *Kuril Kamchatka Biodiversity Studies II - RV Sonne SO250, Tomakomai-Yokohama (Japan), 16.08.-26.09.2016*.

Brandt, A., Błażewicz-Paszkowycz, M., Bamber, R.N., Mühlenhardt-Siegel, U., Malyutina, M. V, Kaiser, S., De Broyer, C. & Havermans, C. (2012) Are there widespread peracarid species in the deep sea (Crustacea: Malacostraca)? *Polish Polar Research* 33, 139–162.

Brandt, A., Brenke, N., Andres, H.G., Brix, S., Guerrero-Kommritz, J., Mühlenhardt-Siegel, U. & Wägele, J.W. (2005) Diversity of peracarid crustaceans (Malacostraca) from the abyssal plain of the Angola Basin. *Organisms Diversity and Evolution* 5, 105–112.

Brandt, A., Elsner, N.O., Malyutina, M. V, Brenke, N., Golovan, O.A., Lavrenteva, A. V & Riehl, T. (2015) Abyssal macrofauna of the Kuril–Kamchatka Trench area (Northwest Pacific) collected by means of a camera–epibenthic sledge. *Deep Sea Research Part II: Topical Studies in Oceanography* 111, 175–187.

Brandt, A., Elsner, N.O., Malyutina, M. V & Golovan, O.A. (2010) *The Russian-German deep-sea expedition (SoJaBio) to the Sea of Japan*

onboard of the R/V Akademik Lavrentyev.

Brandt, A., Frutos, I., Bober, S., Brix, S., Brenke, N., Guggolz, T., Heitland, N., Malyutina, M. V, Minzlaff, U., Riehl, T., Schwabe, E., Zinkann, A.C. & Linse, K. (2018) Composition of abyssal macrofauna along the Vema Fracture Zone and the hadal Puerto Rico Trench, northern tropical Atlantic. *Deep-Sea Research Part II: Topical Studies in Oceanography* 148, 35–44.

Brandt, A. & Malyutina, M. V (2012) *The German-Russian deep-sea expedition KuramBio (Kurile Kamchatka Biodiversity Study) to the Kurile Kamchatka Trench and abyssal plain on board of the R/V Sonne, 223rd Expedition (July 21th – September 7th 2012). Cruise report.* Technische Informationsbibliothek u. Universitätsbibliothek, Hamburg [u.a.]

Brandt, A. & Malyutina, M. V (2015) The German-Russian deep-sea expedition KuramBio (Kurile Kamchatka biodiversity studies) on board of the RV Sonne in 2012 following the footsteps of the legendary expeditions with RV Vityaz. *Deep-Sea Research Part II: Topical Studies in Oceanography*.

Brix, S., Bauernfeind, W., Brenke, N., Błażewicz, M., V, B., Buldt, K., Cannon, J., Díaz Agras, G., Fiege, D., Fiorentino, D., Haraldsdóttir, S., Hoffmann, S., Holst, S., Hüttmann, F., Jeskulke, K., Jennings, R.M., Kocot, K., Khodami, S., Lucas Rodriguez, Yolanda Martinez Arbizu, P., Meißner, K., Mikkelsen, N., Miller, M., Murray, A., Neumann, H., Ostmann, A., Riehl, T., Schnurr, S., Savavarsson Jorundur & Yasuhara, M. (2012) Cruise Report M85 / 3 IceAGE1 2011 with RV Meteor. *Technical Report.*, 41.

Brix, S., Cannon, J., Svavarsson, J., Eilertsen, M., Kenning, M., Schnurr, S., Jennings, R., Hoffmann, S., Martinez, P., Jekulke, K. & Holst, S. (2013) Icelandic marine Animals: Genetics and Ecology. Cruise No. POS456. *Cruise Report POS 456 Kiel – 2 Reykjavik, 20.07. – 04.08.2013* 456, 1–17.

Brix, S., Riehl, T. & Leese, F. (2011) First genetic data for species of the genus Haploniscus Richardson, 1908 (Isopoda: Asellota: Haploniscidae) from neighbouring deep-sea basins in the South Atlantic. *Zootaxa*, 79–84.

Brix, S. & Svavarsson, J. (2010) Distribution and diversity of desmosomatid and nannoniscid isopods (Crustacea) on the Greenland-Iceland-Faeroe Ridge. *Polar Biology* 33, 515–530.

Brix, S., Svavarsson, J. & Leese, F. (2014) A multi−gene analysis reveals multiple highly divergent lineages of the isopod Chelator insignis (Hansen,

1916) south of Iceland. *Polish Polar Research* 35, 225–242.

Bruce, J.R., Colman, J.S. & Jones, N.S. (1963) 44 Journal of the Marine Biological Association of the United Kingdom *Marine Fauna of the Isle of Man and its Surrounding Seas s.* . Cambridge University Press (CUP).

Bückle Ramírez, L.F. (1965) Untersuchungen über die Biologie von Heterotanais oerstendi Kroyer (Crustacea, Tanaidacea). *Zeitschrift für Morphologie und Ökologie der Tiere* 55, 714–782.

Clarke, A. & Gaston, K.J. (2006) Climate, energy and diversity. *Proceedings of the Royal Society B: Biological Sciences* 273, 2257–2266.

Corkum, L.D. & Cronin, D.J. (2004) Habitat complexity reduces aggression and enhances consumption in crayfish. *J Ethol* 22, 23–27.

Danovaro, R., Corinaldesi, C., Dell'Anno, A. & Snelgrove, P.V.R. (2017) The deep-sea under global change. *Current Biology* 27, R461–R465.

Danovaro, R., Gambi, C. & Della Croce, N. (2002) Meiofauna hotspot in the Atacama Trench, eastern South Pacific Ocean. *Deep-Sea Research Part I: Oceanographic Research Papers* 49, 843–857.

Danovaro, R., Snelgrove, P.V.R. & Tyler, P.A. (2014) Challenging the paradigms of deep-sea ecology. *Trends in Ecology and Evolution* 29, 465–475.

Delille, D., Guidi, L.D. & Soyer, J. (1985) Nutrition of Allotanais hirsutus (Crustacea: Tanaidacea) at Kerguelen Island. In: *Antarctic nutrient cycles and food webs.* , pp. 378–380.

Devey, C.W., Augustin, N., Brandt, A., Brenke, N., Köhler, J., Lins, L., Schmidt, C. & Yeo, I.A. (2018) Habitat characterization of the Vema Fracture Zone and Puerto Rico Trench. *Deep Sea Research Part II: Topical Studies in Oceanography* 148, 7–20.

Dojiri, M. & Sieg, J. (1997) Taxonomic atlas of the soft-bottom benthic fauna of the Santa Maria Basin and Western Santa Barbara Channel. In: *Taxonomica Atlas of the Soft-bottom Benthic Fauna of the Santa Maria Basin and Western Santa Barbara Channel.* , pp. 181–268.

Van Dover, C.L. (2000) *The ecology of deep-sea hydrothermal vents*. Princeton University Press.

Esquete, P. & Cunha, M.R. (2018) Additions to Tanaidomorpha (Crustacea:Tanaidacea) from mud volcanoes and coral mounds of the Gulf of Cadiz and Horseshoe Continental Rise. *Zootaxa* 4377, 517–541.

Etter, R.J., Boyle, E.E., Glazier, A., Jennings, R.M., Dutra, E. & Chase, M.R. (2011) Phylogeography of a pan-Atlantic abyssal protobranch bivalve: implications for evolution in the Deep Atlantic. *Molecular Ecology* 20, 829–843.

Etter, R.J., Rex, M.A., Chase, M.R. & Quattro, J.M. (2005) Population differentiation decreases with depth in deep-sea bivalves. *Evolution; international journal of organic evolution* 59, 1479–91.

Evans, K.L., Warren, P.H. & Gaston, K.J. (2005) Species-energy relationships at the macroecological scale: A review of the mechanisms. *Biological Reviews of the Cambridge Philosophical Society* 80, 1–25.

Faurby, S., Jørgensen, A., Kristensen, R.M. & Funch, P. (2011) Phylogeography of North Atlantic intertidal tardigrades: refugia, cryptic speciation and the history of the Mid-Atlantic Islands. *Journal of Biogeography* 38, 1613–1624.

Feller, R.J. (1980) Development of the sand-dwelling meiobenthic harpacticoid copepod huntemannia jadensis Poppe in the laboratory. *Journal of Experimental Marine Biology and Ecology* 46, 1–15.

Gage, J.D. & Tyler, P.A. (1991) 71 Journal of the Marine Biological Association of the United Kingdom *Deep-sea biology: a natural history of organisms at the deep-sea floor*. Cambridge University Press (CUP).

García-Herrero, Á., Sánchez, N., García-Gómez, G., Pardos, F. & Martínez, A. (2019) Two new stygophilic tanaidomorphs (Peracarida, Tanaidacea) from Canary Islands and southeastern Iberian Peninsula. *Marine Biodiversity* 49, 107–130.

Gellert, M. & Błażewicz, M. (2018) New species of Anarthruridae (Tanaidacea: Crustacea) of the western Australian slope. *Marine Biodiversity*.

Glover, A.G., Dahlgren, T.G., Taboada, S., Paterson, G.L.J., Wiklund, H., Waeschenbach, A., Cobley, A., Martinez Arbizu, P., Kaiser, S., Schnurr, S.M., Khodami, S., Raschka, U., Kersken, D., Stuckas, H., Menot, L., Bonifácio, P., Vanreusel, A., Macheriotou, L., Cunha, M.R., Hilário, A., Rodrigues, C., Colaço, A., Ribeiro, P.A., Błażewicz, M., Gooday, A.J.,

Jones, D.O.B., Billett, D., Goineau, A., Amon, D., Smith, C.R., Patel, T., McQuaid, K., Spickermann, R. & Brager, S. (2016) The London Workshop on the Biogeography and Connectivity of the Clarion-Clipperton Zone. *Research Ideas and Outcomes* 2, e10528.

Greve, L. (1965a) New records of some Tanaidacea (Crustacea) from the vicinity of Tromso. *The zoological department Tromso Museum* 27, 1–7.

Greve, L. (1965b) Tanaidacea from Trsndheimsfjorden. *Der Kongelige Norske Videnskabers Selskabs Forhandliger* 38, 140–143.

Greve, L. (1965c) The biology of some tanaidacea from raunefjorden, western norway. *Sarsia* 20, 43–54.

Gutu, M. (2006) New apseudomorph taxa (Crustacea, Tanaidacea) of the world ocean. *Curtea Veche*, 318pp.

Hansen, H.J. (1887) *Oversigt over de paa Dijmphna-Togtet indsamlede Krebsdyr.* Lütken, C.F., Dijmphna-Togtets Zoologisk-Botaniske Udbytte. I Kommission hos H. Hagerup, Kjøbenhavn.

Hansen, H.J. (1913) Crustacea Malacostraca. *The Danish Ingolf-Expedition* 3, 1–145.

Hassack, E. & Holdich, D.M. (1987) The tubicolous habit amongst the Tanaidacea (Crustacea, Peracarida) with particular reference to deep-sea species. *Zoologica Scripta* 16, 223–233.

Havermans, C., Sonet, G., d'Udekem d'Acoz, C., Nagy, Z.T., Martin, P., Brix, S., Riehl, T., Agrawal, S. & Held, C. (2013) Genetic and Morphological Divergences in the Cosmopolitan Deep-Sea Amphipod Eurythenes gryllus Reveal a Diverse Abyss and a Bipolar Species. *PLoS ONE* 8, e74218.

Hereu, B., Zabala, M., Linares, C. & Sala, E. (2005) The effects of predator abundance and habitat structural complexity on survival of juvenile sea urchins. *Marine Biology* 146, 293–299.

Hessler, R.R. & Jumars, P.A. (1974) Abyssal community analysis from replicate box cores in the central North Pacific. *Deep-Sea Research and Oceanographic Abstracts* 21, 246.

Hessler, R.R. & Sanders, H.L. (1967) Faunal diversity in the deep-sea. *Deep-Sea Research* 14, 65–78.

Highsmith, R.C. (1982) Induced Settlement and Metamorphosis of Sand Dollar (Dendraster Ecentricus) Larvae in Predator-Free sites: Adult Sand Dollar Beds. *Ecology* 63, 329–337.

Highsmith, R.C. (1985) Floating and algal rafting as potential dispersal mechanisms in brooding invertebrates. *Marine Ecology Progress Series* 25, 169–179.

Holdich, D.M. & Jones, J.A. (1983) The distribution and ecology of british shallow-water tanaid crustaceans (Peracarida, tanaidacea). *Journal of Natural History* 17, 157–183.

Ingram, C.L. & Hessler, R.R. (1987) Population biology of the deep-sea amphipod Eurythenes gryllus: inferences from instar analyses. *Deep Sea Research Part A, Oceanographic Research Papers* 34, 1889–1910.

Jakiel, A., Stępień, A. & Błażewicz, M. (2018) A tip of the iceberg—Pseudotanaidae (Tanaidacea) diversity in the North Atlantic. *Marine Biodiversity* 48, 859–895.

Jakiel, A., Stępień, A., Jóźwiak, P., Serigstad, B. & Błażewicz-Paszkowycz, M. (2015) First record of tanaidacea (Crustacea) from a deep-sea coral reef in the Gulf of Guinea. *Zootaxa* 3995, 203–228.

Jamieson, A.J., Fujii, T., Mayor, D.J., Solan, M. & Priede, I.G. (2010) Hadal trenches: the ecology of the deepest places on Earth. *Trends in Ecology and Evolution* 25, 190–197.

Jennings, R.M., Brix, S., Bober, S., Svavarsson, J. & Driskell, A. (2018) More diverse than expected: distributional patterns of Oecidiobranchus Hessler, 1970 (Isopoda, Asellota) on the Greenland-Iceland-Faeroe Ridge based on molecular markers. *Marine Biodiversity* 48, 845–857.

Jochumsen, K., Schnurr, S.M. & Quadfasel, D. (2016) Bottom temperature and salinity distribution and its variability around Iceland. *Deep Sea Research Part I: Oceanographic Research Papers* 111, 79–90.

Johannsen, N., Lins, L., Riehl, T. & Brandt, A. (2020) Changes in species composition of Haploniscidae (Crustacea: Isopoda) across potential barriers to dispersal in the Northwest Pacific. *Progress in Oceanography* 180.

Johnson, S.B. & Attramadal, Y.G. (1982a) A functional-morphological model of *Tanais cavolinii* milne-edwards (Crustacea, Tanaidacea) adapted to a

tubicolous life-strategy. *Sarsia* 67, 29–42.

Johnson, S.B. & Attramadal, Y.G. (1982b) A functional-morphological model of Tanais cavolinii milne-edwards (Crustacea, Tanaidacea) adapted to a tubicolous life-strategy. *Sarsia* 67, 29–42.

Jóźwiak, P. & Błażewicz-Paszkowycz, M. (2011) New records of the family Agathotanaidae (Crustacea: Tanaidacea) in the Antarctic, with remarks on Arthrura monacantha (Vanhöffen, 1914). *Zootaxa* 2785, 32–52.

Jumars, P.A. (1976) Deep-sea species diversity: does it have a characteristic scale? *Journal of Marine Research* 34, 217–246.

Jumars, P.A. & Hessler, R.R. (1976) Hadal community structure: implications from the Aleutian Trench. *Journal of Marine Research* 34, 547–560.

Just, J. (1970) *Decapoda, Mysidacea, Isopoda, and Tanaidacea from Jørgen Brønlund Fjord, North Greenland.* C.A. Reitzel.

Kaiser, S., Smith, C.R. & Arbizu, P.M. (2017) Editorial: Biodiversity of the Clarion Clipperton Fracture Zone. *Marine Biodiversity* 47, 259–264.

Koehl, M.A.. (1999) Ecological Biomechanics Of Benthic Organisms: Life History, Mechanical Design And Temporal Patterns Of Mechanical Stress. , 3469–3476.

Koslow, T. (2007) *The silent deep : the discovery, ecology and conservation of the deep sea*. University of Chicago Press.

Kudinova-Pasternak, R. (1991) Trofitcheskie grupy Tanaidacea (Crustacea, Peracarida). *Zoologicheskii Zhurnal* 70, 30–37.

Kudinova-Pasternak, R.K. (1966a) Tanaidacea (Crustacea) of the Pacific ultra-abyssals. *Zoologicheskii Zhurnal* 45, 518–535.

Kudinova-Pasternak, R.K. (1966b) Tanaidacea of the Pacific ultra-abyssals. *Crustaceana* 45, 518–534.

Kudinova-Pasternak, R.K. (1973) Tanaidacea (Crustacea, Malacostraca) collected on the R/V “Vitjas” in regions of the Aleutian Trench and Alaska. *Trudy Instituta Okeanologii, Akademiya Nauk SSSR* 91, 141–168.

Kudinova-Pasternak, R.K. (1975) Tanaidacea, Atlantic sector, Antarctic and subantarctic. *Akademiya Nauk SSSR* 103, 194–229.

Kudinova-Pasternak, R.K. (1978) Tanaidacea (Crustacea, Malacostraca) from the deep-sea trenches of the western part of the Pacific. *Trudy Instituta Okeanologii Akademii Nauk SSSR* 108, 115–135.

Lang, K. (1971a) Die Gattungen Agathotanais Hansen Und Paragatho-Tanais N. Gen. (Tanaidacea). *Crustaceana* 21, 57–71.

Lang, K. (1971b) Taxonomische und phylogenetische Untersuchungen über die Tanadaceen 6. Revision der Gattung *Paranarthrura* Hansen, 1913, und Aufstellung von zwei neuen Familien, vier neuen Gattungen und zwei neiien Arten. *Arkiv för Zoologi* 23, 361–401.

Lang, K. (1973) Taxonomische und phylogenetische Untersuchungen über die Tanaidaceen (Crustacea). *Zoologica Scripta* 2, 197–229.

Larsen, K. (2001) Morphological and molecular investigation of polymorphism and cryptic species in tanaid crustaceans: Implications for tanaid systematics and biodiversity estimates. *Zoological Journal of the Linnean Society* 131, 353–379.

Larsen, K. (2012) Tanaidacea (Peracarida) from macaronesia i. The deep-water fauna off the selvagen Islands, Portugal. *Crustaceana* 85, 571–589.

Larsen, K., Błażewicz-Paszkowycz, M. & Cunha, M.R. (2006) Tanaidacean (Crustacea: Peracarida) fauna from chemically reduced habitats - The Lucky Strike hydrothermal vent system, Mid-Atlantic Ridge. *Zootaxa* 36, 1–36.

Larsen, K. & Eds, M.S. (2007) Tanaidacea (Crustacea: Peracarida) from Japan III. the deep trenches; the Kurile-Kamchatka Trench and Japan Trench. *Zootaxa* 1599, 1–149.

Larsen, K., Gobardhan, S. & Zakir, A. (2013) Description of a new mangrove root dwelling species of *Teleotanais* (Crustacea:Peracarida:Tanaidacea) from India, with a Key to Teleotanaidae. *Species Diversity* 18, 237–243.

Larsen, K. & Shimomura, M. (2007) Foreword. *Zootaxa* 1599, 5–12.

Larsen, K. & Wilson, G.D.F. (2002) Tanaidacean phylogeny, the first step: The superfamily Paratanaidoidea. *Journal of Zoological Systematics and Evolutionary Research* 40, 205–222.

Leung, J.Y.S. (2015) Habitat heterogeneity affects ecological functions of macrobenthic communities in a mangrove: Implication for the impact of

restoration and afforestation. *Global Ecology and Conservation* 4, 423–433.

Levin, L.A. & Gage, J.D. (1998) Relationships between oxygen, organic matter and the diversity of bathyal macrofauna. *Deep-Sea Research Part II: Topical Studies in Oceanography* 45, 129–163.

Lilljeborg, W. (1864) Bidrag til kännedommen om de inom Sverige och Norrige förekommande Crustaceer af Isopodernas underordning och Tanaidernas familj. *Inbjudningsskrift till Åhörande af de Offentliga Föreläsninge* 1865, 1–31.

Logemann, K. (2013) The South Icelandic Current. , 1937–1938.

Lörz, A.N., Jazdzewska, A.M. & Brandt, A. (2018) A new predator connecting the abyssal with the hadal in the Kuril-Kamchatka Trench, NW Pacific. *PeerJ* 2018.

Malyutina, M. V, Brandt, A. & Ivin, V. V (2015) The Cruise Report *The Russian-German deep-sea expedition SokhoBio (Sea of Okhotsk Biodiversity Studies) to the Kurile Basin of the Sea of Okhotsk on board of the R/V Akademik MA Lavrentyev. 71st Cruise, July 6th-August 6th, 2015*.

Malyutina, M. V, Chernyshev, A. V. & Brandt, A. (2018a) Introduction to the SokhoBio (Sea of Okhotsk Biodiversity Studies) expedition 2015. *Deep-Sea Research Part II: Topical Studies in Oceanography* 154, 1–9.

Malyutina, M. V, Frutos, I. & Brandt, A. (2018b) Diversity and distribution of the deep-sea Atlantic Acanthocope (Crustacea, Isopoda, Munnopsidae), with description of two new species. *Deep-Sea Research Part II: Topical Studies in Oceanography* 148, 130–150.

Martinez Arbizu, P. & Haeckel, M. (2015) *EcoResponse Assessing the Ecology, Connectivity and Resilience of Polymetallic Nodule Field Systems*. GEOMAR Rep. Helmholtz-Zentrum für Ozeanforschung Kiel / Helmholtz Centre for Ocean Research Kiel, Kiel.

Martinez Arbizu, P. & Schminke, H.K. (2005) DIVA-1 expedition to the deep sea of the Angola Basin in 2000 and DIVA-1 workshop in 2003. In: *Organisms Diversity and Evolution*. , pp. 1–2.

McCallum, A.W., Woolley, S.N.C.C., Błażewicz-Paszkowycz, M., Browne, J., Gerken, S., Kloser, R., Poore, G.C.B., Staples, D.A., Syme, A., Taylor, J., Walker-Smith, G., Williams, A. & Wilson, R.S. (2015) Productivity

enhances benthic species richness along an oligotrophic Indian Ocean continental margin. *Global Ecology and Biogeography* 24, 462–471.

McClain, C.R. & Hardy, S.M. (2010) The dynamics of biogeographic ranges in the deep sea. *Proceedings of the Royal Society B: Biological Sciences* 277, 3533–3546.

Mikhailov, O. (1972) Some new data on the bottom relief of the Kuril–Kamchatka Trench. Faunao f the Kurile–Kamchatka Trench and Its Environment. 86, 75–79.

Mordasova, V.N. (1997) Some peculiarities of Chlorophyll distribution in the Sea of Okhotsk. *Oceanology* 37, 484–491.

Negoescu, I. & Svavarsson, J. (1997) Anthurideans (crustacea, isopoda) from the north atlantic and the arctic ocean. *Sarsia* 82, 159–202.

Oliver, J.S. & Slattery, P.N. (1985) Destruction and Opportunity on the Sea Floor: Effects of Gray Whale Feeding. *Ecology* 66, 1965–1975.

Pabis, K., Błażewicz-Paszkowycz, M., Jóźwiak, P. & Barnes, D.K.A. (2014) Tanaidacea of the Amundsen and Scotia seas: An unexplored diversity. *Antarctic Science* 27, 19–30.

Pabis, K., Jóźwiak, P., Lörz, A.-N., Schnabel, K.E. & Błażewicz-Paszkowycz, M. (2015) First insights into the deep-sea tanaidacean fauna of the Ross Sea: species richness and composition across the shelf break, slope and abyss. *Polar Biology* 38, 1429–1437.

Pape, E., van Oevelen, D., Moodley, L., Soetaert, K. & Vanreusel, A. (2013) Nematode feeding strategies and the fate of dissolved organic matter carbon in different deep-sea sedimentary environments. *Deep-Sea Research Part I: Oceanographic Research Papers* 80, 94–110.

Patel, T., Robert, H., D'Udekem D'Acoz, C., Martens, K., De Mesel, I., Degraer, S. & Schön, I. (2018) Biogeography and community structure of abyssal scavenging Amphipoda (Crustacea) in the Pacific Ocean. *Biogeosciences Discussions*, 1–36.

Poore, G.C.B., Avery, L., Błażewicz-Paszkowycz, M., Browne, J., Bruce, N.L., Gerken, S., Glasby, C., Greaves, E., McCallum, A.W., Staples, D.A., Syme, A., Taylor, J., Walker-Smith, G., Warne, M., Watson, C., Williams, A., Wilson, R.S. & Woolley, S.N.C.C. (2015) Invertebrate diversity of the unexplored marine western margin of Australia: taxonomy and

implications for global biodiversity. *Marine Biodiversity* 45, 271–286.

Ramirez-Llodra, E., Brandt, A., Danovaro, R., De Mol, B., Escobar, E., German, C.R., Levin, L.A., Martinez Arbizu, P., Menot, L., Buhl-Mortensen, P., Narayanaswamy, B.E., Smith, C.R., Tittensor, D.P., Tyler, P.A., Vanreusel, A. & Vecchione, M. (2010) Deep, diverse and definitely different: Unique attributes of the world's largest ecosystem. *Biogeosciences* 7, 2851–2899.

Ramirez-Llodra, E., Shank, T.M. & German, C.R. (2007) Biodiversity and biogeography of hydrothermal vent species: Thirty years of discovery and investigations. *Oceanography* 20, 30–41.

Rex, M.A. & Etter, R.J. (2010) 47 Choice Reviews Online *Deep-sea biodiversity: pattern and scale*. Harvard University Press, Cambridge, Massachusetts.

Riehl, T., Lins, L. & Brandt, A. (2018) The effects of depth, distance, and the Mid-Atlantic Ridge on genetic differentiation of abyssal and hadal isopods (Macrostylidae). *Deep-Sea Research Part II: Topical Studies in Oceanography* 148, 74–90.

Rishworth, G.M., Perissinotto, R. & Błażewicz, M. (2019) Sinelobus stromatoliticus sp. nov. (Peracarida: Tanaidacea) found within extant peritidal stromatolites. *Marine Biodiversity* 49, 783–794.

Sanders, H.L. Marine Benthic Diversity: A Comparative Study. *The American Naturalist* 102, 243–282.

Sars, G.O. (1882) Revision af gruppen: Isopoda Chelifera med charakteristik af nye herhen hørende arter og slægter. *Archiv for Mathematik og Naturvidenskab* 7, 1–54.

Sars, G.O. (1886) Crustacea. II. *Norwegian North Atlantic Expedition, 1876-1878*, 1–96.

Schnurr, S.M., Brandt, A., Brix, S., Fiorentino, D., Malyutina, M. V & Svavarsson, J. (2014) Composition and distribution of selected munnopsid genera (Crustacea, Isopoda, Asellota) in Icelandic waters. *Deep Sea Research Part I: Oceanographic Research Papers* 84, 142–155.

Schnurr, S.M., Osborn, K.J., Malyutina, M. V, Jennings, R.M., Brix, S., Driskell, A., Svavarsson, J. & Martinez Arbizu, P. (2018) Hidden diversity in two species complexes of munnopsid isopods (Crustacea) at the

transition between the northernmost North Atlantic and the Nordic Seas. *Marine Biodiversity* 48, 813–843.

Shino, S.M. & Shiino, S.M. (1978) Tanaidacea collected by French Scientists on board the survey ship “Marion-Dufresne” in the regions around the Kerguelen Islands and other subantarctic islands in 1972, ’74, ’75, ’76. *Science Report of Shima Marineland.* 5, 1–122.

Shirayama, Y. (1984) Vertical-distribution of meiobenthos in the sediment profile in bathyal, abyssal and hadal deep-sea systems of the western pacific. , 123–129.

Sieg, J. (1973) Zum Problem Der Herstellung Von Dauerpraparaten Von Klein-Crustaceen, Insbesondere Von Typusexemplaren. *Crustaceana* 25, 222–224.

Sieg, J. (1976a) Taxonomische Monographie der Pseudotanaidae (Crustacea, Tanaidacea). *Metteilungens aus dem Zoologischen Mueseum in Berlin* 53, 1–109.

Sieg, J. (1976b) To the natural system of Dikonophora Lang (Crustacea, Tanaidacea). *Crustaceana Monographs* 35, 119–133.

Sieg, J. (1977) Taxonomische Monographie der Familie Pseudotanaidae (Crustacea, Tanaidacea). *Mitteilungen aus dem Museum für Naturkunde in Berlin. Zoologisches Museum und Institut für Spezielle Zoologie (Berlin)* 53, 3–109.

Sieg, J. (1980) Revision der gattung Nototanais Richardson, 1906 (Crustacea, Tanaidacea). *Mitteilungen aus dem Zoologischen Museum in Berlin* 56, 44–70.

Sieg, J. (1984) Neue Erkenntnisse zum System der Tanaidacea. *Eine phylogenetische Studie,* 100-105,126-132.

Sieg, J. (1986) *Crustacea Tanaidacea of the Antarctic and the Subantarctic - part I.*

Sieg, J. & Heard, R.W. (1988) Tanaidacea (Crustacea: Peracarida) of the Gulf of Mexico. V: The family Pseudotanaidae from less than 200 meters, with the description of Pseudotanais mexikolpos, n. sp. and a key to the known genera and species of the world. *Proceedings of the Biological Society of Washington* 101, 39–59.

Siewing, R. (1953) Morphologische Untersuchungen anTanaidaceen und Lophogastriden. *Zeitschrift fu¨r wis-senschaftliche Zoologie* 157, 333–426.

Simon-Lledó, E., Bett, B.J., Huvenne, V.A.I., Schoening, T., Benoist, N.M.A., Jeffreys, R.M., Durden, J.M. & Jones, D.O.B. (2019) Megafaunal variation in the abyssal landscape of the Clarion Clipperton Zone. *Progress in Oceanography* 170, 119–133.

Singh, R., Miljutin, D.M., Vanreusel, A., Radziejewska, T., Miljutina, M.M., Tchesunov, A., Bussau, C., Galtsova, V. & Martinez Arbizu, P. (2016) Nematode communities inhabiting the soft deep-sea sediment in polymetallic nodule fields: do they differ from those in the nodule-free abyssal areas? *Marine Biology Research* 12, 345–359.

De Smet, B., Pape, E., Riehl, T., Bonifácio, P., Colson, L. & Vanreusel, A. (2017) The Community Structure of Deep-Sea Macrofauna Associated with Polymetallic Nodules in the Eastern Part of the Clarion-Clipperton Fracture Zone. *Frontiers in Marine Science* 4, 103.

Smith, C.R., Drazen, J. & Mincks, S.L. (2006a) Deep-sea Biodiversity and Biogeography: Perspectives from the Abyss Nature of the abyssal habitat. *International Seabed Authority Seamount Biodiversity Symposium*, 1–13.

Smith, K.L. (1985) Macrozooplankton of a deep sea hydrothermal vent: In situ rates of oxygen consumption. *Limnology and Oceanography* 30, 102–110.

Smith, K.L., Baldwin, R.J. & Williams, P.M. (1992) Reconciling particulate organic carbon flux and sediment community oxygen consumption in the deep North Pacific. *Nature* 359, 313–316.

Smith, V.H., Joye, S.B. & Howarth, R.W. (2006b) Eutrophication of freshwater and marine ecosystems. *Limnology and Oceanography* 51, 351–355.

Stephensen, K. (1937) Marine Isopoda and Tanaidacea. The Zoology of Iceland. In: F. and S. L. Tmen (Ed), *The Zoology of Iceland III. pART 27*. Copenhagen and Reykjavik . 1937, pp. 26.

Stępień, A., Pabis, K. & Błażewicz, M. (2019) Tanaidacean faunas of the Sea of Okhotsk and northern slope of the Kuril-Kamchatka Trench. *Progress in Oceanography* 178, 102196.

Stransky, B. & Svavarsson, J. (2010) Diversity and species composition of

peracarids (Crustacea: Malacostraca) on the South Greenland shelf: Spatial and temporal variation. *Polar Biology* 33, 125–139.

Taboada, S., Riesgo, A., Wiklund, H., Paterson, G.L.J., Koutsouveli, V., Santodomingo, N., Dale, A.C., Smith, C.R., Jones, D.O.B., Dahlgren, T.G. & Glover, A.G. (2018) Implications of population connectivity studies for the design of marine protected areas in the deep sea: An example of a demosponge from the Clarion-Clipperton Zone. *Molecular Ecology*.

Tews, J., Brose, U., Grimm, V., Tielbörger, K., Wichmann, M.C., Schwager, M. & Jeltsch, F. (2004) Animal species diversity driven by habitat heterogeneity/diversity: the importance of keystone structures. *Journal of Biogeography* 31, 79–92.

Thistle, D. (2003) The deep-sea floor: an overview. *Ecosystems of the world, Ecosystems of the Deep Oceans*, 5–38.

Tittensor, D.P., Rex, M.A., Stuart, C.T., McClain, C.R. & Smith, C.R. (2011) Species-energy relationships in deep-sea molluscs. *Biology Letters* 7, 718–722.

Tyler, R.H., Maus, S. & Lühr, H. (2003) Satellite observations of magnetic fields due to ocean tidal flow. *Science* 299, 239–241.

VanHöffen, E. (1907) *Crustaceans from the small Karajak fjord in West Greenland*. universities zoological museum komenhavn, Krajak-fjord.

VanHöffen, E. (1914) *Die Isopoden der Deutschen Sdpolar-Expedition, 1901-1903*. G. Reimer, Berlin : Available from: http://www.biodiversitylibrary.org/bibliography/10649 (February 2, 2020).

Vanreusel, A., Fonseca, G., Danovaro, R., Da Silva, M.C., Esteves, A.M., Ferrero, T., Gad, G., Galtsova, V., Gambi, C., Da Fonsêca Genevois, V., Ingels, J., Ingole, B., Lampadariou, N., Merckx, B., Miljutin, D., Miljutina, M., Muthumbi, A., Netto, S., Portnova, D., Radziejewska, T., Raes, M., Tchesunov, A., Vanaverbeke, J., Van Gaever, S., Venekey, V., Bezerra, T.N., Flint, H., Copley, J., Pape, E., Zeppilli, D., Martinez, P.A. & Galeron, J. (2010) The contribution of deep-sea macrohabitat heterogeneity to global nematode diversity. *Marine Ecology* 31, 6–20.

Wedding, L.M., Friedlander, A.M., Kittinger, J.N., Watling, L., Gaines, S.D., Bennett, M., Hardy, S.M. & Smith, C.R. (2013) From principles to practice: A spatial approach to systematic conservation planning in the deep sea. *Proceedings of the Royal Society B: Biological Sciences* 280.

Wedding, L.M., Reiter, S.M., Smith, C.R., Gjerde, K.M., Kittinger, J.N., Friedlander, A.M., Gaines, S.D., Clark, M.R., Thurnherr, A.M., Hardy, S.M. & Crowder, L.B. (2015) Managing mining of the deep seabed: Contracts are being granted, but protections are lagging. *Science* 349, 144–145.

Wefer, G. (2003) *Ocean margin systems*. Springer.

Weisshappel, J.B. (2000) Distribution and diversity of the hyperbenthic amphipod family Eusiridae in the different seas around the Greenland-Iceland-Faeroe-Ridge. *Sarsia* 85, 227–236.

Weisshappel, J.B. (2001) Distribution and diversity of the hyperbenthic amphipod family Calliopiidae in the different seas around the Greenland-Iceland-Faeroe-Ridge. *Sarsia* 86, 143–151.

West, A.J., Lin, C.W., Lin, T.C., Hilton, R.G., Liu, S.H., Chang, C.T., Lin, K.C., Galy, A., Sparkes, R.B. & Hovius, N. (2011) Mobilization and transport of coarse woody debris to the oceans triggered by an extreme tropical storm. *Limnology and Oceanography* 56, 77–85.

Wilson, G.D.F. (1987) Crustacean communities of the manganese nodule province (Domes Site A compared with Domes site C). *Report for the National Ocanic....* 0030, 1–43.

Włodarska-Kowalczuk, M., Kukliński, P., Ronowicz, M., Legeżyńska, J. & Gromisz, S. (2009) Assessing species richness of macrofauna associated with macroalgae in Arctic kelp forests (hornsund, svalbard). *Polar Biology* 32, 897–905.

Wolff, T. (1977) Diversity and faunal composition of the deep-sea benthos. *Nature* 267, 780–785.

Woolley, S.N.C.C., Tittensor, D.P., Dunstan, P.K., Guillera-Arroita, G., Lahoz-Monfort, J.J., Wintle, B.A., Worm, B. & O'Hara, T.D. (2016) Deep-sea diversity patterns are shaped by energy availability. *Nature* 533, 393–396.

Wright, S. (1943) Isolation by Distance. *Genetics* 28.

Chapter 2: A tip of the iceberg—Pseudotanaidae (Tanaidacea) diversity in the North Atlantic

A tip of the iceberg—Pseudotanaidae (Tanaidacea) diversity in the North Atlantic

Aleksandra Jakiel, Anna Stępień & Magdalena Błażewicz

Marine Biodiversity

ISSN 1867-1616
Volume 48
Number 2

Mar Biodiv (2018) 48:859-895
DOI 10.1007/s12526-018-0881-x

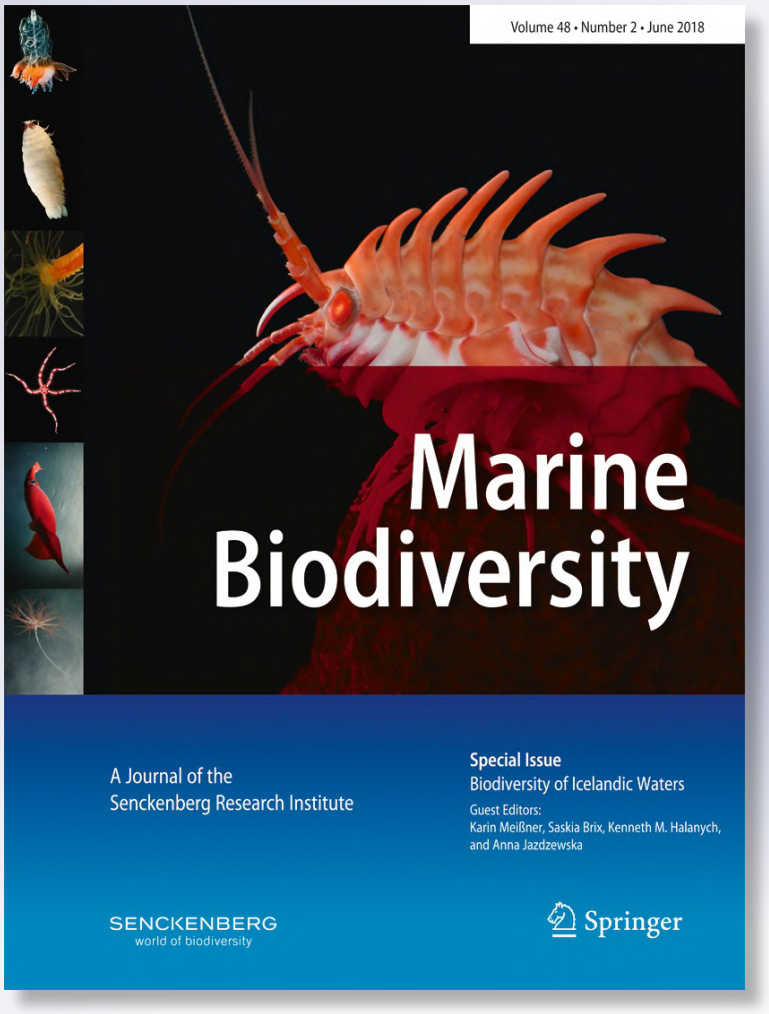

Springer

Marine Biodiversity (2018) 48:859–895
https://doi.org/10.1007/s12526-018-0881-x

SENCKENBERG

BIODIVERSITY OF ICELANDIC WATERS

A tip of the iceberg—Pseudotanaidae (Tanaidacea) diversity in the North Atlantic

Aleksandra Jakiel[1] · Anna Stępień[1] · Magdalena Błażewicz[1]

Received: 13 October 2017 / Revised: 20 March 2018 / Accepted: 21 March 2018 / Published online: 3 May 2018

Abstract

During two IceAGE expeditions, a large collection of Tanaidacea was gathered from the shelf down to the slope (213–2750 m) in six areas off Iceland—the Irminger Basin, the Iceland Basin, the Norwegian Sea, the Denmark Strait, the Iceland-Faroe Ridge, and the Norwegian Channel. In this collection, members of the family Pseudotanaidae were most numerous component. We examined 40 samples collected with different gears (e.g., EBS, VVG. GKG), in which 323 pseudotanaid individuals were counted and covered a total depth from 213.9 to 2746.4 m. Morphological identification of the material has revealed the presence of five species: *Akanthinotanais* cf. *longipes*, *Mystriocentrus biho* sp. n. *Pseudotanais misericorde* sp. n., *P. svavarssoni* sp. n., and *P. sigrunis* sp. n. The description of the four new species has been presented in the paper and a rank of the subgenus *Akanthinotanais* is elevated to a genus rank. A large group of morphologically almost identical specimens, similar with *P. svavarssoni* sp. n. from a wide depth range and from various areas off Iceland was discriminated to species by applying morphometric methods; one distinct species (*P. svavarssoni* sp. n.) and complex of presumably cryptic species the species was discovered. Based on current data and literature records, similarity among fauna of Pseudotanaidae was assessed with applying Bray–Curtis formula. As results, potential zoogeographic regions in the North Atlantic have been distinguished.

Keywords Tanaidacea · Pseudotanaidae · *Pseudotanais* · *Mystriocentrus* · *Akanthinotanais* · New species · Zoogeography IceAGE · Iceland · North Atlantic

Introduction

Iceland is located at the junction of the Mid-Atlantic Ridge and Greenland–Scotland Ridge (Logemann et al. 2013.) The submarine ridges play an essential role in the oceanic circulation and distribution of water masses, and hence, in the distribution of marine fauna (Asthorsson et al. 2007; Brix and Svavarsson 2010; Schnurr et al. 2014). The Greenland–Scotland Ridge hampers the interaction between two water masses: the warm water originated in the southern part of North Atlantic, and the polar water from the Arctic Ocean (Logemann et al. 2013; Jochumsen et al. 2016). The warm and saline Atlantic water flows northwards in the near-surface layer via the Reykjanes Ridge, to continue northernmost as the North Icelandic Irminger Current north-west of Iceland, and over the Iceland-Faroe Ridge east of Iceland (Asthorsson et al. 2007). The cold Arctic water is transported south, partly in the near-surface layer along the Greenland coast (the East Greenland Current), and in part as a bottom current carrying a very cold and dense water from the Nordic Sea down to the south off Iceland (Perkins et al. 1998; Hansen and Osterhus 2000). Since the water masses below the threshold of the Ridge are separated (Jochumsen et al. 2016), biological processes and species composition of faunas in basins located on both sides of the Ridge are thought to be different (Gislason and Astthorsson 2004; Astthorsson et al. 2007).

The specific oceanography of waters surrounding Iceland renders the region an important field laboratory in which to investigate diversity, distribution, and migration of the marine

This article is registered in ZooBank under: urn:lsid:zoobank.org:pub:F65EDFAB-7032-44B2-9484-06EDD56B87D8.

This article is part of the Topical Collection on Biodiversity of Icelandic Waters by Karin Meißner, Saskia Brix, Ken M. Halanych and Anna Jazdzewska.

Communicated by S. Brix

✉ Aleksandra Jakiel
aleksandrajakiel@wp.pl

[1] Department of Invertebrate Zoology and Hydrobiology, University of Łódź, Banacha 12/16, 90-237 Łódź, Poland

fauna. The Icelandic marine Animals Genetic and Ecology (IceAGE) project aimed to understand how underwater physical structures (e.g., submerged ridges) and non-physical barriers (e.g., currents, temperature, salinity) affect the distribution of benthic organisms (Brix et al. 2014). Traditional taxonomic methods as well as modern approaches to biodiversity research (ecological modeling and molecular species discrimination) have been studied for such groups as Isopoda, Tanaidacea, Ophiuroidea, and Mollusca (Brix, 2011; Błażewicz-Paszkowycz et al. 2014; Khodami et al. 2014; Mikkelsen and Todt 2014; Schnurr and Malyutina 2014; Todt and Kocot 2014). Benthic samples collected from an extensive depth range (117−2750 m), at different localities around Iceland, providing an opportunity to test if, and to what extent, topographic and oceanographic barriers (i.e., ridges, currents) influence the distribution, community structure, and diversity of benthic organisms.

The Tanaidacea (Peracarida, Malacostraca) are small marine crustaceans commonly occurring in diverse benthic habitats. As they are brooders and have no planktonic larvae, their mobility is low, and thus their dispersal ability is considered to be limited (Błażewicz-Paszkowycz et al. 2012, 2014). Tanaids may reach high densities (Larsen 2005); under specific environmental conditions (i.e., depth), they were found to be more abundant than amphipods, isopods, or mysids (Bamber 2005). Although the interest in the tanaidacean fauna has been observed to increase during the last decade (e.g., Bamber 2012; Błażewicz-Paszkowycz et al. 2013; Drumm and Bird 2016), the taxon still remains inadequately known. Over 1300 of the species described so far represent some 2–3% of their estimated diversity (Błażewicz-Paszkowycz et al. 2012).

The IceAGE cruises carried out in 2011 and 2013 (Brix et al. 2013) provided an opportunity to obtain a large collection of tanaidaceans and the family Pseudotanaidae Sieg, 1976 accounted for a substantial part of it (unpublished data of the authors). The family is widespread in the world's ocean, and its members being encountered within a wide depth range: from 0.5 to over 7000 m (Bird and Holdich 1989a; Błażewicz-Paszkowycz et al., 2012; Pabis et al. 2015). Pseudotanaids have been reported from different habitats, e.g., hard bottom, algae, coral reefs, cold seeps, mud volcanos, and hydrothermal vents (Bird 1999; Błażewicz-Paszkowycz and Bamber 2011; Larsen, 2012; Stępień unpublished data).

So far, 51 species have been described and 21 species have been recorded in the North Atlantic (Fig. 2). Lilljeborg (1864) was the first to report on pseudotanaids, although the family would be established in 1976 by Sieg (1976). Lilljeborg described *Pseudotanais forcipatus* (Lilljeborg 1864) as *Tanais forcipatus* from the Swedish coast. Almost 20 years later, Sars (1882) erected the genus *Pseudotanais* and synonymized the species of Lilljeborg. Moreover, the list of North Atlantic pseudotanaids was supplemented by records of *P. macrocheles* Sars, 1882 and *P. lilljeborgi* Sars, 1882 from the Norwegian coast (Sars 1882) and *P. affinis* Hansen, 1887 from the Kara Sea (Hansen 1887). Hansen (1913) added new records of the previously known species and described three new species (*P. abyssi* Hansen, 1913; *P. oculatus* Hansen, 1913, and *P. longipes* Hansen, 1913) from off Iceland and Greenland. The wide distribution of those species in arctic, subarctic, and boreal regions was subsequently reported by numerous authors (e.g., Sars 1896; Greve 1965a, b, c: along the Norwegian coast; Stephensoen 1937: off Greenland, Iceland, and Faroe). The number of pseudotanaid species known in the North Atlantic remained unchanged for the next 60 years until two further species (*P. jonesi* Sieg, 1977, *P. similis* Sieg, 1977) were described by Sieg from the Bay of Biscay (Sieg 1977). Furthermore Sieg (1977) proposed splitting genus *Pseudotanais* to two subgenera: *Akanthinotanais* (*A.*) and *Pseudotanais* (*P.*).

In a series of papers describing results of BIOGAS, GASCOR, and EPI VI programmes, Bird and Holdich (1985, 1989a, b) highlighted the high biodiversity of pseudotanaids in the depth range of 1100–4800 m in the North Atlantic, mainly west of Great Britain and in the Bay of Biscay. They erected two new genera—*Mystriocentrus* Bird and Holdich, 1989a and Parapseudotanais Bird and Holdich, 1989b, and described eleven species, namely *Mystriocentrus serratus* Bird and Holdich, 1989a; *Parapseudotanais abyssalis* Bird and Holdich, 1989b; *Pseudotanais* (*P.*) *corollatus* Bird and Holdich, 1989a; *P.* (*P.*) *colonus* Bird and Holdich, 1989b; *P.* (*P*) *denticulatus* Bird and Holdich, 1989a; *P.* (*P.*) *falcicula* Bird and Holdich, 1989b; *P.* (*P*) *longispinus* Bird and Holdich, 1989a; *P.* (*P.*) *scalpellum* Bird and Holdich, 1989b; *P.* (*P.*) *spatula* Bird and Holdich, 1989a; *P.* (*P.*) *spicatus* Bird and Holdich, 1989b; and *P.* (*P.*) *vulsella* Bird and Holdich, 1989a. Finally, one more species, *P.* (*P.*) *falcifer* Błażewicz-Paszkowycz and Bamber, 2011 from a mud volcano off Norway, was added to the list (Błażewicz-Paszkowycz and Bamber 2011).

Our aims in this work were to (1) assess, based on literature data and new records from the IceAGE project, the diversity and distribution of the Pseudotanaidae in the North Atlantic, understood as the area north of 40° N (Dinter 2001); (2) describe new species belonging to the family; and (3) based on current data and literature records to assess the similarity among fauna of Pseudotanaidae in various region of The North Atlantic to pinpoint potential zoogeographic regions.

While working on the IceAGE collection, we found a large group of morphologically almost identical specimens from all the basins off Iceland where the samples were collected (the Iceland and Irminger Basins, Denmark Strait, Norwegian Sea, Iceland-Faroe Ridge and the Faroe-Shetland Channel) from a wide depth range. Considering the low mobility of the Tanaidacea (they are tube-building brooders without planktonic stage) and the presence of geographic barriers around Iceland (i.e., submarine ridges, a complex current system), we hypothesize that those morphologically almost identical

individuals found in different environmental regimes are distinct species. To test the hypothesis, we attempted to discriminate between the species (which are presumably a cryptic species complex) using a morphometric approach.

Study area

Iceland lies at the junction of the Mid-Atlantic Ridge (MAR) and the Greenland–Scotland Ridge (GSR) (Logemann et al. 2013). As a result of the topography, the oceanic area around Iceland is divided into four basins (Fig. 1). The Iceland and Irminger Basins, located south of the island to the east and west, respectively, are separated by the Reykjanes Ridge, an extension of MAR (Malmberg and Valdimarsson 2003). The two basins are bounded by the Greenland–Iceland Sill (Denmark Strait) to the west and by the Iceland–Faroe Ridge to the East (Malmberg and Valdimarsson 2003). The northern and north-eastern basins are the Iceland Sea and the Norwegian Sea, respectively (Malmberg and Valdimarsson 2003), the former being split into two parts by the Kolbeinsey Ridge.

The area south of Iceland is primarily affected by the Atlantic water masses (Fig. 1). The southern and south-eastern shelf is bathed by the South Icelandic Current (SIC) that flows north and north-east and transports the Modified North Atlantic Water (MNAW). Upon reaching the Faroe-Shetland Ridge, SIC turns to the south-east to flow along the ridge and to open out into the Faroe Current. The south-eastern Icelandic slope (at a depth of 500–1100 m) is bathed by the anticlockwise current, made up by the Norwegian Sea Deep Water (NSDW) (Malmberg and Valdimarsson 2003). This water mass, called here the Iceland–Scotland Overflow Water (ISOW), crosses the Iceland–Faroe Ridge, passes the Iceland Basin, and continues into the Irminger Basin (Meißner et al. 2014).

The deep part (deeper than 1500 m) of the Irminger Basin is affected by ISOW as well as by the Denmark Strait Overflow Water (DSOW), which passes though the Denmark Strait and flows south along the Greenland slope) and the Labrador Sea Water (formed in the Labrador Sea) (Malmberg 2004; Meißner et al. 2014) (Fig. 1). The shallower part of the Basin remains under the influence of the Irminger Current (IC), which transports MNAW along the Reykjanes Ridge. IC flows north along the slope (Logemann et al. 2013). Upon reaching the Denmark Strait, IC turns south to flow along the Greenland slope.

The Denmark Strait is, in part, affected by MNAW transported by an IC branch, the North Icelandic-Irminger Current (NIIC) flowing north along the Icelandic shelf edge (Meißner et al. 2014). A cold-water mass [i.e., the Arctic Polar Water (APW, DSOW)] flows along the East Greenland shelf and slope.

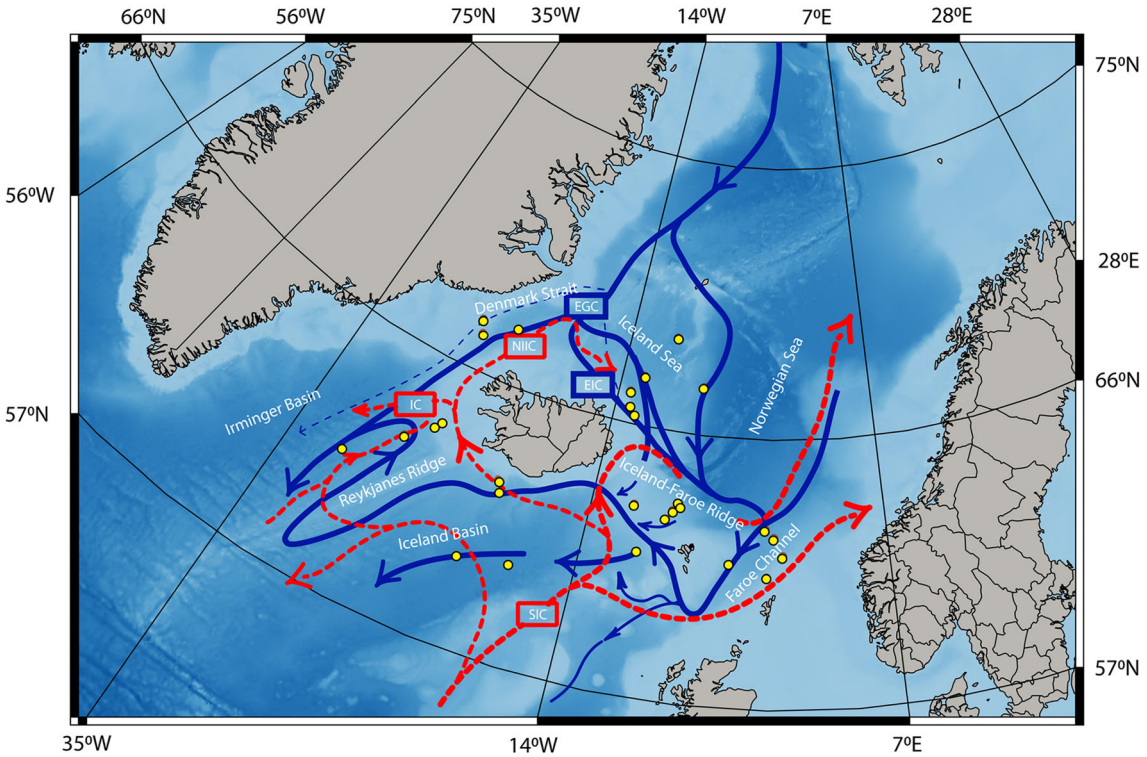

Fig. 1 Study area and location of sampling station (yellow dots) in the N Atlantic during IceAGE expeditions. Red lines: warm currents (branches of North Atlantic Current); blue lines: cold currents of arctic origin; dashed lines: surface currents; not-dashed lines: deep sea current. *EGC* East Greenland Curent, *EIC* East Icelandic Current, *IC* Irminger Current, *NIIC* North Icelandic Irminger Current, *SIC* South Icelandic Current; after Hansen and Osterhus (2000) and Ostmann et al. (2014)

The north and north-eastern areas experience mixing of several water masses (Meißner et al. 2014). NICC transports the Atlantic water which loses heat here. In addition, shallow areas are affected by the Norwegian Sea Arctic Intermediate Water, deeper parts being influenced by NSDW (Fig. 1). East of the Kolbeinsey Ridge, NIIC and the Arctic Water form the East Icelandic Current (EIC) which bathes the north-eastern continental slope to eventually reach the northern flank of the Iceland-Faroe Ridge. EIC is underlain by the North Icelandic Jet, a cold undercurrent which flows west, within the depth range of 200–1000 m, to cross the Kolbeinsey Ridge and reach the northern part of the Denmark Strait.

Material and methods

Samples

This study is based on the pseudotanaid collection obtained during two (2011 and 2013) IceAGE cruises on board the RVs *Meteor* and *Poseidon* (Brix et al. 2014). The samples were collected from the shelf down to the slope (213–2750 m) in six areas off Iceland, henceforth referred to as "basins": the Irminger Basin, the Iceland Basin, the Norwegian Sea, the Denmark Strait, the Iceland-Faroe Ridge, and the Norwegian Channel (Fig. 1).

The pseudotanaid material was obtained with different sampling devices: a Van Veen grab (VV), a Shipek grab (SG), a box corer (GKG), and an epibenthic sledge (EBS). It was sieved (500 μm mesh size) using chilled seawater, and preserved in 4% formaldehyde for morphological research; some individuals were fixed in pre-cooled 96% undenaturated ethanol for molecular analyses (Riehl et al. 2014). For the purpose of this work, the formaldehyde-treated samples were used only.

A total of 40 samples were examined, which yielded 323 pseudotanaid individuals. Four samples were collected in the Iceland Basin, 6 in the Irminger Basin, 6 in the Denmark Strait, 11 in the Norwegian Sea, 5 in the Norwegian Channel, and 8 off the Iceland-Faroe Ridge (Table 1).

Taxonomic description

Representative females were dissected using chemically sharpened tungsten needles; appendages were mounted in glycerine on slides. Working drawings were prepared using a microscope equipped with a *camera lucida*; the publication-quality illustrations were prepared using a digital tablet and Illustrator software (Coleman 2003). The morphological terminology follows that proposed by Błażewicz-Paszkowycz and Bamber (2011). The spatulate setae mentioned by Bird and Holdich (1989a, b) are referred to as the sensory setae here.

The material has been deposited in the Universität Hamburg Zoological Museum Center of Natural History (CeNak) (Germany) (Table 2).

Measurements

We applied a morphometric analysis to strengthen the identification of the most numerous and widely distributed circum-Icelandic species of the genus *Pseudotanais* (described as *P. svavarssoni*, sp. n. see below). Ovigerous females and neutri individuals (similar in size to ovigerous females) from each basin, with unbroken appendages and a complete blade-like spine, were selected for the analysis (Table 3).

The measurements were made with a camera connected to the microscope (Nikon Eclipse Ci-L) and NIS-Elements View software (www.nikoninstruments.com). The body width and the length of the carapace, pereonites, pleonites, and pleotelson were measured on whole specimens. The length was measured along the axis of symmetry, whereas the width, perpendicular to the axis of symmetry, at the widest spot. As the pseudotanaid pleotelson is usually curved, it was often impossible to observe on a slide; therefore, instead of measuring the total body length, we took three measurements (i.e., the lengths of the carapace, total pereonites, and five pleonites). Thus, the body length is a sum of lengths of all the body segments without the pleotelson.

Appendages were measured (length and width) by measuring their articles on dissected specimens. A total of 173 characters and 29 specimens from four different "populations" (with respect to regions and depth: "*population 1*" (P1) from the deep (~2000 m) part of the Norwegian Sea; "*population 2*" (P2) from the deep (~1300–1500 m) part of the southern basins: the Iceland and Irminger; "*population 3*" (P3) from the shallow (~200 m) part of the southern Irminger Basin; and "*population 4*" (P4) from the shallow (~400–600 m) part of the Iceland–Scotland Ridge (the Iceland–Faroe Ridge and the Norwegian Channel) was measured. For the statistical analysis, the following 42 characters/ratios were used:

(1) The combined carapace, pereonite, and pleonite length (CPP)
(2) The CPP to carapace length ratio
(3) The CPP to pereonite-1 length ratio
(4) The CPP to pereonite-2 length ratio
(5) The CPP to pereonite-3 length ratio
(6) Length of CPP to pereonite-4 length
(7) Length of CPP to pereonite-5 length
(8) The CPP to pereonite-6 length ratio
(9) The combined pleonite length to pleon width ratio
(10) The antennule to carapace length ratio
(11) The antennule to antennule article-1 length ratio
(12) The antennule ariticle-3 to article-2 length ratio
(13) The antenna article-2 to article-2 distal spine length ratio

Table 1 Main characteristics of the sampling stations where Pseudotanaidae species were collected during IceAge cruises (according to Brix et al. 2012); (*EBS* epibenthic sledge, *GKG* box corer, *SG* Shipek grab, *VV* Van Veen grab)

Cruise	Area	Station	Gear	Date	Latitude [N]	Longitude [W]	Depth [m]	Temperature [°C]	Salinity	Oxygen [μmol/kg]
IceAge I	Iceland Basin	963-1	EBS	28.08.2011	60° 02.73′	21° 29.86′	2746.4	2.65	34.99	258.38
IceAge I	Iceland Basin	979-1	EBS	30.08.2011	60° 21.48′	18° 08.24′	2567.6	2.65	34.99	258.38
IceAge I	Iceland Basin	1010-1	EBS	02.09.2011	62° 33.10′	20° 23.71′	1384.8	3.88	35.02	254.57
IceAge I	Iceland Basin	1019-1	EBS	03.09.2011	62° 56.32′	20° 44.61′	913.6	5.29	35.08	242.79
IceAge I	Irminger Basin	1043-1	EBS	05.09.2011	63° 55.46′	25° 57.66′	213.9	7.42	35.19	246.74
IceAge I	Irminger Basin	1051-1	GKG	07.09.2011	61° 37.41′	31° 22.11′	2538.9	3.16	34.94	254.17
IceAge I	Irminger Basin	1054-1	EBS	07.09.2011	61° 36.19′	31° 22.60′	2537.3	3.16	34.94	254.17
IceAge I	Irminger Basin	1066	GKG	08.09.2011	62° 59.97′	28° 04.78′	1621.8	4.28	34.99	245.53
IceAge I	Irminger Basin	1072-1	EBS	08.09.2011	63° 00.46′	28° 04.09′	1593.8	4.28	34.99	245.53
IceAge I	Irminger Basin	1086-1	EBS	09.09.2011	63° 42.53′	26° 23.05′	698.1	6.19	35.09	231.52
IceAge I	Denmark Strait	1116-1	GKG	14.09.2011	67° 12.82′	26° 16.31′	683.1	0.07	34.90	292.96
IceAge I	Denmark Strait	1129-1	GKG	14.09.2011	67° 38.77′	26° 44.78′	320.6	0.70	34.62	290.90
IceAge I	Denmark Strait	1132-1	EBS	14.09.2011	67° 38.48′	26° 45.28′	318.1	0.70	34.62	290.90
IceAge I	Denmark Strait	1136-1	EBS	14.09.2011	67° 38.15′	26° 45.99′	315.9	0.70	34.62	290.90
IceAge I	Denmark Strait	1141-1	GKG	15.09.2011	67° 50.22′	23° 42.11′	1241.6	−0.66	34.91	278.77
IceAge I	Denmark Strait	1148-1	EBS	15.09.2011	67° 50.79′	23° 41.76′	1248.8	−0.66	34.91	278.77
IceAge I	Norwegian Sea	1178-1	GKG	20.09.2011	67° 38.71′	12° 10.10′	1818.8	−0.85	34.91	1818.80
IceAge I	Norwegian Sea	1152-1	GKG	17.09.2011	69° 05.60′	09° 56.01′	2172.6	−0.75	34.91	266.74
IceAge I	Norwegian Sea	1155-1	EBS	17.09.2011	69° 06.89′	09° 54.72′	2203.8	−0.75	34.91	266.74
IceAge I	Norwegian Sea	1159-1	EBS	17.09.2011	69° 06.66′	09° 55.02′	2202.8	−0.75	34.91	266.74
IceAge I	Norwegian Sea	1166-1	GKG	19.09.2011	67° 35.28′	06° 57.47′	2401.8	−0.82	34.91	271.26
IceAge I	Norwegian Sea	1168-1	EBS	19.09.2011	67° 36.38′	07° 00.08′	2372.6	−0.82	34.91	271.26
IceAge I	Norwegian Sea	1184-1	EBS	20.09.2011	67° 38.63′	12° 09.72′	1819.3	−0.85	34.91	1819.30
IceAge I	Norwegian Sea	1188-1	GKG	21.09.2011	67° 04.32′	13° 00.89′	1580.6	−0.74	34.90	269.25
IceAge I	Norwegian Sea	1212-1	EBS	22.09.2011	66° 32.63′	12° 52.48′	317.2	1.36	34.84	291.81
IceAge I	Norwegian Sea	1216-1	GKG	22.09.2011	66° 18.06′	12° 22.38′	730.8	−0.40	34.90	283.58
IceAge I	Norwegian Sea	1219-1	EBS	22.09.2011	66° 17.34′	12° 20.82′	579.1	−0.40	34.90	283.58
IceAge II	Norwegian Chanel	871-4	GKG	26.07.2013	62° 45.31′	00° 54.09′	1562.7	−0.78	34.91	298.34
IceAge II	Norwegian Chanel	872-4	EBS	27.07.2013	63° 01.88′	01° 29.91′	1858.3	−0.79	34.91	295.35
IceAge II	Norwegian Chanel	872-5	GKG	27.07.2013	63° 01.80′	01° 27.05′	1842	−0.79	34.91	295.35
IceAge II	Norwegian Chanel	873-2	GKG	28.07.2013	61° 46.63′	03° 52.38′	835.1	−0.70	34.91	303.51
IceAge II	Norwegian Chanel	873-6	EBS	28.07.2013	61° 46.52′	03° 52.38′	833.7	−0.70	34.91	303.51
IceAge II	Iceland-Faroe Ridge	879-2	SG	31.07.2013	63° 06.02′	08° 35.14′	505.9	1.33	34.95	305.41
IceAge II	Iceland-Faroe Ridge	879-5	EBS	31.07.2013	63° 06.10′	08° 34.32′	510.9	1.33	34.95	305.41
IceAge II	Iceland-Faroe Ridge	880-2	EBS	31.07.2013	63° 23.36′	08° 09.42′	686.0	−0.43	34.91	306.23
IceAge II	Iceland-Faroe Ridge	880-3	GKG	31.07.2013	63° 24.79′	08° 11.63′	688.1	−0.43	34.91	306.23
IceAge II	Iceland-Faroe Ridge	881-4	EBS	01.08.2013	63° 34.66′	07° 42.69′	1043.6	−0.57	34.91	303.94
IceAge II	Iceland-Faroe Ridge	881-6	VV	01.08.2013	63° 38.50′	07° 47.03′	1073.4	−0.57	34.91	303.94
IceAge II	Iceland-Faroe Ridge	882-2	VV	02.08.2013	63° 25.01′	10° 58.80′	441.4	0.27	34.90	311.93
IceAge II	Iceland-Faroe Ridge	882-5	EBS	02.08.2013	63° 25.04′	10° 58.20′	440.5	0.27	34.90	311.93

Table 2 Distribution of species described during this study

Area	Station	Depth [m]	*Akanthinotanais* cf. *longipes*	*Mystriocentrus biho* n.sp	*Pseudotanais misericorde* n.sp	*Pseudotanais sigrunis* n.sp	*Pseudotanais svavarssoni* n.sp	*Pseudotanais svavarssoni* complex	Pseudotanaidae indet	Total of individuals
Iceland Basin	963-1	2746.4	–	–	–	1	–	1	–	2
Iceland Basin	979-1	2567.6	–	–	–	–	–	1	–	1
Iceland Basin	1010-1	1384.8	1	–	1	–	–	3	–	5
Iceland Basin	1019-1	913.6	–	1	–	–	–	1	–	2
Irminger Basin	1043-1	213.9	–	–	–	–	–	18	–	18
Irminger Basin	1051-1	2538.9	–	–	–	–	–	1	–	1
Irminger Basin	1054—1	2537.3	–	3	4	–	–	2	–	9
Irminger Basin	1066	1621.8	–	–	1	–	–	–	–	1
Irminger Basin	1072-1	1593.8	–	–	–	–	–	2	–	2
Irminger Basin	1086-1	698.1	–	–	–	–	–	1	–	1
Denmark Strait	1116-1	684.1	–	–	–	1	–	–	–	1
Denmark Strait	1129-1	683.1	–	–	–	–	–	1	–	1
Denmark Strait	1132-1	320.6	–	–	–	–	–	3	–	3
Denmark Strait	1136-1	318.1	–	–	–	–	–	2	–	2
Denmark Strait	1141-1	1241.6	–	–	–	–	–	1	–	1
Denmark Strait	1148-1	1248.8	–	–	–	–	–	5	–	5
Norwegian Sea	1178-1	1818.8	–	–	–	–	–	2	–	2
Norwegian Sea	1152-1	2172.6	–	–	–	–	6	–	5	11
Norwegian Sea	1155-1	2203.8	–	–	–	–	1	–	–	1
Norwegian Sea	1159-1	2202.8	–	–	–	–	127	–	–	127
Norwegian Sea	1166-1	2401.8	–	–	–	–	2	–	–	2
Norwegian Sea	1168-1	2372.6	–	–	–	–	49	–	–	49
Norwegian Sea	1184-1	1819.3	–	–	–	–	–	8	–	8
Norwegian Sea	1188-1	1580.6	–	–	–	–	–	6	–	6
Norwegian Sea	1212-1	317.2	–	–	–	4	–	9	–	13
Norwegian Sea	1216-1	730.8	–	–	–	4	–	6	–	10
Norwegian Sea	1219-1	579.1	–	–	–	2	–	5	–	7
Norwegian Chanel	871-4	1562.7	–	–	–	–	–	2	–	2
Norwegian Chanel	872-4	1858.3	–	–	–	–	–	3	–	3
Norwegian Chanel	872-5	1842	–	–	–	–	–	1	–	1
Norwegian Chanel	873-2	835.1	–	–	–	–	–	2	–	2
Norwegian Chanel	873-6	833.7	–	–	–	–	–	1	–	1
Iceland-Faroe Ridge	879-2	505.9	–	–	–	–	–	2	–	2
Iceland-Faroe Ridge	879-5	510.9	–	–	–	–	–	3	–	3

Table 2 (continued)

Area	Station	Depth [m]	*Akanthinotanais* cf. *longipes*	*Mystriocentrus biho* n.sp	*Pseudotanais misericorde* n.sp	*Pseudotanais sigrunis* n.sp	*Pseudotanais svavarssoni* n.sp	*Pseudotanais svavarssoni* complex	Pseudotanaidae indet	Total of individuals
Iceland-Faroe Ridge	880-2	686.0	–	–	–	–	–	1	–	1
Iceland-Faroe Ridge	880-3	688.1	–	–	–	1	–	–	–	1
Iceland-Faroe Ridge	881-4	1043.6	–	–	–	–	–	1	–	1
Iceland-Faroe Ridge	881-6	1073.4	–	–	–	–	–	1	–	1
Iceland-Faroe Ridge	882-2	441.4	–	–	–	2	–	1	–	3
Iceland-Faroe Ridge	882-5	440.5	–	–	–	2	–	9	–	11
		Total sum	1	4	6	18	185	105	5	323
		%	0.3	1.2	1.8	5.5	57	32.4	1.5	

(14) The antenna article-3 to article-3 distal spine length ratio
(15) The cheliped carpus length to width ratio
(16) The cheliped basis to carpus length ratio
(17) The cheliped propodus length to width ratio
(18) The cheliped fixed finger length to propodus length ratio
(19) The pereopod-1 basis length to width ratio
(20) The pereopod-1 propodus to carpus length ratio
(21) The pereopod-1 propodus to dactylus + unguis length ratio
(22) The pereopod-1 unguis to dactylus length ratio
(23) The pereopod-2 propodus to carpus length ratio
(24) The pereopod-2 propodus to dactylus + unguis length ratio
(25) The pereopod-2 propodus to blade-like spine length ratio
(26) The pereopod-3 propodus to carpus length ratio
(27) The pereopod-3 propodus to dactylus + unguis length ratio
(28) The pereopod-3 propodus to blade-like spine length ratio
(29) The pereopod-4 propodus to carpus length ratio
(30) The pereopod-4 propodus to dactylus + unguis length ratio
(31) The pereopod-4 propodus to blade-like spine length ratio
(32) The pereopod-4 propodus to carpus distal seta length ratio
(33) The pereopod-5 propodus to carpus length ratio
(34) The pereopod-5 propodus to blade-like spine length ratio
(35) The pereopod-4 propodus to carpus distal seta length ratio
(36) The pereopod-6 propodus to carpus length ratio
(37) The pereopod-6 propodus to dactylus + unguis length ratio
(38) The pereopod-6 propodus to blade-like spine length ratio
(39) The pereopod-6 propodus to carpus distal seta length ratio
(40) The pleonite combined length to uropod basis and endopod combined length ratio
(41) The uropod basis length to width ratio
(42) The uropod exopod to endopod length ratio

Statistical analysis

The Kruskal–Wallis test with multiple post-hoc comparison (Statistica 10 software) was used to find out which of the ratios or characters determined significantly differentiate between the four "populations"studied. The characters and ratios identified by the test were used further to perform the principal component analysis (PCA) and analysis of similarity (ANOSIM). PCA is an ordination method in which samples (specimens here) regarded as points in a multi-dimensional space are projected onto a best fit plane (Clarke and Gorley 2006). Prior to the analysis, the data were normalized.

ANOSIM (Clarke and Gorley 2006) was conducted to test for the degree and significance of differences between a priori determined groups ("populations") of specimens: ANOSIM calculates a test statistic (*Global R*) which equals 1 if all individuals within a population are more similar to each other than to any individual in another population, and 0 if there is no difference between populations (Clarke and Gorley 2006). The relevant dissimilarity matrix was constructed using the normalized Euclidean distance.

Table 3 Morphological characters and proportion found in *Pseudotanais svavarssoni* sp. n. individials to be diffrentiated: P1—group of individuals from deep Norwegian Sea, P2—deep Southern Basins, P3—shallow Irminger Basin, P4—shallow Iceland-Faroe Ridge. H—value of Kruskal–Wallis test (df = 3; $N = 29$); probabilities; Z—multiple comparison value

Group	Variable	(V1) combined length of carapace, pereonites and pleonites	(V2) length of pereopod-1 propodus to carpus lenght	(V3) length of pereopod-1 propodus to dactylus + unguis length	(V4) length of pereopod-3 propodus to blade-like spine length	(V5) length of pereopod-6 propodus to distal seta on carpus length	(V6) length of cheliped carpus to width	(V7) length of cheliped propodus to width
P1	Measurements	1.21–1.74	2.28–2.53	1.15–1.29	1.41–1.75	2.62–6.42	1.78–2.15	1.47–1.63
	Range	0.98–1.98	2.35–2.51	1.2–1.38	1.46–1.66	2.98–6.46	1.86–2.08	1.49–1.59
	SD	0.5	0.08	0.09	0.1	1.24	0.11	0.05
P2	Measurements	1.45–1.57	2.48–2.58	0.99–1.28	1.4–1.58	1.48–4.79	1.33–1.73	1.38–1.51
	Range	1.47–1.59	2.46–2.56	1.01–1.29	1.41–1.59	1.6–4.94	1.36–1.76	1.36–1.5
	SD	0.06	0.05	0.14	0.09	1.67	0.20	0.07
P3	Measurements	1.38–1.59	1.78–2.19	0.86–1.06	1.21–1.45	2.98–4.4	1.53–2.01	1.36–1.98
	Range	1.34–1.54	1.56–2.36	0.88–1	1.25–1.41	3.18–4.88	1.56–1.9	1.55–1.93
	SD	0.1	0.11	0.06	0.08	0.85	0.17	0.19
P4	Measurements	0.76–1.75	1.77–2.61	0.78–0.95	1.12–1.62	1.66–3.88	1.55–1.97	1.45–2.01
	Range	0.84–1.44	1.94–2.62	0.82–1.02	1.14–1.46	1.96–3.44	1.57–1.91	1.53–1.89
	SD	0.3	0.34	0.10	0.16	0.74	0.17	0.18
Kruskal-Wallis	H	13.33	13.52	20.01	15.52	9.25	13.92	10.36
	p	0.004	0.003	0.0002	0.001	0.01	0.002	0.01
Multiple comparison	Groups	G1 & G4	G1 & G3	G1 & G3	G1 & G3	G1 & G4	G1 & G2	G1 & G3
	Z	3.48	3.18	3.56	3.25	2.83	2.89	2.72
	p	0.002	0.008	0.002	0.006	0.02	0.02	0.03

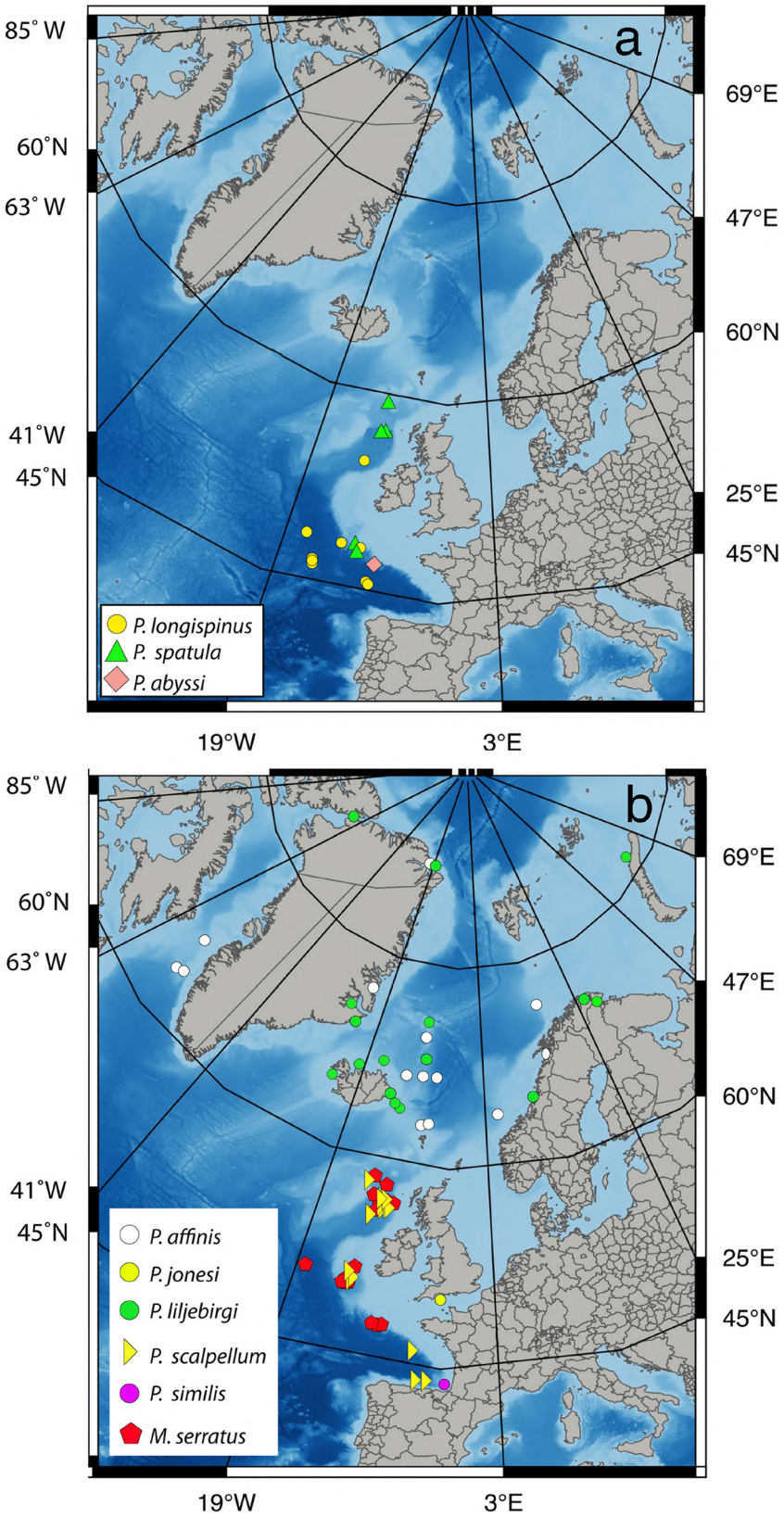

Fig. 2 Distribution of the Pseudotanaidae species in the North Atlantic based on literature (present study not included): Bird and Holdich (1989a, b); Błażewicz-Paszkowycz and Bamber (2011); Bruce et al. (1963); [Dahl] in Sieg (1977); [Debouttéville (1960), Debouttéville et al. (1954)] in Sieg (1983); [Fee, Hatch] in Sieg (1977); Greve (1965a, b, c); Hansen (1887, 1913); Holdich and Bird (1986); Holdich and Jones (1983); Just (1970); Kruuse, Ryder, Wandel in Hansen (1913); Liljeborg (1864); Sars (1882, 1896); Stephensen (1937); Sieg (1977); [Vanhöffen, Kruuse, Ryder, Horring, Sars] in Hansen (1913); [Vanhöffen, R. Horring, H.J. Hansen, Sars, A.M. Norman, Stappers, Th. Scott] in Hansen (1913); see Table 4

Fig. 2 (continued)

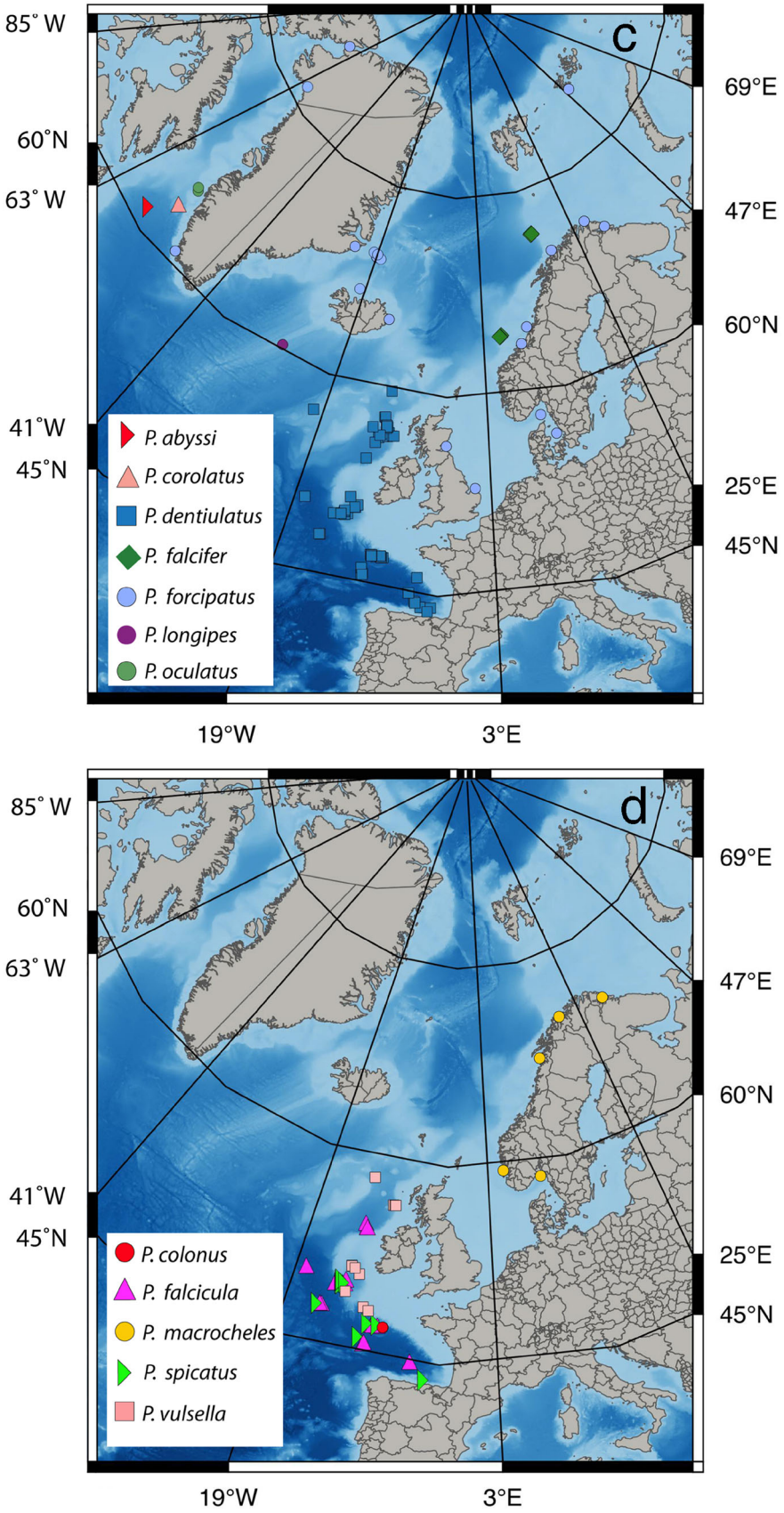

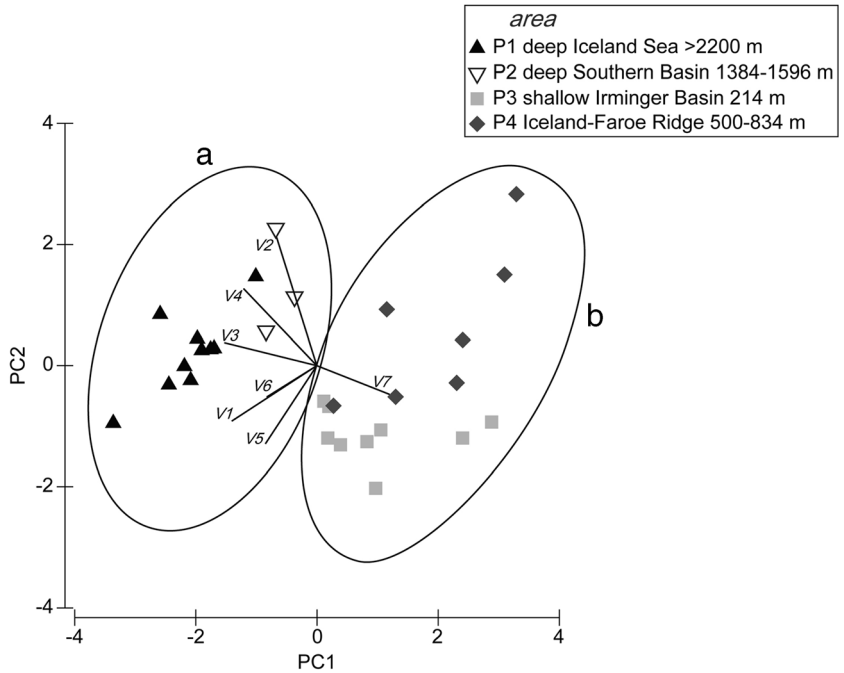

Fig. 3 Plot of principal component analysis based on seven morphometric characters (V1–7) of *P. svavarssoni* sp. n. and *P. svavarssoni* complex. List of character in Table 3

Similarities between the North Atlantic sites of pseudotanaids were determined in multivariate analysis using the group-average cluster and derived from the presence/absence-based Bray-Curtis similarity coefficient. In case of the species with particularly wide distribution (e.g., *P. affinis*, *P. lilljeborgi*, *P. forcipatus*), the records from a type locality and/or vicinity of the type localities only were included to analysis. In this approach, all potentially erroneous records and the records of possible cryptic species were excluded. PCA, ANOSIM, and group-average clustering were run using the PRIMER v. 6 package (Clarke and Gorley 2006).

Results

Species composition

The morphological approach adopted in this study allowed to identify five pseudotanaid species representing three genera: *Akanthinotanais* Sieg, 1977, *Mystriocentrus* Bird and Holdich, 1989b, and *Pseudotanais* Sars, 1882. The third genus yielded three species (including two new for science), *Akanthinotanais* and *Mystriocentrus* being represented by one species each.

Species discrimination

PCA run with the seven morphometric characters initially identified as significantly discriminating (Table 3) was applied to the most numerous pseudotanaid species (*Pseudotanais svavarssoni* sp. n.) and resulted in the first five PCs accounting for 90% of the total variation. Most of the variability in the seven characters is captured in the 2D projection plotted in Fig. 3. The first and the second PC axes (PC1 and PC2) explain 44 and 16% of the total variance, respectively. PC1 axis

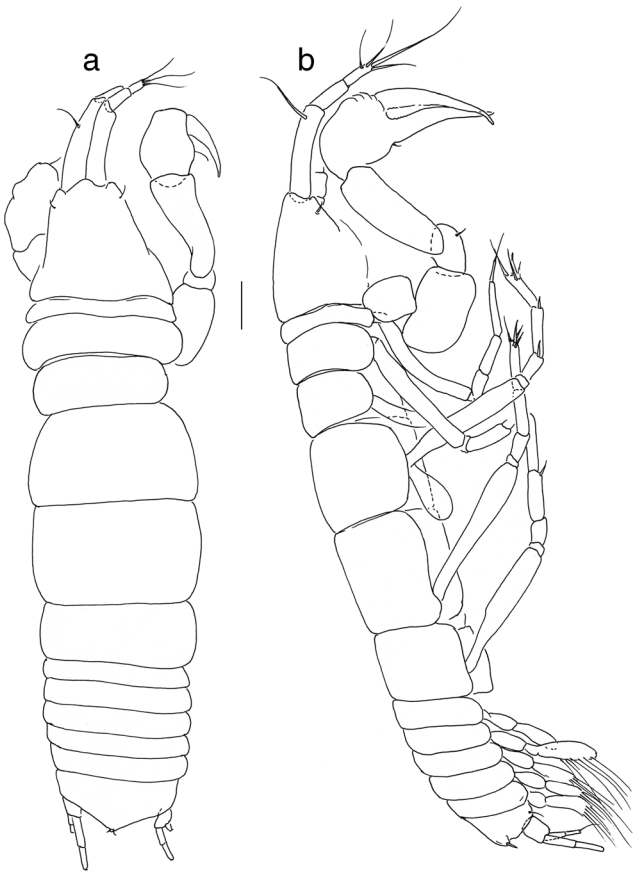

Fig. 4 *Mystriocentrus biho* sp. n., female with oostegites (cat no…). **a** Dorsal view. **b** Lateral view. Scale: 0.1 mm

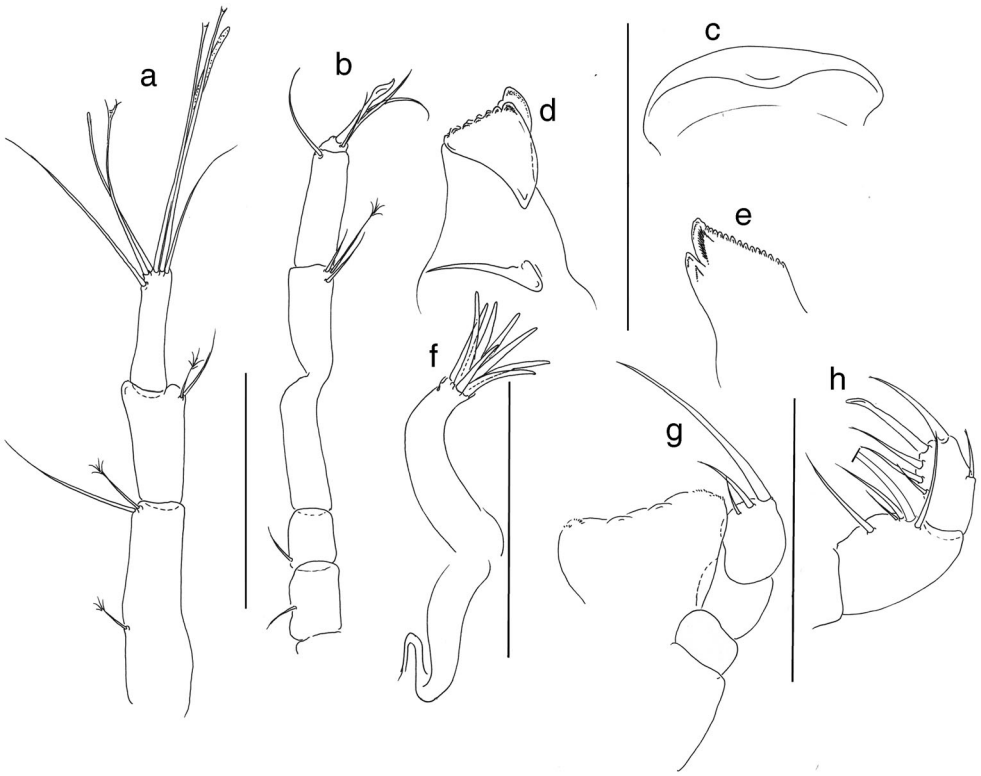

Fig. 5 *Mystriocentrus biho* sp. n., preparatory female, paratype (cat no…). **a** Antennule. **b** Antenna. **c** Labrum. **d** Left mandible. **e** Right mandible. **f** Maxillule. **g** Maxilliped. **h** Details of maxilliped palp. Scale: 0.1 mm for **a**–**b** and 0.01 mm for **c**–**h**

separated the specimens examined into two groups (A, B) (Fig. 3). The group A consists of those individuals collected from deeper stations (> 1300 m) in the Irminger and Iceland Basins as well as the Norwegian Sea, the group B includes specimens found in shallow-water (< 800 m) samples from the Iceland–Scotland Ridge and the Irminger Basin.

Most variables decreased along the PC1 axis (from left to right), the highest values being attained by characters V4, V1, and V2 (Fig. 3, Table 3). An opposite trend (values increasing along PC1) was shown by the V7 (chelae propodus length to width ratio only).

ANOSIM showed significant morphometric differences (*Global* $R = 0.68$, $p = 0.1\%$) between populations from the regions examined. The highest differences were found between the specimens representing "*population 1*" (deeper stations in the Norwegian Sea) and "*population 3*" (shallow stations in the Irminger Basin) (*Global* $R = 0.88$, $p = 0.1\%$) as well as between specimens from "*population 1*" and "*population 4*" (shallow stations in ISR) (*Global* $R = 0.83$; $p = 0.1\%$). Significant, relatively high differences were also detected between specimens from "*population 2*" (deeper stations in the Irminger and Iceland Basins) and "*population 3*" (*Global* $R = 0.74$; $p = 0.5\%$) and between specimens from "*population 1*" and "*population 2*" (*Global* $R = 0.63$, $p = 1\%$). Differences in morphometry between specimens from "*population 3*" and "*population 4*" were weaker (*Global* $R = 0.33$), but still significant ($p = 0.7\%$).

The morphometric analysis confirmed morphological differences between groups of individuals collected from different regions and depths. The differences, although present, are detectable only with careful measurement of the seven characters identified; therefore, the results indicated the presence of at least two (but possibly four) cryptic species. Moreover, as the strongest differences were observed between specimens from deep stations in the Norwegian Sea and all the other individuals (Table 3), we decided to choose a holotype for the newly described species (*P. svavarssoni* sp. n., see below) from those stations. As the differences between the other three sets of specimens (shallow stations in ISR, and Irminger Basin, deeper stations in the Irminger and Iceland Basins) were less pronounced, we decided to retain them as the "*svavarssoni*" complex until genetic data would lend reasonable support to the presence of distinct species.

Taxonomic descriptions

Family Pseudotanaidae Sieg 1976

Genus: *Mystriocentrus* Bird and Holdich, 1989a

Diagnosis (amended after Bird and Holdich, 1989b): pereonite-2 similar in length or longer than pereonites 1 and 3; antenna articles 1 and 2 with simple setae, and with thickened seta on article-6 (terminal); molar process acuminate and simple; maxilliped endites fused, palp article-4 with thickened

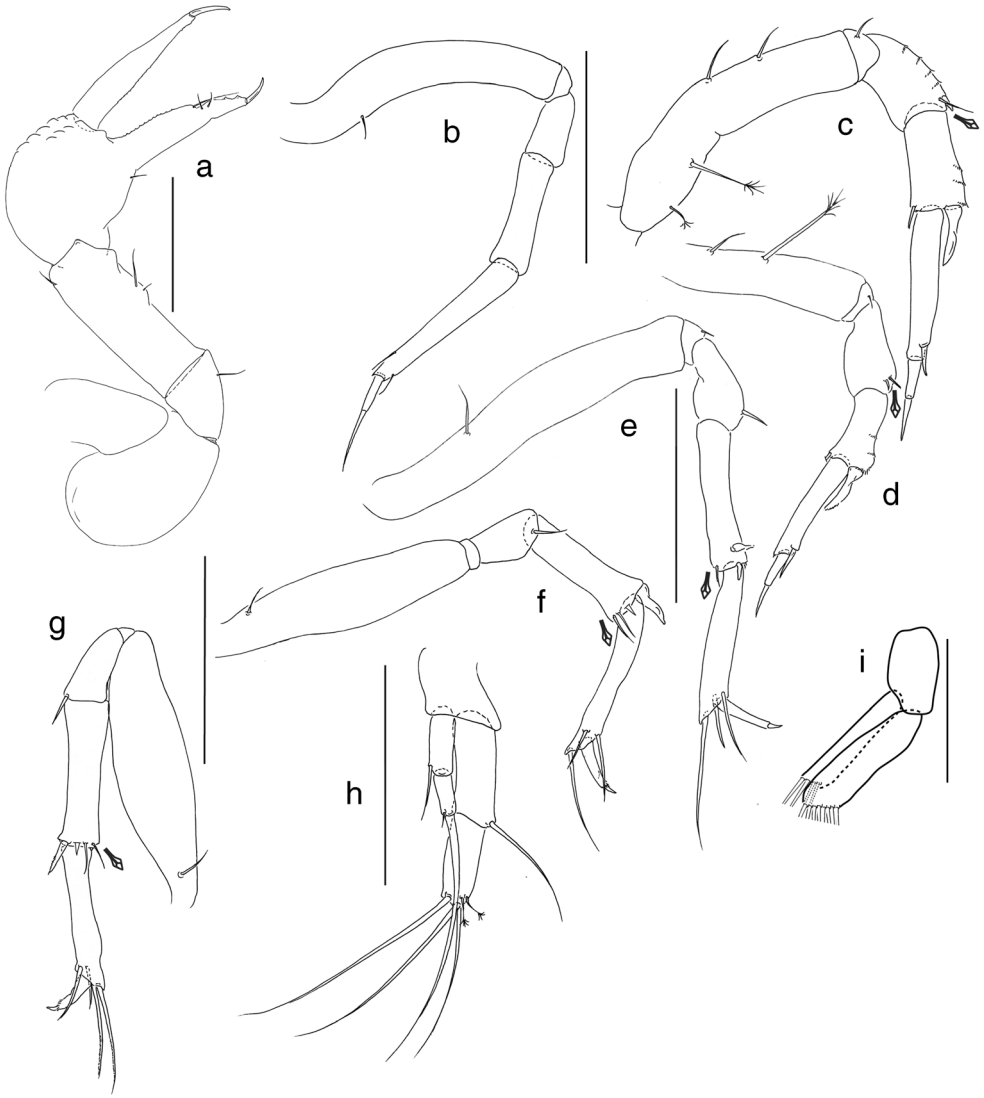

Fig. 6 *Mystriocentrus biho* sp. n., preparatory female. **a** Cheliped. **b** Pereopod-1. **c** Pereopod-2. **d** Pereopod-3. **e** Pereopod-4. **f** Pereopod-5. **g** Pereopod-6. **h** Uropod. **i** Pleopod. Scale: 0.1 mm

seta; cheliped propodus almost as long as wide (1−1.2 times as long as wide), and small folds in distodorsal corner; chela forcipate, with serrate inner margin; pereopods 2−6 with blade-like spine on carpus.

Type species: *M. serratus* Bird and Holdich, 1989a

Species included: *M. serratus* Bird and Holdich, 1989b; *M. biho*, sp. n.

Remarks: Until examination of the Pseudotanaids from IceAGE collection (present studies), the *Mystriocentrus* was monotypic genus. Most of the diagnostic character for genus given as by Bird and Holdich 1989a, b (e.g., relatively long pereonite-2, thickened seta on antennule article-6 and maxilliped palp article-4, forcipate seta with serrate incisive margins and folds in distodorsal corner, and blade like spines on carpus of pereopods 2–6 well define this genus so far. Observed in type species "spatulate setae" on merus and carpus (through which the genus received its name Bird and Holdich 1989a: 277) might not be so robust generic character, although still valid for species identification (see Remarks page 14).

Mystriocentrus biho sp. n. Registered in ZooBank under: urn:lsid:zoobank.org:act:0AED0F58-63D5-4524-A857-FE6EC2883162 Figs. 4, 5, and 6

Material examined: Holotype: Ovigerous female, ZMH K-54850, St 1054-1, 61° 36.82′ N 31° 22.26′ W−61° 36.98′ N 31° 22.18′ W, depth 2545.7−2536.8 m, EBS, 07 Sep 2011.

Paratypes: neutrum (dissected), ZMH K-54852, St. 1019-1, 62° 56.46′ N 20° 44.06′ W−62° 56,52′ N 20° 43,77′ W, depth 916.1−909.4 m, EBS, 03 Sep 2011.

Two neutri, ZMH K-54851, St 1054-1, 61° 36.82′ N 31° 22.26′ W−61° 36.98′ N 31° 22.18′ W, depth 2545.7 −2536.8 m, EBS, 07 Sep 2011.

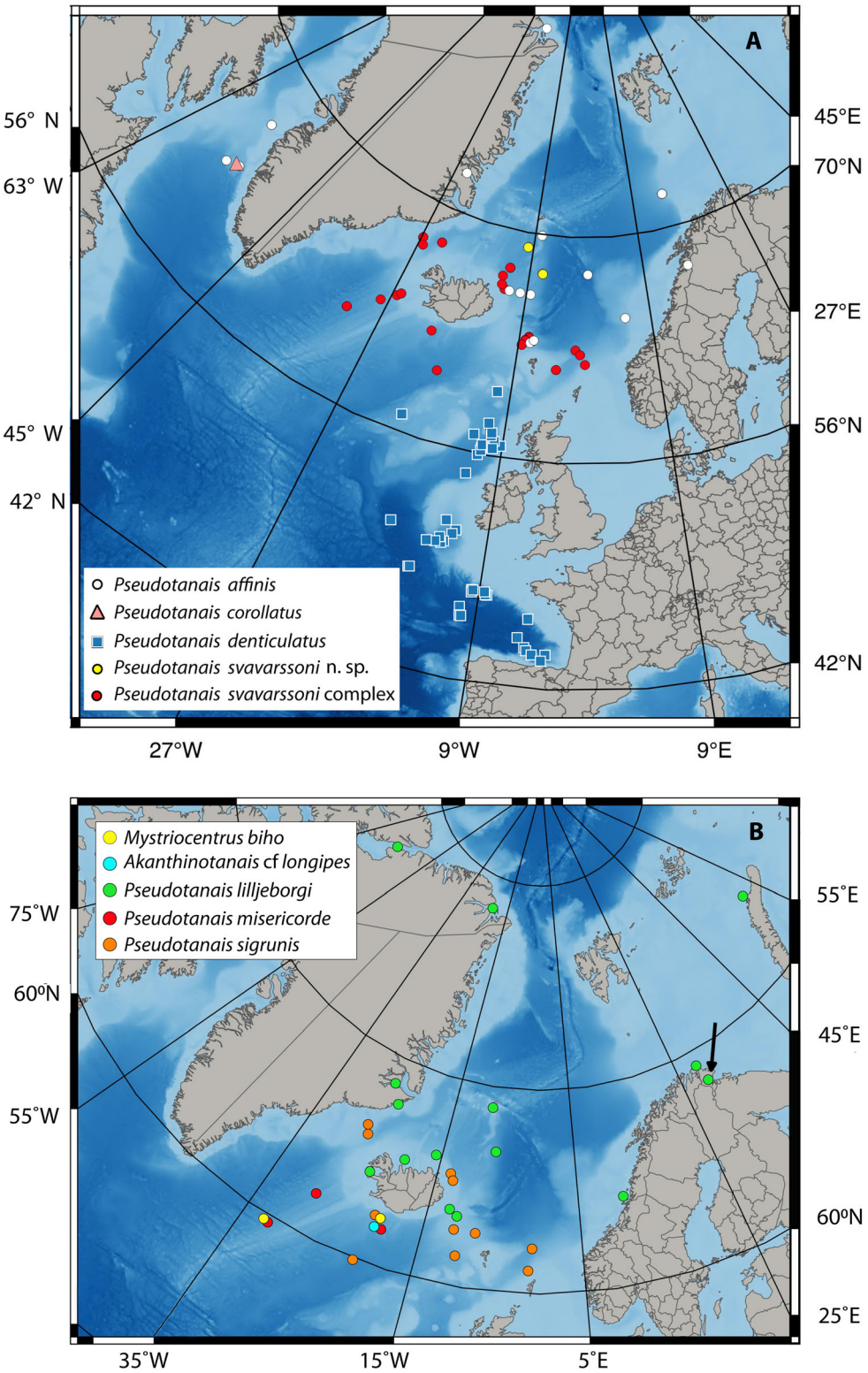

Fig. 7 Distribution of the Pseudotanaidae species collected during IceAGE cruises. Distribution of *Pseudotanais affinis*, *P. corollatus*, *P. denticulatus*, and *P. lilljeborgi* as in the Fig. 2

Diagnosis: Pereonite-2 similar in length to pereonite-3; pereonite-3 clearly narrower, 0.8 times as wide as pereonite-4; maxilliped endites with small tubercles; pereopods 2–3 carpal blade-like spines long, 0.4 times as long as propodus.

Etymology: The name is composed of the first letters from the last names of Graham J. Bird and David M. Holdich, who erected the genus *Mystriocentrus.*

Description of ovigerous female: *Body* (Fig. 4) 1.9 mm length, 3.8 times as long as wide. Carapace 18% of total

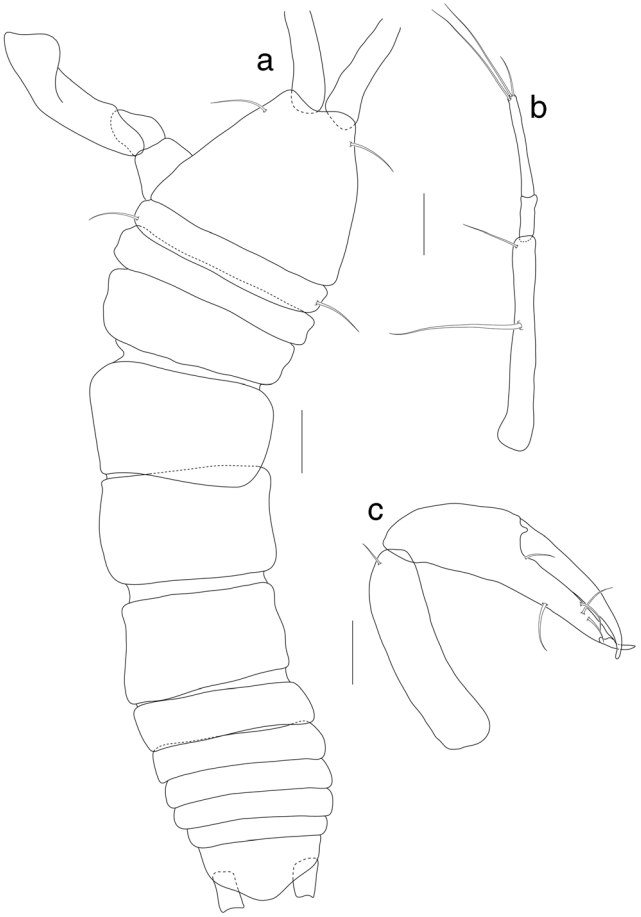

Fig. 8 *Akanthinotanais* cf. *longipes*, preparatory female. **a** Dorsal view. **b** Antennule. **c** Cheliped. Scale: 0.1 mm

body length, subtriangular, 0.8 times as long as wide, with simple setae on each anterio-lateral margin. *Pereon* 55% of total body length, pereonite-1, half times as long as pereonite-2; pereonite-2 0.9 times as long as pereonite-3; pereonite-3, 0.8 times as wide as pereonite-4; pereonite-4 1.2 times as long as pereonte-3; pereonite-5 similar in length and width to pereonite-4; pereonite-6 half times as long as pereonite-5; pereonites 0.1, 0.2, 0.3, 1.2, 1.2, and 0.3 times as long as broad, respectively. *Pleon* 17% of total body length, with five similar in length pleonites, each 0.1 times as long as wide. *Pleotelson* 10% of body length; pleonites together with pleotelson as long as pereonites 4–6 combined length.

Antennule (Fig. 5a) article-1 3.7 times as long as wide, with penicillate middle seta, one penicillate and one simple distal setae on outer margin; article-2 2.1 times as long as wide, half times as long as article-1, with simple and penicillate distal setae on inner margin; article-3 3.5 times as long as wide, as long as article-2, with one subdistal seta, tipped with one aesthetasc, one simple, one distally rounded, three distally furcate setae.

Antenna (Fig. 5b) article-1 fused, broken during dissection; article-2 1.5 times as long as wide, with seta on middle outer margin; article-3 1.3 times as long as wide, 0.8 times as long as article-2, with seta on proximal outer margin; article-4 four times as long as article-3, 6.3 times as long as wide, with two simple and one penicillate distal setae; article-5 3.4 times as long as wide, half times as long as article-4, with distal simple seta; article-6 vestigial, with one thickened, sensory seta and three simple setae distally.

Mouthparts. *Labrum* (Fig. 5c) rounded, hood-shape, naked. *Left mandible* (Fig. 5d) incisor distal margin blunt and serrated, *lacinia mobilis* large and distally serrated; molar acuminate and simple. *Right mandible* (Fig. 5e) with incisor distal margin serrated; *lacinia mobilis* fussed to a small process. *Maxillule* (Fig. 5f) distally bent, with eight slender distal spines. *Maxilliped* (Fig. 5g, h) endites completely fused, distal edges with small tubercles and lateral margins finely setose. Palp article-1 and article-2 naked; article-3 with three and one short setae on inner margin; article-4 with one thickened seta (Fig. 5h) and four simple inner and distal setae and one outer seta.

Cheliped (Fig. 6a) basis 1.6 times as long as wide; merus subtriangular, with simple midventral seta; carpus three times as long as wide, with two midventral setae, and with simple distodorsal seta; propodus (palm) as long as wide, small folds in distodorsal corner and small ventral seta; fixed finger 5.1 times as long as wide, 1.2 times as long as propodus, with serrated inner margin and three small inner setae; dactylus simple with slightly serrated inner margin.

Pereopod-1 (Fig. 6) basis 5.7 times as long as wide, with simple dorsoproximal seta; ischium 0.4 times as long as wide, naked; merus 1.8 times as long as wide, 0.6 times as long as carpus, naked; carpus 2.7 times as long as wide, 0.6 times as long as propodus, naked; propodus 6.6 times as long as wide, with dorsoproximal and distodorsal seta; dactylus 0.1 times as long as propodus, unguis 1.5 times as long as dactylus, together 0.5 times as long as propodus.

Pereopod-2 (Fig. 6c) basis 5.5 times as long as wide, with two simple ventral setae and with two penicillate dorsoproximal setae; ischium half times as long as wide, with simple seta; merus 1.5 times as long as wide, 0.9 times as long as carpus, with microtrichiae ventrally, spine and sensory seta distoventrally; carpus twice as long as wide, 0.6 times as long as propodus, with simple distodorsal seta and blade-like distoventral spine (0.4 times as long as propodus); propodus six times as long as wide, with distoventral spine; dactylus 0.2 times as long as propodus, unguis subequal propodus together almost as long as half of propodus.

Pereopod-3 (Fig. 6d) basis 3.5 times as long as wide, with one simple and one penicillate seta on ventral margin; ischium 0.3 times as long as wide, with simple ventral seta; merus 1.6 times as long as wide, and 1.1 times as long as carpus, with sensory seta and spine distoventrally; carpus half as long as

wide, and 0.6 times as long as propodus, with microtrichiae ventrally, small distodorsal seta and blade-like spine distoventral spine (0.4 times as long as propodus); propodus six times as long as wide, with one distoventral spine; dactylus 0.3 times as long as propodus, unguis 0.6 times as long as dactylus, together 0.6 as long as propodus.

Pereopod-4 (Fig. 6e) basis six times as long as wide, with ventroproximal simple seta; ischium 0.6 times as long as wide, with simple seta; merus 1.8 times as long as wide, 0.6 times as long as carpus with simple distoventral seta; carpus five times as long as wide, subequal propodus, with blade-like spine (broken) and spine distoventrally, and with sensory seta distodorsally; propodus six times as long as wide, with two distoventral setae and long distodorsal seta; dactylus with unguis half as long as propodus; unguis 0.2 as long as dactylus.

Pereopod-5 (Fig. 6f) as pereopods-4, but carpus with one sensory seta and one simple seta, on dorsal margin distally, with one spine and with one blade-like spine ventral margin.

Pereopod-6 (Fig. 6g) similar to pereopod-4 but basis 3.7 times as long as wide, carpus with one sensory seta, one simple seta, one spine and one blade-like spine; propodus with four setae terminally.

Pleopoda (Fig. 6i) basal article 3.6 as long as wide, endopod 5.3 as long as wide, with four distal setae; exopod 3.3 as long as wide, with eight distal setae.

Uropod (Fig. 6h) basal article as long as wide, naked; exopod 1.7 times as long as basis, and as long as endopod article-1, with two articles, article-1 1.3 times as long as article-2, with distal seta, article-2 with one small subdistal and one strong distal setae; endopod 1.8 times as long as exopod, with two articles; article-1 1.2 times as long as article-2, with long simple seta distally on outer margin; article-2 with three long simple and two short penicillate setae distally.

Distribution: *M. biho* sp. n. was recorded in Irminger and Iceland Basins at the depth range 913−2540 m (Fig. 7b). The new species is the second member of the genus *Mystriocentrus*, that is so far known only from the North Atlantic (Fig. 2b).

Remarks: The *Mystricentrus biho* sp. n. can be recognized from the congener *M. serratus* Bird and Holdich, 1989a, b by the proportion of pereonites 2−3. In the new species, the pereonite-2 is similar in length to pereonite-3, but twice as long as pereonite-3 in *M. serratus*. Beside that, pereonite-3 is visibly narrower than rest of the pereonites (0.8 times as wide as pereonite-4) in the new species, but similar size in *M. serratus*. Additionally, *M. biho*. sp. n. has one sensory (spatulate) setae on merus and carpus of the pereopods 2−6, while in *M. serratus* one to three such setae present; blade-like spine on pereopods 2−3 carpus are clearly longer (0.4 times as long as propodus) in *M. biho* than in *M. serratus* (0.1−0.2 times as long as propodus). Finally, the new species can be distinguished by appearance of maxilliped endite that has small tubercles on the distal margin; the distal margin of maxilliped endites in *M. serratus* is smooth.

Genus *Akanthinotanais* Sieg, 1977

Diagnosis (after Sieg 1977): Pereopods without blade-like spines.

Remarks: The Pseudotanaidae is a morphologically consistent family with few autapomorphic characters (Bird and Holdich, 1989a). Distinguished by Sieg (1977), two subgenera—*Akanthinotanis* (Sieg, 1977) and *Pseudotanais* (Sieg, 1977)—were seen by McLelland (2008) distinct enough to erect them as genera or even subfamily. Although the research by McLelland unfortunately were never published, Bird and Larsen (2009) treated the two taxa as valid genera in their phylogenetic analyses adding in its result two other genera *Mystriocentrus* Bird and Holdich, 1989b and *Parapseudotanais* Bird and Holdich, 1989a.

The phylogenetic analysis is beyond the purpose of this paper, but it is essential to mention that molecular markers approach ascertain *Pseudotanais* itself as not monophyletic and highly diverse taxon (Jakiel and Błażewicz, in preparation), that can be straightforwardly split into at least few new genera. Furthermore, the same approach apparently demonstrated that *Akanthinotanais* is not monophyletic with *Pseudotanais* supporting McLelland proposition to treat them both as valid genera.

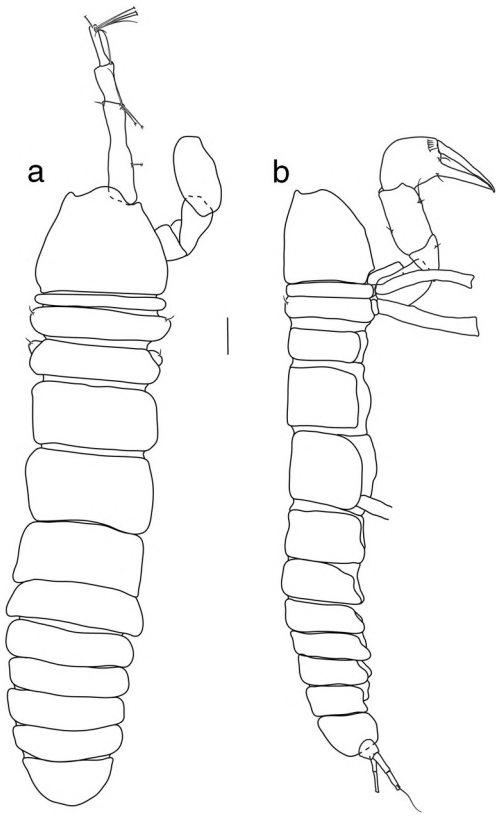

Fig. 9 *Pseudotanais misericorde* sp. n., preparatory female. **a** Dorsal view. **b** Lateral view. Scale: 0.1 mm

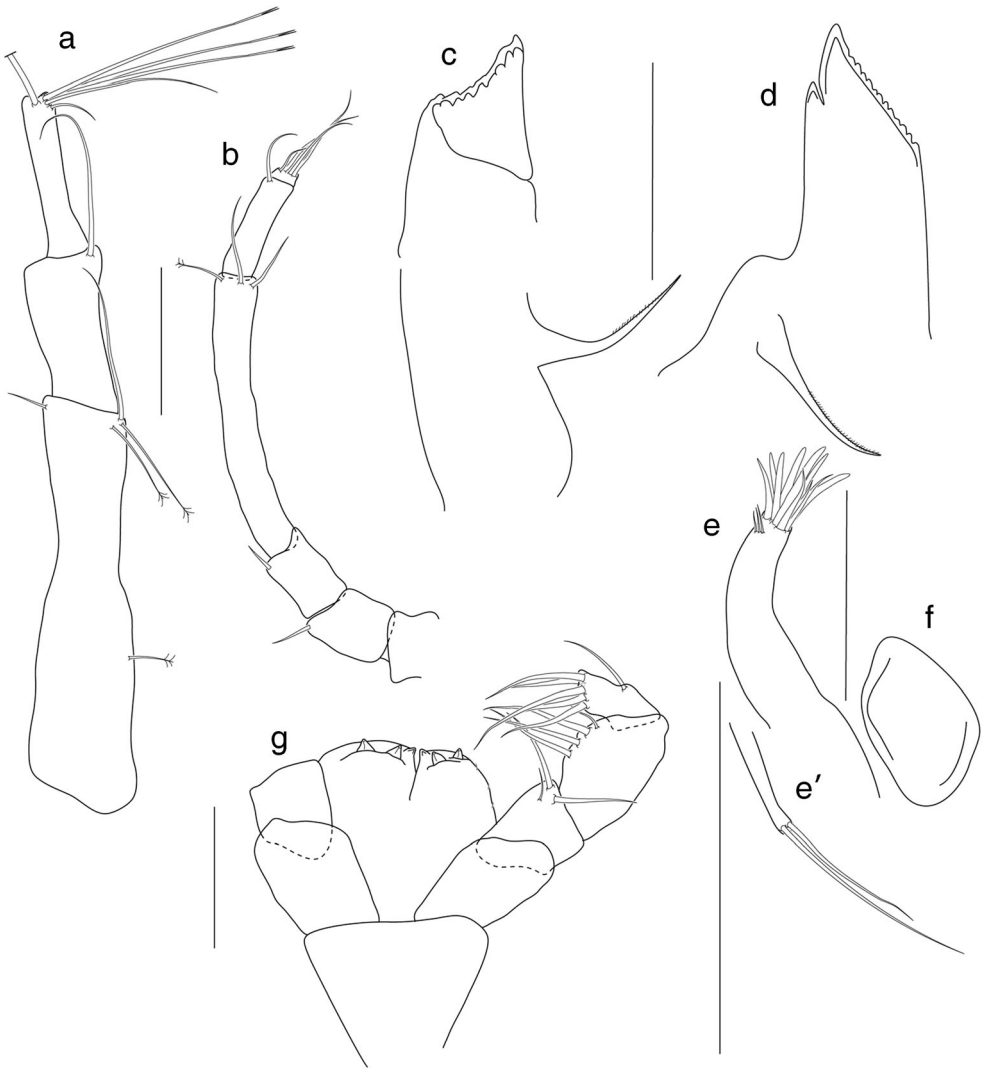

Fig. 10 *Pseudotanais misericorde* sp. n., preparatory female. A antennule, B antenna, C left mandible, D right mandible, E maxillule endite, E' maxillule palp, F maxilla, and G maxilliped. Scale: 0.1 mm for A-B and 0.01 mm for C–G

Akanthinotanais cf. *longipes*

Fig. 8

Material examined: one neutrum, ZMH K-54853, St. 1010-1, 62° 33.17′ N 20° 23.18′ W−62° 33.22′ N 20° 22.88′ W, depth 1383.3−1387.8 m, EBS, 02 Sep 2011.

Distribution: *Akanthinotanais longipes* was described by Hansen (1913) from *Ingolf* Expedition (st. 78; 60° 37′ N 27° 52′ W, depth 364 m, temp. 4.5 °C) in the Iceland Basin and so far it is the only known location of the species (Fig. 2c).

In the IceAGE collection, the only specimen presumably conspecific with *A. longipes* was found in Iceland Basin at the depth 1387 m (Fig. 7b).

Remarks: As the only individual collected during the IceAGE cruises was preserved in poor condition, its full identification and comparison of details with those of *Akanthinotanais longipes* (Hansen, 1913) was not possible. However, the absence of eyes, the presence of slender antennule and cheliped, and the absence of a blade-lik seta on pereopod-1 allowed us to regard it as conspecific with *A. longipes*. Only three akanthinotanaids known at present are blind, but only *A. longipes* is elongated (3.0 times as long as it is wide) and has a not-forcipate cheliped. Two other blind akanthinotanaids *Akanthinotanais gaussi* (Vanhöffen, 1914) and *Akanthinotanais similis* (Sieg, 1977) have rather robust chela which is 2.0 and 2.5 times, respectively, as long as it is wide.

Genus *Pseudotanais* G.O. Sars, 1882

Pseudotanais misericorde sp. n.

Figs. 9, 10, and 11

Material examined: Holotype: neutrum, ZMH K-54854, St. 1054-1, 61° 36.82′ N 31° 22.26′ W−61° 36.98′ N 31° 22.18′ W, depth 2545.7−2536.8 m, EBS, 07 Sep 2011.

Paratypes: neutrum (dissected), ZMH K-54855, St. 1010–1, 62° 33.17′ N 20° 23.18′ W−62° 33.22′ N 20° 22.88′ W, depth 1383.3−1387.8 m, EBS, 02 Sep 2011; three neutri (two dissected), ZMH K-54856, St. 1054–1, 61° 36.82′ N 31° 22.26′ W−61° 36.98′ N 31° 22.18′ W, depth 2545.7 −2536.8 m, EBS, 07 Sep 2011; neutrum ZMH K-54857, St.

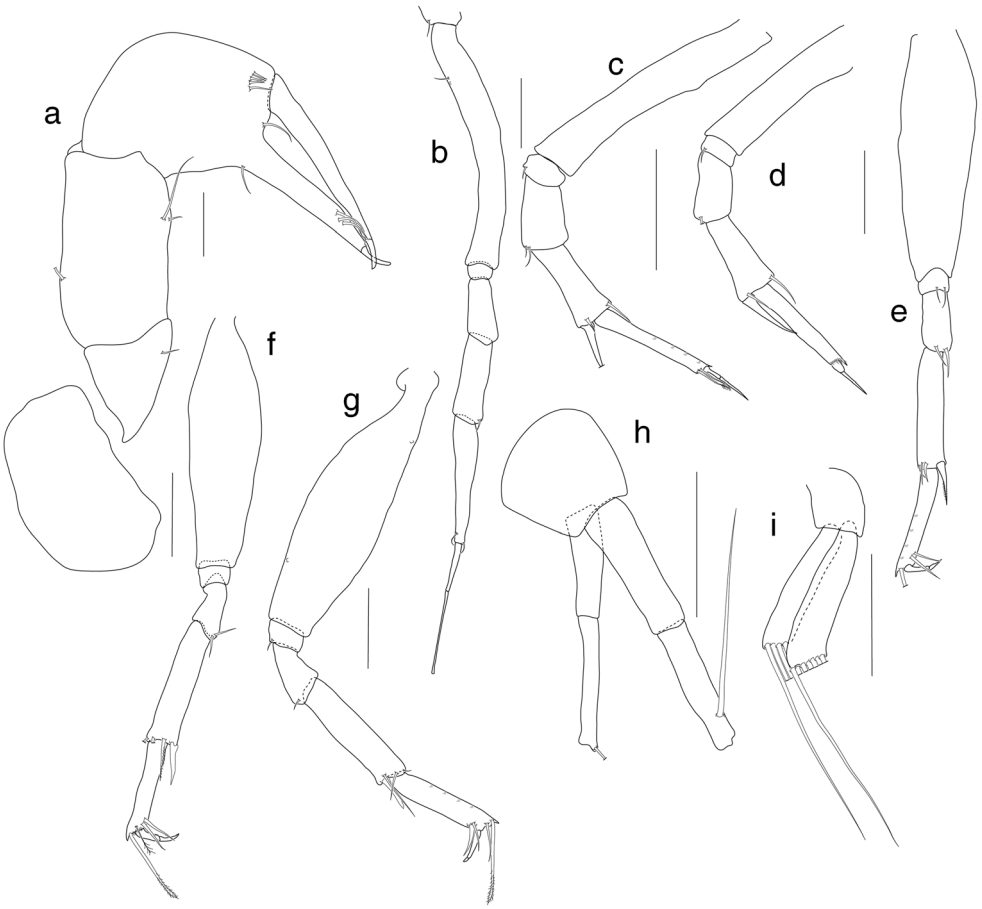

Fig. 11 *Pseudotanais misericorde* sp. n., preparatory female. **a** Cheliped. **b** Pereopod-1. **c** Pereopod-2. **d** Pereopod-3. **e** Pereopod-4. **f** Pereopod-5. **g** Pereopod-6. **h** Uropod. **i** Pleopod. Scale: 0.1 mm

1066, 62° 59.97′ N 028° 04.78′ W, depth 1621.8 m, GKG, 08 Sep 2011.

Diagnosis: Eyes absent. Pereonites 2–3 the same length. Antennule article-1 six times as long as wide. Antenna articles 2–3 with simple setae. Maxilliped molar pointed with upper margin serrated. Maxilliped endites with conical tubercles. Cheliped carpus 1.6 times as long as wide. Chela forcipate, unguis, and dactylus distal spines inside bent. Pereopods 2–6 blade-like spine slender and pointed. Uropod exopod two articulated, 0.8 times as long as endopod.

Etymology: From Latin *misericorde* was called the long and narrow knife used in medieval for delivering a mercy stroke. The name refers to the unusual shape of the blade-like spine on pereopods 2–6, that is long and pointed.

Description of neutrum: *Body* (Fig. 9a, b) 1.8 mm; 5.0 times as long as broad. Carapace almost as long as pereonites 1–3 and half of pereonite-4 combined, naked, lateral margin gently rounded. Pereon 39% of total body length, pereonite-1 half as long as pereonite-2; pereonites 2 the same length and pereonites 3, wilt lateral setae; pereonite-3 half as long as pereonite-4; pereonite-4 as long as pereonites-5; pereonite-5 1.2 times as long as pereonites-6, pereonites 0.1, 0.2, 0.2, 0.5, 0.5, and 0.4 times as long as broad, respectively (data for the holotype). *Pleon* 22.7% of total body length, pleonite-1 slightly wider than all other pleonites. *Pleotelson* 13% of total body length pleonites together with pleotelson almost as long as pereonites 2–6 combined length.

Antennule (Fig. 10a) article-1 six times as long as wide, with middle penicillate seta, one simple and two penicillate distal setae on inner margin and simple distal seta on outer margin; article-2 2.1 times as long as wide, with distal seta longer that article-3 on inner margin; article-3 just longer than article-2, with six distal setae: two simple and three distally trifurcate seta, one seta broken.

Antenna (Fig. 10b) shorter than antennule; article-1 fussed with body; article-2 1.1 times as long as wide, with one seta on outer margin; article-3 1.5 times as long as wide, subequal to article-2 with one seta on outer margin; article-4 3.5 times as long as article 3, 7.4 times longer than broad, with two simple and one penicillate setae distally; article-5 0.3 times as long as article-4, with one simple seta distally; article 6 vestigial, with four simple setae distally.

Mouthparts. Labium not observed. Left mandible (Fig. 10c) incisor distal margin blunt and serrated, *lacinia mobilis* large, and distally serrated; molar acuminate; right mandible (Fig. 10d) with incisor distal margin serrated; *lacinia mobilis* fussed to a small process. *Maxillule* (Fig. 10e) distally bent, with eight spines and two setae

distally, three fine setae subdistally on outer margin; endite (Fig. 10e') with two distal setae. *Maxilla* (Fig. 10f) ovoid, naked. *Maxilliped* (Fig. 10g) endites completely fused except the most distal fragment, where they stay well separated; distal margin with two conical tubercles, each with visible distal hole, and finely setose lateral margins. Palp article-1 naked, article-2 with three inner setae (two long one short), article-3 with four inner setae (three long and one short), article-4 with and five simple inner and distal setae and one middle outer seta.

Cheliped (Fig. 11a) basis 1.6 times as long as wide; merus subtriangular with single midventral seta; carpus 1.7 times as long as broad, with two midventral (long and short) setae; dorsal margin with simple submiddle distal seta not seen; chela forcipate, propodus (palm) 1.3 times as long as wide and 0.9 times as long as fixed finger, with ventral seta and one seta near dactylus insertion; row of five small setae on inner surface; fixed finger with three seta, distal spine bent upward; dactylus simple as long as fixed finger, distal spine bent downward.

Pereopod-1 (Fig. 11b) slender, basis 7.9 times as long as wide with two dorsoproximal setae (one broken); ischium naked; merus 2.3 times as long as wide, 0.2 times as long as basis, naked; carpus 3 times as long as wide 0.6 times as long as propodus, with fine distodorsal seta; propodus 7 times as long as wide, with two fine distal seta; dactylus 0.3 as long as propodus, dactylus 0.6 times as long as unguis; dactylus and unguis combined as long as propodus.

Pereopod-2 (Fig. 11c) basis 6.5 times as long as wide; ischium with simple seta; merus 1.5 times as long as wide, 0.7 times as long as carpus, with two setae distally; carpus 2.7 times as long as wide, 0.7 times as long as propodus with two setae and one blade-like spine, very slender spine (distally broken) distally; propodus 8.3 times as long as wide with plumose seta distally, ventral margin with microtrichiae; unguis twice as long as dactylus, combined half as long as propodus.

Pereopod-3 (Fig. 11d) similar to pereopod-2, but carpus 2.6 times as long as propodus and propodus 5 times as long as wide, without microtrichiae; blade-like spine on carpus 0.6 times as long as propodus.

Pereopod-4 (Fig. 11e) basis 3.3 times as long as wide, naked; ischium with two setae; merus 0.2 times as long as wide; 0.4 times as long as carpus, with two distal setae; carpus 4.5 times as long as wide, 1.2 times as long as propodus, with blade-like spine (0.4 times as long as propodus) and with three setae distally; propodus 6.2 times as long as wide, with two ventrodistal simple setae and dorsodistal seta broken; dactylus twice as long as unguis.

Pereopod-5 (Fig. 11f) basis 3.4 times as long as wide; ischium naked (setae probably broken off); merus 2.6 times as long as wide, 0.5 times as long as carpus, with two distal setae; carpus 4.3 times as long as wide, 1.2 times as long as propodus, with blade-like spine (0.4 times as long as propodus) and three setae distally (one serrate, two broken); propodus 5.2 times as long as wide, with two distoventral simple setae, one subdistal penicillate seta and one dorsodistal serrated, distally flatten seta; dactylus 1.4 times as long as unguis.

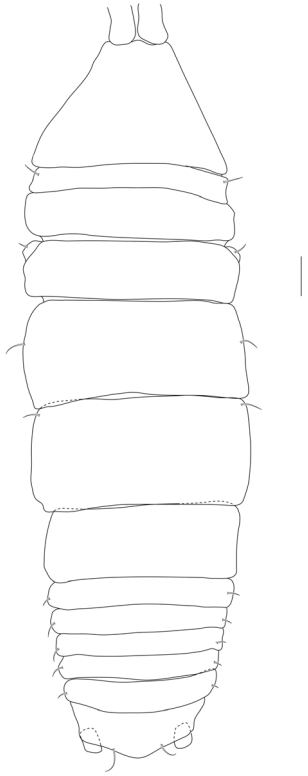

Fig. 12 *Pseudotanais svavarssoni* sp. n., neutrum, holotype (cat no…), dorsal view. Scale: 0.1 mm

Pereopod-6 (Fig. 11g) basis 3.8 times as long as wide with dorsoproximal seta (broken off); ischium with one seta (second seta probably broken off); merus 2.1 times as long as carpus with one distal seta (second seta probably broken off); carpus 3.8 times as long as wide and 1.1 times as long as propodus, with three simple setae and one blade-like spine (0.3 times as long as propodus), distally; propodus 4.8 times as long as wide with two simple distoventral setae, one simple and one distally serrated, dorsodistal flatten setae; dactylus 5 times as long as unguis.

Pleopod (Fig. 11i) endopod 4.5 times as long as wide, with four distal setae; exopod four times as long as wide with seven distal setae.

Uropod (Fig. 11h) basis naked; exopod 0.8 times as long as endopod, with two articles, article-1 0.8 times as long as article-2, article-2 with at least one distal seta (broken); endopod with two, subequal articles, article-2 with at least one subdistal seta.

Distribution: *P. misericorde* was recorded in the Iceland and Irminger Basins (Fig. 7) at the depth range: from 1383 to 2545 m.

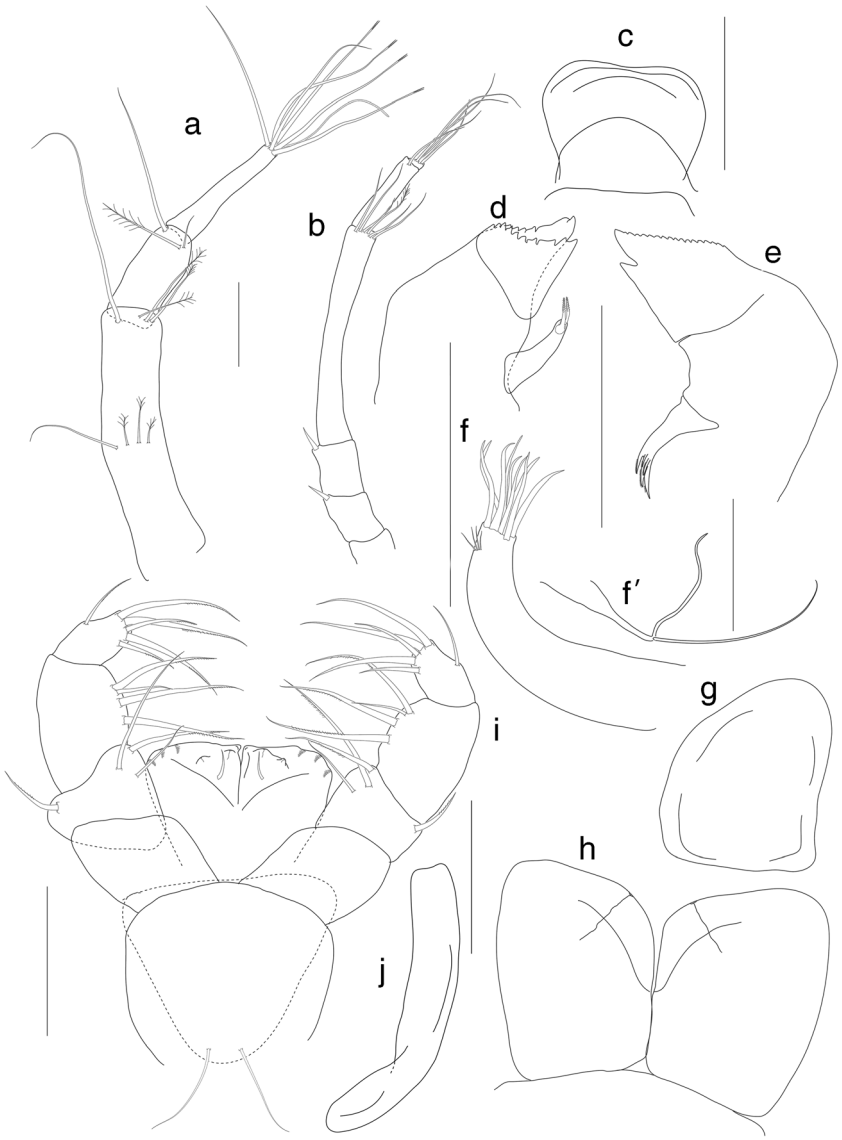

Fig. 13 *Pseudotanais svavarssoni* sp. n., preparatory female. A antennule, B antenna, C labrum, D left mandible, E right mandible, F maxillule endite, F' maxillule palp, G maxilla, H labium, I maxilliped, J epignath. Scale: 0.1 mm for A–B and 0.01 for C–J

Remarks: *Pseudotanais misericorde* sp. n. represents the group of blind pseudotanaids with a forcipate chela and exopod of the uropod almost as long as the endopod. These two characters delineate also *Pseudotanais vulsella* Bird and Holdich, 1989b and *P. falcicula* Bird and Holdich, 1989a, both recorded in Porcupine Bank and Rockall Trough.

P. misericorde, as *P. vulsella*, has the same conical tubercles on distal margin of maxilliped endites but the new species can be distinguished from *P. vulsella* by slender blade-like carpal spines ("blade" part is much narrower than in all other species). In *P. falcicula* tubercles in edge of the maxilliped endites are very small (Bird and Holdich, 1989b, Fig. 19g) besides straight distal spines in chela dactylus and fixed finger, what allow to comfortably distinguish it *P. falcicula* from the new species.

Pseudotanais svavarssoni sp. n.

Figs. 12, 13, and 14

Material examined: Holotype: neutrum ZMH K-54858, 1168-1, 67° 36.38' N 007° 00.08′ W, depth 2372.6 m, EBS, 19 Sep 2011.

Paratypes: five neutri, one manca, ZMH K-54859, St. 1152-1, 69° 5.60′ N 9° 56.01′ W, depth 2172.6 m, GKG, 17 Sep 2011; neutrum, ZMH K-54860, St. 1155-1, 69° 06.89′ N 009° 54.72′ W, depth 2203.8 m, EBS, 17 Sep 2011; 92 neutri, 35 juvenile males, ZMH K-54861, St. 1159-1, 69° 06.66′ N 009° 55.02′ W, depth 2202.8 m, EBS, 17 Sep 2011; one neutrum, one juvenile male, ZMH K-54862, St.1166-1, 67° 35.28′ N 6° 57.47′ W, depth 2401.8 m, GKG, 19 Sep 2011; 43 neutri, (one dissected), five juvenile males ZMH K-54863, 1168-1, 67° 36.38′ N 007° 00.08′ W, depth 2372.6 m, EBS, 19 Sep 2011.

Diagnosis: Eyes absent. Carapace, pereonites, and pleonites combined length range between 1.2 and 1.7 mm. Pereonite-1 the shortest. Antennule article-1 four times as long

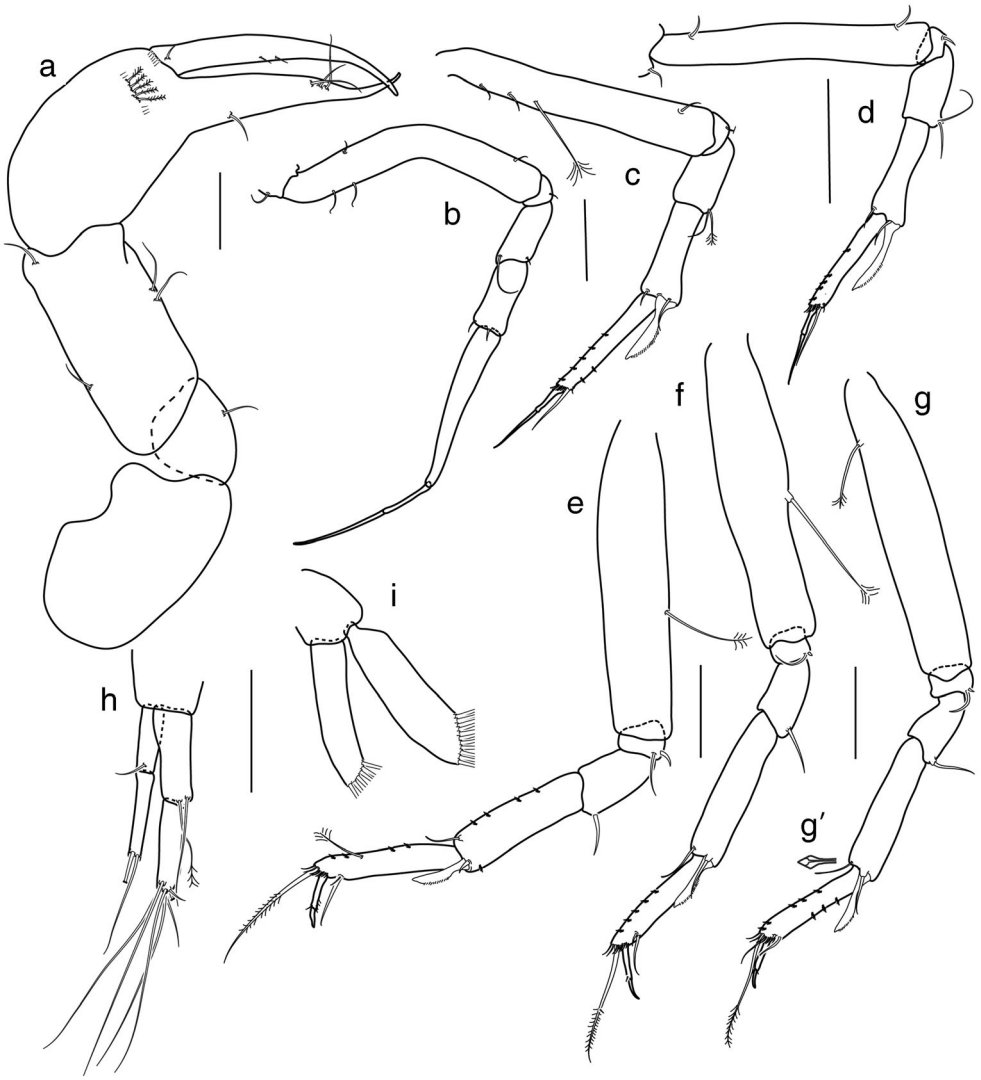

Fig. 14 *Pseudotanais svavarssoni* sp. n., preparatory female. A cheliped, B pereopod-1, C pereopod-2, D pereopod-3, E pereopod-4, F pereopod-5, G pereopod-6, H uropod, and I pleopod. Scale: 0.1 mm

as wide. Antenna articles 2–3 with distal simple setae. Left mandible with two teeth. Maxilliped endites with small tubercles. Cheliped elongated, carpus 1.7–2.1 times as long as wide, propodus 1.4–1.6 times as long as wide. Pereopod-1 propodus 2.2–2.5 times as long as carpus, propodus 1.1–1.3 times as long as combined length of dactylus and unguis. Pereopods 2−6 carpal blade-like spine well developed. Pereopod-3 propodus 1.4–1.7 times as long as blade-like spine. Pereopod-6 propodus 2.6–6.4 times as long as distal carpal seta ratio. Females with pleopods. Uropod exopod two articulated, 0.8 times as long as endopod.

Etymology: The species named after Jörundur Svavarsson, a professor in marine biology at the University of Iceland, the great enthusiast of Icelandic nature and wonderful fellow on the land as well as on the sea.

Description of neutrum: *Body* (Fig. 12) 1.7 mm long, over three times as long as wide. Carapace 18% of total body length, subtriangular, naked. *Pereon* 58% of total body length, pereonite-1, 0.4 times as long as pereonite-2; pereonite-2 0.9 times as long as pereonite-3; pereonite-3 0.6 times as wide as pereonite-4; pereonite-4 0.8 times as long as pereonte-5; pereonite-5 1.5 times as long as pereonite-6; pereonites 1−6: 0.1, 0.3, 0.3, 0.4, 0.5, and 0.4 times as long as wide, respectively; pereonites 1, 4, and 5 with one lateral seta on each margin. *Pleon* 18.8% of total body length, with five similar in length pleonites, each 6.4 times as long as wide, with one seta on lateral margin. *Pleotelson* 6% of total body length; pleonites together with pleotelson almost as long as pereonite-2, two setae on pleotelson distal margin.

Antennule (Fig. 13a) article-1 4.0 times as long as wide, with long simple, and three midlength penicillate setae, and three penicillate and long simple seta distally; article-2 2.2 times as long as wide, and 0.4 times as long as article-1, with one outer distal seta longer that article-3, one penicillate and one simple seta distally; article-3 1.2 times as long as article-2, with two simple and four distally trifurcate and one aesthetasc, distally.

Table 4 Geographical distribution of North Atlantic Pseudotanaidae species. * type localities/source of type localities; 1: Lillieborg 1864, 2: Sars 1882, 3: Hansen 1887, 4: Sars, 1869, 5: Hansen 1913, 6: Hansen H.J. in Hansen 1913, 7: Horring in Hansen 1913, 8: Kruuse in Hansen 1913, 9: Norman in Hansen 1913, 10: Ryder in Hansen 1913, 11: Sars in Hansen 1913, 12: Scott in Hansen 1913, 13: Stappers in Hansen 1913, 14: Vanhoffen in Hansen 1913, 15: Wandel in Hansen 1913, 16: Stephensen 1937, 17: Delamare-Deboutteville 1960, 18: Bruce et al. 1963, 19: Greve 1965a, b, c, 20: Just 1970, 21: Dahl in Sieg 1977, 22: Fee in Sieg 1977, 23: Hatch in Sieg 1977, 24: Sieg 1977, 25: Delamare-Deboutteville et al. 1955 in Sieg 1983, 26: Holdich and Jones 1983, 27: Bird and Holdich, 1989a, 28: Bird and Holdich, 1989b, 29: Błażewicz-Paszkowycz and Bamber 2011, 30: Vanhoffen in Sieg 1977, 31: Kudinova-Pasternak in Sieg 1977

Area	Species/localities	Latitude [N]	*A. longipes*	*A. similis*	*Mystriocetrus serratus*	*Parapseudtanais abyssalis*	*P. abyssi*	*P. affinis*	*P. colonus*	*P corolatus*
Bay of Biscay	South	44	–	–	–	–	–	–	–	–
Biscay Abyssal Plains		46	–	–	–	–	–	–	–	–
Bay of Biscay	North	47	–	–	+	+*	–	–	+*	–
Roscoff/Bloscon		48	–	+	–	–	–	–	–	–
Porcupine Abyssal Plains		48–50	–	–	+	–	–	–	–	–
British coast	Braden, Plymouth	50	–	–	–	–	–	–	–	–
Porcupine Seabight		50–51	–	–	+	–	–	–	–	–
Celtic and Armorican Slope		50–51	–	–	–	–	–	–	–	–
British coast	Isle of Man	55	–	–	–	–	–	–	–	–
Feni Ridge		54–55	–	–	+	–	–	–	–	–
Rockall Trough		54–57	–	–	+*	–	–	–	–	–
Sweaden coast	Sund	55	–	–	–	–	–	–	–	–
Sweaden coast	Kategatt	56	–	–	–	–	–	–	–	–
British coast		56	–	–	–	–	–	–	–	–
Hebridean Slope		56–58	–	–	–	–	–	–	–	–
Sweaden coast	Skagerrak	58	–	–	–	–	–	–	–	–
Sweaden coast	Gullmar fiord	58	–	–	–	–	–	–	–	–
Norwey coast	south of Bergen	60	–	–	–	–	–	–	–	–
Iceland coast	Iceland Basin	60–63	–	–	–	–	–	+	–	–
Iceland coast	Irminger Basin	60–63	+*	–	–	–	–	–	–	–
Norwegian coast		60–72	–	–	–	–	–	–	–	–
Norwey coast	Trondheimfiord	63	–	–	–	–	–	–	–	–
Davis Strait		61–66	–	–	–	–	+*	+	–	+*
Iceland coast	IF Ridge	63–64	–	–	–	–	–	+	–	–
Greenland coast	Ameralik fiord	64	–	–	–	–	–	–	–	–
Greenland coast	Angmasivik	64	–	–	–	–	–	–	–	–
Iceland coast	Denmark Strait	65–67	–	–	–	–	–	–	–	–
Norwey coast	vicinity of Nesna	66	–	–	–	–	–	–	–	–
Iceland coast	Norwegian Sea	66–67	–	–	–	–	–	+	–	–
Iceland coast	Iceland Sea	66–67	–	–	–	–	–	+	–	–
Norwey coast	Raunefiord	67	–	–	–	–	–	–	–	–
Greenland coast	Kap Dalton	69	–	–	–	–	–	–	–	–
Greenland coast	Turner Sound	69	–	–	–	–	–	–	–	–
Norwey coast	Balsfjord	69	–	–	–	–	–	–	–	–
Norwey coast	vicinity of Malangen	69	–	–	–	–	–	–	–	–
Norwey coast	Ullsfjord	69	–	–	–	–	–	–	–	–
Norwey coast	Ramfiord	69	–	–	–	–	–	–	–	–
Finmark coast		69	–	–	–	–	–	–	–	–

Table 4 (continued)

Area	Species/localities	Latitude [N]	*A. longipes*	*A. similis*	*Mystriocetrus serratus*	*Parapseudtanais abyssalis*	*P. abyssi*	*P. affinis*	*P. colonus*	*P corolatus*
	close upon the frontiers of Russia									
Greenland coast	Denmark Island	70	–	–	–	–	–	–	–	–
Greenland coast	Karajak Fiord	70	–	–	–	–	–	–	–	–
Jan Mayen		70	–	–	–	–	–	+	–	–
Norwey coast	vicinity of Kvalsund	70	–	–	–	–	–	–	–	–
Norwey coast	vicinity of Kvaloy	70	–	–	–	–	–	–	–	–
Norwey coast	Varanger Fjord	70	–	–	–	–	–	+	–	–
Greenland coast	Forsblad fiord	72	–	–	–	–	–	+	–	–
Greenland coast	Upernivik	72	–	–	–	–	–	–	–	–
Norwey coast	Håkon Mosby Mud Volcano	72	–	–	–	–	–	+	–	–
Barents Sea		76	–	–	–	–	–	–	–	–
Norwey coast	Spitsbergen	76–79	–	–	–	–	–	–	–	–
Greenland coast	Jørgen Brønlund Fiord	82	–	–	–	–	–	+	–	–
Source			5	17, 24*, 25	28	28	5	3*, 5, 20, 29	27	27
Localities other than N Atlantic							Antarktyka	Kra Sea*; Alaska		
Source							30	31		

Area	*P. denticulatus*	*P. facifer*	*P. falicula*	*P. forcipatus*	*P. jonesi*	*P. lilieborgie*	*P. longispinsus*	*P. macrocheles*	*P. oculatus*	*P. scalpellum*
Bay of Biscay	+	–	–	–	–	–	–	–	–	–
Biscay Abyssal Plains	+	–	+	–	–	–	+	–	–	–
Bay of Biscay	+	–	+	–	–	–	+*	–	–	–
Roscoff/Bloscon	–	–	–	–	–	–	–	–	–	–
Porcupine Abyssal Plains	+	–	+	–	–	–	+	–	–	–
British coast	–	–	–	–	+*	–	–	–	–	–
Porcupine Seabight	+*	–	+	–	–	–	+	–	–	+
Celtic and Armorican Slope	+	–	–	–	–	–	–	–	–	–
British coast	–	–	–	–	+	–	–	–	–	–
Feni Ridge	+	–	–	–	–	–	–	–	–	–
Rockall Trough	+	–	+*	–	–	–	+	–	–	+*
Sweaden coast	–	–	–	+	–	–	–	–	–	–
Sweaden coast	–	–	–	+	–	–	–	–	–	–
British coast	–	–	–	+	+	–	–	–	–	–
Hebridean Slope	+	–	–	–	–	–	–	–	–	–
Sweaden coast	–	–	–	+	–	–	–	–	–	–
Sweaden coast	–	–	–	+*	–	–	–	–	–	–
Norwey coast	–	–	–	–	–	–	–	+	–	–
Iceland coast	–	–	–	–	–	–	–	–	–	–
Iceland coast	–	–	–	–	–	–	–	–	–	–

Table 4 (continued)

Area	*P. denticulatus*	*P. facifer*	*P. falicula*	*P. forcipatus*	*P. jonesi*	*P. lilieborgie*	*P. longispinsus*	*P. macrocheles*	*P. oculatus*	*P. scalpellum*
Norwegian coast	–	–	–	+	–	–	–	–	–	–
Norwey coast	–	–	–	+	–	–	–	–	–	–
Davis Strait	–	–	–	–	–	–	–	–	+*	–
Iceland coast	–	–	–	+	–	+	–	–	–	–
Greenland coast	–	–	–	+	–	–	–	–	–	–
Greenland coast	–	–	–	–	–	+	–	–	+	–
Iceland coast	–	–	–	–	–	+	–	–	–	–
Norwey coast	–	–	–	+	–	–	–	–	–	–
Iceland coast	–	–	–	–	–	–	–	–	–	–
Iceland coast	–	–	–	+	–	+	–	–	–	–
Norwey coast	–	–	–	–	–	–	–	+	–	–
Greenland coast	–	–	–	+	–	+	–	–	–	–
Greenland coast	–	–	–	+	–	–	–	–	–	–
Norwey coast	–	–	–	+	–	–	–	–	–	–
Norwey coast	–	–	–	+	–	–	–	–	–	–
Norwey coast	–	–	–	+	–	–	–	+	–	–
Norwey coast	–	–	–	+	–	–	–	–	–	–
Finmark coast	–	–	–	+	–	–	–	–	–	–
Greenland coast	–	–	–	+	–	+	–	–	–	–
Greenland coast	–	–	–	+	–	+	–	–	–	–
Jan Mayen	–	–	–	–	–	+	–	–	–	–
Norwey coast	–	–	–	+	–	+	–	–	–	–
Norwey coast	–	–	–	+	–	–	–	–	–	–
Norwey coast	–	–	–	–	–	+*	–	+*	–	–
Greenland coast	–	–	–	–	–	–	–	–	–	–
Greenland coast	–	–	–	–	–	–	–	–	+	–
Norwey coast	–	+*	–	–	–	–	–	–	–	–
Barents Sea	–	–	–	+	–	+	–	–	+	–
Norwey coast	–	–	–	–	–	–	–	–	+	–
Greenland coast	–	–	–	–	–	+	–	–	–	–
Source	27*	29	28	1*, 5, 6, 7, 9, 11, 12, 13, 14, 16, 19, 21	18, 24*, 26, 27	4*, 5, 7, 8, 10, 11, 14, 16, 19, 20, 28	28*	2*, 19	5*, 8, 10, 15, 22, 23, 24	28*
Localities other than N Atlantic				Franz Joseph Land						
Source				12						

Area	*P. spatula*	*P. spicatus*	*P. vulsella*	*A.* cf. *longipes*	*Mystriocetrus biho* n. sp	*P. misericorde* n sp.	*P. sigrunis n sp.*	*P. svavarrsoni n sp.*	*P. svavarrsoni complex*
Bay of Biscay	+	+	–	–	–	–	–	–	–
Biscay Abyssal Plains	–	–	–	–	–	–	–	–	–
Bay of Biscay	–	+	–	–	–	–	–	–	–
Roscoff/Bloscon	–	–	–	–	–	–	–	–	–
Porcupine Abyssal Plains	–	+	–	–	–	–	–	–	–

Table 4 (continued)

Area	*P. spatula*	*P. spicatus*	*P. vulsella*	*A.* cf. *longipes*	*Mystriocetrus biho* n. sp	*P. misericorde* n sp.	*P. sigrunis n sp.*	*P. svavarrsoni n sp.*	*P. svavarrsoni complex*
British coast	–	–	–	–	–	–	–	–	–
Porcupine Seabight	+*	+*	+*	–	–	–	–	–	–
Celtic and Armorican Slope	+	–	+	–	–	–	–	–	–
British coast	–	–	–	–	–	–	–	–	–
Feni Ridge	–	–	+	–	–	–	–	–	–
Rockall Trough	–	+	+	–	–	–	–	–	–
Sweaden coast	–	–	–	–	–	–	–	–	–
Sweaden coast	–	–	–	–	–	–	–	–	–
British coast	–	–	–	–	–	–	–	–	–
Hebridean Slope	+	–	+	–	–	–	–	–	–
Sweaden coast	–	–	–	–	–	–	–	–	–
Sweaden coast	–	–	–	–	–	–	–	–	–
Norwey coast	–	–	–	–	–	–	–	–	–
Iceland coast	–	–	–	–	–	–	–	–	+
Iceland coast	–	–	–	+	+	+	+	–	+
Norwegian coast	–	–	–	–	–	–	–	–	–
Norwey coast	–	–	–	–	–	–	–	–	–
Davis Strait	–	–	–	–	–	–	–	–	–
Iceland coast	–	–	–	–	–	–	+	–	+
Greenland coast	–	–	–	–	–	–	–	–	–
Greenland coast	–	–	–	–	–	–	–	–	–
Iceland coast	–	–	–	–	–	–	+	–	+
Norwey coast	–	–	–	–	–	–	–	–	–
Iceland coast	–	–	–	–	–	–	–	–	–
Iceland coast	–	–	–	–	–	–	+	+	–
Norwey coast	–	–	–	–	–	–	–	–	–
Greenland coast	–	–	–	–	–	–	–	–	–
Greenland coast	–	–	–	–	–	–	–	–	–
Norwey coast	–	–	–	–	–	–	–	–	–
Norwey coast	–	–	–	–	–	–	–	–	–
Norwey coast	–	–	–	–	–	–	–	–	–
Norwey coast	–	–	–	–	–	–	–	–	–
Finmark coast	–	–	–	–	–	–	–	–	–
Greenland coast	–	–	–	–	–	–	–	–	–
Greenland coast	–	–	–	–	–	–	–	–	–

Table 4 (continued)

Area	*P. spatula*	*P. spicatus*	*P. vulsella*	*A.* cf. *longipes*	*Mystriocetrus biho* n. sp	*P. misericorde* n sp.	*P. sigrunis n sp.*	*P. svavarrsoni n sp.*	*P. svavarrsoni complex*
Jan Mayen	–	–	–	–	–	–	–	–	–
Norwey coast	–	–	–	–	–	–	–	–	–
Norwey coast	–	–	–	–	–	–	–	–	–
Norwey coast	–	–	–	–	–	–	–	–	–
Greenland coast	–	–	–	–	–	–	–	–	–
Greenland coast	–	–	–	–	–	–	–	–	–
Norwey coast	–	–	–	–	–	–	–	–	–
Barents Sea	–	–	–	–	–	–	–	–	–
Norwey coast	–	–	–	–	–	–	–	–	–
Greenland coast	–	–	–	–	–	–	–	–	–
Source	28*	28*	28						
Localities other than N Atlantic Source									

Antenna (Fig. 13b) shorter than antennule; article-1 fussed with body, broken during dissection; article-2 1.1 times as long as wide, with spine on outer margin; article-3 as article-2; article-4 8.0 times as long as wide, with five simple and one penicillate setae, distally; article-5 2 times as long as wide, 0.3 times as long as article-4, with simple distal seta; article-6 short, with five simple distal setae.

Mouthparts. *Labrum* (Fig. 13c) rounded, hood-shape, naked. *Left mandible* (Fig. 13d) incisor margin irregularly serrated, *lacinia mobilis* large and irregularly serrated; molar acuminate with two serrated distal spines. *Right mandible* (Fig. 13e) with regularly serrated incisor, *lacinia mobilis* fussed to a small process; molar acuminate, with five serrated distal spines. *Maxillule* (Fig. 13f) distally bent, with nine distal setae and four subdistal fine setae on outer margin endite (Fig. 13f') with two distal setae. *Maxilla* (Fig. 13g) suboval distally, proximal margin flattened, naked. *Labium* (Fig. 13h) simple (accessory lobe not seen), naked. *Maxilliped* (Fig. 13i) basis short, almost as long as wide with two simple proximal setae directed posteriorly to main axis of the body; endites partly fussed, distally separated, distal edge with one seta and a pair of small tubercles on each side, lateral margins finely setose. Palp article-1 naked; article-2 with three setae on inner margin and one seta on outer margin.; article-3 with three long and one short seta on inner margin; article-4 with five simple setae on inner distal margin and one seta on outer margin. *Epignath* (Fig. 13j) naked, linguiform.

Cheliped (Fig. 14a) basis 1.5 times as long as broad; merus subtriangular, with midventral seta; carpus 2.0 times as long as broad, with two midventral setae, and with one subproximal and one distal setae on dorsal margin; chela not-forcipate, slender; propodus (palm) 1.9 times as long as wide, little shorter than fixed finger, and row of five serrated setae on inner side; fixed finger with three setae on cutting edge and one ventral seta, distal spine bent upward; dactylus as long as fixed finger with two seta on inner margin, with distal spine bent downward.

Pereopod-1 (Fig. 14b) slender, coxa with simple seta; basis 6.7 times as long as wide, with two dorsoproximal and one distoventral setae; ischium with one seta, merus 2 times as long as wide, 0.8 times as long as carpus with short distoventral and long dorsoproximal setae; carpus 2.5 times as long as wide, 0.4 times as long as propodus, with two small distal setae; propodus 6.6 times as long as wide, naked; dactylus 0.3 times as long as propodus; unguis 1.8 times as long as dactylus, combined 0.9 times as long as propodus.

Pereopod-2 (Fig. 14c) basis seven times as long as wide, with two simple and one penicillate seta dorsoproximally, one distoventral seta; ischium with small simple seta; merus 1.8 times as long as wide, 0.7 times as long as carpus, with simple and penicillate setae distoventrally; carpus 3.3 times as long as wide, 0.6 times as long as propodus, with two simple setae and long blade-like spine propodus 7 times as long as wide, with simple distal seta; numerous microtrichiae in distal half;

Table 5 Characters of the "affinis," "denticulatus," and "longisetosus"' group

		Reference	Antenna article 2–3	Mandibles	Pereopod-1 merus distodorsal seta	Pereopod-1 carpus distodorsal ornamentation	Pereopods 2–3 merus distoventral ornamentation	Number of the pereonite bearing setae	Number of the pleonite bearing setae
Affinis'	*P. affinis*	Hansen 1886/87; Ingolf st 25 (Davis Strait)	Spines	?	Long	Short	Spine	4–6	2,4,5
	P. scalpellum	Bird and Holdich 1989	Spines	Acuminate (4 spines)	Long	Short	Spine and seta	1, 4–6	1,2
	P. svavarssoni sp. n.	present study	Spines (slender)	Acuminate 2 spines (L); 5 spines (R)	Long	Short	Two long setae (one serrated)	1, 4, 5	1–5
	Pseudotanais sp. P	McLelland 2008	Spines	Acuminate (3–5 spines)	Absent	Long	Spine	1, 3–6	1–5
Denticulatus'	*P. corollatus*	Hansen 1913, Sieg 1977	Spines	Wide	Short	Short	Two setae	0	0
	P. denticulatus	Bird and Holdich 1985	Spines	Wide	Short	Short	Spine and seta	1, 4–6	0
	Pseudotanais sp. A	McLelland 2008	Spines	Wide	Absent	Short			
Longisetosus'	*P. longisetosus*	Sieg, 1977	Spine and seta	Acuminate (central spine long)	Long	Long	Spine and seta	0	0
	P. longispinus	Bird and Holdich 1989a, b	Spines	Acuminate (central spine long)	Long	Long	Spine and seta	0	0
	P. nipponicus	McLelland 2007	Spines	Acuminate (central spine long)	Long	Long	Spine and seta	1, 4–6 (dorso lateral), 2–6 (antero-lateral), 4–5 (medio-lateral seta)	5 (2 pairs)
	P. spatula	Bird and Holdich 1989a, b	Spines	Acuminate	Long	Long	Spine and seta	1,3	0
	Pseudotanais sp. O	McLelland 2008	"Stout spiniform seta"	Acuminate (one spine long)	Long	Long	Spine and seta	3–6	1–5

L left, *R* right

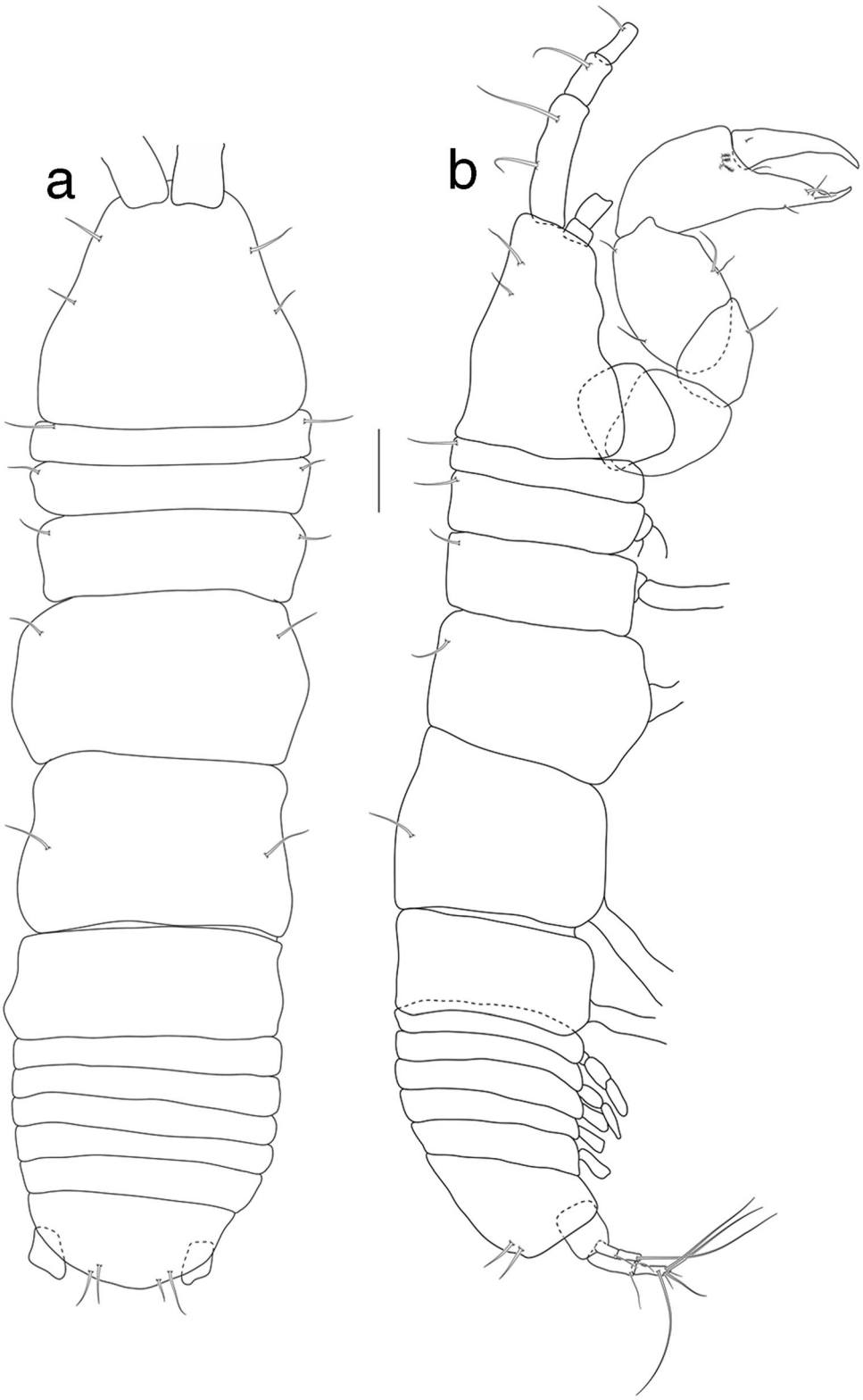

Fig. 15 *Pseudotanais sigrunis* sp. n. preparatory female, holotype (cat no…). **a** Dorsal view. **b** Lateral view. Scale: 0.1 mm

dactylus 0.6 times as long as propodus, unguis 1.7 times as long as dactylus, together 0.9 times as long as propodus.

Pereopod-3 (Fig. 14d) similar to pereopod-2, but basis with ventroproximal and ventrodistal simple setae; carpus 0.9 times as long as propodus, blade-like spine 0.7 times as long as propodus; propodus 7.3 times as long as wide.

Pereopod-4 (Fig. 14e) 4.1 times as long as wide, with penicillate midventral seta; ischium with one short and one long

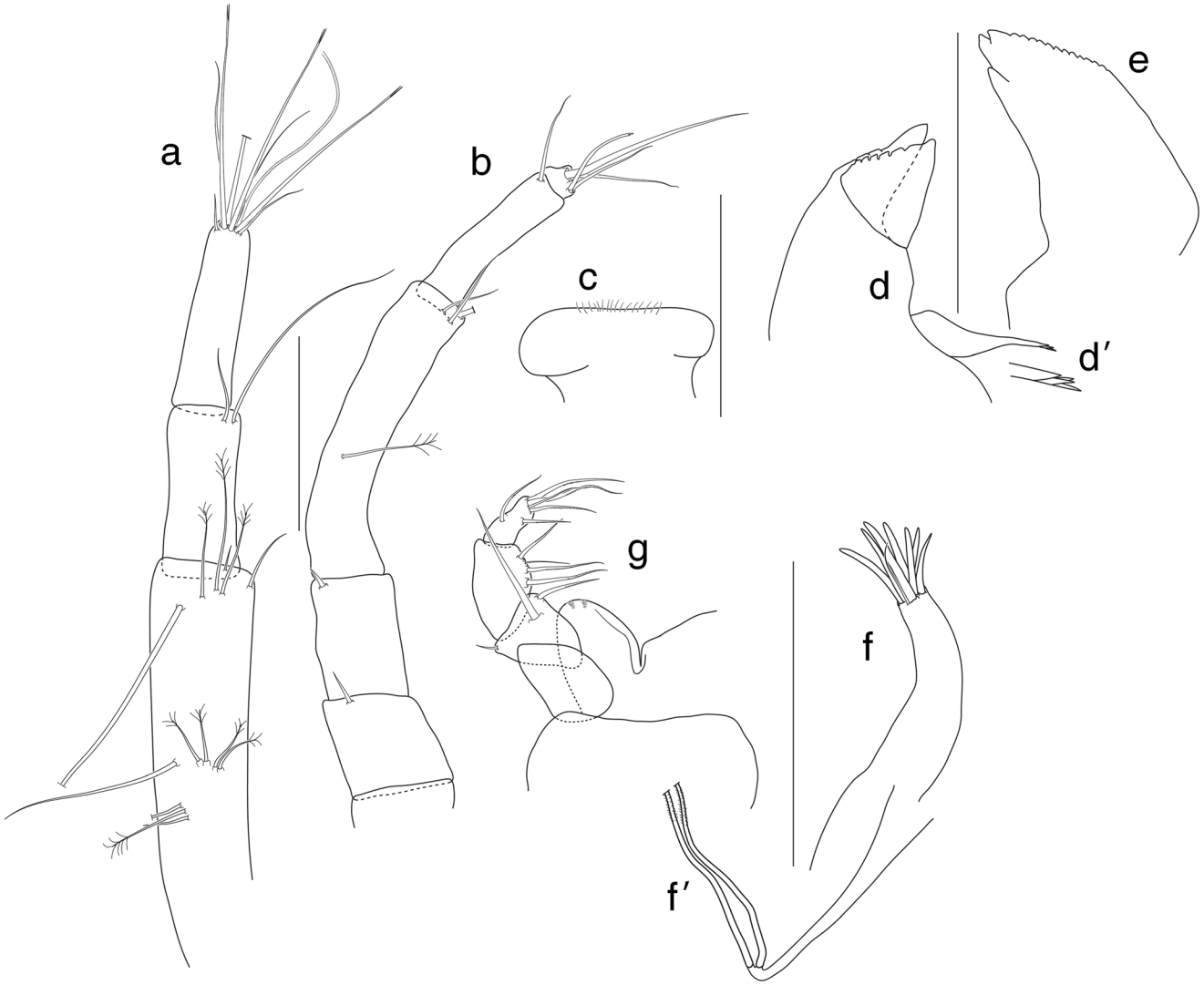

Fig. 16 *Pseudotanais sigrunis* sp. n. preparatory female. A antennule, B antenna, C labrum, D left mandible, D' molar of left mandible, E right mandible, F maxillule endite, F' maxillule palp, G maxilliped. Scale: 0.1 mm for A, B and 0.01 for C–F

simple setae; merus 1.5 times as long as wide, 0.5 times as long as carpus, with one distoventral seta; carpus 3.3 times as long as wide, 0.9 times as long as propodus, dorsal margin with microtrichiae, distodorsal sensory seta and distoventral small spine and blade-like spine (0.4 times as long as propodus); propodus 6 times as long as wide, with distal margin setose and dorsal margin with microtrichiae, short and long ventrodistal setae and long (as long as propodus) penicillate, distodorsally; dactylus 0.2 times as long as propodus, unguis 0.3 times as long as dactylus, combined 0.3 times as long as propodus.

Pereopod-5 (Fig. 14f) similar to pereopod-4.

Pereopod-6 (Fig. 14g) similar to pereopod-4, but propodus with additional longer seta.

Pleopod (Fig. 14i) endopod 4.6 times as long as wide, with six distal setae; exopod 3.2 times as long as wide, with eleven distal setae.

Uropod (Fig. 14h) basis naked; exopod 0.8 times as long as endopod, with two articles, article-1 0.8 times as long as article-2, with distal seta, article-2 with at two distal setae; endopod with two subequal articles, article-1 with one simple and penicillate distal setae, article-2 with four long, two short simple setae and one plumose seta terminally (Table 4).

Distribution: *Pseudotanais svavarssoni* sp. n. was represented in Norwegian Sea, in the depth range 2172.6–2401.8 m (Fig. 7a).

Remarks: *Pseudotanais svavarssoni* sp. n. with characters such as (1) spines on antenna articles 2−3, (2) acuminate molar, (3) long distodorsal seta on pereopod-1 merus, and (4) elongated uropods, with exopod somewhat shorter than endopod, can be unequivocally regarded as representing the "*affinis*" group. It is distinguished from other members of the group by (1) relatively slender spines on antenna articles 2−3 (the spines are strong in *P. affinis*, *P. scalpellum*, and

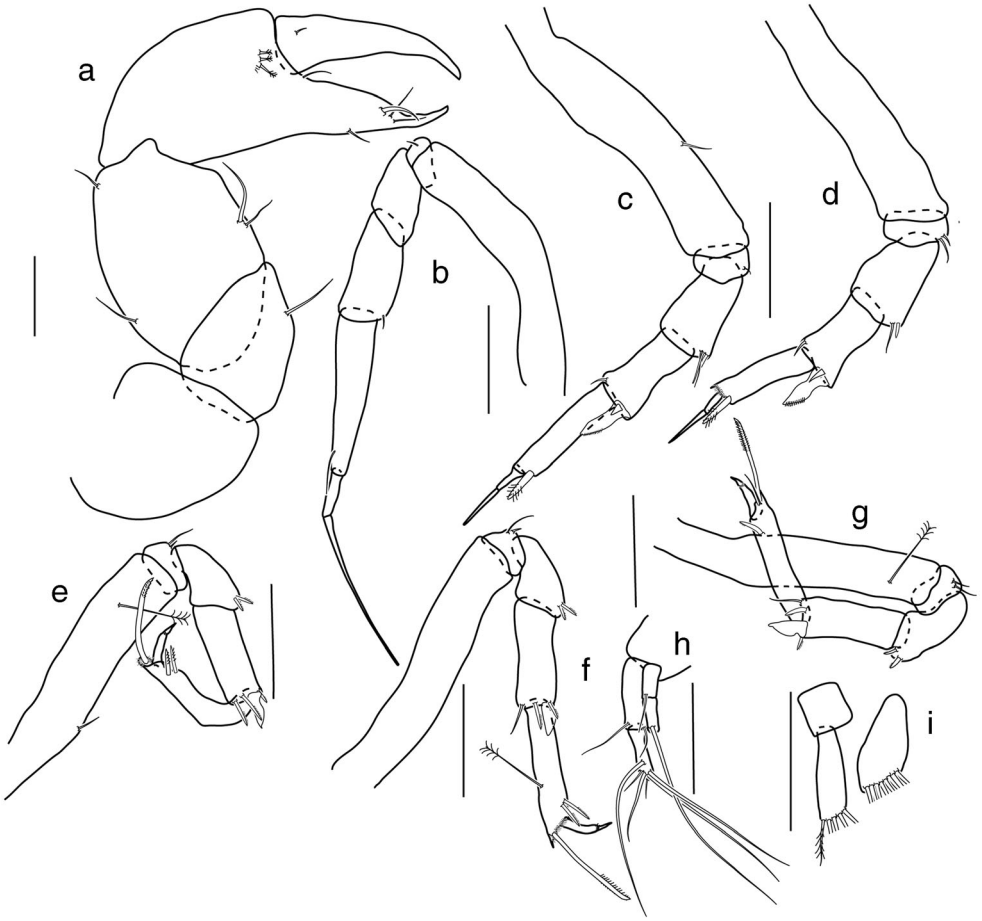

Fig. 17 *Pseudotanais sigrunis* sp. n., preparatory female. **a** Cheliped. **b** Pereopod-1. **c** Pereopod-2. **d** Pereopod-3. **e** Pereopod-4. **f** Pereopod-5. **g** Pereopod-6. **h** Uropod. **i** Pleopod. Scale: 0.1 mm

Pseudotanais sp. P), (2) the presence of two setae on merus of the pereopods 2–3 (the spine in *P. affinis* and *P. scalpellum*, and the spine and seta in *Pseudotanais* sp. P are relatively long), as well as a slender dactylus and unguis in the pereopods 4–6 (see Table 5).

The history of the "*affinis*: group is quite convoluted (Bird and Holdich 1985, 1989a). The first species, *Pseudotanais affinis* Hansen, 1887, was described from Kara Sea; it was subsequently recognized, based on the Ingolf collection, in numerous locations, e.g., the Davis Strait, around Iceland, south of Jan Mayen, an East Greenland fjord (Hansen 1913; Fig. 2b). Morphological differences between the specimens studied by Hansen (1913) were considered the intraspecific variation, although the eurytopic distribution of the species, reported from both "warm" (2.4–4.5 °C) and "cold" (0.4–0.9 °C) areas over a relatively wide depth range (582–2196 m) suggests a complex of (possibly) cryptic species. Later on, the distribution range of the species was extended to cover an area between off the British coasts down to the Bay of Biscay (Bird and Holdich, 1989b).

The wide distribution and interspecific morphological variability of pseudotanaids was addressed by Bird and Holdich, 1989a). Having conducted comprehensive morphological studies which involved re-examination of Hansen's collection, they concluded that the species Sieg (1977) identified and illustrated as *P. affinis* was hardly a member of the "*affinis*" group on account of its wide mandible molar and the setae on antenna articles 2–3. As a result, they erected two new species: *P. corollatus* Bird and Holdich, 1989b to accommodate the former *P. affinis* from the Davis Strait (Hansen 1913), and *P. denticulatus* for the former *P. affinis* from off the west coast of Great Britain and the Bay of Biscay (Bird and Holdich, 1989a).

The presence of the wide mandible led Bird to assume that *P. denticulatus* and *P. corollatus* may come from the same group of species, the "*denticulatus*." Another species that could be assigned to the group is *Pseudotanais* sp. A (McLelland, 2008). Differences between the "*affinis*" and the "*denticulatus*" species-groups are listed in Table 5.

As emphasized by Bird and Holdich (1989b), we are far away from fully recognizing the complexity of the "*affinis*" species-group. Based on the existing knowledge, they provisionally assigned three other species to the group: *P. spatula* Bird and Holdich, 1989a; *P. scalpellum* Bird and Holdich, 1989b; and *P. longispinus* Bird and Holdich, 1989a. Although all those species are, most likely, phylogenetically closely related to the "*affinis*" group (Jakiel unpublished data), they may represent two separate evolutionary lines. The

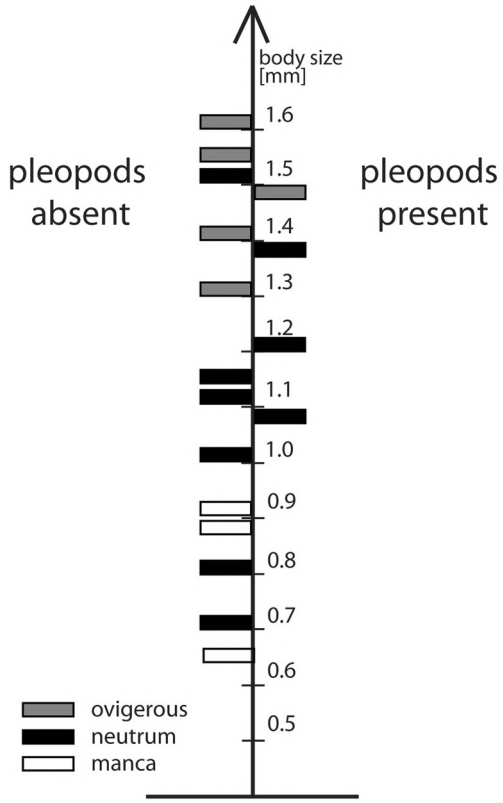

Fig. 18 Morphological variability of the occurrence of the pleopods in different life stages in *Pseudotanaid sigrunis* sp. n.

first (*Pseudotanais longisetosus* Sieg, 1977; *P. longispinus* Bird and Holdich, 1989a; *P. nipponicus* McLelland, 2007; *P. spatula* Bird and Holdich, 1989b; and *Pseudotanais* sp. O, McLelland, 2008) is defined by two autapomorphies: the presence of a long seta on the merus and carpus of pereopod-1 and a few setae on the pereopod 1–3 basis. Members of the other line show a long seta only on the merus of pereopod-1 and few (if any) setae on the basis of pereopods 1–3. Further analysis of other *Pseudotanais* species with an acuminate mandible and the uropod exopod slightly shorter than the endopod support distinguishing still one more species-group, the "*longisetosus*." Differences between the "*affinis*" and "*longisetosus*" groups are listed in Table 5.

Pseudotanais svavarssoni species complex

Material examined: two neutri (ZMH K-54810), St. 871-4, 62° 45.31′ N 000° 54.09′ W, depth 1562.7 m, GKG, 26 Jul 2013; two neutri, one juvenile male (ZMH K-54811), St. 872-4, 63° 01.88′ N 001° 29.91′ W, EBS, depth 1858.3 m, 27 Jul 2013; manca (ZMH K-54812), St. 872-5, 63° 01.80′ N 001° 27.05′ W, depth 1842 m, GKG, 27 Jul 2013; two neutri (ZMH K-54813), St. 873-2, 61° 46.63′ N 003° 52.38′ W, depth 835.1 m, GKG, 28 Jul 2013; juvenile male, St. 873-6, 61° 46.52′ N 003° 52.38′ W, depth 833.7 m, EBS, 28 Jul 2013; two neutri (ZMH K-54814), St. 879-2, 63° 06.02′ N 008° 35.14′ W, depth 505.9 m, SG, 31 Jul 2013; two neutri, one manca (ZMH K-54815), St. 879-5, 63° 06.10′ N 008° 34.32′ W, EBS, depth 510.9 m, 31 Jul 2013; neutrum (ZMH K-54816), St. 880-2, 63° 23.36′ N 008° 09.42′ W, depth 686 m, EBS, 31 Jul 2013; juvenile male, (ZMH K-54817), St. 881-4, 63° 34.66′ N 007° 42.69′ W, depth 1043.6 m, EBS, 01 Aug 2013; neutrum (ZMH K-54818), St. 881-6, 63° 38.50′ N 007° 47.03′ W, depth 1073.4 m, VV, 01 Aug 2013; ovigerous female, (ZMH K-54819), St. 882-2, 63° 25.01′ N 010° 58.80′ W, depth 441.4 m, VV, 02 Aug 2013; three neutri, four ovigerous females, two juvenile males, (ZMH K-54820), St. 882-5, 63° 25.04′ N 010° 58.20′ W, 440.5 m, EBS, 02 Aug 2013; neutrum, (ZMH K-54821), St. 963-1, 60° 2.72′ N 21° 29.52′ W–60° 2.73′ N 21° 29.86′ W; depth 2746 m, EBS, 29 Aug 2011; neutrum, (ZMH K-54822) , St. 979-1, 60° 20.87′ N 18° 8.52′ W–60° 20.72′ N 18° 8.60′ W, 2568.8–2571 m, EBS, 30 Aug 2011; three neutri, (ZMH K-54823) , St. 1010-1, 62° 33.17′ N 20° 23.18′ W–62° 33.22′ N 20° 22.88′ W, 1383.3–1387.8 m, EBS, 02 Sep 2011; neutrum, (ZMH K-54824), St. 1019-1, (62° 56.46′ N 20° 44.06′ W–62°

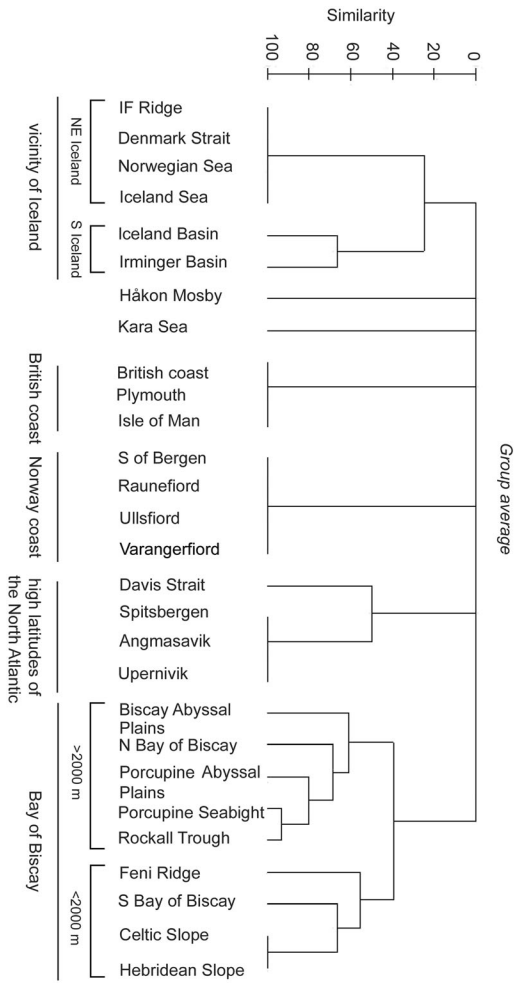

Fig. 19 Dendrogram of similarity (Bray Curtis, average linkage clustering method) of occurrence of Pseudotanaidae fauna in the North Atlantic based on both present study and literature data (see caption of Table 4)

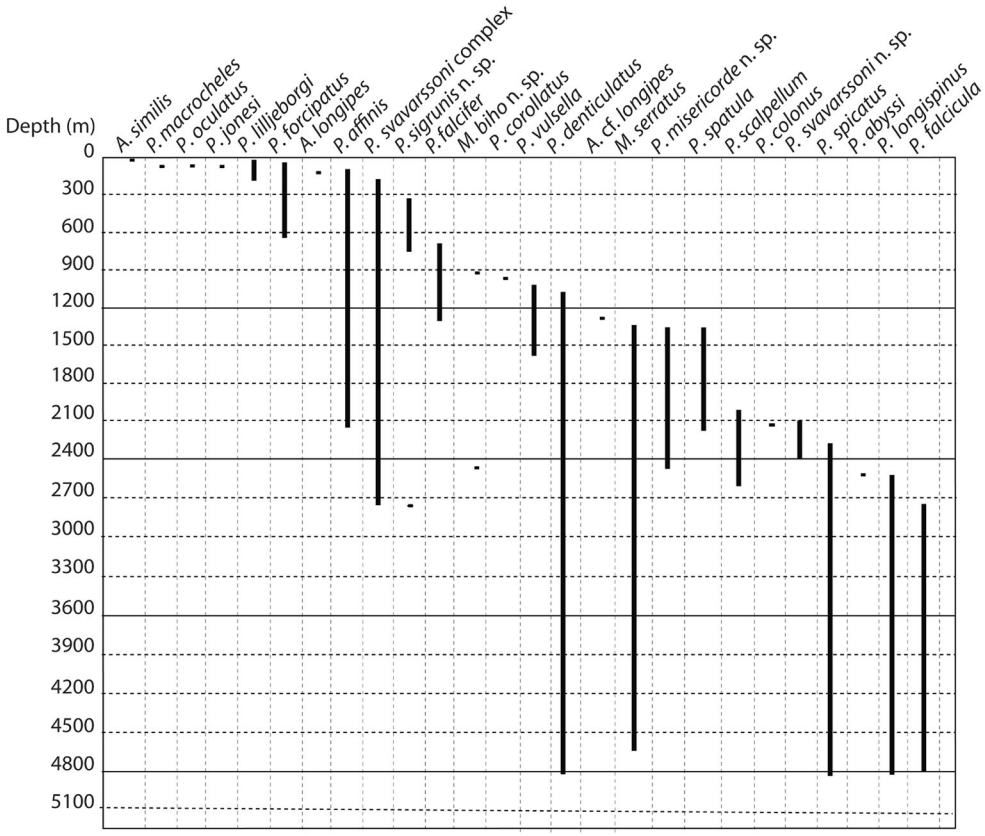

Fig. 20 Bathymetric distribution of the Pseudotanaidae species recorded in the N Atlantic from both the IceAGE collection and literature data. For literature data, see Table 4 caption

56.52′ N 20° 43.77′ W, depth 916.1−909.4 m, EBS, 03 Sep 2011; 15 neutri, three juvenile males, (ZMH K-54825), St. 1043-1, 63° 55.53′ N 25° 57.54′ W−63° 55.62′ N 25° 57.36′ W, depth 214.9−216.5 m, EBS, 05 Sep 2011; neutrum, (ZMH K-54826), St. 1051-1, 61° 37.40′ N 31° 22.11′ W, 2547.5 m, GKG, 07 Sep 2011; two neutri, (ZMH K-54827), St. 1054-1, 61° 36.82′ N 31° 22.26′ W−61° 36.98′ N 31° 22.18’ W, 2545.7–2536.8 m, EBS, 07 Sep 2011; two neutri, (ZMH K-54828), St. 1072-1, 63° 0.97′ N 28° 3.35′ W−63° 1.10′ N 28° 3.15′ W, depth 1564.2–1567 m, EBS, 09 Sep 2011; neutrum, (ZMH K-54829), St. 1086-1, 63° 42.66′ N 26° 22.78′ W−63° 42.78′ N 26° 22.54′ W, depth 688.4−680.3 m, EBS, 09 Sep 2011; neutrum, (ZMH K-54830), St. 1129-1, 67° 38.77′ N 26° 44.78′ W, depth 320.6 m, GKG, 14 Sep 2011; three neutri, (ZMH K-54831), St. 1132-1, 67° 38.48′ N 026° 45.28′ W, 318.1 m, EBS, 14 Sep 2011; neutrum, ovigerous female, (ZMH K-54832), St. 1136-1, 67° 38.06′ N 26° 46,19′ W−67° 37.96′ N 26° 46.42′ W, depth 315.9 m, EBS, 14 Sep 2011; neutrum, (ZMH K-54833), St. 1141-1, 67° 50.22′ N 23° 42.11′ W, depth 1241.6 m, GKG, 15 Sep 2011; four neutri, juvenile male, (ZMH K-54834), St. 1148-1, 67° 50.79′ N 023° 41.76′ W, depth 1248.8 m, EBS, 15 Sep 2011; neutrum male, manca, (ZMH K-54835), St. 1178-1, 67° 38.72′ N 12° 10.10′ W, depth 1818.9 m, GKG, 20 Sep 2011; six neutri, two ovigerous females, (ZMH K-54836), St. 1184-1, 67° 38.63′ N 012° 09.72′ W, depth 1819.3 m, EBS, 20 Sep 2011; three neutri females, two juvenile males, manca, (ZMH K-54837), St. 1188-1, 67° 4.32′ N 13° 0.89′ W, depth 1580.6 m, GKG, 21 Sep 2011; seven neutri, two juveniles male (ZMH K-54838), St. 1212-1, 66° 32.63′ N 012° 52.48′ W, depth 317.2 m, EBS, 22 Sep 2011; five neutri, juvenile male, (ZMH K-54839), St. 1216-1, 66° 18.06′ N 12° 22.38′ W, 730.8 m, GKG, 22 Sep 2011; 5 neutri, (ZMH K-54840), 1219-1, 66° 17.34′ N 012° 20.82′ W, depth 579.1 m, EBS, 22 Sep 2011.

Diagnosis: carapace, pereonites, and pleonites combined length 0.7–1.7 mm; cheliped carpus 1.3–2.0 times as long as wide, propodus 1.3–2.0 times as long as wide; pereopod-1 propodus 1.7–2.6 times as long as carpus, propodus 0.7–1.2 times as long as combined length of dactylus and unguis; pereopod-3 propodus 1.1–1.6 times as long as blade-like spine; pereopod-6 propodus 1.4–4.7 times as long as distal carpal seta.

Distribution: *P. svavarssoni* species complex is widely represented in the studied area and in the widest depth range (214–2746 m). It occurs in all investigated regions: Iceland-Faroe Ridge, Iceland Basin, Irminger Basin, Denmark Strait Norwegian Channel, and Norwegian Sea (Fig. 7a).

Pseudotanais sigrunis sp. n.

Figs 15, 16, and 17

Material examined: Holotype neutrum (ZMH K-54841); St. 1216-1, 66° 1.06′ N 12° 22.38′ W, depth 730.8 m, 22 Sep 2011.

Two ovigerous female, (ZMH K-54842), St. 882-2, 63° 25.01′ N 010° 58.80′ W, depth 441.4 m, 02 Aug 2013; one neutrum, ovigerous female, (ZMH K-54843), St. 882-5, 63° 25.04′ N 010° 58.20′ W, depth 440.5 m, EBS02 Aug 2013; manca (ZMH K-54844), St. 880-3, 63° 24.79′ N 008° 11.63′ W, depth 688.1 m, GKG, 31 Jul 2013; neutrum (ZMH K-54845), St. 963-1, 60° 2.72′ N 21° 29.52′ W–60° 2.73′ N 21° 29.86′ W, depth 2746.4−2746 m, EBS, 29 Aug 2011; neutrum, (ZMH K-54846), St. 1116-1, 67° 12.82′ N 26° 16.31′ W, depth 683.1 m, GKG, 14 Sep 2011; three neutri, ovigerous female, manca, (ZMH K-54847), St. 1212-1, 66° 32.63′ N 012° 52.48′ W, depth 317.2 m, EBS, 22 Sep. 2011; two neutri, manca, (ZMH K-54848), St. 1216-1, 66° 18.06′ N 12° 22.38′ W, depth 730.8 m, GKG, 22 Sep 11; neutrum, ovigerous female, (ZMH K-54849), St. 1219-1, 66° 17.34′ N 012° 20.82′ W, depth 579.1 m, EBS, 22 Sep 2011.

Diagnosis: Eyes absent. Antennule article-1 four times as long as wide. Antenna article-2 with seta, article-3 with spine. Mandible molar acuminate with four spines. Maxilliped endites simple. Cheliped robust, chela not forcipate; carpus 1.6 times as long as wide; unguis and dactylus distal spines inside bent. Pereopods 2−6 carpal blade-like spine well developed. Uropod exopod two articulated, as long as endopod article-1.

Etymology: The species named after Sigrún Haraldsdóttir, a great fellow during cruise IceAGE, who tirelessly helped in sorting of the benthic samples onboard.

Description of neutrum: *Body* (Fig. 15) more than three times as long as broad. Cephalothorax 22% of total body length subtriangular, with two pairs of lateral simple seta. Eyes absent. *Pereon* 55% of total body length. Pereonite-1 0.6 times as long as pereonite-2; pereonite-2 0.7 times as long as pereonite-3; pereonite-3 0.6 times as long as pereonite-4; pereonites-4 0.7 times as long as pereonites-5; pereonites-5 twice as long as pereonite-6; pereonites 0.1, 0.2, 0.3, 0.5, 0.6, and 0.4 times as long as broad respectively (measurements for the holotype); pereonites 1–5 each with a pair of simple lateral setae. Pleonites 15% of total length, as long as pereonite-5. Pleotelson 8% of total length, as long as three pleonites combined length, with two pairs of distal seta.

Antennule (Fig. 16a) article-1 3.7 times as long as wide, with outer medial and distal tufts penicillate (3–5) and simple (1–3) setae. Article-2 2.3 times as long as wide and 0.4 times as long as article-1 with short and long outer distal setae; article-3 as long as article-2, with one aestetasc, four simple, three distally trifurcate and one broken seta.

Antenna (Fig. 16b) aricle-1 fussed with body, article-2 as long as wide with one thin spine, article-3 1.4 times as long as wide, and 1.2 times as long as article-2, with small distal spine; article-4 four times as long as wide and 2.5 times as long as article-3, with one midlength penicillate seta and three distal setae (one broken); article-5 4.2 times as long as wide and 0.5 times as long as article-4, with one distal seta; article-6 short, with three simple and one bifurcated distal setae.

Mouthparts: *Labrum* hood-shaped, weakly setose (Fig. 16c); *left mandible* (Fig. 16d) incisor margin weakly serrated, *lacinia mobilis* large and irregularly serrated; molar acuminate with four distal spines (Fig. 16d'). *Right mandible* (Fig. 16e) with regularly serrated incisor, *lacinia mobilis* fussed to a small process; molar not seen. *Maxillule* (Fig. 16f) tipped with seven spines and one seta; endite (Fig. 16f') with two distal setae. *Labium* not observed. *Maxilliped* (Fig. 16g) endites distally separated, simple, with microtrichiae in distal corners; palp article-1 naked, article-2 with two inner setae (short and log) and one outer seta; article-3 with four inner setae, article-4 with five simple inner and distal setae and one outer seta. *Epignath* not seen.

Cheliped (Fig. 17a) basis 0.9 times as long as broad; merus triangular with midventral seta; carpus elliptical, 1.5 times as long as wide, with two midventral setae and subproximal and distal setae dorsally; chela not-forcipate, propodus (palm) 1.7 times as long as wide, almost as long as fixed finger with two ventral seta and row of three serrated setae on inner side; fixed finger with three setae on cutting edge and one simple seta in near dactylus insertion; dactylus with dorsoproximal seta.

Pereopod-1 (Fig. 17b) basis 6.1 times as long as broad; ischium with simple seta; merus 1.5 times as long as wide, 0.7 times as long as carpus, naked; carpus 2.2 times as long as wide, 0.6 times as long as propodus, with one fine distodorsal seta; propodus 5.8 times as long as wide, with distoventral seta; dactylus 0.3 times as long as propodus, unguis four times as long as dactylus; unguis and dactylus combined 1.3 times as long as propodus.

Pereopod-2 (Fig. 17c) basis 5.4 times as long as wide with middle simple seta; ischium with simple seta; merus 2.1 times as long as wide, 1.1 times as long as carpus, with simple seta and spine distoventrally; carpus 2.4 times as long as wide, 0.7 times as long as propodus with blade-like spine 0.4 times as long as propodus, one distodorsal seta and short distoventral spine; propodus five times as long as wide, with serrated distal spine; dactylus 0.2 times as long as propodus, unguis twice as long as dactylus, dactylus and unguis combined 0.6 times as long as propodus.

Pereopod-3 (Fig. 17d) similar to pereopod-2, but merus with short spine and seta distoventrally; propodus three times as long as wide.

Pereopod-4 (Fig. 17e) basis 5.1 times as long as wide, with one simple seta midlength and one penicillate seta subdistally; ischium with short and long setae; merus 1.6 times as long as wide, 0.6 times as long as carpus, with two serrated distoventral setae; carpus 2.8 times as long as wide and 0.9 times as long as propodus, with blade-like spine 0.3 times as

long as propodus and three serrated spines distally; propodus 5.7 times as long as wide, with two distoventral serrated spines and dorsodistal serrated seta; dactylus 0.3 times as long as propodus, unguis 0.1 times as long as propodus, dactylus and unguis combined 0.3 times as long as propodus.

Pereopod-5 (Fig. 17f) similar to pereopod-4; propodus five times as long as wide, with one distodorsal penicillate seta.

Pereopod-6 (Fig. 17g) similar to pereopod-4; but propodus with one additional simple seta distally.

Pleopoda (Fig. 17i) basal article as long as wide, 3.5 times as long as wide, with five distal setae; exopod 1.9 times as long as wide, with eight distal setae.

Uropod (Fig. 17h) basis naked; exopod 0.6 times as long as endopod, with two articles; article-1 times as long as article-2 with one distal seta; article-2 with two setae (one broken); endopod two articles, article-1 with two distal setae; article-2 with two short and four long distal setae.

Distribution: *P. sigrunis* sp. n. was well represented in IceAGE material. It was recorded at Iceland Faroe Ridge, in Norwegian Channel, Iceland Basin, Denmark Strait, and Norwegian Sea (Fig. 7b) at the depth range from 317 to 731 m and 2746 m.

Morphology variables

Some of the specimens of *P. sigrunis* sp. n. had fully developed pleopods, while the others missed those appendages (4 with and 13 without pleopods). This presence/absence of the pleopods was irrespective to locality, depth, body size, and, in some cases, also to the life stage (Fig. 18), although all studied mancas (0.6 −0.9 mm) apparently missed the pleopods. *Pseudotanais sigrunis* sp. n. was a series of just 17, widely distributed specimens, what hampers further analysis and any reliable conclusion. If the studied individuals are really conspecific, we can hypothesize the presence and the absence of the pleopods can be rationalized by presence in the life-history a dispersal stage.

Remarks: *P. sigrunis* sp. n. with a robust cheliped, acuminate mandible molar, and short, bi-articulated exopod on the uropods is the most similar to *Pseudotanais lilljeborgi* Sars, 1882. Two other species with also an acuminate molar and a regular (non-forcipate) chela (*P. colonus* Bird and Holdich, 1989b and *P. falcifer* Błażewicz-Paszkowycz and Bamber, 2011) show a non-articulated exopod on the uropods.

Pseudotanais lilljeborgi Sars, 1882 is a *Pseudotanais* with a wide geographic distribution (Fig. 2b) and numerous records in the literature (e.g., Sars 1896; Hansen 1913; Greve 1965a, b, c; Stephensen 1937; Just 1970; Bird and Holdich, 1989a), all records being confined to a relatively narrow depth range (139–536 m). The species was described by Sars (1882) based on the type material from Varangerfjord (northern part of Norway) and diagnosed as a non-forcipate member of the genus with eyes and a relatively short exopod on the uropod (not longer than the proximal article of the endopod), the uropod endopod proximal article being longer than the distal one. Moreover, the species shows long setae on articles 2–3 of the antenna.

Sieg (1977) redescribed *P. lilljeborgi* using the Ingolf material collected off Iceland and Jan Mayen Island by Hansen (1913); he disregarded Hansen's note that the "Icelandic" specimens lacked eyes and their carapace shape differed from that of the "Norwegian" individuals (Hansen 1913, p. 27). In addition, the *P. lilljeborgi* studied by Sieg (1977) showed short setae on the antenna articles 2 and 3, and the exopod uropod somewhat longer than the endopod proximal article, while they were apparently long in the type specimens.

The newly described *Pseudotanais sigrunis* sp. n. shows setae on the antenna articles 2–3 to be as short as those in *P. lilljeborgi* studied by Sieg (1977), the exopod uropod being somewhat longer than the endopod proximal article. Therefore, we assume that the part of the Ingolf collection studied by Sieg (1977) is conspecific with *P. sigrunis*.

It is important to emphasize that all except one specimens were found in relatively shallow areas (317–731 m) in nearly all the basins around Iceland, a single individual only being collected at a deeper station (2746 m, the Icelandic Basin). Morphological analyses failed to reveal differences between the "shallow" and the "deep" individuals. Nevertheless, we anticipate that molecular studies involving a larger collection of specimens should show whether (1) the "shallow-water" and the "deep-water" populations of the species are conspecific rather than forming a complex of cryptic species, and (2) other records of *P. lilljeborgi* (e.g., from off the northern part of Norway: vicinity of Kvalsund (Greve 1965a, c), Barents Sea (Strapper unpublished data), and East Greenland (Hansen 1913)) belong to the only one species.

Discussion

The Pseudotanaidae are currently represented by 51 nominal species known worldwide (WoRMS 2018). In the North Atlantic, the number of nominal pseudotanaid species known at present is, together with the new species described in this paper, 25 (Table 4). The IceAGE collection represented by 323 specimens was dominated by *Pseudotanais svavarssoni* sp. n. which accounted for 57% of the specimens examined, followed by *Pseudotanais sigrunis* sp. n., *Pseudotanais misericorde* sp. n., *Mystriocentrus biho* sp. n., and *Akanthinotanais* cf. *longipes*, which made up 5.5, 1.8, 1.2, and 0.3% of all the identified specimens, respectively. Because of poor preservation condition, five specimens from the collection we studied could not be identified to the species level (Table 2).

Most of those taxa have a limited zoogeographical range (i.e., one, relatively well-defined basin) and a distinct bathymetric range (Fig. 19). The Bray-Curtis similarity-based

cluster analysis separated the different a priori designated areas into groups based on the pseudotanaid faunas:

- Off the British coast: *P. corollatus* and *P. jonesi*
- Off the Norwegian coast: *P. macrocheles*
- High latitudes of the North Atlantic: *P. oculatus*
- The Bay of Biscay and the Porcupine Abyssal Plain: *P. abyssi*, *P. colonus*, *P. denticulatus*, *P. falcicula*, *P. longispinosus*, *P. scalpellum*, *P. serratus*, *A. similis*, *P. spatula*, *P. spicatus*, and *P. vulsella*
- Off Iceland: north—*P. svavarssoni* sp. n.; south—*A. longipes*, *M. biho* sp. n., *P. misericorde* sp. n., *P. svavarssoni* complex

A separate group in the dendrogram was made up by *P. falcifer* known from mud volcanoes off Norway (Błażewicz-Paszkowycz and Bamber 2011). In addition, the Kara Sea with the original locality of *P. affinis* produced a separate branch in the dendrogram. Three species, namely *P. forcipatus*, *P. affinis*, and *P. lilljeborgi*, are particularly widely distributed, their range extending from the high Arctic (the Barents Sea) to the British coast of the North Sea (e.g., *P. forcipatus*) or from Novaya Zemlya to the coasts of Norway and Iceland to the west coast of Greenland (*P. affinis* and *P. lilljeborgi)* (Table 4).

The bathymetric range of N Atlantic pseudotanaids extends from the upper shelf down to 4800 m (Fig. 20), few of them showing a narrow range (e.g., *A. similis*, *P. macrocheles*, *P. oculatus*, *P. jonesi*, *P. corollatus*, *P. colonus*, *P. abyssi*). Unsurprisingly, all of those species have very narrow zoogeographical distribution and they are often restricted to the type locality (Fig. 2). An exception is *P. macrocheles* that occurs only in Norwegian fjords (Fig. 2d). A few other pseudotanaids recorded in the North Atlantic show a depth range extending from some hundred meters up to 2500 m (e.g., *P. sigrunis* sp.*n.*, 317–731 m; *P. svavarssoni* sp. n., 2172–2401 m; *M. biho* sp. n.; 913–2537 m; *P. scalpellum*, 2081–2634 m; *P. falcifer*, 722–1263 m; *P. spatula*, 1400–2200 m; *P. vulsella*, 1028–1640 m; and *P. misericorde*, 1385, 1621, 2537 m) and have a relatively narrow zoogeographical distribution (Figs. 2 and 7). Five species (*P. longispinus*, *P. spicatus*, *P. falcicula*, *M. serratus*, and *P. denticulatus*) spans their bathymetric range over 3000 m, although the distribution is relatively narrow (Fig. 20). Two of them, *P. denticulatus* and *P. serratus*, show the widest depth range (around 3700 and 3100 m, respectively). Quite a wide depth range has been also found in the *P. svavarssoni* complex (2500 m) and *P. affinis* (1700 m), accompanied by a wide zoogeographical range (Fig. 7), in contrast to *P. lilljeborgi* and *P. forcipatus*, both showing shallower depth ranges (< 500 m), but wide zoogeographical distributions (Fig. 2b).

Conclusion

In the IceAGE collection made in waters surrounding Iceland (Irminger Basin, Iceland Basin, Norwegian Sea, Denmark Strait, Iceland–Faroe Ridge, and Norwegian Channel), five species of pseudotanaids were identified; four of them were new for science (*Mystriocentrus biho* sp. n., *P. misericorde* sp. n., *P. sigrunis* sp. n., and *P. svavarssoni* sp. n.). Apart from species new to the knowledge, *Akanthinotanais* cf. *longipes* was collected from close place to type locality *A. longipes* Hansen, 1913 that is known only from that original location. One species that is probably complex of closely related species morphologically was very similar with *P. svavarssoni* sp. n. The morphometric approach and analysis highlighted significant differences between specimens collected in northern and southern Icelandic basins; distinct differences were also apparent between specimens collected from shallow and deep waters. Molecular approach is required to confirm our findings. Pseudotanaidae of Iceland are currently represented by seven nominal species.

Distinguished in the analysis, zoogeographical regions are represented by distinct pseudotanaid fauna. Our results stay in contrast to the earlier observation for bivalves (Dijkstra et al. 2009) or munnopsids (Schnurr et al. 2014). The wide distribution of these isopods in the North Atlantic and marine basins are rationalized by their efficient swimming abilities and potentially high ecological plasticity.

Considering a restricted dispersal ability of pseudotanaids, the North Atlantic could be divided into several zones, where distinct species, or discrete group of species, are noted (see Fig. 19). For example, some taxa are known only for the Bay of Biscay while *P. oculatus* were noted in high latitudes in the North Atlantic, but *P. macrocheles* was collected from fiords along Norway coast.

Four of the pseudotanaid species in the North Atlantic are widely distributed. *P. affinis*, *P. macrocheles*, *P. lilljeborgi*, and *P. forcipatus* were noted in various marine basisn located around Iceland, Norway, and Greenland. Those records need to be re-examined, and it is highly probable that they represent complex of sister (or cryptic) species.

Acknowledgments We appreciate Captain Michael Schneider, the crew of R/V Meteor and Klaus Ricke with his crew of R/V Poseidon, the scientist participating in the IceAGE programs as well as pickers and sorters for their valuable help on and off board. We are thankful to Kelly Merrlin for language editions. We are grateful to two anonymous reviewers for comments and critiques that helped to improve this article. This study was funded by the National Science Centre of Poland (grant number UMO-2014/13/B/NZ8/04702).

Funding This study was funded by Polish National Science Centre grant (UMO-2014/13/B/NZ8/04702).

Compliance with ethical standards

Conflict of interest The authors declare that they have no conflict of interest.

Ethical approval All applicable international, national, and/or institutional guidelines for the care and use of animals were followed by the authors.

Field study Permits and approval of field or observational studies are not applicable for authors.

References

Astthorsson OS, Gislason A, Jonsson S (2007) Climate variability and the Icelandic marine ecosystem. Deep Sea Res II 54:2456–2477

Bamber RN (2005) The Tanaidaceans (Arthropoda: Crustacea: Peracarida: Tanaidacea) of Esperance, Western Australia, Australia. In: Wells FE, Walker DI, Kendrick GA (eds) The marine Flora and Fauna of Esperance, Western Australia: proceedings of the twelfth international marine biological workshop. Western Australia museum, Perth, pp 613–728

Bamber RN (2012) Littoral Tanaidacea (Crustacea: Peracarida) from Macaronesia: allopatry and provenance in recent habitats. J Mar Biol Assoc UK:1–22. https://doi.org/10.1017/S0025315412000252

Bird GJ (1999) A new species of *Pseudotanais* (Crustacea, Tanaidacea) from cold seeps in the deep Caribbean, collected by the French submersible *Nautile*. Zoosystema 21:445–451

Bird GJ, Holdich DM (1985) A remarkable tubicolous tanaid (Crustacea: Tanaidacea) from the Rockall trough. J Mar Biol Assoc U K 65: 563–572

Bird GJ, Holdich DM (1989a) Tanaidacea (Crustacea) of the north-East Atlantic: the subfamily Pseudotanainae (Pseudotanaidae) and the family Nototanaidae. Zool J Lin Soc Lond 97:233–298

Bird GJ, Holdich DM (1989b) Recolonisation of artificial sediments in the deep Bay of Biscay by Tanaidaceans (Crustacea: Peracarida), with a description of a new species of *Pseudotanais*. J Mar Biol Assoc UK 69:307–317

Bird GJ, Larsen K (2009) Tanaidacean phylogeny: the second step. The basal paratanaoidean families. Arthropod Syst Phylogeny 67:137–158

Błażewicz-Paszkowycz M, Bamber RN (2011) Tanaidomorph Tanaidacea (Crustacea: Peracarida) from mud-volcano and seep sites on the Norwegian margin. Zootaxa 3061:1–35

Błażewicz-Paszkowycz M, Bamber RN, Anderson G (2012) Diversity of Tanaidacea(Crustacea: Peracarida) in the world's oceans—how far have we come? PLoS One 7:e33068

Błażewicz-Paszkowycz M, Bamber RN, Jóźwiak P (2013) Tanaidaceans (Crustacea: Peracarida) from the SoJaBio joint expedition in slope and deeper waters in the sea of Japan. Deep Sea Res II 86:181–213

Błażewicz-Paszkowycz M, Jennings RM, Jeskulke K, Brix S (2014) Discovery of swimming males of Paratanaoidea (Tanaidacea). Pol Polar Res 35:415–453

Brix S (2011) A report from the IceAGE Expedition. http://Www.Ifm.Zmaw.De/Fileadmin/Files/Leitstelle/Meteor/M85/M85-3-Scr.Pdf

Brix S, Svavarsson J (2010) Distribution and diversity of desmosomatid and nannoniscid isopods (Crustacea) on the Greenland–Iceland–Faeroe ridge. Polar Biol 33:515–530. https://doi.org/10.1007/S00300-009-0729-8

Brix S, Svavarsson J, Leese F (2014) A multi-gene analysis reveals multiple highly divergent lineages of the isopod *Chelator Insignis* (Hansen, 1916) south of Iceland. Pol Polar Res 35:225–242

Bruce JR, Colman JS and Jones NS (1963) Marine Fauna of the Isle of Man. Liverpool University Press, Liverpool, pp 307–307

Clarke K, Gorley R (2006) PRIMER v6: User manual/tutorial, PRIMER-E. Plymouth

Coleman CO (2003) Digital inking: how to make perfect line drawings on computers. Org Divers Evolv http://Senckenberg.De/Odes/03-14.Htm,1–14

Delamare-Deboutteville C (1960) Biologie des Eaux Souterraines Littorales et Continentales. Hermann, Paris pp 740

Delamare-Deboutteville CS Gerlach, Siewing RS (1955) Recherches sur la faune des eaux souterraines littorales du Golfe de Gascogne. Littoral des Landes. Vie Milieu 5:373–407

Dijkstra HH, Warén A, Gudmundsson G (2009) Pectinoidea (Mollusca: Bivalvia) from Iceland. Mar Biol Res 5:207–243

Dinter W (2001) Biogeography of the OSPAR maritime area. A synopsis and synthesis of biogeographical distribution patterns described for the north-east Atlantic. Federal Agency for Nature Conservation, Bonn

Drumm D, Bird G (2016) New deep-sea Paratanaoidea (Crustacea: Peracarida: Tanaidacea) from the northeastern Gulf of Mexico. Zootaxa 4154:389–414. https://doi.org/10.11646/Zootaxa.4154.4.2

Gislason A, Astthorsson OS (2004) Distribution pattern of zooplankton around Iceland in spring. Sarsia 20:85–94

Greve L (1965a) The biology of some Tanaidacea from Raunefjorden, western Norway. Sarsia 20:43–54

Greve L (1965b) Tanaidacea from Trondheimsfjorden. Det Kongelige Norske Videnskabers Selskabs Forhandlinger 38:140–143

Greve L (1965c) New records of some Tanaidacea (Crustacea) from the vicinity of Tromsö. Astarte 27:2–6

Hansen HJ (1887) Oversigt over de paa dijmpha-togtet indsamlede krebsdyr. Dijmphna Togtets Zool Bot Udbytte, Kopenhagen, pp 183–286

Hansen HJ (1913) Crustacea, malacostraca. II. IV. The order Tanaidacea. Danish Ingolf. Expedition 3:1–145

Hansen B, Osterhus S (2000) North Atlantic–Nordic seas exchanges. Prog Oceanogr 45:109–208

Holdich DM, Bird GJ (1986) A preliminary report on 'Dikonophoran' tanaidaceans (Crustacea). In: Laubier L, Monniot C (eds) Peuplements profonds du Golfe de Gascogne. Centre National De Tri D'oceanographie Biologique. Centob Ifremer, Brest, pp 441–447

Holdich DM, Jones JA (1983) The distribution and ecology of British shallow-water tanaid crustaceans (Peracarida, Tanaidacea). J Nat Hist 17:157–183

Jochumsen K, Schnurr SM, Quadfasel D (2016) Bottom temperature and salinity distribution and its variability around Iceland. Deep Sea Res 111:79–90

Just J (1970) Decapoda, Mysidacea, Isopoda, and Tanaidacea from Jørgen Brønlund Fjord, North Greenland. Meddelelser om Grønland udgivne af Kommissionen for Videnskabelige Undersøgelser i Grønland 184(9):1–32

Khodami S, Martinez Arbizu P, Stöhr S, Laakmann S (2014) Molecular species delimitation of Icelandic brittle stars (Echinodermata: Ophiuridea) pol. Polar Res 35:243–260

Larsen K (2005) Deep-Sea Tanaidacea (Peracarida) from the Gulf of Mexico. Crustaceana Monogr 5:1–381

Larsen K (2012) Tanaidacea (Peracarida) from Macaronesia I. The deep-water fauna off the Selvagen Islands, Portugal. Crustaceana 85:571–589

Lilljeborg W (1864) Bidrag till kännedomen om de inom sverige och norrige förekommande Crustaceer af isopodernas underordning och tanaidernas familj. Inbjudningsskrifter Universitet i Uppsala, Uppsala. PAGES

Logemann K, Ólafsson J, Snorrason Á, Valdimarsson H, Andmarteinsdóttir G (2013) The circulation of Icelandic waters—a modelling study. Ocean Sci 9:931–955

Malmberg SA (2004) The Iceland Basin–Topography and Oceanographic Features. Hafrannsóknir, No. 109, Reykjavík 2004: pp41.

Malmberg S, Valdimarsson H (2003) Hydrographic conditions in Icelandic waters, 1990–1999. In Ices mar Sc 219:50–60

McLelland JC (2007) Family Pseudotanaidae Sieg, 1976. In: Larsen K & Shimomura M. (Eds) 2007. Tanaidacea (Crustacea: Peracarida) from Japan III. The deep trenches; the Kurile-Kamchatka Trench and Japan Trench. Zootaxa 1599:87–99

McLelland JA (2008) A systematic and taxonomic review of the family Pseudotanaidae (Crustacea: Peracarida: Tanaidacea) based primarily on morphometric cladistic analyses. Dissertation, University Of Southern Mississippi

Meißner K, Brenke N, Svavarsson J (2014) Benthic habitats around Iceland investigated during the IceAGE expeditions. Pol Polar Res 35:179–204

Mikkelsen NT, Todt C (2014) Diversity of Caudofoveata (Mollusca) around Iceland and description of *Psilodens Balduri* sp. n. Pol Polar Res 35:279–290. https://doi.org/10.2478/Popore-2014-0014

Ostmann A, Schnurr S, Martínez AP (2014) Marine environment around Iceland: hydrography, sediments and first predictive models of icelandic deep-sea sediment1039 characteristics. Pol Polar Res 35: 151–176. https://doi.org/10.2478/Popore-2014-0021

Pabis K, Jóźwiak P, Lorz AN, Schnabel K, Błażewicz-Paszkowycz M (2015) First insights into the deep-sea tanaidacean fauna of the RossSea–species richness and composition across the shelf break, slopeand abyss. Polar Biol 38:1429–1437

Perkins H, Hopkins TS, Malmberg SA, Poulain PM, Warn-Varnas A (1998) Oceanographic conditions east of Iceland. J Geophys Res 103:21531–21542

Riehl T, Brenke N, Brix S, Driskell A, Kaiser S, Brandt A (2014) Field and laboratory methods for DNA studies on deep-sea isopod crustaceans. Pol Polar Res 35:205–226

Sars GO (1869) Undersøgelser over Christianiafjordens Dybvandsfauna. Nyt Mag Naturv 16:305–362

Sars GO (1882) Revision af gruppen Chelifera med charakteristik af nye herhen hørende arter og slaegter. Archiv For Matematik Og Naturvidenskab 7:1–54

Sars GO (1896) An account of the Crustacea of Norway with short descriptions and figures of all the species. Isopoda. Bergen Museum 2:1–270

Schnurr S, Malyutina MS (2014) Two new species of the genus Eurycope (Isopoda, Munnopsidae) from Icelandic waters. Pol Polar Res 35: 361–388

Schnurr S, Brandt A, Brix S, Fiorentino D, Malyutina M, Svavarsson J (2014) Composition and distribution of selected munnopsid genera (Crustacea, Isopoda, Asellota) in Icelandic waters. Deep Sea Res I 84:142–155

Sieg J (1976) Zum Natürlichen system Der Dikonophora Lang (Crustacea, Tanaidacea). Zool Syst Evol 14:177–198

Sieg J (1977) Taxonomische monographie der familie Pseudotanaidae (Crustacea, Tanaidacea). Mitteilungen aus dem zoologischen museum in Berlin 53:1–109

Stephensen K (1937) Marine Isopoda and Tanaidacea. In Munksgaard E (Ed) The zoology of Iceland Vol. III, Kopenhagen, Reykjavik, pp 1–25

Todt C, Kocot KM (2014) New records for the solenogaster *Proneomenia sluiteri* (Mollusca) from icelandic waters and description of *Proneomenia custodiens* sp. n. Pol Polar Res 35:291–310

Załącznik nr 4 do Regulaminu przyznawania nagród z funduszu nagród oraz trybu sporządzania i opiniowania wniosków o przyznawanie nagród Rektora UŁ za osiągnięcie związane z pracami badawczymi, dydaktycznymi i organizacyjnymi.

5 January 2020

STATEMENT

In agreement with all co-authors of the publication entitled:

A tip of the iceberg — Pseudotanaidae (Tanaidacea) diversity in the North Atlantic

published in *Marine Biodiversity*

(2018): 48: 859-895; doi 10.1007/s12526-018-0881-x

I declare that my contribution in this work is:

author	Contribution (%)	signature
Jakiel Aleksandra	50	
Stępień Anna	25	
Błażewicz Magdalena	25	

Chapter 3: Deep ocean seascape and Pseudotanaidae (Crustacea: Tanaidacea) diversity at the Clarion-Clipperton Fracture Zone

SCIENTIFIC REPORTS
nature research

OPEN

Deep ocean seascape and Pseudotanaidae (Crustacea: Tanaidacea) diversity at the Clarion-Clipperton Fracture Zone

Aleksandra Jakiel[1,4], Ferran Palero[1,2,3,4*] & Magdalena Błażewicz[1]

Understanding the diversity and spatial distribution of benthic species is fundamental to properly assess the impact of deep sea mining. Tanaidacea provide an exceptional opportunity for assessing spatial patterns in the deep-sea, given their low mobility and limited dispersal potential. The diversity and distribution of pseudotanaid species is characterized here for the Clarion and Clipperton Fractures Zone (CCZ), which is the most extensive deposit field of metallic nodules. Samples were taken from the Belgian, German and French license areas, but also from the APEI 3 (Area of Particular Environmental Interest 3) of the Interoceanmetal consortium associates. The combination of morphological and genetic data uncovered one new pseudotanaid genus (*Beksitanais* n. gen.) and 14 new species of *Pseudotanais* (2 of them virtual taxa). Moreover, our results suggest that spatial structuring of pseudotanaid diversity is correlated with deep-sea features, particularly the presence of fractures and seamount chains crossing the CCZ. The presence of geographical barriers delimiting species distributions has important implications for the establishment of protected areas, and the APEI3 protected area contains only one third of the total pseudotanaid species in CCZ. The specimen collection studied here is extremely valuable and represents an important first step in characterizing the diversity and distribution of pseudotanaids within the Tropical Eastern Pacific.

The influence of habitat heterogeneity on species diversity has puzzled biologists for a long time and still raises many questions[1–3]. High habitat heterogeneity and spatial complexity provide shelter for many invertebrate taxa and might result in higher diversity of benthic organisms[4]. Competition and influence of predators are restricted in heterogeneous areas[5,6] while the number of potential ecological niches increases[7]. Studies concerning benthic marine fauna have traditionally focused on shallow-water areas, so that knowledge on deep-sea habitat heterogeneity and its influence at various spatial scales is still lacking[8]. The deep-sea ecosystem was considered as a rather homogeneous environment in the past, but the application of state-of-the-art technologies for habitat mapping has proven otherwise[1]. McClain and Barry (2010)[9] have shown that habitat heterogeneity is an important factor driving the structure of benthic assemblages and that significant species turnover can be observed at relatively small scales (<1 km)[8]. Abyssal hills increase habitat heterogeneity, benthic megafaunal biomass and diversity[10]. Furthermore, benthic meiofauna studies also show that deep sea nodule fields facilitate the coexistence of species with different modes of life, ranging from sediment dwelling to epifaunal[11].

The Clarion and Clipperton Fractures Zone (CCZ) is a 6 million km^2 region located in international waters of the Tropical Eastern Pacific. Well-known to mining corporations, this is the most extensive deposit field of metallic nodules, rich in manganese, nickel, copper and cobalt[12,13]. The attraction for deep sea nodules has raised in the last few years because they host large quantities of other critical metals needed for high-tech, green-tech, and energy applications[14]. The exploration and exploitation of the CCZ is currently managed by the International Seabed Authority (ISA), an intergovernmental body that regulates mining and related activities in the seabed beyond national jurisdiction[15]. ISA has recently granted 15 mining licences in the CCZ area and selected 9 Areas

[1]Department of Invertebrate Zoology and Hydrobiology, Faculty of Biology and Environmental Protection, University of Lodz, ul. Banacha 12/16, 90-237, Łódź, Poland. [2]Centre d'Estudis Avançats de Blanes (CEAB-CSIC), Carrer d'accés a la Cala Sant Francesc 14, 17300, Blanes, Spain. [3]Associate Researcher, Department of Life Sciences, The Natural History Museum, Cromwell Road, London, SW7 5BD, UK. [4]Aleksandra Jakiel and Ferran Palero contributed equally. *email: fpalero@ceab.csic.es

Licence area	Station	Latitude [N]	Longitude [W]	Depth [m]	Pseudotanaid presence
BGR	20	11° 49.81′	117° 00.28′	4093	✓
BGR	24	11° 51.52′	117° 01.19′	4100	✓
BGR	50	11° 49.92'	117° 29.31'	4330	✓
BGR	59	11° 48.55'	117° 29.03′	4342	✓
IOM	81	11° 03.97'	119° 37.67'	4365	✓
IOM	99	11° 02.61'	119° 39.52'	4401	✓
GSR	117	13° 52.39'	123° 15.30′	4496	✓
GSR	133	13° 50.98′	123° 15.07′	4507	✓
IFREMER	158	14° 03.41′	130° 07.99'	4946	✓
IFREMER	171	14° 02.68′	130° 05.97'	5030	×
APEI3	192	18° 44.81′	128° 21.87'	4877	✓
APEI3	197	18° 48.66'	128° 22.75′	4805	✓
APEI3	210	18° 49.27′	128° 25.80′	4700	×

Table 1. Pseudotanaidae presence (✓) or absence (×) on the surveyed stations. APEI3: Area of Particular environmental Interest 3; BGR: Bundesanstalt fur Geowissenschalfen und Rofstoffe (Germany); IOM: Interoceanometal; GSR: Global Sea Mineral Resources NV (Belgium); IFREMER: Institut Français de Recherche pour l'Exploitation de la Mer (France).

of Particular Environmental Interest (APEI) as non-mining, reference areas. Fields rich in polymetallic nodules represent heterogeneous habitats, which increases regional diversity[11,16,17], but removing nodules, together with the resuspension and redeposition of the sediment, affects local fauna[18]. Experimental work suggests that mining may cause major disturbances on nodule-associated fauna and reduce biodiversity[19]. Therefore, understanding connectivity and spatial distribution of benthic species is fundamental to properly assess the impact of mining[20].

Tanaidacea are small peracarid crustaceans, benthic brooders, living on tubes or buried in the sediment. Tanaidacean abundance is usually underestimated[21,22], but they can be more numerous than amphipods or isopods[23]. They have low mobility and limited dispersal potential, and provide an exceptional opportunity for assessing connectivity patterns in the deep-sea. Morphological identification of tanaidaceans is difficult because of their small size and sexual dimorphism[23], and some currently accepted taxa might form in fact species complexes, considering their low dispersal abilities and reproductive biology[24]. The use of molecular techniques before thorough morphological evaluation (i.e. reverse taxonomy) can be advantageous when the occurrence of cryptic species is expected[25,26]. Nevertheless, the scarcity of data in public databases such as GenBank or BOLD is a limiting factor for the study of genetic variation in Tanaidacea. From a total of 346 tanaid sequences deposited in GenBank, ~25% are simply identified as 'unclassified Tanaidacea', which clearly hinders the use of DNA barcoding approaches. This is particularly pressing on the Pseudotanaidae, for which the only sequence available in public databases corresponds to the Histone 3 gene of *Pseudotanais* sp[27], and without any DNA barcoding data published so far.

Pseudotanaidae (Sieg 1976) species represent a frequent and diverse element of deep-sea benthic assemblages, only exceeded by polychaetes[28,29]. The genus *Pseudotanais* is the most speciose within the family, formed by four species-groups: 'affinis', 'denticulatus', 'forcipatus' and 'longisetosus', based on morphological variation in key traits (e.g. antenna article 2–3, mandibles, chelipeds, and setation and ornamentation on pereopods 1–3) (see[30] and[31]). However, the validity of these groups is unclear and the systematics of pseudotanaids has never been studied using molecular methods. From the 55 pseudotanaid species known, only 9 have been reported from the Pacific Ocean, 7 restricted to this area (*Akanthinotanais makrothrix* Dojiri and Sieg, 1997; *Pseudotanais californiensis* Dojiri and Sieg, 1997; *P. abathagastor* Błażewicz-Paszkowycz *et al*., 2013; *P. intortus* Błażewicz-Paszkowycz *et al*., 2013; *P. soja* Błażewicz-Paszkowycz *et al*., 2013; *P. nipponicus* McLelland, 2007 and *P. vitjazi* Kudinova-Pasternak, 1966; WoRMS 2018) and two species originally described from the Atlantic Ocean namely, *P. affinis* Hansen, 1887 and *P. nordenskioldi* Sieg, 1977 (reported by Kudinova-Pasternak[31] but unlikely to belong to these two Atlantic species).

The present study was designed to characterize the diversity and distribution of pseudotanaid species in the CCZ area. The mitochondrial gene coding for the subunit I of the cytochrome oxidase was selected to help filling the current gap in molecular databases. The combination of morphological and molecular genetic data uncovered the presence of one new genus (*Beksitanais* n. gen.) and 14 new species of *Pseudotanais* (two of them virtual taxa). Moreover, our results suggest that genetic structuring of pseudotanaid diversity is correlated with deep-sea landscape and the presence of seamounts and fractures crossing the CCZ.

Results

Phylogenetic analyses. Pseudotanaids were found in 87% (13 out of 15) of the stations surveyed, which confirms the generalized presence of these tanaids in the deep-sea benthos (Table 1). The bathymetric range where pseudotanaids were captured was large, spanning from 4093 m to 4877 m depth. A total of 67 individuals were used for molecular analysis and gave positive DNA barcoding results (Table 2). A total of 16 different COI haplotypes were obtained (Fig. 1), representing one *Beksitanais* and 14 *Pseudotanais* species (two virtual taxa, without a voucher left for morphological analysis). The sequence alignment spanned 691 bp before trimming and was reduced to 611 bp after running Gblocks. The Hasegawa-Kishino-Yano (HKY + G + I) model showed the lowest BIC score (BIC = 9947.97) and it is considered to describe the substitution pattern the best. Non-uniformity of

Area	Station	*B. apocalyptica*	*P. uranos*	*P. gaiae*	*P. yenneferae*	*P. geralti*	*P. julietae*	*P. romeo*	*P. georgesandae*	*P. oloughlini*	*virtual sp A*	*P. chaplini*	*P. mariae*	*P. chopini*	*P. kobro*	*virtual sp B*
BGR	20							1				1	1	3		1
	24							4						4		
	50													3		
	59													2	1	
IOM	81	3				2							2		1	
	99					4							1	1	3	
GSR	117					1					1				1	
	133						1									
IFREMER	158											1				
	171															
APEI3	192			3	1				1	2						
	197		5		9					3						

Table 2. Pseudotanaidae species abundance on the CCZ stations surveyed.

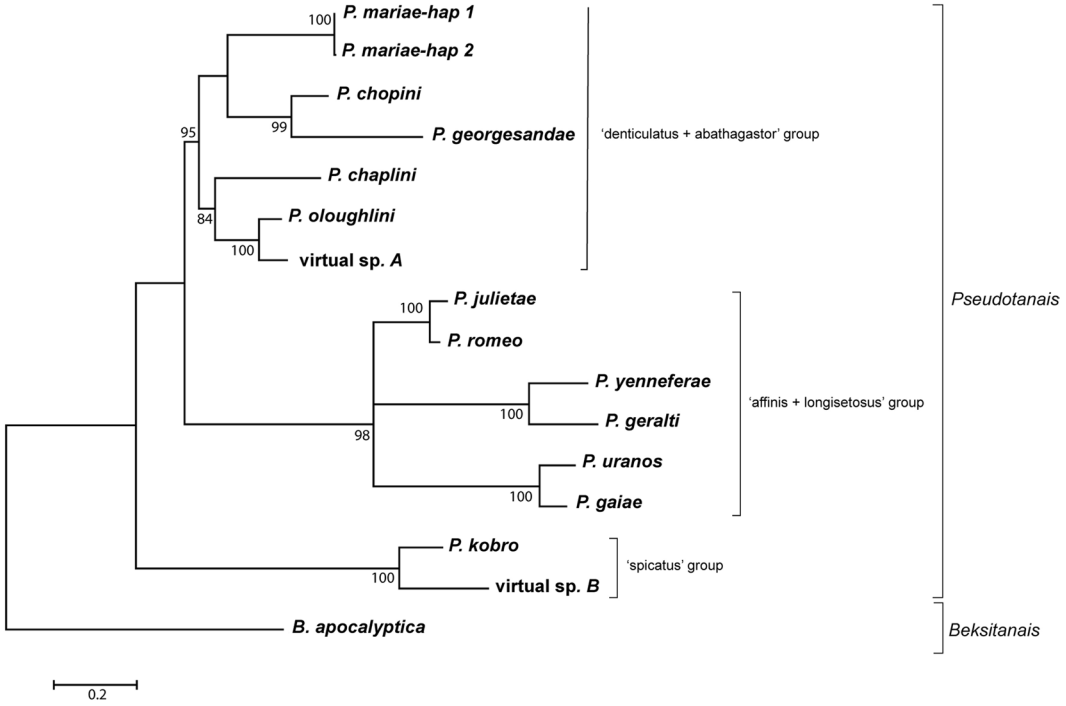

Figure 1. Evolutionary relationships between Pseudotanaidae species inferred by using the COI sequences and the Maximum Likelihood method. The percentage of trees in which the associated taxa clustered together (bootstrap support) is shown next to the branches. Only values above 70% are shown.

evolutionary rates among sites was modelled using a Gamma distribution ($+G = 0.85$) and the rate variation model allowed for some positions to be evolutionarily invariable ($+I = 37.61\%$ sites). The Maximum Likelihood tree with the highest log likelihood value ($\ln L = -4841.74$) is shown in Fig. 1. *Pseudotanais* species grouped into three well-supported clades namely, 1) the 'spicatus' group (including *P. kobro* and virtual species B); 2) the 'affinis + longisetosus' group (including three pairs of sister taxa: *P. romeo*/*P. julietae*, *P. geralti*/*P. yenneferae* and *P. uranos*/*P. gaiae*) and 3) the 'abathagastor + denticulatus' group (including *P. mariae*, the sister species *P. chopini*/*P. georgesandae* and a clade formed by *P. chaplini*, *P. oloughlini* and virtual species A). The genetic clustering of COI sequences in the ML tree corresponds to the morphological identification of taxa (see below).

Pairwise genetic *p*-distances between COI sequences ranged between 0 and 35.5% (Table S1). Intraspecific genetic variation was very low, as expected given the limited sample size per species, and only *P. mariae* showed more than one haplotype. Estimates of average evolutionary divergence over sequence pairs within groups of *Pseudotanais* species showed similar mean divergences within the 'abathagastor + denticulatus' group (0.228 ± 0.022) and within the 'affinis + longisetosus' group (0.277 ± 0.030), and lower divergences within the 'spicatus' group (0.060 ± 0.008). Net evolutionary divergences over sequence pairs between groups of species were larger between *Beksitanais* and any *Pseudotanais* clade than between *Pseudotanais* species groups. Within

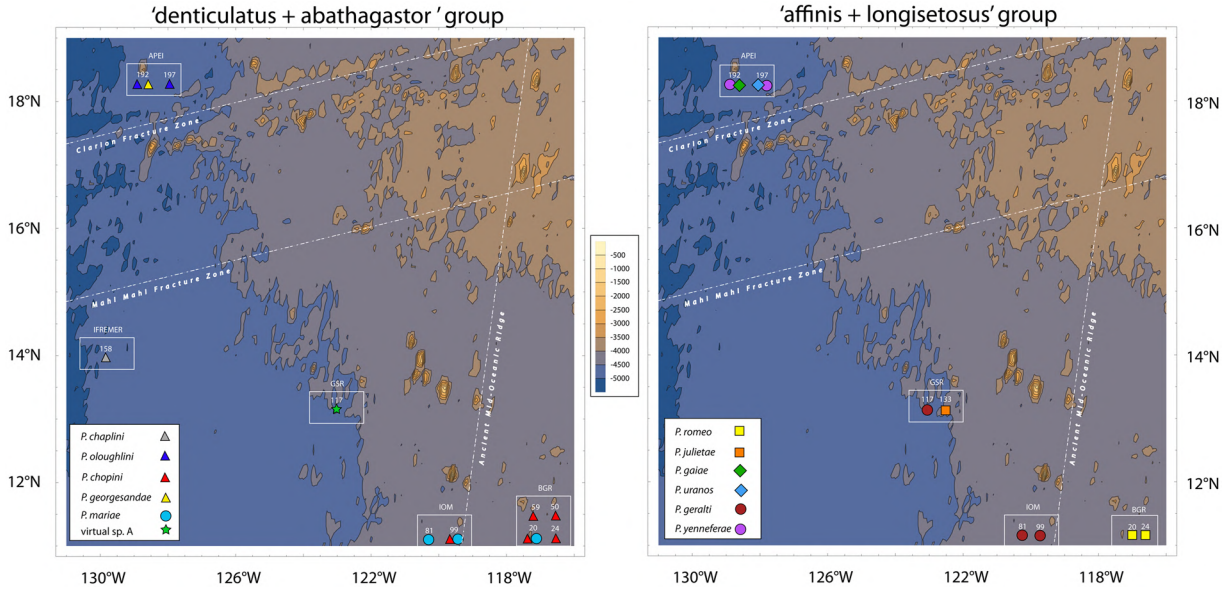

Figure 2. Contour plot showing the bathymetry of the studied area and the spatial distribution of the newly described Pseudotanaidae. Station numbers are shown in white. Mountain chains can be identified as a series of concentric contours running adjacent to the Clarion Fracture Zone or the ancient Mid-Ocean Ridge.

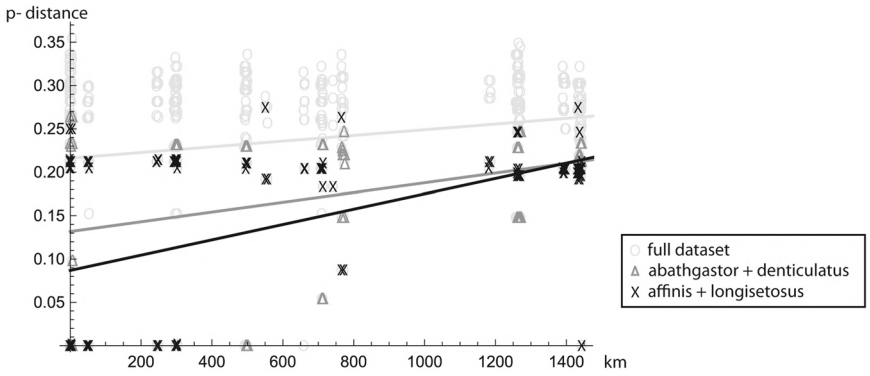

Figure 3. Correlation between genetic and geographic distances for the Pseudotanaidae species sampled. Symbols indicate comparison between all taxa (O), between samples from the 'affinis + longisetosus' clade (X) or between samples from the 'abathagastor + denticulatus' clade (Δ).

Pseudotanais, the 'spicatus' group and either the 'affinis + longisetosus' (0.429 ± 0.051) or the 'abathagastor + denticulatus' (0.402 ± 0.055) clades show divergences almost twice as large as those observed between 'abathagastor + denticulatus' and 'affinis + longisetosus' (0.275 ± 0.037).

Spatial modelling and genetic gradients. The 3D-model based on mean sea level data reveal an extremely heterogeneous deep sea landscape at the CCZ, with the presence of several seamounts and knolls (Fig. 2). In fact, two underwater mountain chains cross the studied area: one rise running east-to-west around latitude 17°N and another running south-southwest around longitude 120°W. The first isolates the APEI3 area (located around 18°N) from the remaining sampling sites, and includes seamountains about 4000 m high, reaching to 250 m under the surface (see Discussion). The second runs over the IOM area and separates the BGR area (located around 117°W) from the rest. Plotting the distribution of the newly identified taxa on the 3D spatial model revealed several species (*P. oloughlini*, *P. yenneferae*, *P.georgesandae* and the sister species *P. gaiae* and *P. uranos*) to be restricted to the APEI3 area. Another group of species were only found in the BGR and/or IOM areas (*P. romeo*, *P. mariae*, *B. apocalyptica*, virtual *Pseudotanais* sp. B and *P. chopini*). The virtual *Pseudotanais* sp. A, *P. julietae*, *P. geraldi* and *P. kobro* were found together in the GSR area, although *P. kobro* was also collected in the BGR and IOM areas, and *P. geraldi* was also found in the IOM area. The Spearman rank coefficient revealed a significant correlation between geographical and genetic distances for the complete dataset ($\rho = 0.046$; p-value = 0.032), and this spatial correlation was even higher when each well-supported phylogenetic clade 'affinis + longisetosus' ($\rho = 0.121$; p-value = 0.009) or 'abathagastor + denticulatus' ($\rho = 0.224$; p-value ≤ 0.001) was analysed independently. The linear fitting of an isolation by distance model gave similar results, with the

genetic gradient being two times (for the 'affinis + longisetosus' clade) or even three times (for the 'abathagastor + denticulatus' clade) steeper than for the global dataset (Fig. 3).

Morphological analyses and species description.

Family: Pseudotanaidae Sieg, 1976

Diagnosis: Following Bird & Holdich (1989) and McLelland (2008), Pseudotanaidae can be characterized by: Eyelobes pigmented, rudimentary or absent. Medium body calcification. Pereon with six free pereonites, first reduced in length. Pleon with five free pleonites. Antennule with three articles. Antenna with six articles, articles 2 and 3 with or without stout spiniform setae. Mandible pars molaris broad or narrow, with or without terminal setation. Maxillule palp terminating with two setae and endite terminating with usually nine spiniform setae (two exceptions). Maxilla rudimentary. Maxilliped bases completely fused and endites completely or partially fused and bearing simple setae, cusps, or naked. Cheliped attached to body via sclerite. Chelae forcipate or not. Cheliped carpus with usually two inferior setae (three exceptions). Cheliped fixed finger usually with one inferior setae (four exceptions). Cheliped proximal dactylus seta present or absent. Marsupium formed by one pair of oostegites. Pereopods 2 to 6 carpus with or without modified blade-like setae. Pereopods 4 to 6 ischium with one or two setae, merus with one or two setae and dactylus fused with unguis forming claw. Pleopods usually elongate with terminal setae only (three exceptions). Uropod exopods and endopods with one or two articles or one pseudo-articulate article.

Genus: *Beksitanais* n. gen.

Diagnosis: Antennula article-3 with thickened rod seta. Antenna article 2 and 3 with seta; article-6 without thickened rod seta. Maxiliped palp article-4 without thickened rod seta. Chela forcipate with serrate incisive margin, propodus (palm) without small folds in distodorsal corner, cheliped with one interior seta on fixed finger. Pereopods 4–6 dactylus and unguis fused with a small hook on tip. Uropod exopod with one article, 0.5x endopod, endopod with pseudoarticulation.

Type species: *Beksitanais apocalyptica* n. sp.

Etymology: The genus is named to honour the famous Polish painter Zdzisław Beksiński.

Remarks: Beksitanais n. gen. is most similar to *Mystriocentrus*, but the presence of a thick rod seta on antennule article-3, lack of folds on distodorsal corner of the cheliped, absence of thick rod seta on antenna article-6, as well as lack of thick rod seta on maxilliped palp article-4 allow to distinguish both genera. *Beksitanais* can be separated from the genus *Akanthinotanais* by presence of blade-like spine on carpus of pereopod 2 and 3 and a forcipate chela. From the genus *Parapseudotanais* it can be distinguished by the presence of one interior seta on fixed finger and exopod uropod with one article only. Serrate inner margin on fixed finger and relative length of propodus of pereopod-1 allow to differentiate *Beksitanais* from *Pseudotanais*.

***Beksitanais apocalyptica* n. sp.**

Figures 4–8.

Material examination. Holotype: neuter, BL = 0.9 mm, ZMH K-56558. St. 81, 11° 3.97′N, 119° 37.67′W, 4365 m, EBS, 1 Apr 2015.

Paratypes: two neuters, BL = 0.8 mm (one dissected), ZMH K-56557.

ZMH K-56558, ZMH K-56559 (dissected): adult (swimming male), BL = 1.8 mm (dissected), ZMH K-56556. St. 81, 11° 3.97′N, 119° 37.67′W, 4365 m, EBS, 1 Apr 2015; neuter, BL = 1 mm (dissected), ZMH K-56562. St. 128, 13° 51,10′N 123° 15,12′W, 4510.7 m, Box Core, 9 Apr 2015; two mancas, ZMH K-56560, ZMH K-56561. St. 137, 13° 51,36′N 123° 14,28′W, 4509 m, Box Core, 11 Apr 2015.

Diagnosis: Antenna article-6 and maxilliped palp article-4 without thickened rod seta. Uropod exopod with one article, 0.5x endopod; endopod with pseudoarticulation.

Etymology: The species is named by one of the period of artwork of Zdzisław Beksiński suffused by the post-apocalyptic images.

Description of neuter. BL = 0.9 mm. Body robust (Fig. 4), 3.9 L:W. Carapace 0.7 L:W, 3.6x pereonite-1, 0.2x BL. Pereonites 0.6x BL, pereonites-1–6: 0.2, 0.2, 0.5, 0.6, 0.5 and 0.4 L:W, respectively. Pleon short, 0.2x BL. Pleonites 0.8 L:W.

Antennule (Fig. 5A) article-1 0.6x total length, 7.0 L:W, 2.6x article-2, with one simple, four penicillate mid-length setae, strong subdistal seta and three penicillate distal setae; article-2 3.0 L:W, 1.4x article-3, with subdistal seta; article-3 2.4 L:W, with five simple, one bifurcate and one penicillate setae, and one aestetasc.

Antenna (Fig. 5B) article-1 1.2 L:W; article-2 0.8x article-3, with seta 0.7x the article; article-3 1.8 L:W, 0.2x article-4, with seta 0.5x the article; article-4 8.8 L:W, 2.7x article-5, with one simple and three penicillate subdistal setae, one simple and three penicillate setae distally; article-5 4.1 L:W, 5.8x article-6, with seta; article-6 0.8 L:W, with four setae.

Mouthparts. Left mandible (Fig. 5C) *lacinia mobilis* well developed, distally serrate, incisor distal margin serrate. Right mandible (Fig. 5D) incisor distal margin serrate, *lacina mobilis* merged to small process. Maxilliped (Fig. 5E) basis 0.7 L:W; endites partly merged, distal margin with two tubercles (gustatory cusps); article-2 inner margin with three setae; article-3 with three inner setae, article-4 with six setae: one subdistal, five distal.

Cheliped (Fig. 6A) slender; basis 1.3 L:W; merus with ventral seta; carpus 2.1 L:W, with dorso-distal and dorsosubproximal setae; chela forcipate; palm 1.2 L:W, with row of five setae on inner side; fixed finger distal spine pointed, regular size, with three ventral setae; dactylus 6.3 L:W, cutting edge serrate, proximal seta present.

Pereopod-1 (Fig. 6B) basis 10.4 L:W, 4.3x merus with two simple setae dorsally; ischium naked; merus 2.4 L:W, 0.7x carpus naked; carpus 3.4 L:W, 0.7x propodus, with one simple seta; propodus 5.4 L:W, 1.8x dactylus and unguis combined length, with one simple seta; dactylus 0.5x unguis.

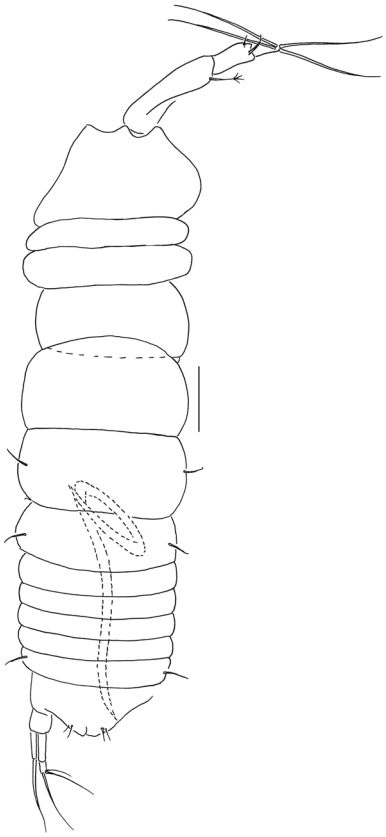

Figure 4. *Beksitanais apocalyptica* n. sp., ZMH K-56558, holotype, neuter, dorsal view in distal part of the animal parasitic nematode is observed. Scale bar: 0.1 mm.

Pereopod-2 (Fig. 6C) basis 6.5 L:W, 3.1x merus with one simple and one penicilate seta dorsally; ischium naked; merus 1.8 L:W, 1.3x carpus, with one simple seta; carpus 1.8 L:W, 0.7x propodus, with one simple seta and one blade-like spine, 0.3x propodus; propodus 4.2 L:W, 1.5x dactylus and unguis combined length; dactylus 1x unguis.

Pereopod-3 (Fig. 6D) basis broken; ischium with ventral seta; merus 2.1 L:W, 1.2x carpus naked; carpus 1.7 L:W, 0.5x propodus, with three simple and blade-like spine, 0.2x propodus; propodus 5.4 L:W, 2.5x dactylus and unguis combined length, with one spine; dactylus 0.7x unguis, dactylus with simple seta.

Pereopod-4 (Fig. 6E) basis 5.6 L:W, 3.5x merus; ischium with seta; merus 1.8 L:W, 0.5x carpus, with serrate seta; carpus 4.1 L:W, 1x propodus, with two simple setae, one rod seta 0.2x propodus, and one blade-like spine 0.2x propodus; propodus 6.6 L:W, 2.5x dactylus and unguis combined length, with three setae; dactylus and unguis fused with a small hook on tip.

Pereopod-5 (Fig. 6F) basis 5.6 L:W, 5.0x merus, with two ventral penicillate setae; ischium with ventral seta; merus 1.8 L:W, 0.4x carpus, with seta; carpus 5.0 L:W, propodus, with two simple setae, one rod seta 0.2x propodus, and one blade-like spine 0.3x propodus; propodus 4.8 L:W, 2.9x dactylus and unguis combined length, with two setae on ventral and seta on dorsal margin; dactylus and unguis fused with a small hook on tip.

Pereopod-6 (Fig. 6G) basis 7.5 L:W, 43.5x merus; ischium naked; merus 2.4 L:W, 0.6x carpus, with serrate seta; carpus 4.7 L:W, 1x propodus, with two simple setae, rod seta 0.3x propodus, and blade-like spine 0.2x propodus; propodus 5.6 L:W, 2.8x dactylus and unguis combined length, with four serrate setae; dactylus and unguis fused with a small hook on tip.

Pleopods (Fig. 6E) exopod with four, endopod with 7 plumose setae.

Uropod (Fig. 6F) peduncle 0.9 L:W; exopod one articled, 6.7 L:W, with strong seta 0.5x endopod; endopod article-1 3.9 L:W, article-2 2.4 L:W, with four simple and one penicillate seta.

Male description. BL = 1.8 mm. Body robust (Fig. 7A,B), 3.9 L:W. Carapace 0.7 L:W, 4.8x pereonite-1, 0.2x BL. Pereonites 0.3x BL, pereonites 1–6: 0.2, 0.2, 0.3, 0.3, 0.3 and 0.3 L:W, respectively. Pleon short, 0.5x BL. Pleonites 0.4 L:W.

Antennule (Fig. 8A) 7-articled; article-1 0.3x total length, 1.9 L:W, 1.7x article-2, with one penicillate and nine simple setae (six broken); article-2 wide, 2.5x article-3, with two penicillate setae; article-3 0.7 L:W, 0.9x article-4, with three setae; article-4 1.2 L:W, 0.8x article-5; article-5 0.7 L:W, 0.2x article-6; article-6 4.5 L:W, 1.6 article-7; article 4–6 with dense row of aestetascs; article-7 5.7 L:W, with three setae.

Antenna (Fig. 8B) 7-articled; article-1 fused to body; article-2 0.8x article-3; article-3 0.3x article-4; article-4 0.5 article-5; article-5 1.4x article-6, with three penicillate setae in mid-length and with one penicillate and three

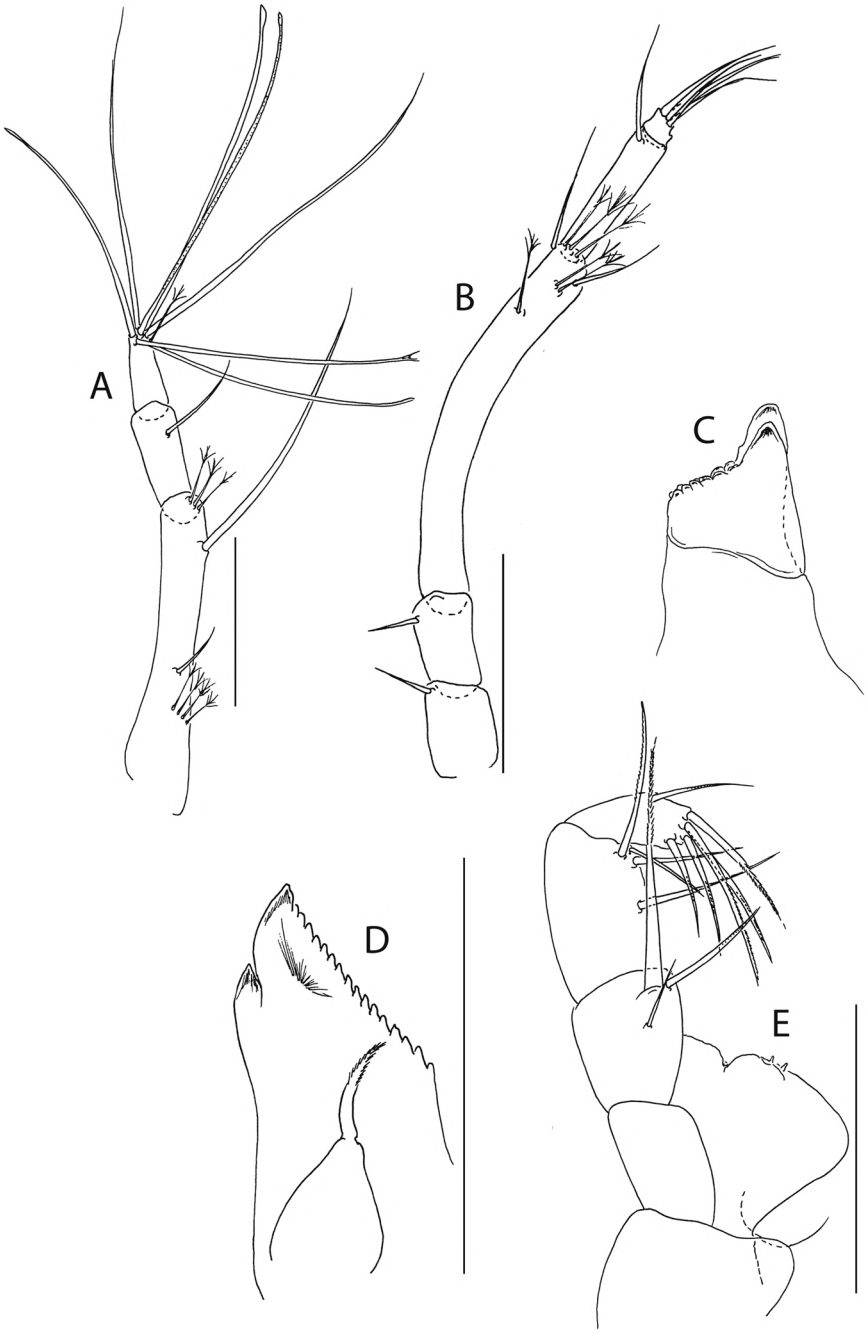

Figure 5. *Beksitanais apocalyptica* n. sp., ZMH K-56559, neuter. Mouthparts. (**A**), antennule; (**B**), antenna; (**C**), left mandible; (**D**), rigth mandible; (**E**), maxilliped. Scale bar: 0.1 mm.

simple setae; article-6 2.2x article-7, with two penicillate setae in mid-length and with two penicillate and one simple seta distally; article-7 with subdistal seta and four distal setae.

Maxilliped (Fig. 8C) basis 0.9 L:W, endites separated, distal margin naked; article-3 with three setae; article-4 with five setae.

Cheliped (Fig. 8D) slender, basis 1.6 L:W; merus with seta; carpus 1.7 L:W, with dorso-distal seta and two ventral setae; chela non-forcipate; palm 1.7 L:W, with row of eight short and one long setae on inner side; fixed finger distal spine pointed, regular size, with three ventral setae, and two dorsal setae, cutting edge serrate, dactylus 4.3 L:W, proximal seta present.

Pereopod-1 (Fig. 8E) basis 6.2 L:W, 2.8x merus, with two setae; ischium with ventral seta; merus 3.6 L:W, 0.7x carpus, with one seta; carpus 4.0 L:W, 0.8x propodus, with four setae; propodus 7.5 L:W, with two setae.

Pereopod-2 (Fig. 8F) basis 6.4 L:W, 3.0x merus, with three simple and one penicillate setae; ischium with ventral seta; merus 2.5 L:W, 0.7x carpus, with spine; carpus 4.2 L:W, 0.7x propodus, with two simple setae and one spine; propodus 7.0 L:W, with two setae and one spine.

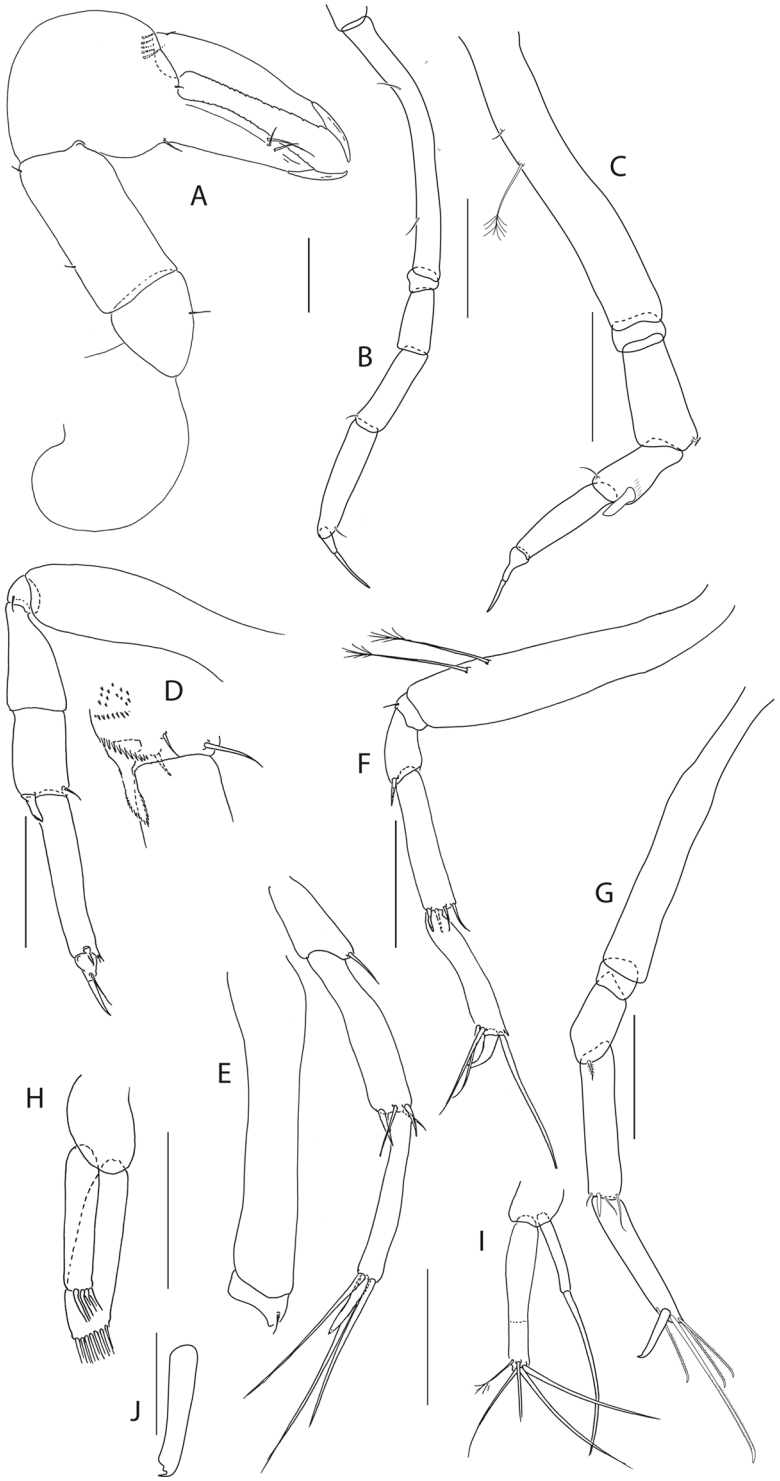

Figure 6. *Beksitanais apocalyptica* n. sp., ZMH K-56559, neuter. (**A**), cheliped; (**B**), pereopod-1; (**C**), pereopod-2; (**D**), pereopod-3; (**E**), pereopod-4; (**F**), pereopod-5; (**G**), pereopod-6; (**H**), pleopod; (**I**), uropod; (**J**), magnified dactylus and unguis for pereopods 4–6. Scale bars: 0.1 mm.

Pereopod-3 (Fig. 8G) basis 6.4 L:W, 3.4x merus, with two simple and one penicillate setae; ischium with ventral seta; merus 2.2 L:W, 0.6x carpus, with seta and spine; carpus 4.0 L:W, with two setae and three spines.

Pereopod-4 (Fig. 8H) basis 3.7 L:W, 2.5x merus, with three setae; ischium with two setae; merus 2.8 L:W, 0.9x carpus, with spine; carpus 2.8 L:W, 1.4x dactylus and unguis combined length, with two spines; dactylus 1.8x unguis.

Pereopod-5 (Fig. 8I) basis 3.2 L:W, 2.7x merus, with two simple setae; ischium with two setae; merus 2.4 L:W, 0.9x carpus, with two distal spines; carpus 2.7 L:W, with seta and two spines.

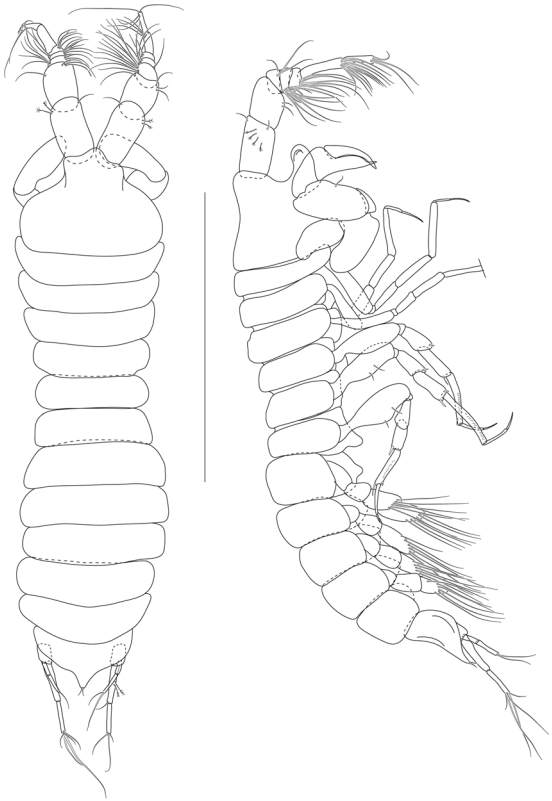

Figure 7. *Beksitanais apocalyptica* n. sp., ZMH K-56556, male. A, dorsal view; B, lateral view. Scale bar: 1 mm.

Pereopod-6 (Fig. 8J) basis 3.3 L:W, 2.2x merus, with three simple setae; ischium with two ventral setae; merus 2.6 L:W and carpus, with one seta and three spines; carpus 7.7 L:W, 1.5x dactylus and unguis combined length, with three spines; dactylus 1.6x unguis.

Pleopods (Fig. 8K) exopod with eleven, endopod with 14 plumose setae.

Uropod (Fig. 8L) peduncle 1.3 L:W; exopod with two articles, 0.6x endopod, article-1 3.3 L:W, article-2 5.5 L:W, with simple seta; endopod article-1 4.2 L:W, with row of six penicillate mid-length setae and two penicillate distal setae; article-2 7.0 L:W, with three short and one long setae.

Distribution: *B. apocalyptica* n. sp. is known from three stations located in the licence area of the consortium Interoceanometal (IOM) at 4365 m depth and in the Belgium license area (GSR) at 4510 m depth in the Central Pacific.

Remarks: In the holotype specimen, a parasitic nematode was observed in the distal part of the body (Fig. 4).

Genus: *Pseudotanais* G.O. Sars, 1882

Diagnosis: Antenna article-6 and maxilliped palp article-4 without rod (thickened) seta. Chela cutting edges simple; fixed finger with one seta. Pereopod 2–6 carpus with blade-like spine.

Pseudotanais species described in the present study are grouped into previously erected morpho-groups by Bird and Holdich (1989)[31] and Jakiel *et al.* (2018)[32]. A list of characters that define each group are included before the species descriptions. An identification key is included at the end of the Results section as well to enable easier identification and clear separation of morpho-groups.

'affinis + longisetosus' group

Diagnosis: Antenna article 2–3 with spines. Mandible acuminate or wide. Chela non-forcipate. Pereopod-1 merus with long seta. Pereopod-2 carpus with long blade-like spine. Uropod slender with exopod uropod about 3/4th the endopod or equal to endopod.

Species included: *Pseudotanais affinis* Hansen, 1887; *P. longisetosus* Sieg, 1977; *P. longispinus* Bird & Holdich, 1989; *P. macrochelis* Sars, 1882; *P. nipponicus* McLelland, 2007; *P. nordenskioldi* Sieg, 1977; *P. spatula* Bird & Holdich, 1989; *P. scalpellum* Bird & Holdich, 1989; *P. svavarssoni* Jakiel, Stępień & Błażewicz, 2018; *P. vitjazi* Kudinova-Pasternak, 1966; *Pseudotanais* sp. O (McLelland, 2008); *Pseudotanais* sp. P (McLelland 2008); *P. gaiae* n. sp.; *P. geralti* n. sp.; *P. julietae* n. sp.; *P. romeo* n. sp.; *P. uranos* n. sp.; *P. yenneferae* n. sp.

***Pseudotanais uranos* n. sp.**

Figures 9–11.

Material examined: Holotype: neuter, BL = 1.5 mm, ZMH K-56606. St 197, 18° 48.66′N 128° 22.75′W, 4805 m, EBS, 22 Apr 2015.

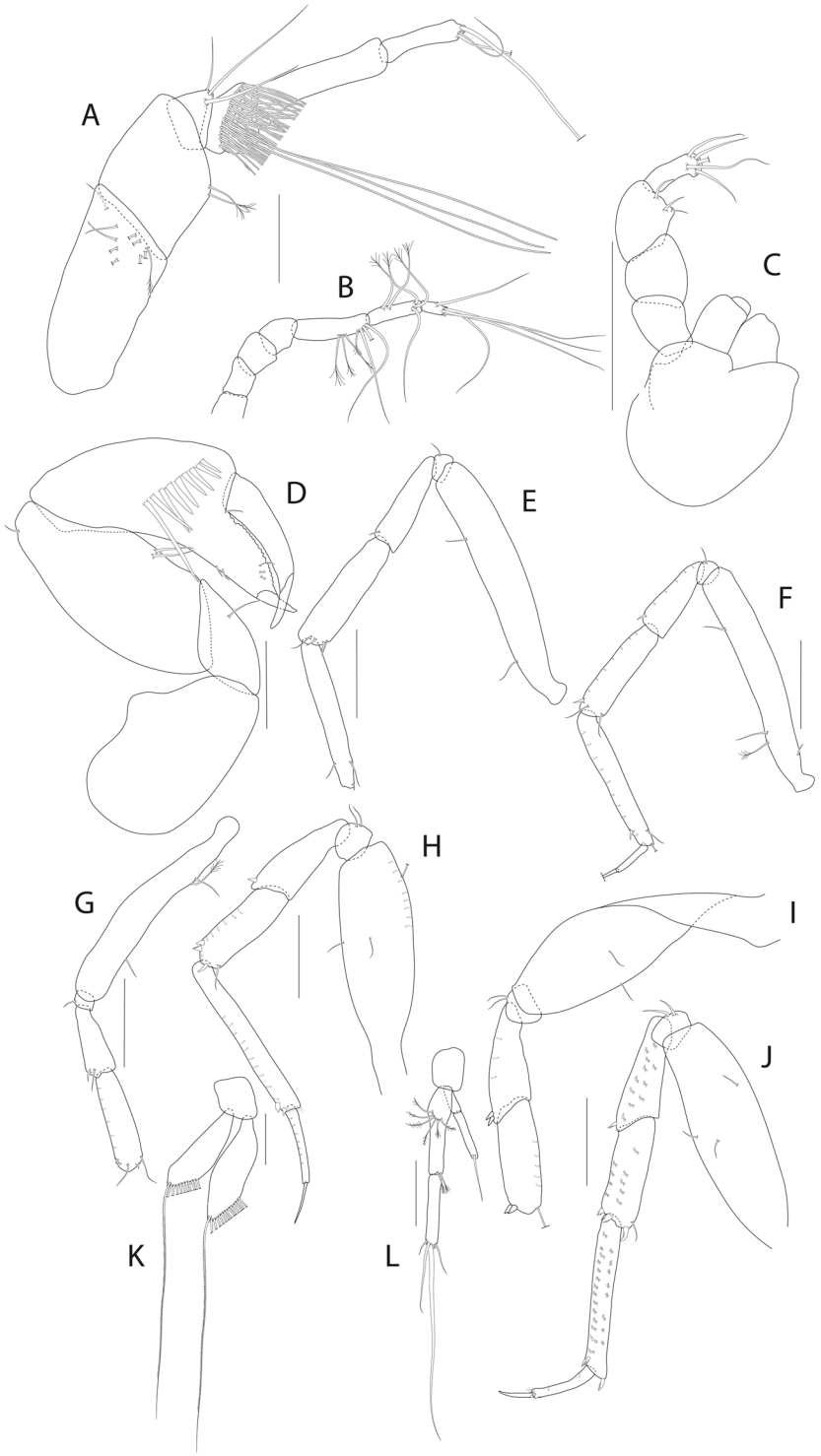

Figure 8. *Beksitanais apocalyptica* n. sp., ZMH K-56556, male. (**A**), antennule; (**B**), antenna; (**C**), maxilliped; (**D**), cheliped; (**E**), pereopod-1; (**F**), pereopod-2; (**G**), pereopod-3; (**H**), pereopod-4; (**I**), pereopod-5; (**J**), pereopod-6; (**K**), pleopod; (**L**), uropod. Scale bars: 0.1 mm.

Paratypes: four neuters, BL = 1.4–1.8 mm, ZMH K-56604 (dissected), ZMH K-56605, ZMH K-56607, ZMH K-56608. St 197, 18° 48.66′N 128° 22.75′W, 4805 m, EBS, 22 Apr 2015.

Diagnosis: Mandible molar acuminate without central spine. Pereopod-1 basis with three setae. Pereopod 5–6 carpus rod seta long (≥0.8x propodus).

Etymology: The name is dedicated to Uranos, the Greek god personifying the sky.

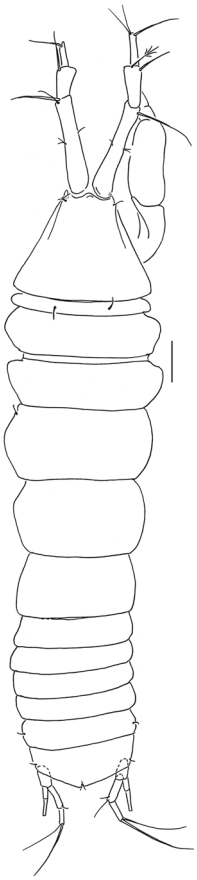

Figure 9. *Pseudotanais uranos* n. sp., ZMH K-56605, holotype neuter. Dorsal view. Scale bar: 0.1 mm.

Description of neuter. BL = 1.5 mm. Body slender (Fig. 9), 4.0 L:W. Carapace 1.2 L:W, 6.8x pereonite-1, 0.2x BL. Pereonites 0.5x BL, pereonites-1–6: 0.2, 0.9, 0.4, 0.5, 0.6 and 0.5 L:W, respectively. Pleon short, 0.3x BL. Pleonites 0.9 L:W. Pleotelson 0.7x pereonite-6.

Antennule (Fig. 10A) article-1 0.5x total length, 6.8 L:W, 2.3x article-2, with six penicillate setae arranged in two rows at mid-length, and four penicillate and one simple setae; article-2 4.0 L:W, 1.1x article-3, with one penicillate and one simple setae; article-3 6.8 L:W, with one penicillate, one bifurcate and two simple setae, and with aestetasc distally.

Antenna (Fig. 10B) article-2 2.1 L:W; article-2 0.8x article-3, with spine 0.3x article-2; article-3 2.2 L:W, 0.3x article-4, with spine 0.2x the article-3; article-4 10.0 L:W, 2.4x article-5, with two simple and four penicillate setae distally; article-5 5.0 L:W, 10.0x article-6, with seta; article-6 0.7 L:W, with five setae.

Mouthparts. Labrum (Fig. 10C) hood-shape. Left mandible (Fig. 10D) *lacinia mobilis* well developed, distally serrate, incisor distal margin serrate, molar acuminate. Right mandible (Fig. 10E) incisor distal margin serrate, *lacina mobilis* merged to small process. Maxillule (Fig. 10F) with eight distal spines. Maxilliped (Fig. 10G) endites merged, with groove at mid-length, distal margin with two tubercles (gustatory cusps); palp article-2 inner margin with three setae, outer margin with seta; article-3 with four inner setae; article-4 with six distal and subdistal setae.

Cheliped (Fig. 11A) slender; basis 1.7 L:W, carpus 3.0 L:W, with two ventral and one dorsosubdistal setae; chela non-forcipate, palm 1.3 L:W, with row of six setae on inner side, fixed finger distal spine pointed, regular size, with three ventral setae; dactylus 6.5 L:W, ventral margin smooth, proximal seta present.

Pereopod-1 (Fig. 11B) coxa with seta; basis 9.3 L:W, with two ventral setae and one dorsal seta; ischium with ventral seta; merus 1.8 L:W, 1.5x carpus, with one short and one long setae; carpus 2.5 L:W, 0.5x propodus, with seta; propodus 10.2 L:W, with seta, 1.3x dactylus and unguis combined length; dactylus 0.6x unguis.

Pereopod-2 (Fig. 11C) basis 5.8 L:W, 3.4x merus, with two simple ventral setae, and with one simple and one penicillate setae dorsally; ischium with seta; merus 1.9 L:W, 0.8x carpus, with serrate seta; carpus 2.8 L:W, 0.8x propodus, with one seta and one blade-like spine (broken); propodus 7.0 L:W, 1.5x dactylus and unguis combined length, with distal seta and microtrichia on ventral margin; dactylus 0.6x unguis.

Pereopod-3 (Fig. 11D) coxa with seta; basis 6.7 L:W, 3.9x merus, with one ventral and one dorsal setae; ischium with ventral seta; merus 2.4 L:W, 0.7x carpus, with serrate seta; carpus 4.0 L:W, 0.8x propodus, with one simple and one wide-base seta and with blade-like spine 0.5x propodus; propodus 7.8 L:W, 1.5x dactylus and unguis combined length, with distal seta and microtrichiae on ventral margin; dactylus 0.7x unguis.

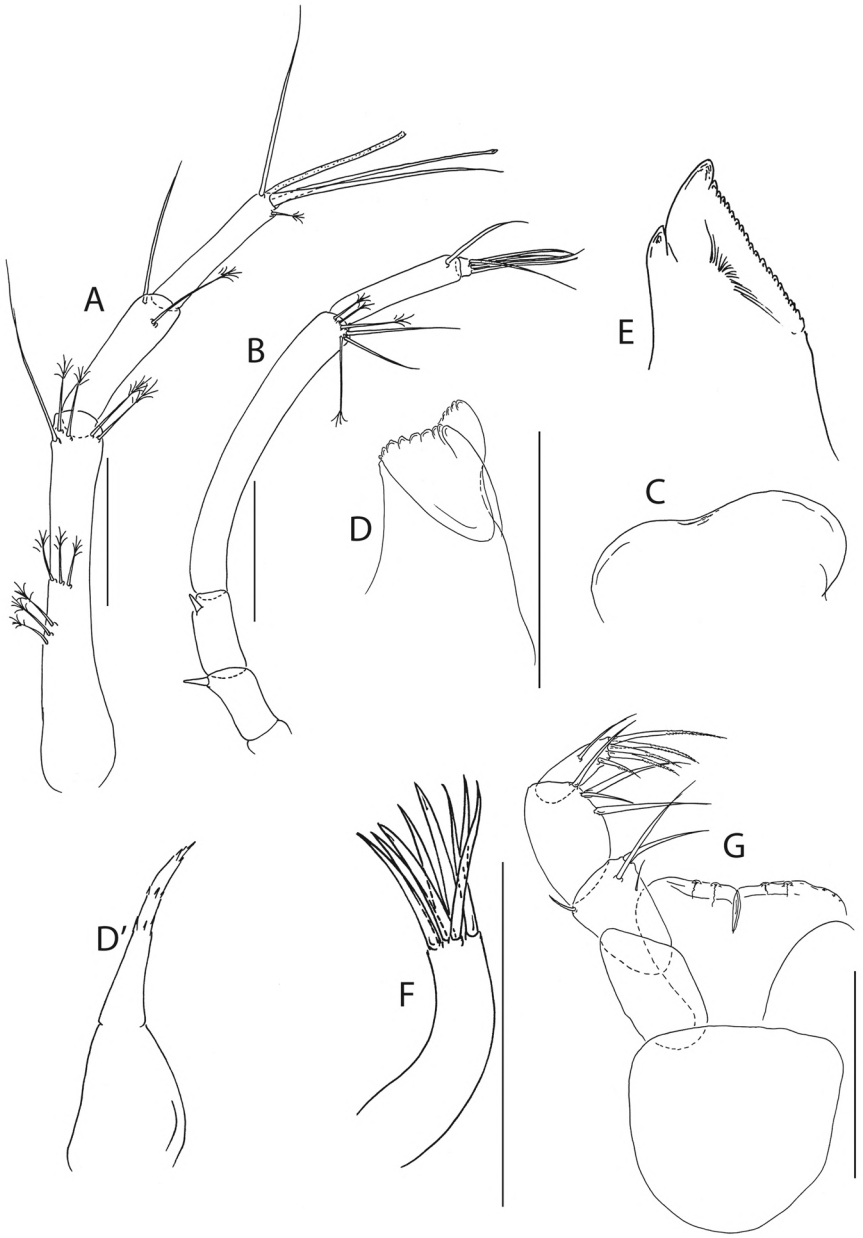

Figure 10. *Pseudotanais uranos* n. sp., ZMH K-56606, neuter. (**A**), antennule; (**B**), antenna; (**C**), labrum; (**D**), left mandible; D' left molar; (**E**), right mandible; (**F**), maxillule; (**G**), maxilliped. Scale bar: 0.1 mm.

Pereopod-4 (Fig. 11E) basis 6.2 L:W, 4.1x merus, with penicillate ventral seta; ischium with seta; merus 2.5 L:W, 0.6x carpus, with seta; carpus 3.6 L:W, with two short and one rod setae, and with blade-like spine 0.3x propodus; propodus 5 L:W, 2.3x dactylus and unguis combined length, with one simple and two serrate setae subdistally, and with serrate seta distally 0.8x propodus and microtrichiae on ventral margin; dactylus 2.7x unguis.

Pereopod-5 (Fig. 11F) basis 5.6 L:W, 4.1x merus, with rod seta at mid-length; merus 3.0 L:W, 0.5x carpus; carpus 3.5 L:W, 1.3x propodus, with two simple and one rod setae 0.7x propodus, and with blade-like spine 0.4x propodus; propodus 4.5 L:W, 3.0x dactylus and unguis combined length, with two serrate subdistal setae, serrate distal seta (broken) and microtrichiae on ventral margin; dactylus 2.0x unguis.

Pereopod-6 (Fig. 11G) basis 5.5 L:W, 4.7x merus; ischium with ventral seta; merus 1.7 L:W, 0.5x carpus, with one simple and one serrate setae; carpus 3.0 L:W, 1.1x propodus, with two simple and one rod setae, and with blade-like spine 0.4x propodus, rod seta 0.8x propodus; propodus 4.0 L:W, 2.2x dactylus and unguis combined length, with two serrate setae subdistally, serrate distal seta broken and with microtrichiae on ventral margin; dactylus 1.7x unguis.

Uropod (Fig. 11H) peduncle 0.8 L:W; exopod with two articles, article-1 2.7 L:W; article-2 6.7 L:W with distal seta; endopod article-1 4.7 L:W, with one simple and two penicillate setae; article-2 5.5 L:W, with one penicillate and two simple setae. Exopod 0.7x endopod.

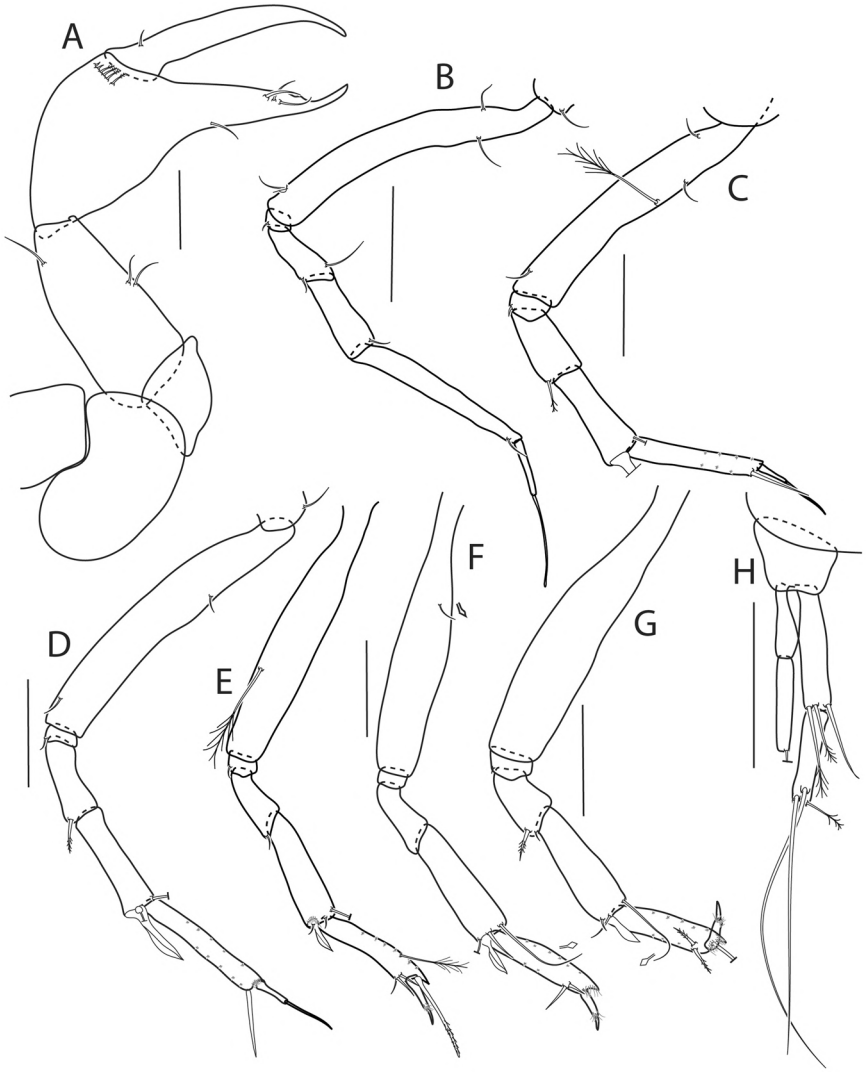

Figure 11. *Pseudotanais uranos* n. sp., ZMH K-56606, neuter (**A**), cheliped; (**B**), pereopod-1; (**C**), pereopod-2; (**D**), pereopod-3; (**E**), pereopod-4; (**F**), pereopod-5; (**G**), pereopod-6; (**H**), uropod. Insets at (**F**,**G**) show detail of tip of the rod seta. Scale bars: 0.1 mm.

Distribution: *P. uranos* n. sp. is known only from APEI3 on the Clarion and Clipperton Fractures Zone, Central Pacific.

Remarks: Long rod seta on pereopods 5–6 of *P. uranos* n. sp. allows to distinguish this species from *Pseudotanais affinis*, *P. macrochelis*, *P. nordenskioldi*, *P. scalpellum*, *P. svavarssoni*, *P. vitjazi* and *Pseudotanais* sp. P (McLelland, 2008), which have short rod seta on pereopod 5–6 carpus. *P. uranos* has only three seta on basis of pereopod-1, whereas *P. longispinus* and *P. nipponicus* have more (5–7) setae. *P. uranos* n. sp. pereonite-1 is shorter than pereonite-2 whereas *P. longisetosus* has pereonite-1 as long as pereonite-2. Finally, *P. uranos* n. sp. has a semilong (0.5x propodus) blade-like spine on carpus of pereopod-3, while *P. spatula* and *Pseudotanais* sp. O[33] have a long (≥=0.6x propodus) blade-like spine on carpus of pereopod-3.

***Pseudotanais gaiae* n. sp.**

Figure 12 and 13.

Material examined: Holotype: neuter (dissected), BL = 1.5 mm, ZMH K-56576. St 192, 18° 44.81′N 128° 21.87′W, 4877 m, EBS, 21 Apr 2015.

Diagnosis: Mandible molar acuminate with central, elongated spine. Pereopod-1 basis without setae. Pereopod 5–6 carpus rod seta long.

Etymology: The species is named after Gaia, the ancestral mother of all life – Mother Earth; the wife of Uranos.

Description. Antennule (Fig. 12A) article-1 0.5x total length, 5.0 L:W, 2.3x article-2, with two setae; article-2 0.4 L:W, 0.8x article-3; article-3 4.2 L:W, with one simple, three bifurcate and one broken setae distally.

Antenna (Fig. 12B) article-2 1.5 L:W, 0.8x article-3, with spine 0.3x the article-2; article-3 1.8 L:W, 0.3x article-4, with spine 0.3x the article-3; article-4 7.5 L:W, 2.2x article-5, with three simple setae; article-5 9.6 L:W, 9.0x article-6, with distal seta; article-6 0.7 L:W, with five setae.

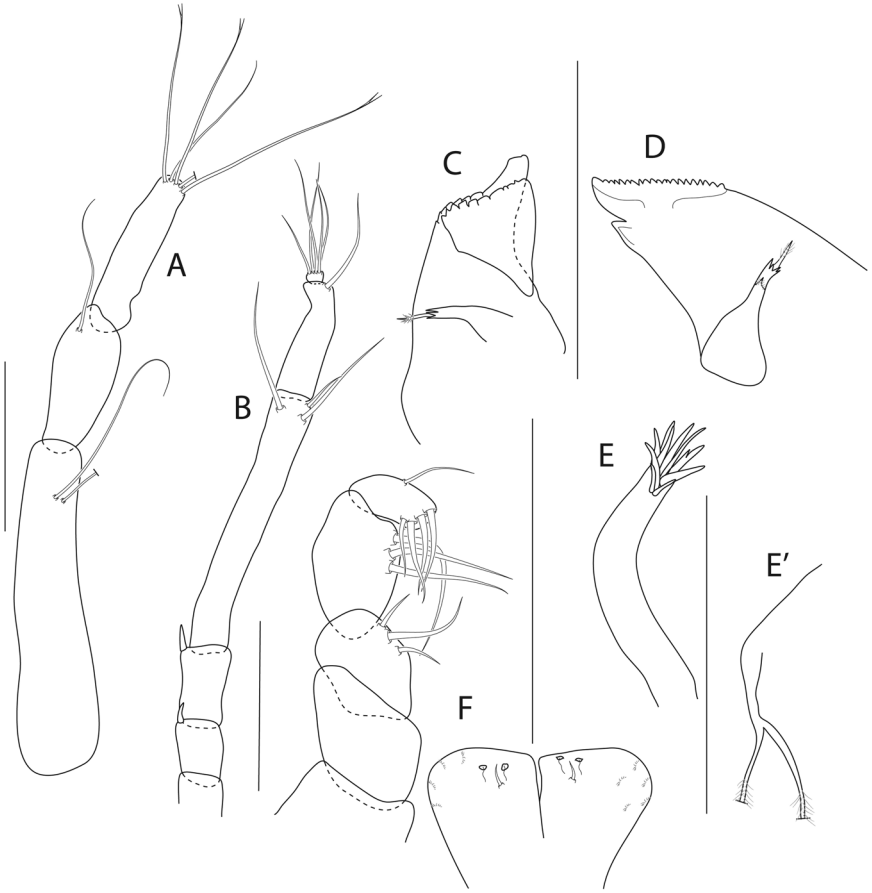

Figure 12. *Pseudotanais gaiae* n. sp., ZMH K-56576, holotype neuter. (**A**), antennule; (**B**), antenna; (**C**), left mandible; (**D**), right mandible; (**E**), maxillule; E' endit; (**F**), maxilliped. Scale bar: 0.1 mm.

Mouthparts. Left mandible (Fig. 12C) *lacinia mobilis* well developed and serrate distally, incisor distal margin serrate, molar pointed, with central, elongated spine. Right mandible (Fig. 12D) incisor distal margin serrate, *lacina mobilis* merged to small process; molar as in mandible left. Maxillule (Fig. 12E,E') with eight simple and one bifurcate distal spines. Maxilliped (Fig. 12F) endites merged, with groove in the mid-length, distal margin with two tubercles (gustatory cusps) and seta; article-2 inner margin with three inner setae; article-3 with three setae, article-4 with five setae.

Cheliped (Fig. 13A) slender; basis 2.0 L:W; carpus 1.8 L:W, with two ventral setae and subdistal dorsal seta; palm 1.1 L:W, with row of four setae on inner side; fixed finger distal spine pointed, regular size, 2.3x palm, with three ventral setae; dactylus 6.0 L:W, proximal seta present.

Pereopod-1 (Fig. 13B) coxa with seta; basis 8.0 L:W; ischium with ventral seta; merus 2.2 L:W, 0.8x carpus; carpus 2.8 L:W with seta, 0.4x propodus; propodus 7.2 L:W, 2.4x dactylus and unguis combined length, with seta; dactylus 0.6x unguis.

Pereopod-2 (Fig. 13C) coxa with seta; basis 8.6 L:W, 10.0x merus; ischium with ventral seta; merus 2.0 L:W, 0.7x carpus, with seta; carpus 2.4 L:W, 0.6x propodus, with blade-like spine 0.6x propodus; propodus 5.8 L:W, with microtrichia.

Pereopod-3 (Fig. 13D) basis, ischium and merus broken (not seen); merus with serrate seta; carpus 2.6 L:W, 0.7x propodus, with wide-base seta and one blade-like spine, 0.5x propodus; propodus 5.2 L:W, 1.5x dactylus and unguis combined length, with one simple and one serrate seta and microtrichia on ventral margin; dactylus 0.7x unguis.

Pereopod-5 (Fig. 13E) basis 7.8 L:W, 3.2x merus; merus 2.1 L:W, 0.7x carpus, with serrate seta; carpus three L:W, 1.1x propodus, with one simple, one rod setae, and one blade-like spine (broken), rod seta propodus; propodus 3.7 L:W, 2.4x dactylus and unguis combined length, two serrate setae subdistally, one simple and one serrate setae distally 1x propodus; dactylus 1.2x unguis.

Pereopod-6 (Fig. 13F) basis 5.0 L:W, 3.5x merus, merus 2.0 L:W, 0.6x carpus, with seta; carpus 3.4 L:W, propodus, with serrate seta, rod seta propodus and blade-like spine 0.4x propodus; propodus 6.0 L:W, 2.0x dactylus and unguis combined length, with one penicillate and two serrate setae subdistally, and serrate seta distally; dactylus 2.0x unguis.

Pleopods (Fig. 13G) exopod with seven and endopod with eight plumose setae.

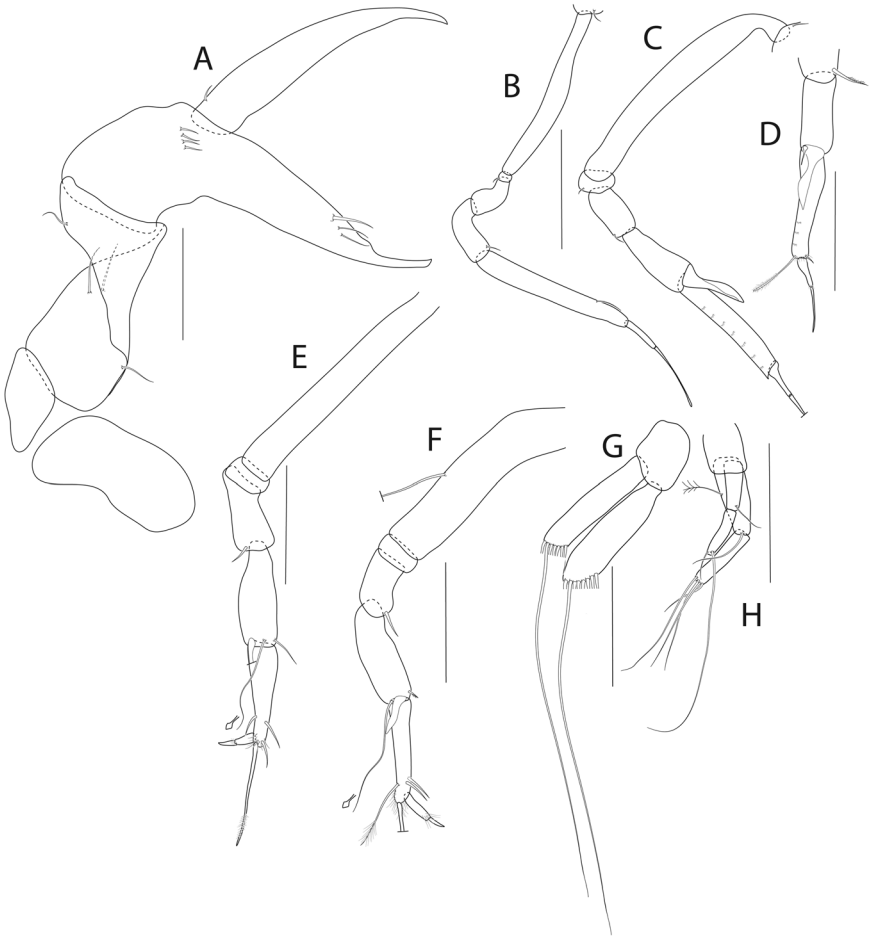

Figure 13. *Pseudotanais gaiae* n. sp., ZMH K-56576, holotype neuter. (**A**), cheliped; (**B**), pereopod-1; (**C**), pereopod-2; (**D**), pereopod-3; (**E**), pereopod-5; (**F**), pereopod-6; (**G**), pleopod; (**H**), uropod. Insets at (**E**,**F**) show detail of tip of the rod seta. Scale bar: 0.1 mm.

Uropod (Fig. 13H) 1.4 L:W, exopod with two articles, 0.7x endopod; article-1 2.7 L:W, with seta; article-2 3.6 L:W, with two setae; endopod article-1 3.0 L:W, with one mid-length penicillate and one distal setae; article-2 3.7 L:W, with four simple setae.

Distribution: *P. gaiae* n. sp. is known only from APEI3 of the Clarion and Clipperton Fractures Zone, Central Pacific.

Remarks: *Pseudotanais gaiae* n. sp. is most similar to *P. uranos* (Fig. 1) and therefore is distinguished from *Pseudotanais affinis*, *P. macrochelis*, *P. nordenskioldi*, *P. scalpellum*, *P. svavarssoni*, *P. vitjazi*, *Pseudotanais* sp. P (McLelland, 2008), *P. longispinus* and *P. nipponicus* by the same set of characters as *P. uranos* (see remarks under *P. uranos*). *P.gaiae* n. sp., with two prickly tubercles (gustatory cusps) and a seta in the maxilliped endites, is distinguished from *P. longisetosus,* which maxilliped endite is naked. *P. gaiae* n. sp. with short seta (0.2x carpus) on pereopod-1 carpus is separated from *P. spatula* that has pereopod-1 carpus with seta long (0.9x carpus). *P. gaiae* and *P. uranos* represent cryptic species, with minute morphological differences, that can be separated using molecular data. The main morphological character that allows distinguishing *P. gaiae* from *P. uranos* is the presence of a central elongated spine on the mandible molar.

***Pseudotanais julietae* n. sp.**

Figures 14–16.

Material examined: Holotype: neuter, BL = 1.8 mm (partly dissected), ZMH K-56584. St 133, 13° 50.98′N 1 23° 15.07′W, 4507 m, 10 Apr 2015.

Diagnosis: Maxilliped endites ornamented with two tubercles (gustatory cusps) and one seta. Pereopods 1–3 basis with six, five and five setae respectively. Pereopod 5–6 carpus with long distodorsal rod seta. Exopod of the uropod as long as endopod.

Etymology: The species is named after Juliet Capulet, the lover of Romeo from William Shakespeare's tragedy *Romeo and Juliet*.

Description of neuter. BL = 1.8 mm. Body robust (Fig. 14), 3.4 L:W. Carapace 0.8 L:W, 8.0x pereonite-1, 0.2x BL. Pereonites 0.6x BL, pereonites-1–6: 0.1, 0.2, 0. 2, 0. 6, 0.6 and 0.5 L:W, respectively. Pleon short, 0.2x BL. Pleonites 0.9 L:W.

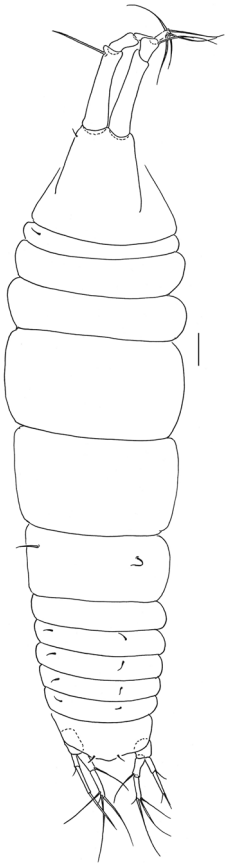

Figure 14. *Pseudotanais julietae* n. sp., ZMH K-56584, holotype neuter. Dorsal view. Scale bar: 1 mm.

Antennule (Fig. 15A) article-1 0.6x total length, 4.5 L:W, 3.1x article-2, with one simple and nine penicillate mid-length setae, and with one simple and three penicillate distal setae; article-2 1.9 L:W, 0.8x article-3, with one simple and two penicillate setae distally; article-3 4.6 L:W, with one simple, four bifurcate setae, and one aestetasc.

Antenna (Fig. 15B) 1.3 L:W; article-1 not observed; article-2 1.2x article-3, with spine 0.4x the article-2; article-3 1.4 L:W, 0.3x article-4, with spine, 0.4x the article-3; article-4 7.8 L:W, 2.1x article-5, with penicillate mid-length seta, one penicillate subdistal seta, three simple and three penicillate distal setae; article-5 4.1 L:W, 6.6x article-6, with distal seta; article-6 0.7 L:W, with four simple setae.

Mouthparts. Labrum (Fig. 15C) hood-shape, setose. Left mandible (Fig. 15D) *lacinia mobilis* well developed and distally serrate, incisor distal margin serrate. Right mandible (Fig. 15E) incisor distal margin serrate, *lacina mobilis* merged to small process, molar lost during dissection. Maxillule (Fig. 15F) with 7 distal spines and three subdistal setae. Labium (Fig. 15G) lobes with distolateral corner weakly setose. Maxilliped (Fig. 15H) endites merged, with groove in mid-length, distal margin with two tubercles (gustatory cusps) and seta; palp with article-2 three inner serrate setae; article-3 with three setae; article-4 with six setae.

Cheliped (Fig. 16A) slender; basis 1.8 L:W; merus with simple seta; carpus 1.8 L:W, with two ventral setae and dorsal seta; chela non-forcipate; palm 1.6 L:W, with row of six setae on inner side; fixed finger distal spine pointed, regular size, with three ventral setae; dactylus 9.2 L:W, with proximal seta.

Pereopod-1 (Fig. 16B) coxa with seta; basis 6.9 L:W, with six ventral setae and with two dorsal setae (broken); ischium with ventral seta; merus 2.8 L:W, 0.8x carpus, with two setae; carpus 2.8 L:W, 0.5x propodus, with two (long and short) setae; propodus 7.0 L:W, 1.1x dactylus and unguis combined length, with two setae; dactylus 0.5x unguis.

Pereopod-2 (Fig. 16C) basis 5.8 L:W, 3.7x merus with five ventral setae and dorsal penicillate seta; ischium with ventral seta; merus 1.6 L:W, 0.7x carpus, with two setae; carpus 2.7 L:W, 0.8x propodus, with two simple setae and blade-like spine 0.6x propodus; propodus 8.0 L:W, 1.7x dactylus and unguis combined length, with serrate distal seta and microtrichia on ventral margin; dactylus 0.7x unguis.

Pereopod-3 (Fig. 16D) coxa with seta; basis 5.6 L:W, 3.3x merus, with five ventral setae and two dorsal setae (broken); ischium with ventral seta; merus 1.7 L:W, 0.7x carpus, with two setae; carpus 3.5 L:W, 0.9x propodus, with two simple setae and with one blade-like spine 0.7x propodus; propodus 8.0 L:W, 1.6x dactylus and unguis combined length, with serrate distal seta and microtrichia on ventral margin; dactylus 0.7x unguis.

Pereopod-4 (Fig. 16E) basis 7.1 L:W, 4.1x merus, with four simple and one penicillate setae ventrally; ischium with ventral seta; merus 2.8 L:W, 0.6x carpus, with seta; carpus 4.6 L:W, 1.1x propodus, with two simple setae,

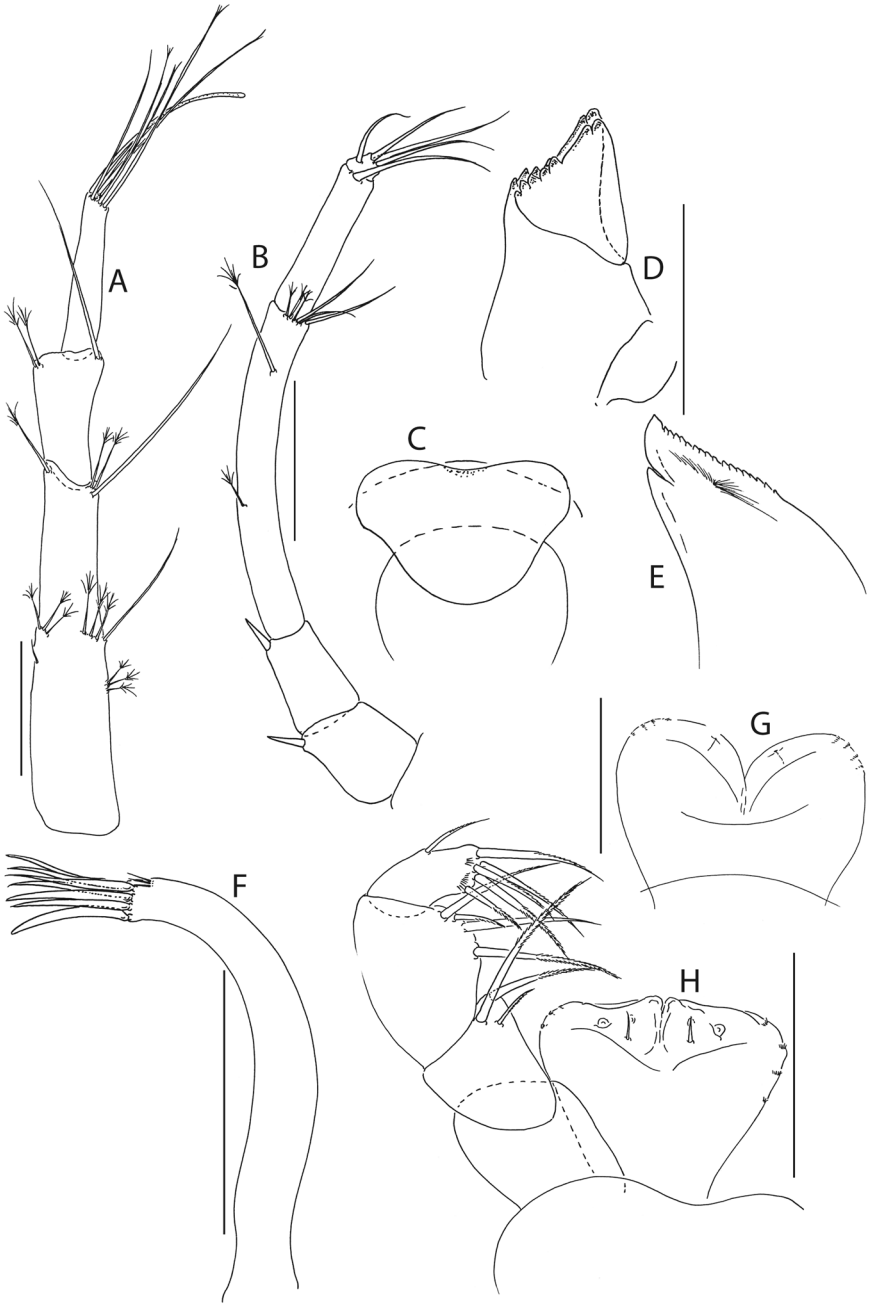

Figure 15. *Pseudotanais julietae* n. sp., ZMH K-56584, holotype neuter. (**A**), antennule; (**B**), antenna; (**C**), labrum; (**D**), left mandible; (**E**), right mandible; (**F**), maxillule; (**G**), labium; (**H**), maxilliped. Scale bar: 0.1 mm.

one rod setae 0.4x propodus and one blade-like spine 0.4x propodus; propodus 5.0 L:W, 2.9x dactylus and unguis combined length, with one simple, one serrate and one penicillate setae subdistally, one serrate distal seta 0.7x propodus, and microtrichia on ventral margin; dactylus 2.5x unguis.

Pereopod-6 (Fig. 16F) basis 3.1 L:W, 3.4x merus, with two ventral setae; ischium with ventral seta; merus 2.0 L:W, 0.6x carpus, with seta; carpus 3.3 L:W, with two simple and one rod setae, and one blade-like spine.

Pleopods (Fig. 16G) exopod with six and endopod with 10 plumose setae.

Uropod (Fig. 16H) peduncle 0.9 L:W, exopod 0.9x endopod with two articles; article-1 4.3 L:W, with seta; article-2 8.5 L:W, with two setae; endopod article-1 4.2 L:W, with one simple, one penicillate setae distally; article-2 5.7 L:W, with four simple and one penicillate setae.

Distribution: *P. julietae* n. sp. is known from the Belgium licence area (GSR) of the Central Pacific.

Remarks: *P. julietae* can be distinguished from all other species of 'affinis + longisetosus' group because the exopod in uropods is always shorter than in all other members of the group (*Pseudotanais affinis*; *P. macrochelis*; *P. nordenskioldi*; *P. scalpellum*; *P. svavarssoni*; *P. vitjazi*; *Pseudotanais* sp. P; *P. longisetosus*; *P. longispinus*; *P. nipponicus*; *P. spatula*).

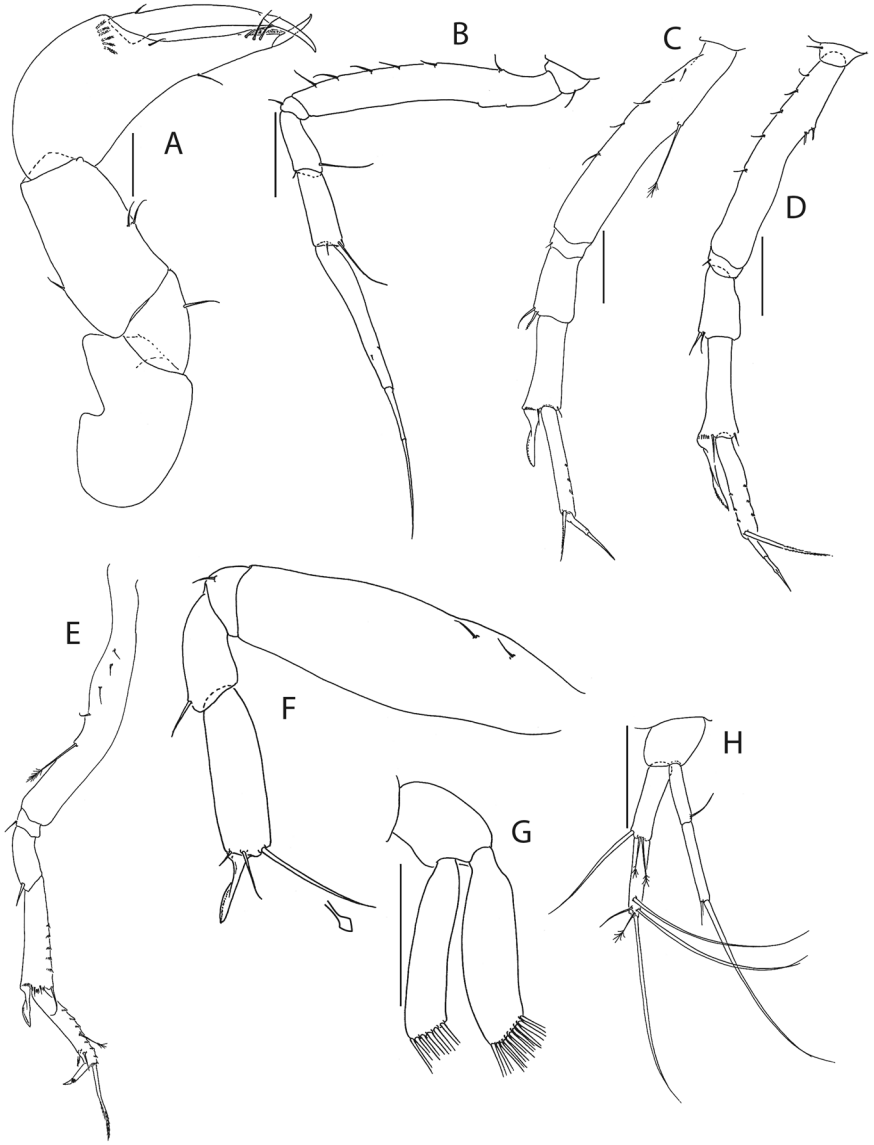

Figure 16. *Pseudotanais julietae* n. sp., ZMH K-56584, holotype neuter. (**A**), cheliped; (**B**), pereopod-1; (**C**), pereopod-2; (**D**), pereopod-3; (**E**), pereopod-4; (**F**), pereopod-6; (**G**), pleopod; (**H**), uropod. Inset at (**F**) show detail of tip of the rod seta. Scale bar: 0.1 mm.

***Pseudotanais romeo* n. sp.**

Figures 17–19.

Material examined: Holotype: neuter, 1.7 mm, ZMH K-56601. St 24, 11° 51.52′N 117° 1.19′W, 4100 m, 22 Mar 2015.

Paratypes: neuter, BL = 1.6 mm, ZMH K-56599. St 20, 11° 49.81′N 117° 0.28′W, 4093 m, 22 Mar 2015; three neuters, BL = 1.4–1.8 mm (one dissected), ZMH K-56600 (dissected), ZMH K-56602, ZMH K-56603. St 24, 11° 51.52′N 117° 1.19′W, 4100 m, 22 Mar 2015.

Diagnosis: Maxilliped endite naked. Cheliped cutting edge on dactylus with two spines. Pereopods 1–3 basis with five, six and three setae respectively. Pereopod 5–6 carpus with long distodorsal rod seta. Exopod of the uropod as long as endopod.

Etymology: The species is named after Romeo Montague, the lover of Juliet from William Shakespeare's tragedy *Romeo and Juliet*.

Description of neuter. BL = 1.7 mm. Body robust (Fig. 17), 3.3 L:W. Carapace 0.6 L:W, 6.2x pereonite-1, 0.2x BL. Pereonites 0.6x BL, pereonites-1–6: 0.1, 0.2, 0.3, 0.6, 0.6 and 0.4 L:W, respectively. Pleon short, 0.1x BL. Pleonites 0.6 L:W.

Antennule (Fig. 18A) article-1 0.6x total length, 7.0 L:W, 2.7x article-2, with one simple, eight penicillate mid-length setae and five penicillate distal setae; article-2 3.2 L:W, 0.9x article-3, with one simple and two penicillate distal setae; article-3 5.8 L:W, with one penicillate and four bifurcate setae, and one aestetasc.

Antenna (Fig. 18B) article-2 1.1 L:W, 0.7x article-3, with spine 0.4x the article-2; article-3 1.7 L:W, 0.3x article-4, with spine 0.2x the article-3; article-4 7.8 L:W, 2.5x article-5, with two penicillate mid-length setae, and

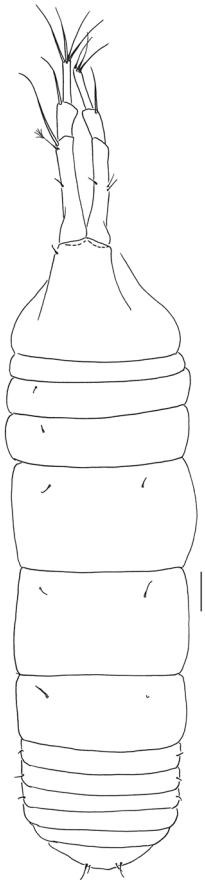

Figure 17. *Pseudotanais romeo* n. sp., ZMH K-56601, holotype neuter. Dorsal view. Scale bar: 1 mm.

two simple and four penicillate setae distally; article-5 4.0 L:W, 9.3x article-6, with distal seta; article-6 0.6 L:W, with four simple setae.

Mouthparts. Left mandible (Fig. 18C) *lacinia mobilis* well developed, distally serrate, incisor distal margin serrate. Right mandible (Fig. 18D) incisor distal margin serrate, *lacina mobilis* merged to a small process. Maxillule (Fig. 18E) with nine distal spines, endit with two distal setae (Fig. 18E'). Maxilliped (Fig. 18F) basis with groove 0.9 L:W, endites merged, with a groove in mid-length, naked; palp article-2 inner margin with three inner setae, outer margin with seta; article-3 with three setae; article-4 with five setae. Epignath (Fig. 18G) distally rounded.

Cheliped (Fig. 19A) robust; basis 1.6 L:W, with distoproximal seta; merus with seta; carpus 2.3 L:W, with two ventral setae; chela non-forcipate; palm 2.0 L:W; fixed finger distal spine pointed, regular size, with three ventral setae; dactylus 6.4 L:W, cutting edge with two spines.

Pereopod-1 (Fig. 19B) basis 7.5 L:W, with ventral seta and five dorsal setae; ischium with ventral seta; merus 3.0 L:W, 9.0x carpus, with two (long and short) setae; carpus 2.8 L:W, 0.5x propodus, with long seta; propodus 7.0 L:W, dactylus and unguis combined length, with seta; dactylus 0.1x unguis.

Pereopod-2 (Fig. 19C) basis 6.4 L:W, 4.7x merus, with six ventral setae and one dorsal seta; ischium with ventral seta; merus 1.6 L:W, 0.5x carpus, with two setae; carpus 2.7 L:W, 0.8x propodus, with seta and blade-like spine, 0.5x propodus; propodus 6.4 L:W, 1.8x dactylus and unguis combined length, with serrate seta and microtrichia on ventral margin; dactylus as long as unguis.

Pereopod-3 (Fig. 19D) basis 5.9 L:W, 3.6x merus, with three ventral setae; ischium naked; merus 2.0 L:W, 0.6x carpus, with two setae; carpus 3.6 L:W, 1.1x propodus, with one seta (broken), one spine (broken) and one blade-like spine 0.8x propodus; propodus 5.4 L:W, 2.2x dactylus and unguis combined length, with seta and microtrichia on ventral margin; dactylus 0.7x unguis.

Pereopod-4 (Fig. 19E,E') basis 5.6 L:W, 3.3x merus, with penicillate ventral seta and two penicillate dorsal setae; ischium naked, merus 1.7 L:W, 0.4x carpus; carpus 5.6 L:W, 1.5x propodus, with rod setae as long as propodus, two spines and with blade-like spine 0.4x propodus; propodus 6 L:W, 2.5x dactylus and unguis combined length, with two ventral setae, one serrate dorsal seta 0.8x propodus and microtrichia on ventral margin; dactylus 2.0x unguis.

Pereopod-5 (Fig. 19F) basis 7.3 L:W, 7.3x merus; ischium naked; merus 1.1 L:W, 0.3x carpus, with seta; carpus 3.5 L:W, 1.2x propodus, with two simple setae, one rod seta 0.9x propodus, and with blade-like spine 0.5x propodus; propodus 6.0 L:W, 2.5x dactylus and unguis combined length, with two simple setae on ventral margin, one seta on dorsal margin, and microtrichia on ventral margin; dactylus 2.0x unguis.

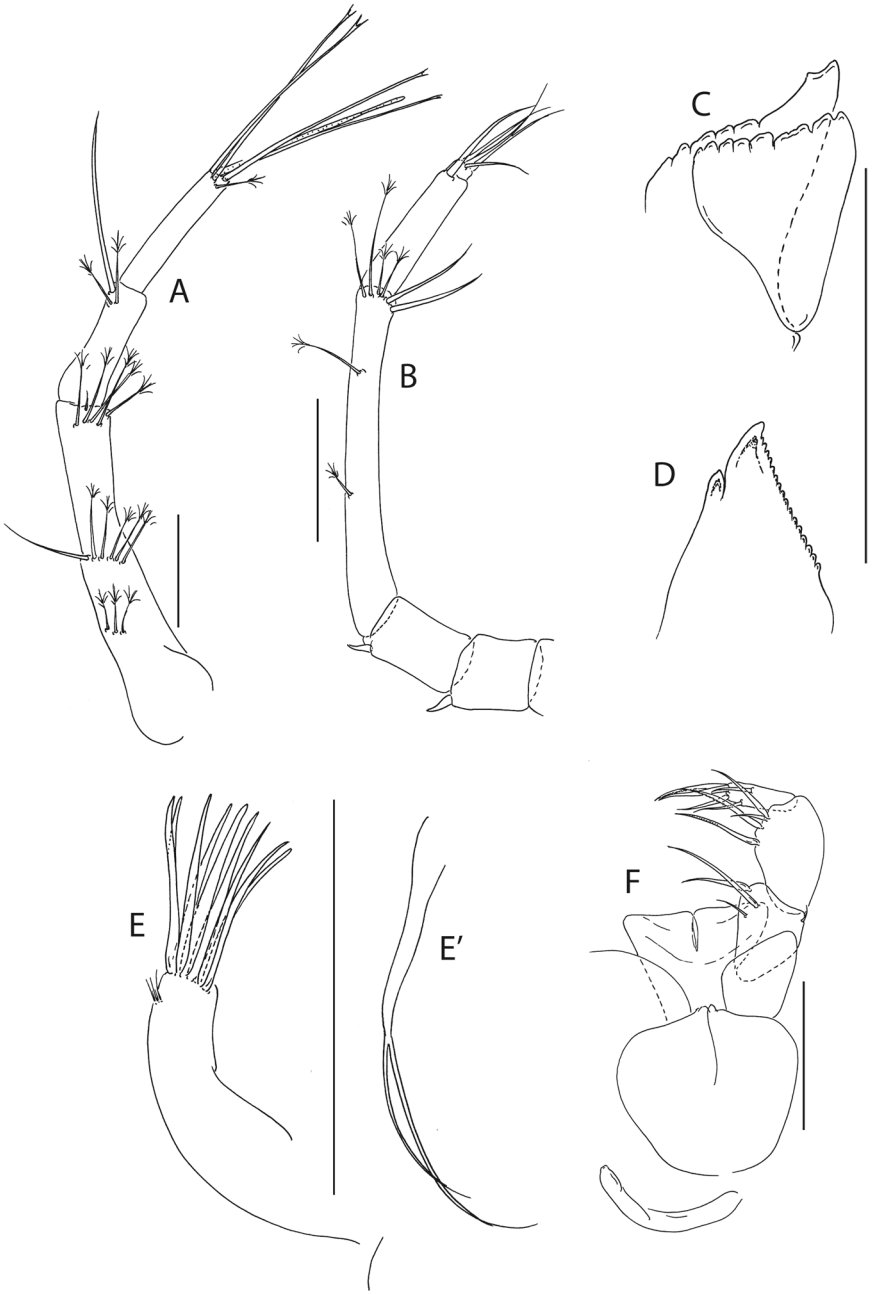

Figure 18. *Pseudotanais romeo* n. sp., ZMH K-56600, neuter. (**A**), antennule; (**B**), antenna; (**C**), left mandible; (**D**), right mandible; (**E**), maxillule; E' endit. Scale bar: 0.1 mm.

Pleopods (Fig. 19G) exopod with seven and endopod with 10 plumose setae.

Uropod (Fig. 19H) peduncle 1.0 L:W; exopod 0.9x endopod, with two articles; article-1 4.6 L:W, with seta; article-2 6.2 L:W, with two setae; endopod article-1 4.3 L:W, with two penicillate distal setae; article-2 7.0 L:W, with five distal setae (broken).

Distribution: *P. romeo* n. sp. is known from the Belgium licence area (GSR) of the Central Pacific.

Remarks: *Pseudotanais romeo* n. sp. is morphologically and genetically most similar to *P. julietae* (Fig. 1) and it is distinguished from all other members of the 'affinis + longisetosus' group by the same character set as *P. julietae* (see remarks under *P. julietae*). *P. romeo* is distinguished from *P. julietae* by the number of setae on basis of pereopod 1–3: 5, 6, 3 and 6, 5, 5, respectively. *P. romeo* has naked maxillped endites whereas *P. julietae* has maxilliped endites ornamented with two tubercles (gustatory cusps) and one seta. The presence of two spines on cutting edge of the cheliped in *P. romeo* also allow to separate it from *P. julietae* with smooth cutting edge.

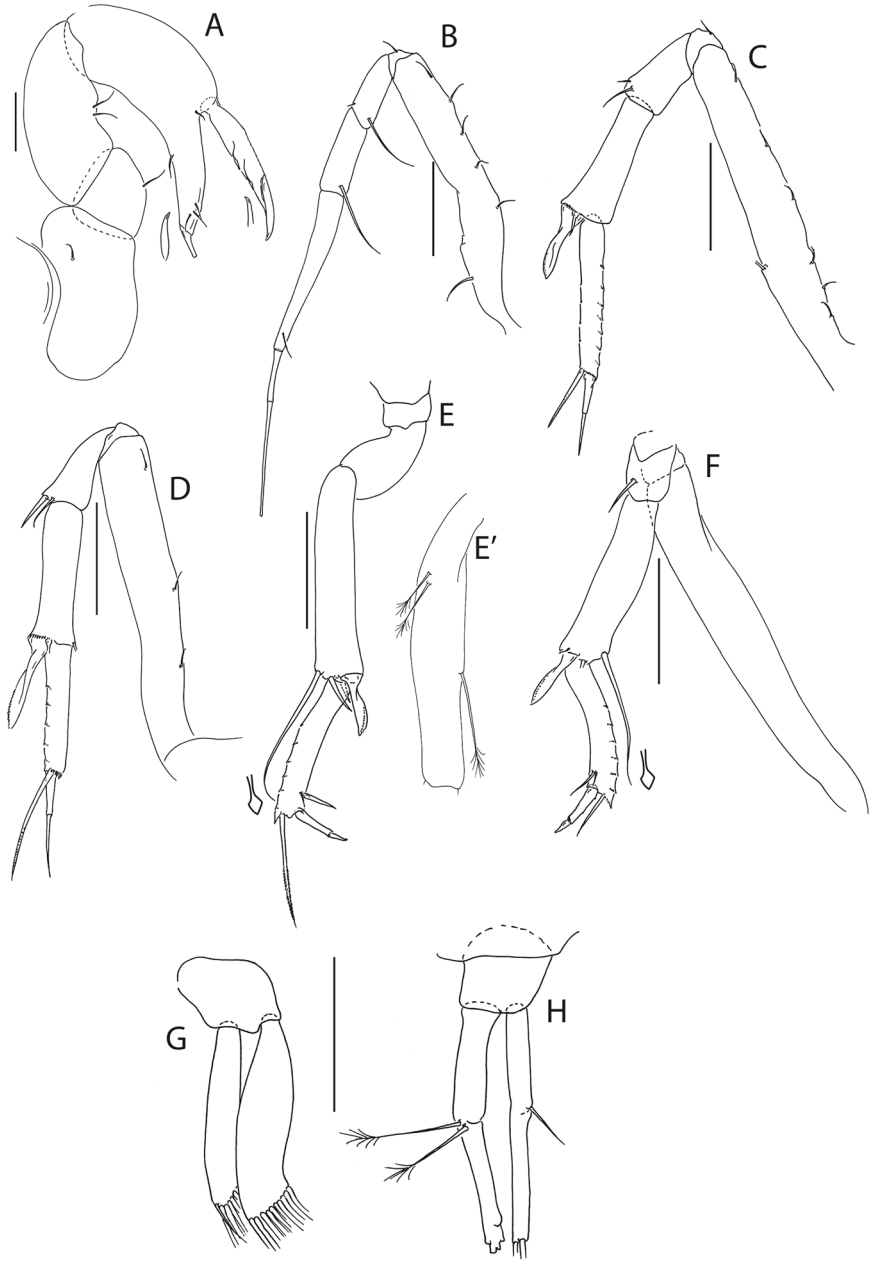

Figure 19. *Pseudotanais romeo* n. sp., ZMH K-56600, neuter. (**A**), cheliped; (**B**), pereopod-1; (**C**), pereopod-2; (**D**), pereopod-3; (**E**), pereopod-4; E', basis of pereopod-4; (**F**), pereopod-5; (**G**), pleopod; (**H**), uropod. Insets at (**E**,**F**) show detail of tip of the rod seta. Scale bar: 0.1 mm.

***Pseudotanais yenneferae* n. sp.**

Figures 20–22.

Material examined: Holotype: female, BL = 1.5 mm, ZMH K-56609. St. 197, 18° 48.66′N 128° 22.75′W, 4805 m, 21 Apr 2015.

Paratype: neuter, BL = 1.1 mm, ZMH K-56618. St. 192, 18° 44.81′N 128° 21.87′W, 4877 m, 21 Apr 2015; eight neuters BL = 1.3–1.9 mm (one dissected), ZMH K-56610, ZMH K-56611, ZMH K-56612, ZMH K-56613, ZMH K-56614, ZMH K-56615, ZMH K-56616 (disstected), ZMH K-56617. St.197, 18° 48.66′N 128° 22.75′W, 4805 m, 22 Apr 2015.

Diagnosis: Mandible molar wide. Pereopod-1 basis with two setae. Pereopod 5–6 carpus with short distodorsal rod seta.

Etymology: The species is named after the female protagonist partner of Polish fantasy novel 'Wiedźmin' (eng. The Witcher) written by Andrzej Sapkowski.

Description of neuter. BL = 1.5 mm. Body slender (Fig. 20A,B), 4.4 L:W. Carapace 0.9 L:W, 7.2x pereonite-1, 0.2x BL. Pereonites 0.5x BL pereonites-1–6: 0.1, 0.3, 0.3, 0.5, 0.6 and 0.5 L:W, respectively. Pleon short, 0.2x BL. Pleonites 1.1 L:W.

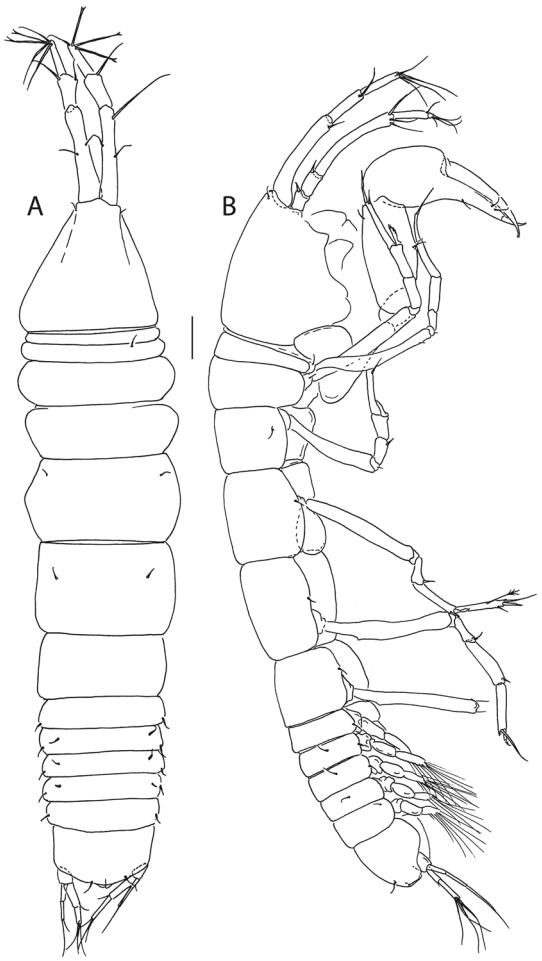

Figure 20. *Pseudotanais yenneferae* n. sp., ZMH K-56609, holotype female. A, dorsal view; B lateral view. Scale bar: 1 mm.

Antennule (Fig. 21A) article-1 0.5x total length, 7.6 L:W, 2.3x article-2, with one simple, one penicillate seta at mid-length, and one simple, three penicillate setae distally; article-2 3.6 L:W, 1.1x article-3, with two simple and one penicillate setae distally; article-3 5.4 L:W, with three simple, three bifurcate setae and one aestetasc.

Antenna (Fig. 21B) article-2 1.4 L:W; article-3, with spine 0.4x the article-2; article-3 1.9 L:W, 0.2x article-4, with spine 0.3x the article-3; article-4 10.0 L:W, 2.2x article-5, with penicillate mid-length seta and two simple, and three penicillate setae distally; article-5 5.4 L:W, 13.5x article-6, with distal seta; article-6 0.5 L:W, with five setae.

Mouthparts. Labrum (Fig. C) naked. Left mandible (Fig. 21D) *lacinia mobilis* well developed and distally serrate, incisor distal margin serrate. Right mandible (Fig. 21E) incisor distal margin serrate, *lacina mobilis* merged to a small process. Maxillule (Fig. 21F) with 8 distal spines. Maxilla (Fig. 21G) semioval. Labium (Fig. 21H) lobe distolateral corner naked. Maxilliped (Fig. 21I) basis 0.9 L:W; endites partly merged, distal margin, with tubercles (gustatory cusps); palp article-2 inner margin, with three setae, outer margin with seta; article-3 with three setae; article-4 with six setae. Epignath not seen.

Cheliped (Fig. 22A) slender; basis 1.6 L:W, with distoproximal seta; merus with seta, carpus 2.3 L:W, with ventral and subproximal setae; chela non-forcipate; palm 1.3 L:W, with row of three setae on inner side; fixed finger distal spine pointed, regular size, with three ventral setae; dactylus 5 L:W, cutting edge smooth, proximal seta present.

Pereopod-1 (Fig. 22B) coxa with seta; basis 8.3 L:W, with two ventral and one dorsal seta; ischium with ventral seta; merus 2.2 L:W and, 0.7x carpus with two seta; carpus 2.5 L:W, 0.4x propodus; propodus 8.2 L:W, 1.3x dactylus and unguis combined length, with two setae; dactylus 0.7x unguis.

Pereopod-2 (Fig. 22C) coxa with seta; basis 9.1 L:W, 4.9x merus with two ventral seta and one dorsal seta; ischium with ventral seta; merus 1.9 L:W, 0.6x carpus, with seta; carpus 2.6 L:W, 0.7x propodus, with two simple and one blade-like spine, 0.5x propodus; propodus six L:W, 2x dactylus and unguis combined length, with distal seta and microtrichia on ventral margin; dactylus 0.6x unguis.

Pereopod-3 (Fig. 22D) basis 6.5 L:W, 4.1x merus, with one simple and one penicillate ventral setae and penicillate dorsal seta; ischium with ventral seta; merus 1.8 L:W, 0.8x carpus, with seta; carpus 2.6 L:W, 0.7x propodus, with blade-like spine 0.7x propodus; propodus 4.7 L:W, with seta.

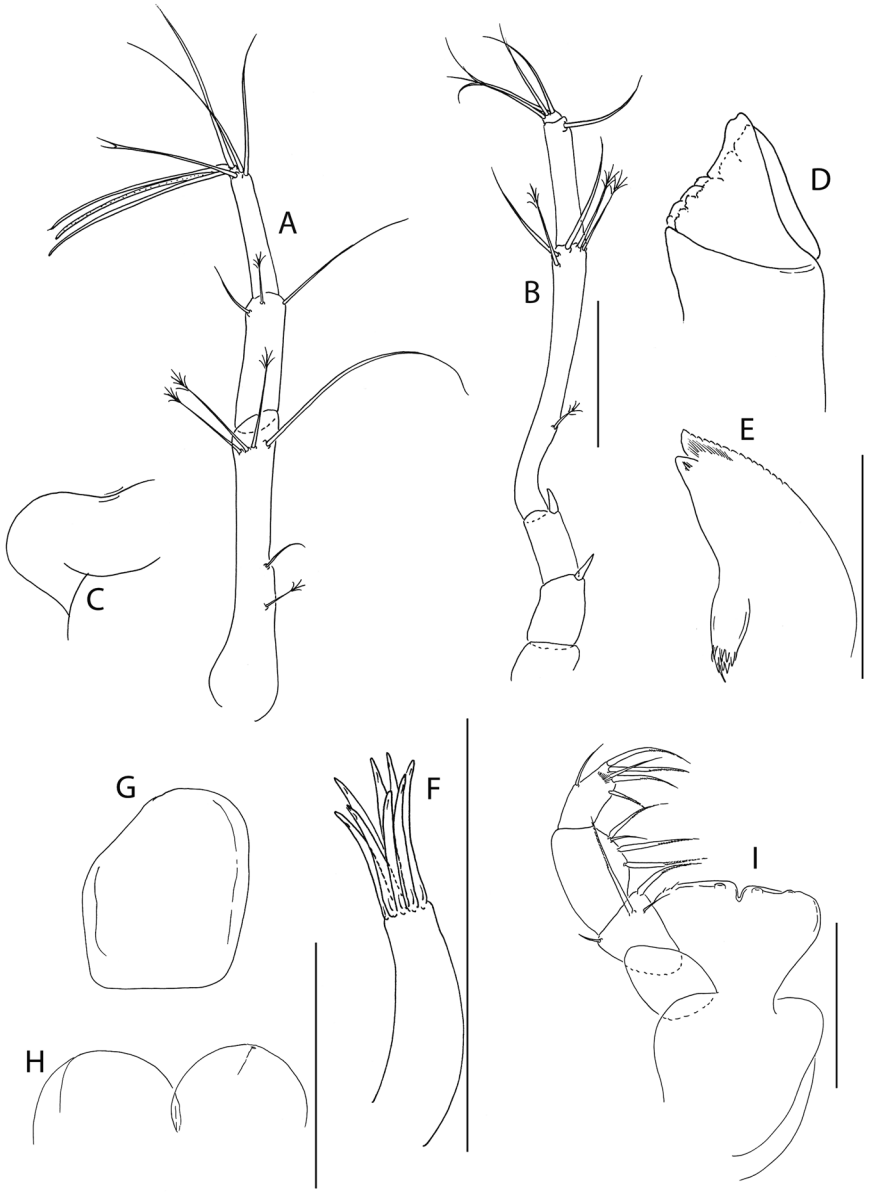

Figure 21. *Pseudotanais yenneferae* n. sp., ZMH K-56616, neuter. (**A**), antennule; (**B**), antenna; (**C**), labium; (**D**), left mandible; (**E**), right mandible; (**F**), maxillule; (**G**), maxilla; (**H**), labium; (**I**), maxilliped: (**J**), epignath. Scale bar: 0.1 mm.

Pereopod-4 (Fig. 22E) basis 7.0 L:W, 4.4x merus; ischium with ventral seta; merus 2.0 L:W, 0.5x carpus, with seta; carpus 3.6 L:W, 0.9x propodus, with one simple and one rod setae 0.3x propodus, one spine and one blade-like spine 0.2x propodus,; propodus 5.2 L:W, 2.6x dactylus and unguis combined length, with one simple and one serrate seta 1x propodus and microtrichia on ventral margin; dactylus 3.0x unguis.

Pereopod-5 (Fig. 22F) basis 7.8 L:W, 1.2x merus, with simple ventral seta and penicillate dorsal seta; ischium with ventral seta; merus 2.0 L:W, 0.6x carpus, with seta; carpus 4.0 L:W, 0.9x propodus, with three simple setae, one rod seta 0.4x propodus, and one blade-like spine 0.3x propodus; propodus 5.0 L:W, 1.9x dactylus and unguis combined length, with two ventral seta and one serrate dorsal seta 0.9x propodus and microtrichia on ventral margin; dactylus 0.2x unguis.

Pereopod-6 (Fig. 22G) basis 7.6 L:W, 5.2x merus; ischium with ventral seta; merus 2.0 L:W, 0.6x carpus, with two setae; carpus 3.5 L:W, propodus, with one simple, one sensory 0.4x propodus and one blade-like spine 0.3x propodus; propodus 4.0 L:W, 2.1x dactylus and unguis combined length, with two simple ventral setae, one simple, and one serrate dorsal setae 1.1x propodus; dactylus 1.6x unguis.

Pleopods (Fig. 22H) exopod with four, endopod with seven plumose setae.

Uropod (Fig. 22I) peduncle 1.2 L:W; exopod 0.8x endopod, with two articles; article-1 5.5 L:W, with seta; article-2 7.0 L:W, with two setae; endopod article-1 3.4 L:W, with two distal penicillate setae; article-2 4.0 L:W, with five setae.

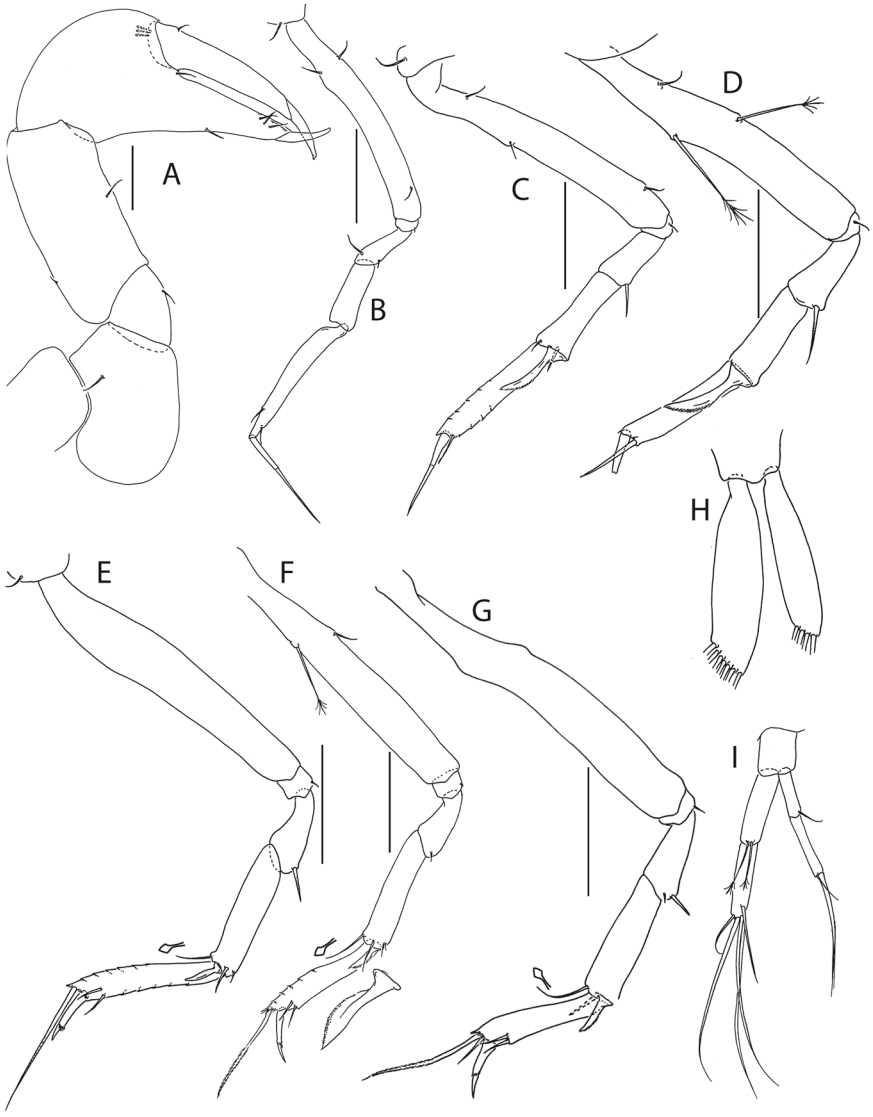

Figure 22. *Pseudotanais yenneferae* n. sp., ZMH K-56616, neuter. (**A**), cheliped; (**B**), pereopod-1; (**C**), pereopod-2; (**D**), pereopod-3; (**E**), pereopod-4; (**F**), pereopod-5; (**G**), pereopod-6; (**H**), pleopod; (**I**), uropod. Insets at (**E**–**G**) show detail of tip of the rod seta; on (**F**) a magnification of the blade-like spine. Scale bar: 0.1 mm.

Distribution: *P. yenneferae* n. sp. is known only from APEI3 of the Clarion and Clipperton Fractures Zone, Central Pacific.

Remarks: *P. yenneferae* n. sp. with short rod setae on pereopods 5–6 carpus can be distinguished from *P. longisetosus*, *P. longispinus*, *P. nipponicus*, *P. spatula*, *Pseudotanais* sp. O, *Pseudotanais romeo* and *P. julietae*, which have long rod setae on pereopods 5–6 carpus. Also, it can be distinguished from. *P. affinis*, *P. macrochelis* and *P. nordenskioldi*, *P. scalpellum*, *P. svavarssoni*, *P. vitjazi* and *Pseudotanais* sp. P (McLelland, 2007) by the wider molar of the mandible.

***Pseudotanais geralti* n. sp.**

Figures 23–25.

Material examined: Holotype: neuter, BL = 1.4 mm, ZMH K-56578 (partly disseceted). St 81, 11° 3.97′N 119° 37.67′W, 4365 m, 1 Apr 2015.

Paratypes: neuter, BL = 1.1 mm, ZMH K-56579 (partly dissected). St. 81, 11° 3.97′N 119° 37.67′W, 4365 m, 1 Apr 2015; three neuters, BL = 1.1–1.3 mm, ZMH K-56581 (dissected), ZMH K-56582, ZMH K-56583. St. 99, 11° 2.61′N 119° 39.52′W, 4401 m, 4 Apr 2015; neuter, BL = 1.1 mm, ZMH K-56580. St. 117, 13° 52.39′N 123° 15.30′W, 4496 m, 7 Apr 2015.

Diagnosis: Mandible molar wide. Pereopod-1 basis with two setae. Pereopod 5–6 carpus with short distodorsal rod seta.

Etymology: The species is named after the character from a Polish fantasy novel 'Wiedźmin' (eng. 'The Witcher') written by Andrzej Sapkowski.

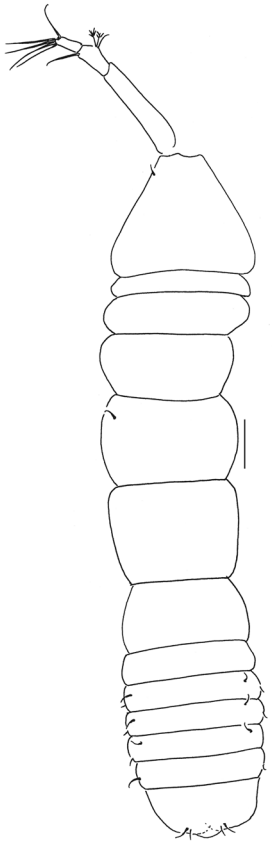

Figure 23. *Pseudotanais geralti* n. sp., ZMH K-56578, holotype neuter. Dorsal view. Scale bar: 1 mm.

Description of neuter. BL = 1.4 mm. Body slender (Fig. 23), 4.7 L:W. Carapace 0.8 L:W, 5.2x pereonite-1, 0.2x BL. Pereonites 0.5x BL, pereonites-1–6: 0.2, 0.3, 0.5, 0.6, 0.8 and 0.5 L:W, respectively. Pleon short, 0.2x BL. Pleonites 0.9 L:W.

Antennule (Fig. 24A) article-1 0.5x total length, 5.0 L:W, 1.9x article-2, with two simple and three mid-length penicillate setae, and two simple and two penicillate distal setae; article-2 2.5 L:W, 0.9x article-3, with two setae; article-3 5.7 L:W, with three simple, one bifurcate seta and one aestetasc.

Antenna (Fig. 24B) article-2 1.8 L:W; 1.1x article-3, with spine 0.3x article-2; article-3 1.3 L:W, article-4, with spine 0.6x article-3; article-4 1.4 L:W, 0.6x article-5, with simple mid-length seta, two simple and two penicillate distal setae; article-5 4.0 L:W, 7.0x article-6, with seta; article-6 0.8 L:W, with five setae.

Mouthparts. Left mandible (Fig. 24C) *lacinia mobilis* well developed and distally serrate, incisor distal margin gently serrate. Right mandible (Fig. 24D) incisor distal margin serrate, *lacina mobilis* merged to a small process. Maxillule (Fig. 24E) with 8 distal spines and three subdistal setae. Maxilliped (Fig. 24F) endites partly merged, distal margin without tubercles (gustatory cusps) and seta; palp article-1 naked; palp article-2 inner margin with two setae, outer margin, with seta; article-3 with four setae; article-4 with five setae.

Cheliped (Fig. 25A) slender; basis 1.7 L:W, with distoproximal seta; merus, with seta; carpus 2.39 L:W, with two ventral setae, and with distal and subproximal setae dorsally; chela non-forcipate; palm 1.5 L:W; fixed finger distal spine pointed, regular size, with three ventral setae; dactylus 5.3 L:W, cutting edge with two spines, proximal seta present.

Pereopod-1 (Fig. 25B) basis 6.1 L:W, with two ventral setae; ischium with ventral seta; merus 2.2 L:W, 0.7x carpus, with seta; carpus 2.6 L:W, 0.4x propodus, with seta; propodus 7.2 L:W, 1.2x dactylus and unguis combined length, with seta; dactylus 0.6x unguis.

Pereopod-2 (Fig. 25C) coxa with seta; basis 5.7 L:W, 3.1x merus, with ventral seta and penicillate dorsal seta; ischium with ventral seta; merus 2.5 L:W, 0.9x carpus, with seta; carpus 2.7 L:W, 0.7x propodus, with two simple setae and blade-like spine, 0.7x propodus; propodus 7.2 L:W, 1.2x dactylus and unguis combined length, with seta and microtrichia on ventral margin, dactylus 0.6x unguis.

Pereopod-5 (Fig. 25D) basis 6.4 L:W, 4.1x merus, with penicillate ventral seta and with simple dorsal seta; ischium with ventral seta; merus 1.7 L:W, 0.5x carpus, with seta; carpus 3.7 L:W, 1.2x propodus, with one simple seta, one sensory 0.4x propodus, and one blade-like spine 0.4x propodus; propodus 4.6 L:W, 2.1x dactylus and unguis combined length, with penicillate seta at mid-length and serrate seta distally; dactylus 0.1x unguis.

Pereopod-6 (Fig. 25E) basis 4.1 L:W, 3.4x merus, with one simple and one penicillate setae ventrally; ischium with one short and one long setae; merus 2.2 L:W, 0.6x carpus, with one short and one long serrate setae; carpus 3.7 L:W, 0.9x propodus, with one serrate, one rod setae 0.3x propodus and one blade-like spine 0.45x propodus;

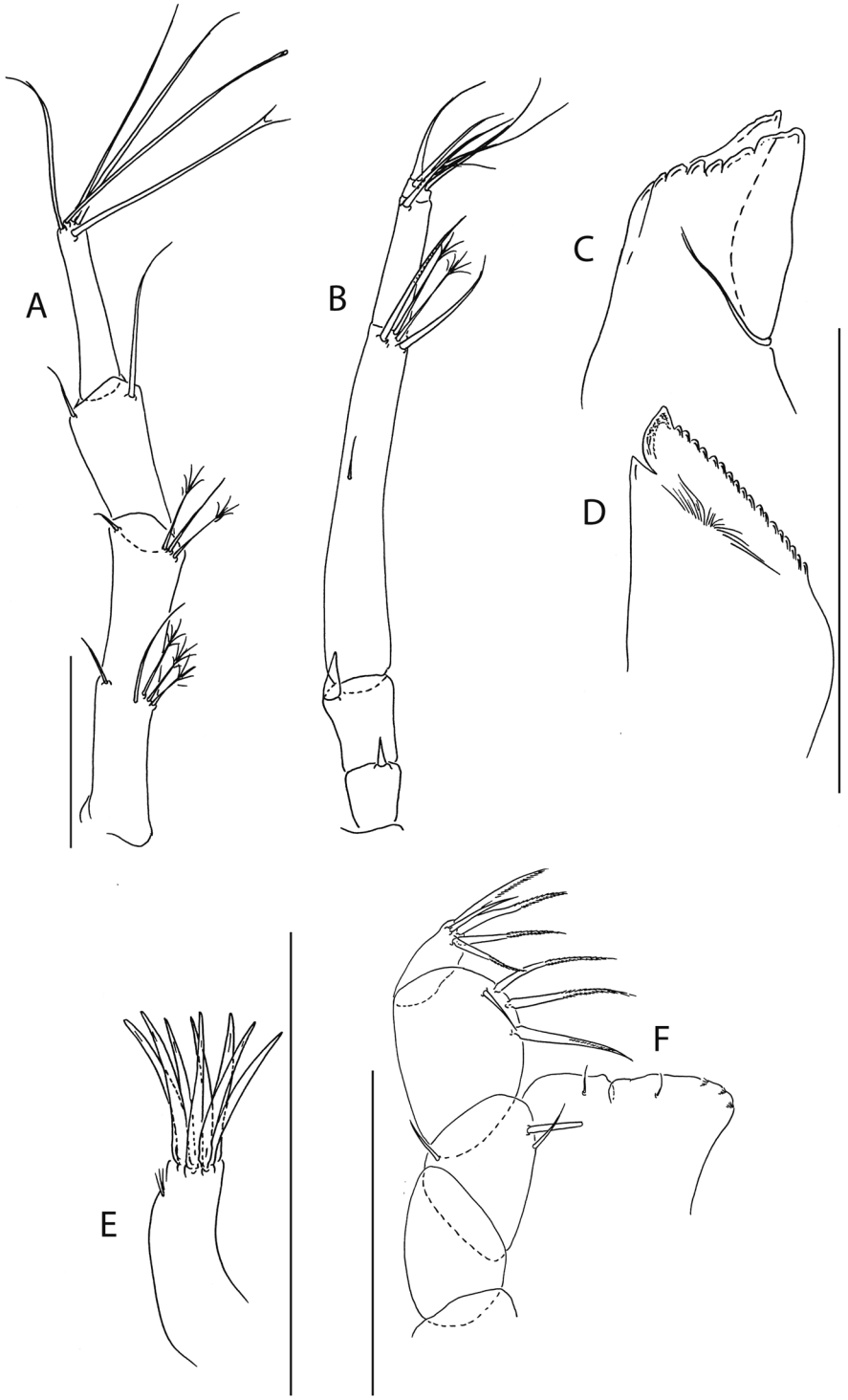

Figure 24. *Pseudotanais geralti* n. sp., ZMH K-56581, neuter. (**A**), antennule; (**B**), antenna; (**C**), left mandible; (**D**), right mandible; (**E**), maxillule; (**F**), maxilliped. Scale bar: 0.1 mm.

propodus 5.2 L:W, 2.4x dactylus and unguis combined length, with two ventral setae, and one serrate dorsal seta 0.8x propodus, and microtrichia on ventral margin; dactylus 1.6x unguis.

Pleopods (Fig. 25F) exopod with four; endopod with 7 plumose setae.

Uropod (Fig. 25G) 1.2 L:W; exopod 0.6x endopod, with two articles; article-1 3.2 L:W, with seta; article-2 4.7 L:W, with two setae; endopod article-1 3.1 L:W; article-2 2.8 L:W, with five setae.

Distribution: *P. geralti* n. sp. is known from the Belgium (GSR) and Interoceanmetal (IOM) licence areas of the Central Pacific.

Remarks: *P. geralti* can be distinguished from the other species in this group by the same characters as listed in *P. yenneferae*. *P. geralti* is morphologically closer to *P. yenneferae* from which is distinguished by its relatively

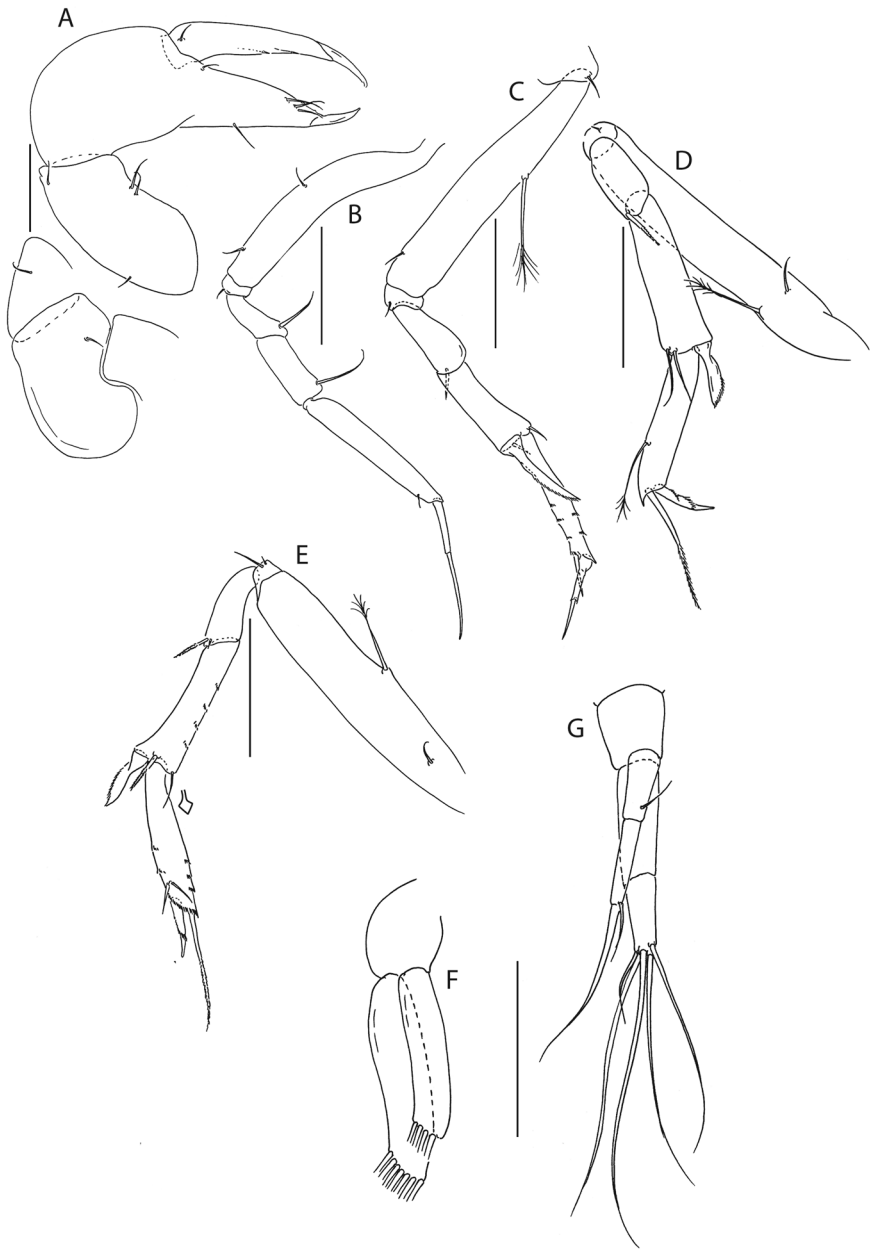

Figure 25. *Pseudotanais geralti* n. sp., ZMH K-56581, neuter. (**A**), cheliped; (**B**), pereopod-1; (**C**), pereopod-2; (**D**), pereopod-5; (**E**), pereopod-6; (**F**), pleopod; (**G**), uropod pereopod-6. Inset at (**E**) show detail of tip of the rod seta. Scale bar: 0.1 mm.

long dorso-distal seta on merus of pereopod-1 (short in *P. yenneferae*), and shorter cheliped carpus (at least twice as wide in *P. yenneferae*).

'denticulatus + abathagastor' group

Diagnosis: Antenna article 2–3 with spines or setae. Mandible molar wide or acuminate. Chela non-forcipate. Pereopod-1 basis with few (1–3) setae. Merus and carpus distodorsal seta short. Pereopod-2 with short, semilong or long blade-like spine on carpus. Pereopods 5–6 carpus distodorsal seta short. Unguis of pereopod 4–6 elongated. Uropod slender, exopod longer or slightly shorter than endopod

Species included: *Pseudotanais corollatus* Bird & Holdich, 1984; *P. denticulatus* Bird & Holdich, 1984; *P. abathagastor* Błażewicz-Paszkowycz, Bamber & Jóźwiak, 2013; *Pseudotanais* sp. C (McLelland 2008); *Pseudotanais chopini* n. sp.; *Pseudotanais georgesandae* n. sp.; *Pseudotanais chaplini* n. sp.; *Pseudotanais oloughlini* n. sp.; *P. mariae* n. sp.

Remarks: The '*denticulatus* + *abathagasthor*' group can be distinguished from the 'affinis + longisetosus' group by the presence of a long seta on merus pereopod-1 in the 'affinis + longisetosus' clade.

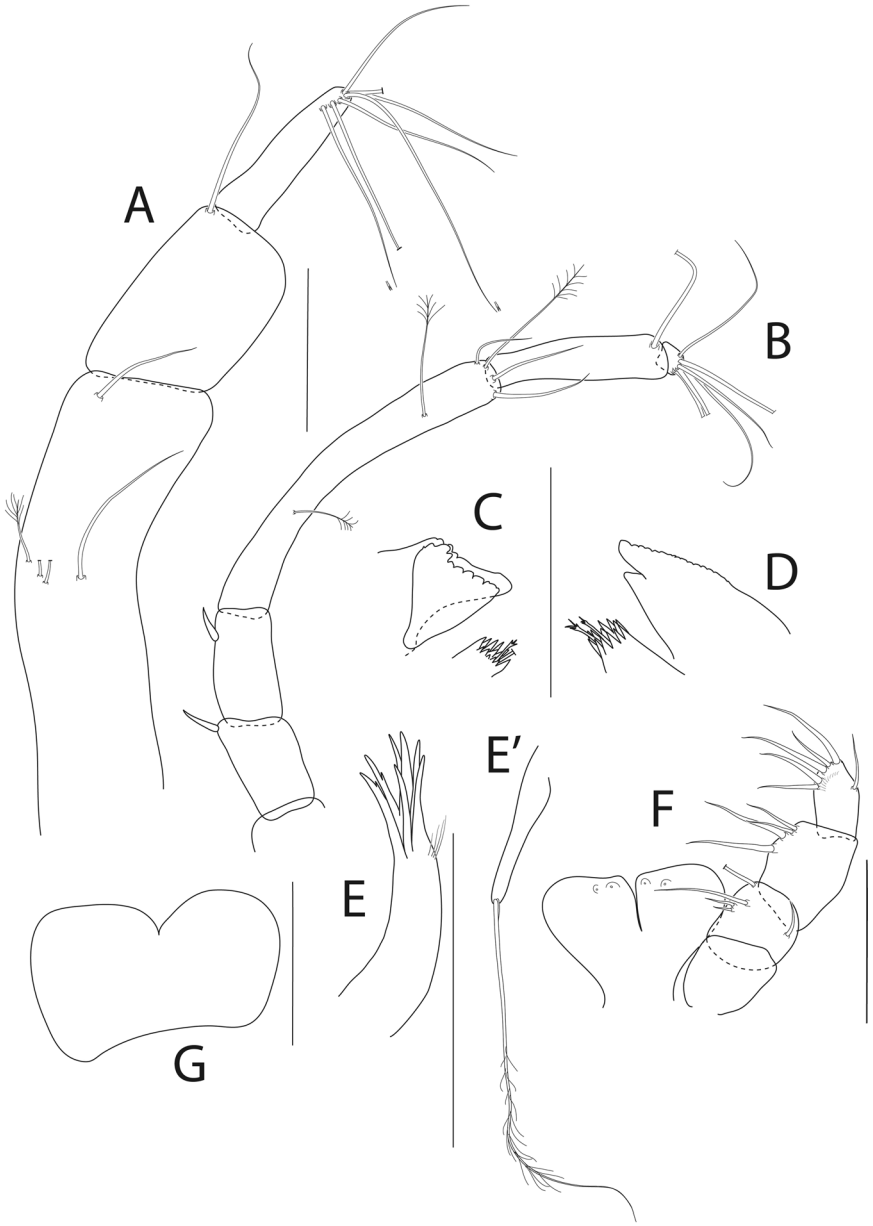

Figure 26. *Pseudotanais georgesandae* n. sp., ZMH K-56577, holotype neuter. (**A**), antennule; (**B**), antenna; (**C**), left mandible; (**D**), right mandible; (**E**), maxillule; E', endit; (**F**), maxilliped (**G**), labium. Scale bar: 0.1 mm.

***Pseudotanais georgesandae* n. sp.**

Figures 26 and 27.

Material examined: Holotype: neuter BL = 1.5 mm, ZMH K-56577 (partly dissected). St 192, 18° 44.81′N 128° 21.87′W, 4877 m, 21 Apr 2015.

Diagnosis: Mandible molar wide. Antenna article 2 and 3 with spine. Pereopod-2 carpus with short blade-like spine. Uropod exopod slightly shorter than endopod.

Etymology: The species is named in recognition of Amantine Lucile Aurore Dupin known as George Sand, a French novelist and essayist, well known for her partnership with the composer and pianist Frédéric Chopin.

Description of neuter. Antennule (Fig. 26A) 3.2 L:W, 2.3x article-2, article-2 1.4 L:W, 1.1x article-3, article-3 4.0 L:W, with five simple and two bifurcate setae.

Antenna (Fig. 26B) 1.4 L:W; article-2 0.8x article-3; article-3 1.7 L:W, 0.3x article-4; article-4 8.4 L:W, 2.0x article-5; article-5 4.0 L:W, 8.0x article-6; article-6 wide.

Mouthparts. Left mandible (Fig. 26C) *lacinia mobilis* well developed and serrate distally. Right mandible (Fig. 26D) molar wide with two spines in the middle. Maxillule (Fig. 26E,E') with five simple and two bifurcate distal spines with four subdistal setae. Maxilliped (Fig. 26F) endites merged with groove in the mid-length, distal margin with two tubercles (gustatory cusps); palp article-2 inner margin with four setae, outer margin with

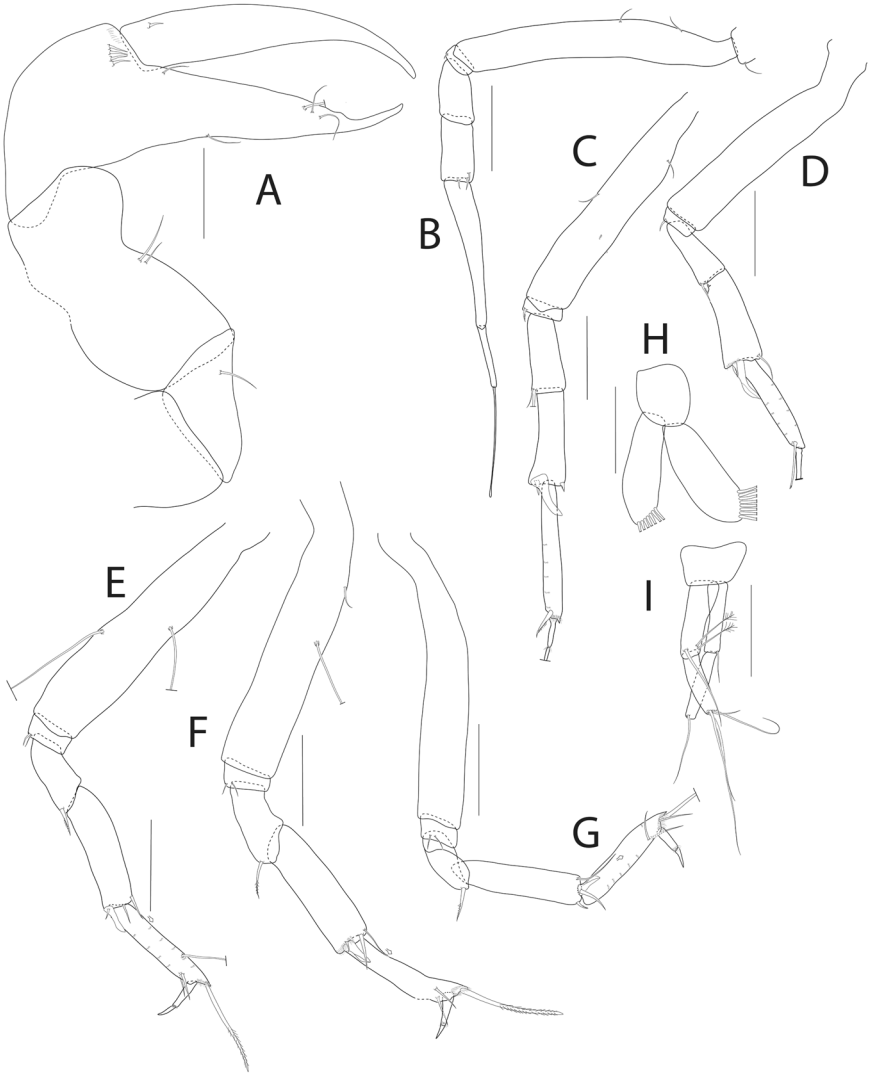

Figure 27. *Pseudotanais georgesandae* n. sp., ZMH K-56577, holotype neuter. (**A**), cheliped; (**B**), pereopod-1; (**C**), pereopod-2; (**D**), pereopod-3; (**E**), pereopod-4; (**F**), pereopod-5; (**G**), pereopod-6; (**H**), pleopod; (**I**), uropod. Insets at (**E**,**F**) show detail of tip of the rod seta. Scale bar: 0.1 mm.

seta; article-3 with four setae, article-4 with five setae on inner margin and one seta on outer margin. Labium (Fig. 26G) lobes distolateral corner naked.

Cheliped (Fig. 27A) slender; carpus 1.8 L:W, with two ventral setae; chela non-forcipate; palm 1.8 L:W, 1.2x palm; dactylus 5.7 L:W with proximal seta.

Pereopod-1 (Fig. 27B) basis 7.7 L:W; merus 1.6 L:W, 0.8x carpus; carpus 2.3 L:W, 0.4x propodus with three setae; propodus 6.3 L:W, 0.8x dactylus and unguis combined length; dactylus 0.6x unguis.

Pereopod-2 (Fig. 27C) basis 5.9 L:W, 3.1x merus; merus 2.8 L:W, 0.8x carpus; carpus 3.4 L:W, 0.7x propodus, with blade-like spine 0.3x propodus; propodus 7.0 L:W.

Pereopod-3 (Fig. 27D) basis 6.0 L:W, 3.3x merus; ischium with seta; merus 2.6 L:W, 0.8x carpus with one simple seta and one serrate spine; carpus 2.8 L:W, 0.8x propodus with one simple seta, one serrate seta, one spine and one blade-like spine 0.4x propodus; propodus 5.4 L:W with serrate spine and microtrichia on ventral margin.

Pereopod-4 (Fig. 27E) basis 5.0 L:W, 4.0x merus with two plumoe setae; ischum with two setae; merus 2.2 L:W, 0.6x carpus with one serrate spine; carpus 3.2 L:W, propodus, with one simple seta, one rod seta 0.2x propodus, one serrate spine and one blade-like spine 0.2x propodus; propodus 5.8 L:W, 2.2x dactylus and unguis combined length with serrate seta 0.9x propodus.

Pereopod-5 (Fig. 27F) basis 5.7 L:W, 3.7x merus; merus 2.2 L:W, 0.6x carpus; carpus 3.3 L:W, 1.2x propodus, with one rod seta 0.3x propodus and one blade-like spine 0.2x propodus; propodus 5.3 L:W, 2.6x dactylus and unguis combined length with serrate seta 0.9x propodus; dactylus 2.0x unguis.

Pereopod-6 (Fig. 27G) basis 6.4 L:W, 4.8x merus; merus 2.0 L:W, 0.5x carpus; carpus 4.0 L:W, 1.2x propodus, with one rod seta 0.5x propodus and one blade-like spine 0.2x propodus; propodus 4.5 L:W, 2.2x dactylus and unguis combined length; dactylus 1.4x unguis.

Pleopods (Fig. 27H) exopod with seven, endopod with eight plumose setae.

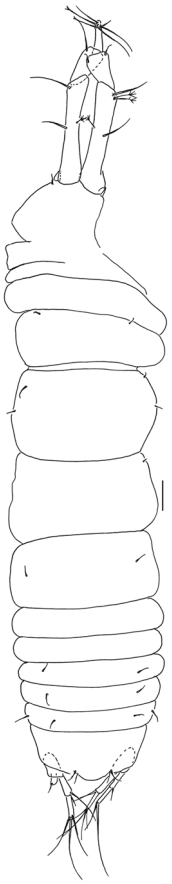

Figure 28. *Pseudotanais chopini* n. sp., ZMH K-56568, holotype neuter. Dorsal view. Scale bar: 1 mm.

Uropod (Fig. 27I) peduncle 1.5 L:W; exopod article-1 6.0 L:W with seta; article-2 5.6 L:W with at least one seta (other broken); endopod article-1 3.5 L:W with one simple and two penicillate; article-2 4.0 L:W with four setae. Exopod 0.9x endopod.

Distribution: *P. georgesandae* n. sp. is known only from APEI3 of the Clarion and Clipperton Fractures Zone, Central Pacific.

Remarks: *Pseudotanais georgesandae* n. sp. can be distinghuished from all the other members of the 'denticulatus + abathagastor' group by the wide mandible molar. The molar of *P. georgesandae* has two bifurcate long spines, which are absent in *P. corollatus* and *P. denticulatus*. The molar of *Pseudotanais* sp. C has one straight spine.

***Pseudotanais chopini* n. sp.**

Figures 28–30.

Material examined: Holotype: neuter, BL = 1.9 mm, ZMH K-56568. St 24, 11° 51.52′N 117° 1.19′W, 4100 m, 22 Mar 2015.

Paratypes: three neuters, BL = 1.1–2 mm, ZMH K-56565, ZMH K-56566, ZMH K-56567. St 20, 11° 49.81′N 117° 0.28′W, 4093 m, 22 Mar 2015; two neuters, BL = 1.5–2 mm, ZMH K-56569, ZMH K-56570. St 24, 11° 51.52′N 117° 1.19′W, 4100 m, 22 Mar 2015; two neuters BL = 1.8–1.9 mm, ZMH K-56573 (dissected), ZMH K-56574. 50, 11° 49.92′N 117° 29.31′W, 4330 m, 27 Mar 2015; two neuters, BL = 1.2–1.3 mm, ZMH K-56571, ZMH K-56572. St 59, 11° 48.55′N 117° 29.03′W, 4342 m, 28 Mar 2015; neuter, BL = 1.2 mm, ZMH K-56575. St 99, 11° 2.61′N 119° 39.52′W, 4401 m, 4 Apr 2015.

Diagnosis: Mandible molar acuminate. Antenna article 2 and 3 with spine. Pereopod-2 with semilong blade-like spine. Uropod exopod slightly shorter than endopod.

Etymology: The species is dedicated to Frédéric Chopin, a Polish composer and virtuoso pianist.

Description. BL = 1.9 mm. Body robust (Fig. 28), 3.7 L:W. Carapace 0.6 L:W, 6.2x pereonite-1, 0.1x BL. Pereonites 0.58x BL, pereonites-1–6: 0.1, 0.2, 0.4, 0.6, 0.5 and 0.5 L:W, respectively. Pleon short, 0.2x BL. Pleonites 0.8 L:W.

Antennule (Fig. 29A) article-1 0.5x total length, 6.0 L:W, 2.8x article-2, with two simple and nine penicillate mid-length setae, one simple and four penicillate distal setae; article-2 2.0 L:W, 0.8x article-3, with two simple and one penicillate distal setae; article-3 6.8 L:W, with three simple, two bifurcate setae and one aestetasc.

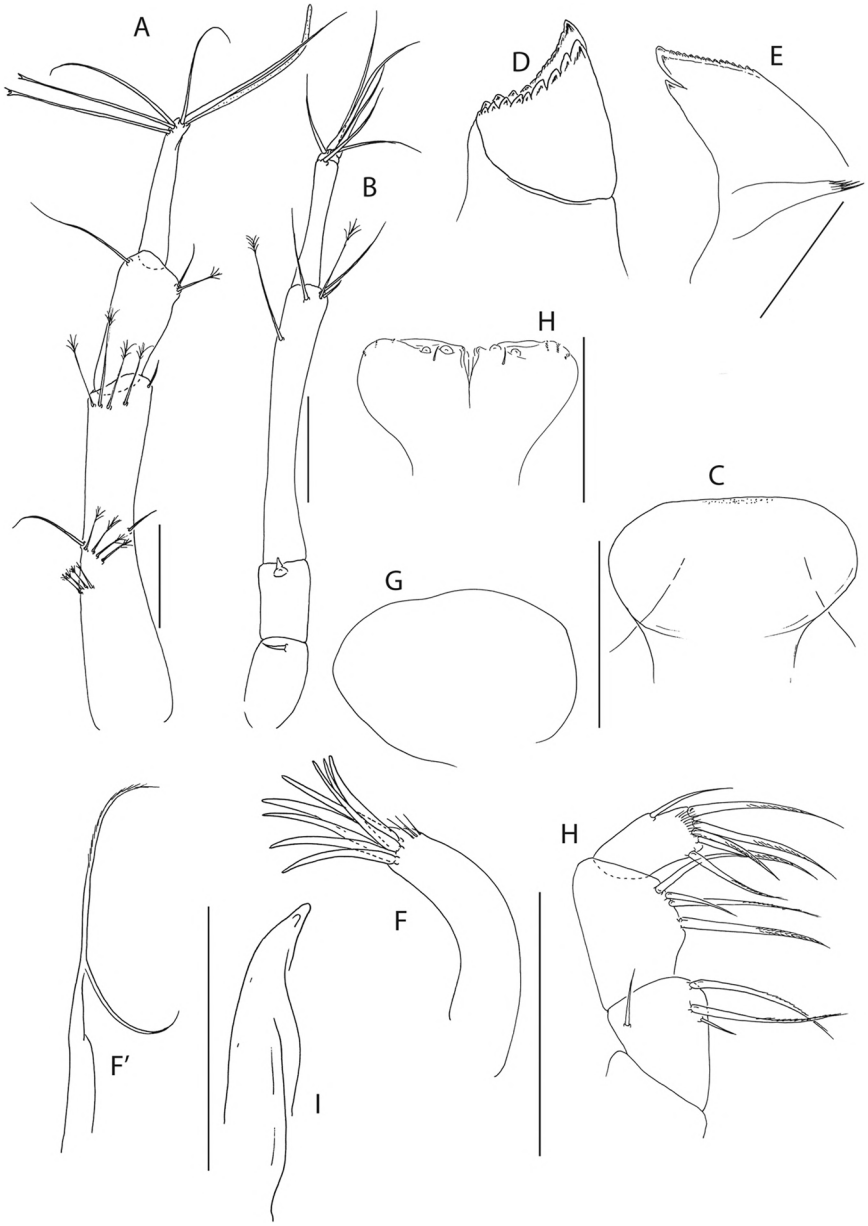

Figure 29. *Pseudotanais chopini* n. sp., ZMH K-56573, neuter. (**A**), antennule; (**B**), antenna; (**C**), labrum; (**D**), left mandible; (**E**), right mandible; (**F**), maxillule; F' endit; (**G**), maxilla; (**H**), maxilliped: (**I**), epignath. Scale bar: 0.1 mm.

Antenna (Fig. 29B) 1.7 L:W; article-2 1.2x article-3, with seta, 0.3x the article; article-3 1.3 L:W, 0.3x article-4, with spine 0.2x the article; article-4 6.9 L:W, 2.2x article-5, with penicillate subdistal seta, and three simple and one penicillate setae distally; article-5 4.7 L:W, 14x article-6, with distal seta; article-6 0.4 L:W, with five simple setae.

Mouthparts. Labrum (Fig. 29C) hood-shaped, naked. Left mandible (Fig. 29D) *lacinia mobilis* well developed and serrate distally, incisor distal margin gently serrate molar broken during dissection. Right mandible (Fig. 29E) incisor distal margin serrate, *lacina mobilis* merged to a small process. Maxillule (Fig. 29F,F') with eight distal spines and three subdistal setae, endite with two setae. Maxilla (Fig. 29G) semioval. Maxilliped (Fig. 29H,H') endites merged with groove in the mid-length, distal margin with two tubercles (gustatory cusps) and with seta; palp article-2 inner margin with three setae, outer margin with seta; article-3 with three setae, article-4 with six setae. Epignath (Fig. 29I) distally pointed.

Cheliped (Fig. 30A) basis 1.6 L:W, with distoproximal seta; merus with seta; carpus 2.3 L:W, with two ventral setae, and with one dorsodistal and one dorsosubproximal setae; chela non-forcipate; palm 2.2 L:W, with row of six setae on inner side; fixed finger distal spine pointed, with three ventral setae; dactylus 6.7 L:W.

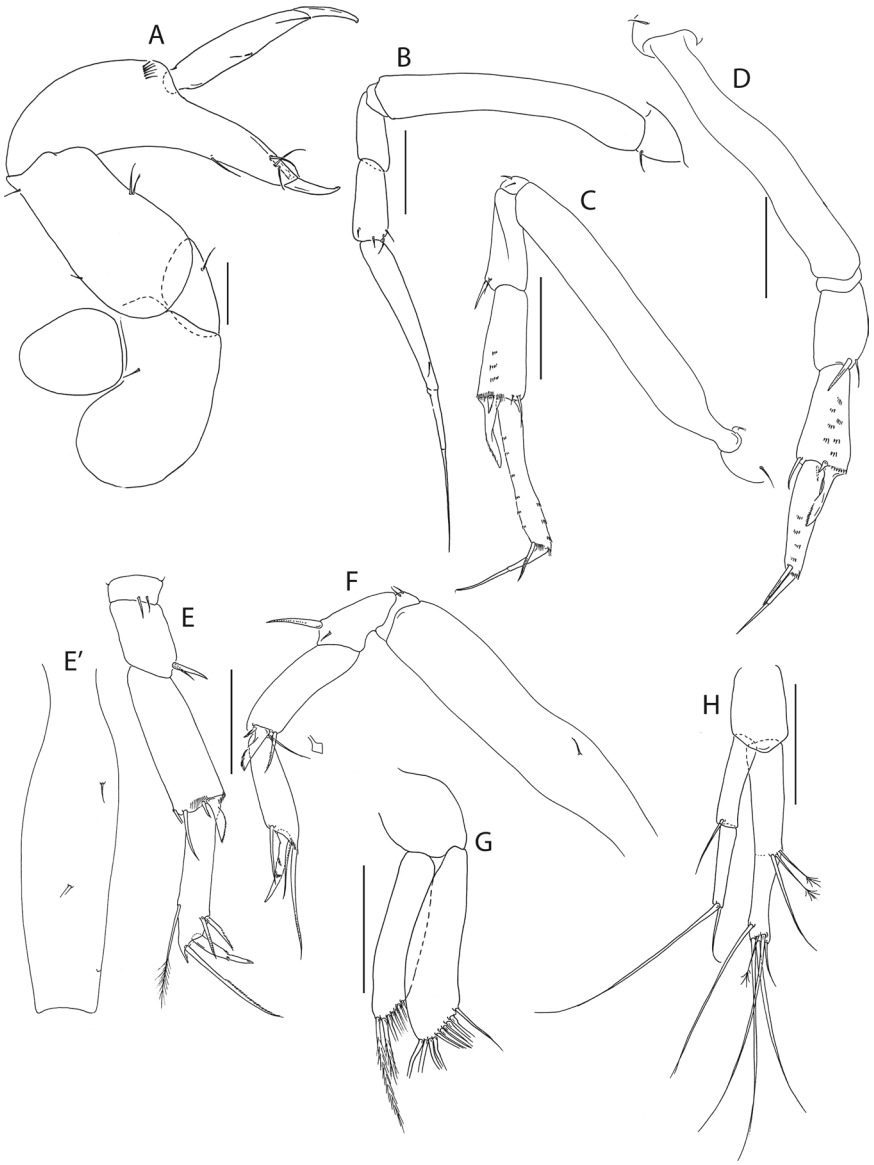

Figure 30. *Pseudotanais chopini* n. sp., ZMH K-56573, neuter. (**A**), cheliped; (**B**), pereopod-1; (**C**), pereopod-2; (**D**), pereopod-3; (**E**), pereopod-4; E' basis of pereopod-3; (**F**), pereopod-6; (**G**), pleopod; (**H**), uropod. Inset at (**F**) show detail of tip of the rod seta. Scale bar: 0.1 mm.

Pereopod-1 (Fig. 30B) coxa with seta; basis 6.8 L:W; merus 2.4 L:W and 0.9x carpus; carpus 2.5 L:W, 0.7x propodus, with four setae; propodus 6.8 L:W, 1.5x dactylus and unguis combined length, with seta; dactylus 0.8x unguis.

Pereopod-2 (Fig. 30C) coxa with seta; basis 6.7 L:W, 3.9x merus; ischium with two ventral setae; merus 1.42 L:W, 0.8x carpus, with two setae; carpus 1.8 L:W, 0.9x propodus, with two setae, one spine and one blade-like spine 0.5x propodus; propodus 6.8 L:W, 1.5x dactylus and unguis combined length, with seta and microtrichia on ventral margin; dactylus 0.7x unguis.

Pereopod-3 (Fig. 30D) coxa with seta; basis 6.7 L:W, 3.9x merus; merus 1.4 L:W, 0.8x carpus, with two setae; carpus 1.8 L:W, 0.9x propodus, with two simple setae, one spine and one blade-like spine 0.6x propodus; propodus 4.2 L:W, 1.4x dactylus and unguis combined length, with seta and microtrichia on ventral margin; dactylus as long as unguis.

Pereopod-4 (Fig. 30E,E') basis 3.8 L:W, 4.5x merus, with two simple ventral setae; ischium with two ventral setae; merus 1.5 L:W, 0.5x carpus, with two setae; carpus 0.9 L:W, 1.1x propodus, with one simple and one sensory (broken) setae, and with one spine and one blade-like spine 0.3x propodus; propodus 4.7 L:W, 2.1x dactylus and unguis combined length, with two serrrated setae on ventral margin, one penicillate and one serrate seta on dorsal margin 1x propodus; dactylus 1.7x unguis.

Pereopod-6 (Fig. 30F) basis 5.0 L:W, 3.7x merus, with ventral seta; ischium with two ventral seta; merus 1.8 L:W, 0.7x carpus, with two setae; carpus 3.0 L:W, 1.1x propodus, with one serrate and one rod setae 0.4x

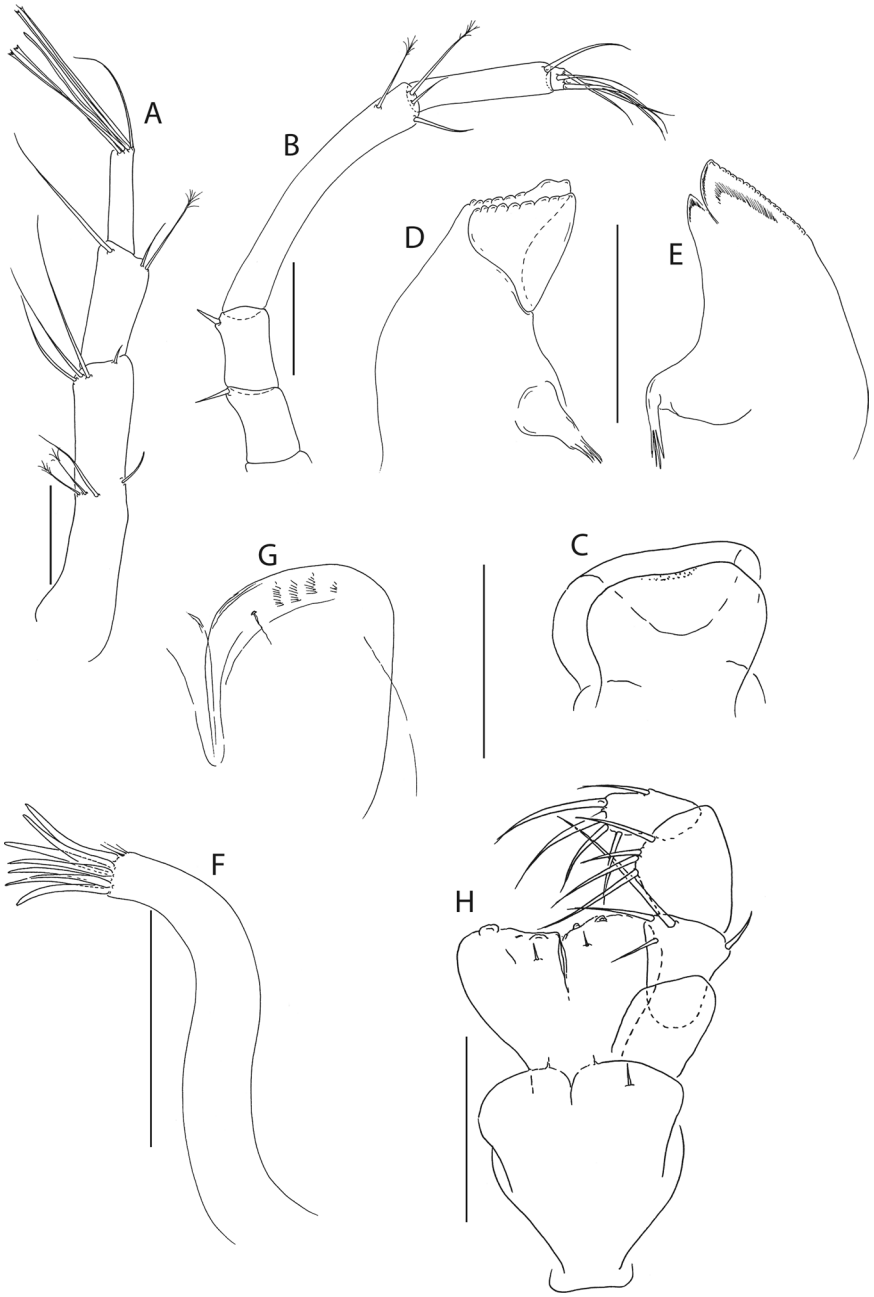

Figure 31. *Pseudotanais chaplini* n. sp., ZMH K-56564, holotype neuter. (**A**), antennule; (**B**), antenna; (**C**), labrium; (**D**), left mandible; (**E**), right mandible; (**F**), maxillule; (**G**), labium; (**H**), maxilliped. Scale bar: 0.1 mm.

propodus, and with one spine and one blade-like spine 0.4x propodus; propodus 3.1 L:W, 1.6x dactylus and unguis combined length, with simple ventral seta and two serrate dorsal setae; dactylus 1.7x unguis.

Pleopods (Fig. 30G) exopod with seven, endopod with ten plumose setae.

Uropod (Fig. 30H) peduncle 1.5 L:W, exopod with two articles, 0.9x endopod; article-1 4.0 L:W, with simple seta; article-2 6 L:W, with two setae; endopod article-1 3.6 L:W, with one simple and two penicillate setae; article-2 3.8 L:W, with five simple and one penicillate seta.

Distribution: *P. chopini* n. sp. is known from the Belgium (GSR) and Interoceanmetal (IOM) licence areas of the Central Pacific.

Remarks: The acuminate mandible molar distinguishes *P. chopini* from other members of the 'denticulatus + abathagastor' group, such as *P. abathagastor*, *P. corollatus*, *P. denticulatus* and *P. georgesandae*, which have wide molars. *Pseudotanais chopini* can be further distinguished from *Pseudotanais* sp. C by the presence of a semilong (0.5x propodus) blade-like spine in pereopod-2 (long in *Pseudotanais* sp. C).

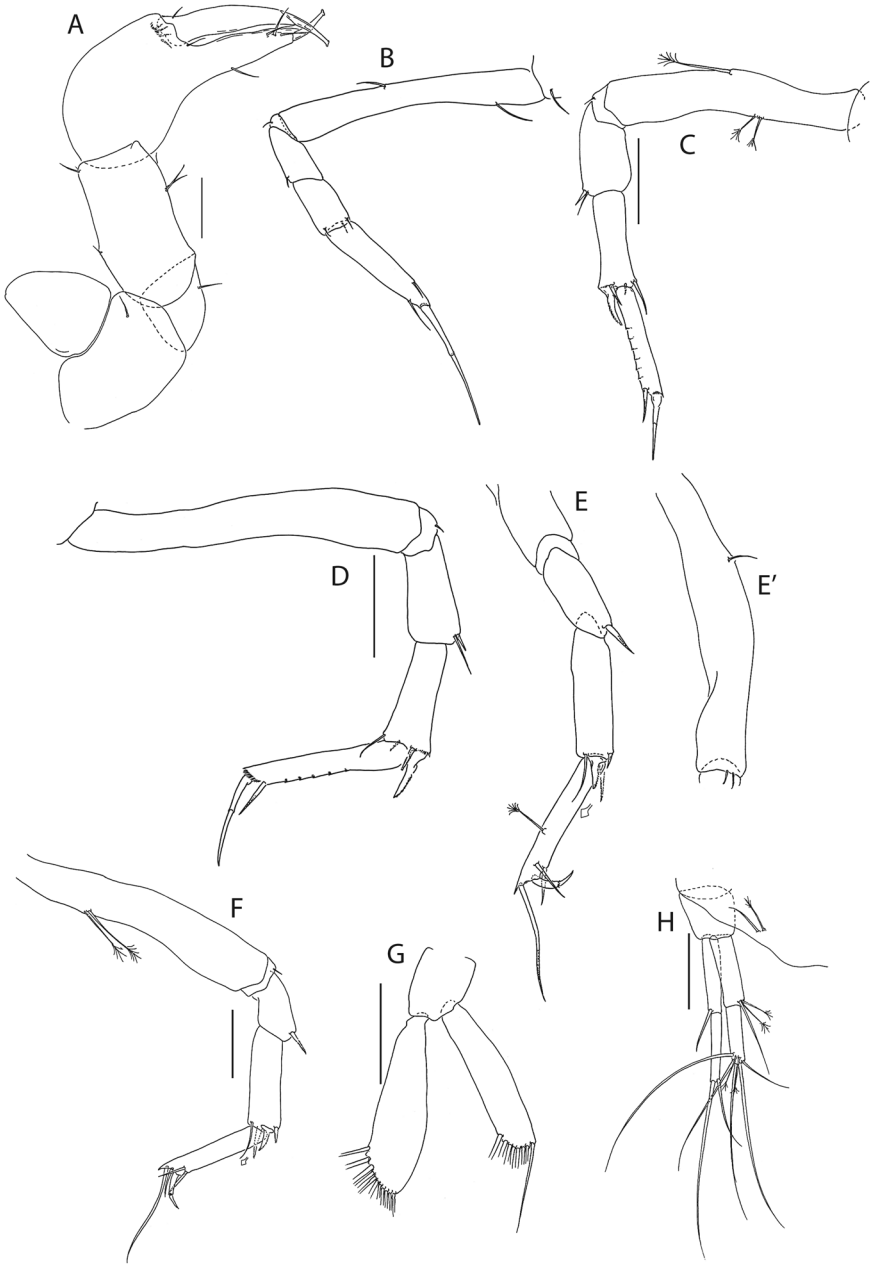

Figure 32. *Pseudotanais chaplini* n. sp., ZMH K-56564, holotype neuter. (**A**), cheliped; (**B**), pereopod-1; (**C**), pereopod-2; (**D**), pereopod-3; (**E**), pereopod-4; E' basis of pereopod-4; (**F**) pereopod-6; (**G**), pleopod; (**H**), uropod. Insets at (**E**,**F**) show detail of tip of the rod seta. Scale bar: 0.1 mm.

***Pseudotanais chaplini* n. sp.**

Figures 31 and 32.

Material examined: Holotype: neuter, BL = 1.5 mm, ZMH K-56564 (partly dissected). St 158, 14° 3.41′N 130° 7.99′W, 4946 m, 15 Apr 2015.

Paratypes: neuter, BL = 1.5 mm, ZMH K-56563 (partly dissected). St 20, 11° 49.81′N 117° 0.28′W, 4093 m, 22 Mar 2015.

Diagnosis: Antenna articles 2–3 with spines. Pereopod 2 and 3 carpus with short blade-like spine. Uropod exopod longer than endopod.

Etymology: The name of the species is dedicated to the great actor and film director of the silent film epoch Charles 'Charlie' Chaplin.

Description. Antennule (Fig. 31A) article-1 0.6x total length, 4.6 L:W, 2.6x article-2, with two simple and two penicillate mid-length setae and four distal setae; article-2 2.3 L:W, 1.1x article-3, with one penicillate and two simple setae; article-3 4.0 L:W, with one simple, four bifurcate setae, and one aestetasc.

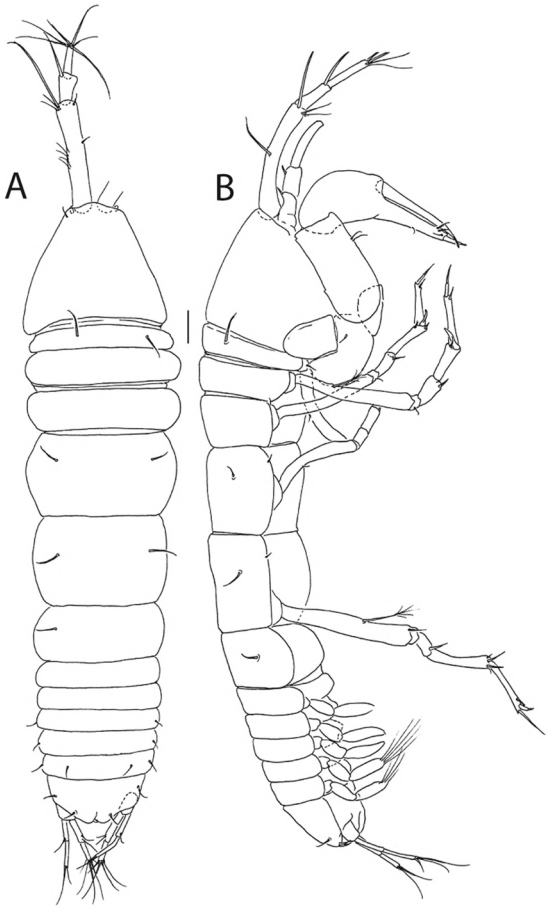

Figure 33. *Pseudotanais oloughlini* n. sp., ZMH K-56596, holotype neuter. (**A**), dorsal view; (**B**) lateral view. Scale bar: 1 mm.

Antenna (Fig. 31B) article-2 1.5 L:W; article-2 0.8x article-3, with spine 0.5x article-2; article-3 1.8 L:W, 0.3x article-4, with spine 0.3x article-3; article-4 8.6 L:W, 2.0x article-5, with two simple and two penicillate setae; article-5 5.0 L:W, 10.0x article-6, with seta; article-6 0.6 L:W, with six setae.

Mouthparts. Labrum (Fig. 31C) hood-shaped, setose. Left mandible (Fig. 31D) *lacinia mobilis* well developed and serrate distally, molar acuminate. Right mandible (Fig. 31E) incisor distal margin serrate, *lacina mobilis* merged to a small process. Maxillule (Fig. 31F) with 8 distal spines. Labium (Fig. 31G) distolateral corner lobes weakly setose. Maxilliped (Fig. 31H) distal margin with two tubercles (gustatory cusps) and seta; palp article-2 inner margin with three inner setae, outer margin with seta; article-3 with four setae, article-4 with five setae.

Cheliped (Fig. 32A) slender; basis 1.5 L:W, with distoproximal seta; merus with simple seta; carpus 2.1 L:W, with two ventral setae, and with one subdistal and one subproximal setae; chela non-forcipate; palm 1.2 L:W, with row of five setae on inner side; fixed finger distal spine pointed, 1.2x palm, with three ventral setae; dactylus 6.7 L:W, cutting edge smooth, proximal seta present.

Pereopod-1 (Fig. 32B) coxa with seta; basis 7.2 L:W, with one ventral and one dorsal setae; ischium with ventral seta; merus 1.7 L:W; carpus, with short seta; carpus 1.5 L:W, 0.4x propodus, with three short setae; propodus 4.6 L:W, 0.9x dactylus and unguis combined length, with two subdistal setae and one distal seta; dactylus 0.7x unguis, without proximal seta.

Pereopod-2 (Fig. 32C) basis 5.7 L:W, 3.6x merus; one ventral and two dorsal penicillate setae; ischium with ventral seta; merus 1.6 L:W, 0.7x carpus, with one seta and one spine; carpus 3.7 L:W, 0.9x propodus, with two simple setae, one serrate spine and one blade-like spine 0.4x propodus; propodus 6.2 L:W, 1.7x dactylus and unguis combined length, with seta and microtrichia on ventral margin; dactylus 0.9x unguis.

Pereopod-3 (Fig. 32D) basis 7.6 L:W, 3.4x merus; ischium with ventral seta; merus 2.2 L:W, 0.9x carpus, with simple seta and spine; carpus 2.8 L:W, 0.6x propodus, with two setae, one spine and one blade-like spine 0.3x propodus; propodus 7.0 L:W, 1.7x dactylus and unguis combined length, with seta and microtrichia on ventral margin; dactylus 0.7x unguis.

Pereopod-4 (Fig. 32E,E') basis 6.2 L:W, 3.1x merus, with ventral seta; ischium with two ventral setae; merus 2.4 L:W, 0.7x carpus, with serrate seta; carpus 4.0 L:W, propodus, with one simple, one rod seta, one spine and blade-like spine, 0.2x propodus, rod seta 0.2x propodus; propodus 6.4 L:W, 2.9x dactylus and unguis combined length, with two ventral setae and one serrate dorsal seta 0.8x propodus; dactylus 1.7x unguis.

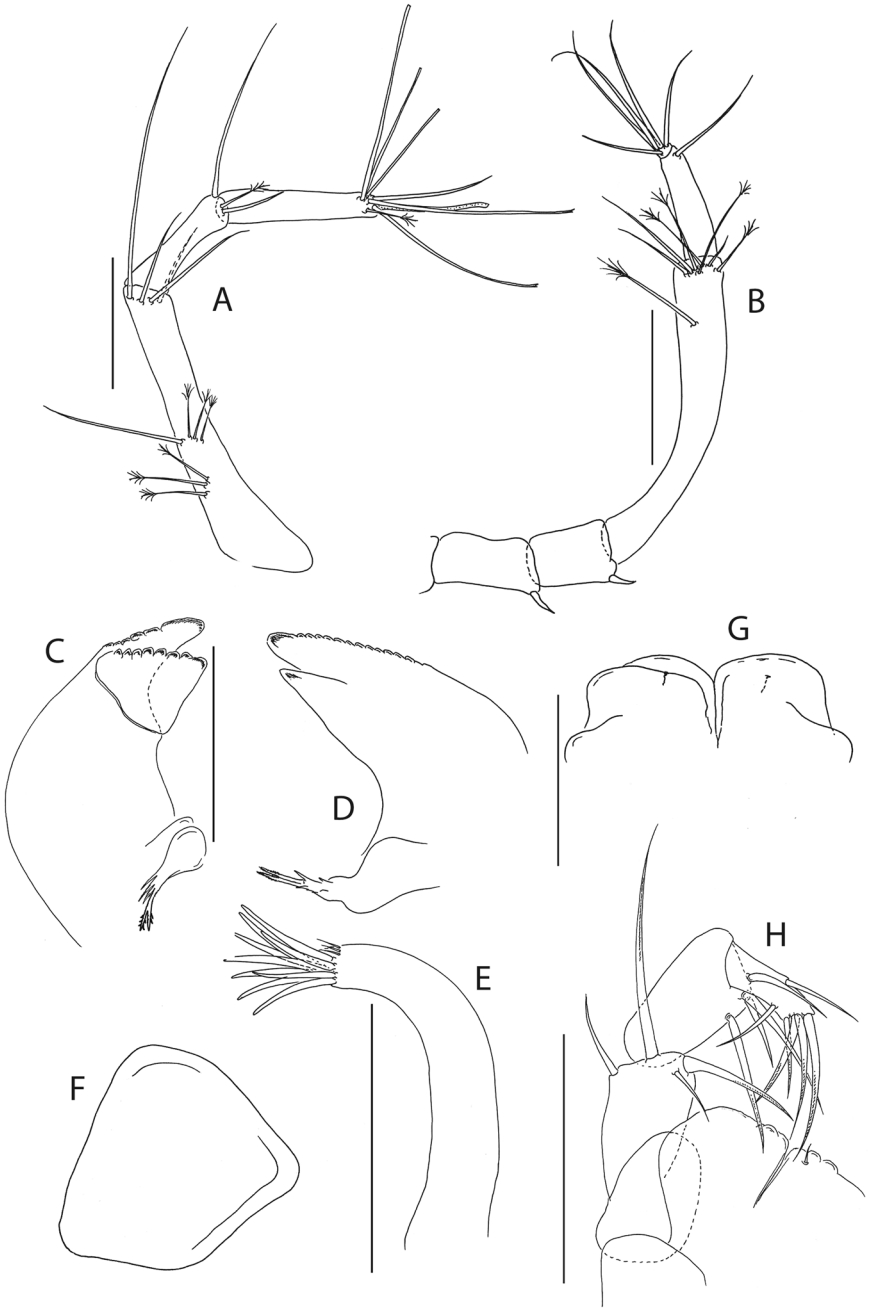

Figure 34. *Pseudotanais oloughlini* n. sp., ZMH K-56595, neuter. (**A**), antennule; (**B**), antenna; (**C**), left mandible; (**D**), right mandible; (**E**), maxillule; (**F**), maxilla; (**G**), labium; (**H**), maxilliped. Scale bar: 0.1 mm.

Pereopod-6 (Fig. 32F) basis 6.0 L:W, 4.3x merus, with two penicillate dorsal setae; ischium with ventral seta; merus 1.7 L:W, 0.6x carpus, with serrate seta; carpus 3.8 L:W, propodus, with rod seta 0.4x propodus, two spines and blade-like spine 0.2x propodus; propodus 5.5 L:W, 2.7x dactylus and unguis combined length, with one seta, two ventral spines ventrally and one serrate seta 1x propodus; dactylus 1.4x unguis.

Pleopods (Fig. 32G) exopod with eight, endopod with eleven plumose setae.

Uropod (Fig. 32H) peduncle 1.2 L:W; exopod with two articles, 1.1x endopod; article-1 5.7 L:W, with seta; article-2 7.5 L:W, with two simple setae; endopod article-1 3.2 L:W, with one simple and two penicillate setae; article-2 4.3 L:W, with two penicillate and five simple setae.

Distribution: *P. chaplini* n. sp. is known from the IFREMER and IOM licence areas of the Central Pacific.

Remarks: The exopod uropod being longer than endopod allows for distinguishing the new species from *P. abathagastor*, *P. corollatus*, *P. denticulatus*, *P. georgesandae*, *P. chopini* and *Pseudotanais* sp. C, as well as from all other species of the genus *Pseudotanais*.

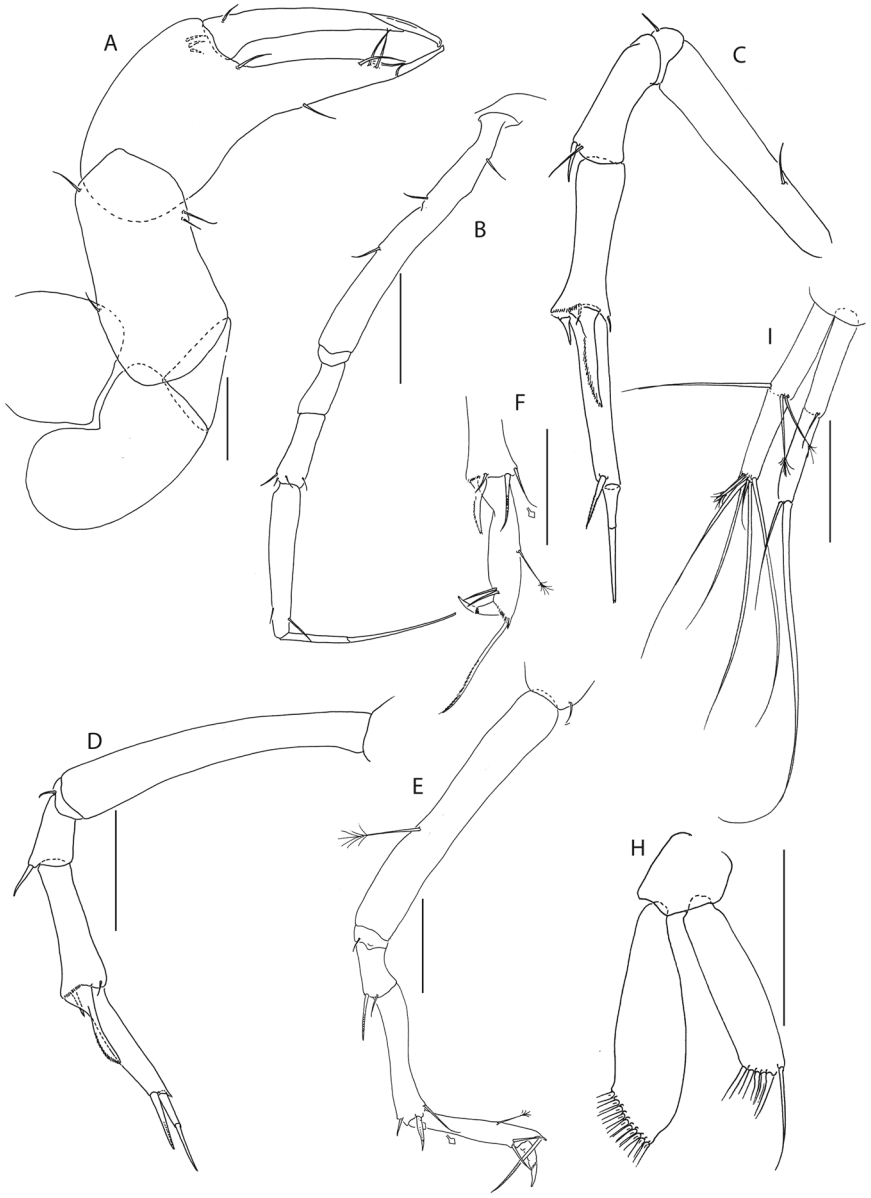

Figure 35. *Pseudotanais oloughlini* n. sp., ZMH K-56595, neuter. (**A**), cheliped; (**B**), pereopod-1; (**C**), pereopod-2; (**D**), pereopod-3; (**E**), pereopod-4; (**F**), pereopod-5; (**G**), pleopod; (**H**), uropod. Inset at (**E**) show detail of tip of the rod seta. Scale bar: 0.1 mm.

***Pseudotanais oloughlini* n. sp.**

Figures 33–35.

Material examined: Holotype: neuter, BL = 1.9 mm, ZMH K-56596. St 197, 18° 48.66′N 128° 22.75′W, 4805 m, 21 Apr 2015.

Paratypes: two neuters, BL = 2 mm, ZMH K-56597, ZMH K-56598. St 192, 18° 44.81′N 128° 21.87′W, 4877 m, 21 Apr 2015; two neuters, BL = 2–2.6 mm, ZMH K-56594 (dissected), ZMH K-56595 (dissected). St 197, 18° 48.66′N 128° 22.75′W, 4805 m, 21 Apr 2015.

Diagnosis: Mandible molar acuminate with bifurcate distal tooth. Antennal articles 2–3 with spine. Pereopods 2 and carpus with long blade-like spine. Uropod exopod longer than endopod.

Etymology: The species is named in recognition of the great holothurian specialist and wonderful friend and colleague – Dr. Mark O'Loughlin.

Description of neuter. BL 1.9 mm. Body slender (Fig. 33A,B), 3.9 L:W. Carapace 0.8 L:W, 5.4x pereonite-1, 0.2x BL. Pereonites 0.5x BL, pereonites-1–6: 0.1, 0.2, 0.2, 0.5, 0.6 and 0.4 L:W, respectively. Pleon short, 0.2x BL. Pleonites 0.9 L:W.

Antennule (Fig. 34A) article-1 0.5x total length, 6.0 L:W, 2.4x article-2, with one simple and six penicillate mid-length setae, and four simple setae (one very long); article-2 4.2 L:W, 0.8x article-3, with two simple and one

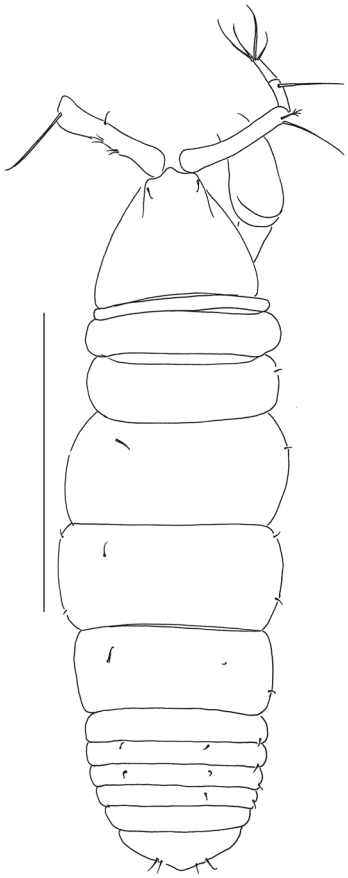

Figure 36. *Pseudotanais mariae* n. sp., ZMH K-56592, holotype neuter. Dorsal view. Scale bar: 1 mm.

penicillate seta; article-3 5.5 L:W, with one simple, two bifurcate, one penicillate and three broken setae, and one aestetasc.

Antenna (Fig. 34B) article-2 2.1 L:W; article-2 1.2x article-3, with spine 0.3x article-2; article-3 1.6 L:W, 0.3x article-4, with spine 0.3x article-3; article-4 6.8 L:W, 3.1x article-5, with penicillate subdistal seta and three simple, four penicillate distal setae; article-5 3.7 L:W, 11.0x article-6, with seta; article-6 0.5 L:W, with five setae.

Mouthparts. Left mandible (Fig. 34C) *lacinia mobilis* well developed and distally serrate, incisor distal margin serrate, molar acuminate, with distal bifurcate spine. Right mandible (Fig. 34D) incisor distal margin serrate, *lacina mobilis* merged to a small process. Maxillule (Fig. 34E) with 9 distal spines and three subdistal setae. Maxilla (Fig. 34F) with semi-triangular shape. Labium (Fig. 34G) lobes distolateral corner naked. Maxilliped (Fig. 34H) endites merged, with groove in the mid-length, distal margin with two tubercles (gustatory cusps) and seta; article-2 inner margin with three inner setae, outer margin with seta; article-3 with three setae; article-4 with five setae.

Cheliped (Fig. 35A) slender; basis 1.8 L:W; carpus 2.2 L:W, with two ventral setae, and with distal and subproximal dorsal setae; chela non-forcipate; palm 1.5 L:W, with row of three setae on inner side; fixed finger distal spine pointed, with three ventral setae; dactylus 6.5 L:W, proximal seta present.

Pereopod-1 (Fig. 35B) basis 9.1 L:W, with one ventral and two dorsal setae; merus 2.0 L:W, and 0.7x carpus; carpus 2.7 L:W, 0.5x propodus, with four setae; propodus 5.8 L:W, 0.9x dactylus and unguis combined length, with two setae; dactylus 0.6x unguis.

Pereopod-2 (Fig. 35C) basis 5.4 L:W, 1.9x merus, with ventral seta; ischium with ventral seta; merus 2.6 L:W, 0.8x carpus, with seta and spine; carpus 3.1 L:W, 0.8x propodus, with two simple setae, one regular spine and one blade-like spine 0.6x propodus; propodus 5.9 L:W, 1.5x as long dactylus and unguis combined length, with serrate distal seta; dactylus 0.6x unguis.

Pereopod-3 (Fig. 35D) basis 6.2 L:W, 4.9x merus; ischium with ventral seta; merus 0.7 L:W, 0.5x carpus, with seta; carpus 3.3 L:W, 1.1x propodus, with simple seta, regular spine and blade-like spine 0.7x propodus; propodus 4.7 L:W, 1.4x dactylus and unguis combined length, with serrate distal seta; dactylus 0.8x unguis.

Pereopod-4 (Fig. 35E) basis 7.3 L:W, 5.5x merus, with penicillate ventral seta; ischium with ventral seta; merus 1.5 L:W, 0.4x carpus, with two distal setae; carpus six L:W, 1.1x propodus, with one simple, one sensory, one regular spine and one blade-like spine (distally broken), rod seta 0.4x propodus; propodus 5.4 L:W, 2.7x dactylus and unguis combined length, with two ventral setae, one penicillate, and one serrate setae on dorsal margin 0.6x propodus; dactylus 1.5x unguis.

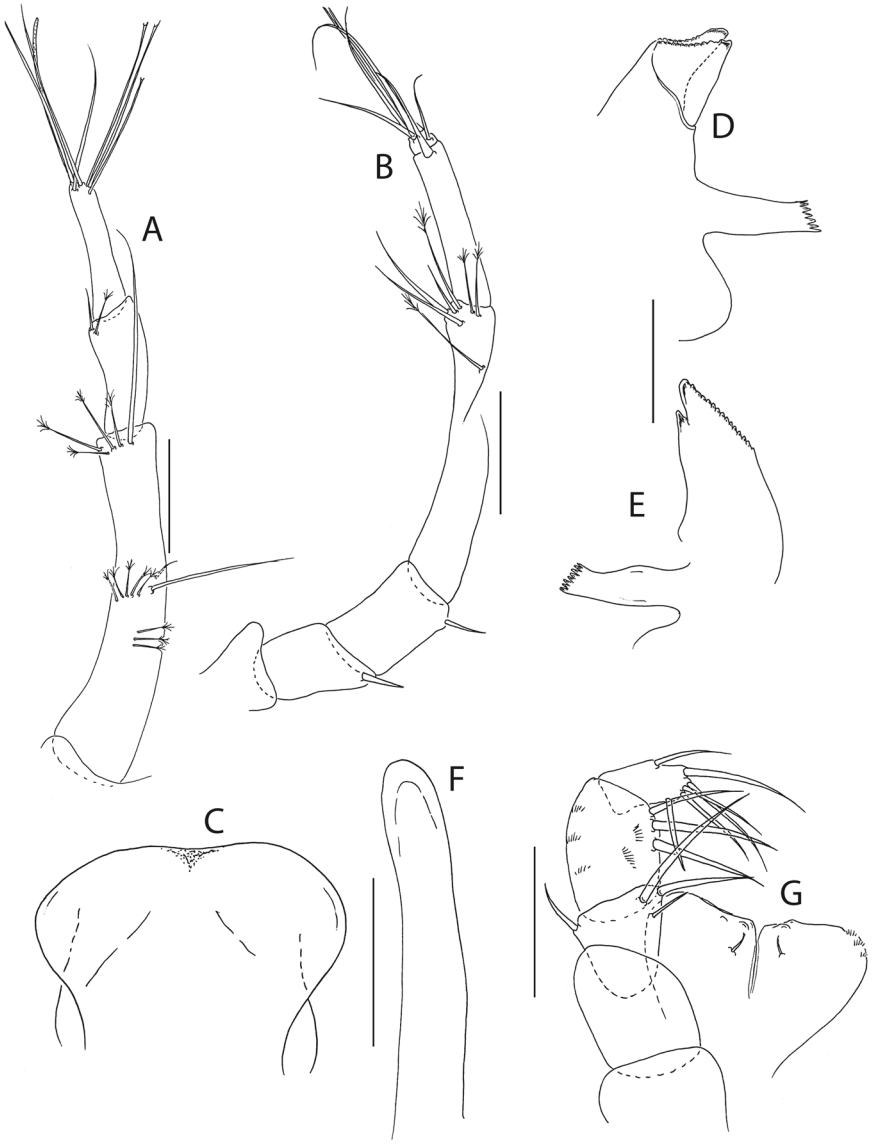

Figure 37. *Pseudotanais mariae* n. sp., ZMH K-56591, neuter. (**A**), antennule; (**B**), antenna; (**C**), labrum; (**D**), left mandible; (**E**), right mandible; (**F**), maxilliped, (**G**), epignath. Scale bar: 0.1 mm.

Pereopod-5 (Fig. 35F) carpus with two simple, one sensory 0.3x propodus, one blade-like spine 0.25x propodus; propodus 4.4 L:W, 3.1x dactylus and unguis combined length, with two ventral setae, one penicillate and one serrate dorsal seta 0.9x propodus; dactylus as long as unguis.

Pleopods (Fig. 35G) exopod with five, endopod with 10 plumose setae.

Uropod (Fig. 35H) exopod 1.1.x endopod, with two articles; article-1 5.0 L:W, with seta; article-2 4.2 L:W, with two setae. Endopod article-1 3.7 L:W, with one simple and two penicillate setae; article-2 4.0 L:W, with five simple and two penicillate setae;

Distribution: *P. oloughlini* n. sp. is known only from APEI3 of the Clarion and Clipperton Fractures Zone, Central Pacific.

Remarks: Uropod exopod longer than endopod separates *Pseudotanais oloughlini* from *P. abathagastor*, *P. corollatus*, *P. denticulatus*, *P. georgesandae*, *P. chopini* and *Pseudotanais* sp. C. *P. oloughlini* is most similar to *P. chaplini* but can be distinguished by its long blade-like spine on carpus of pereopods 2 and 3 (short blade-like spine in *P. chaplini*).

***Pseudotanais mariae* n. sp.**

Figures 36–38.

Material examined: Holotype: neuter, BL = 2.4 mm, ZMH K-56592. St. 81, 11° 3.97′N 119° 37.67′W, 4365 m, 1 Apr 2015.

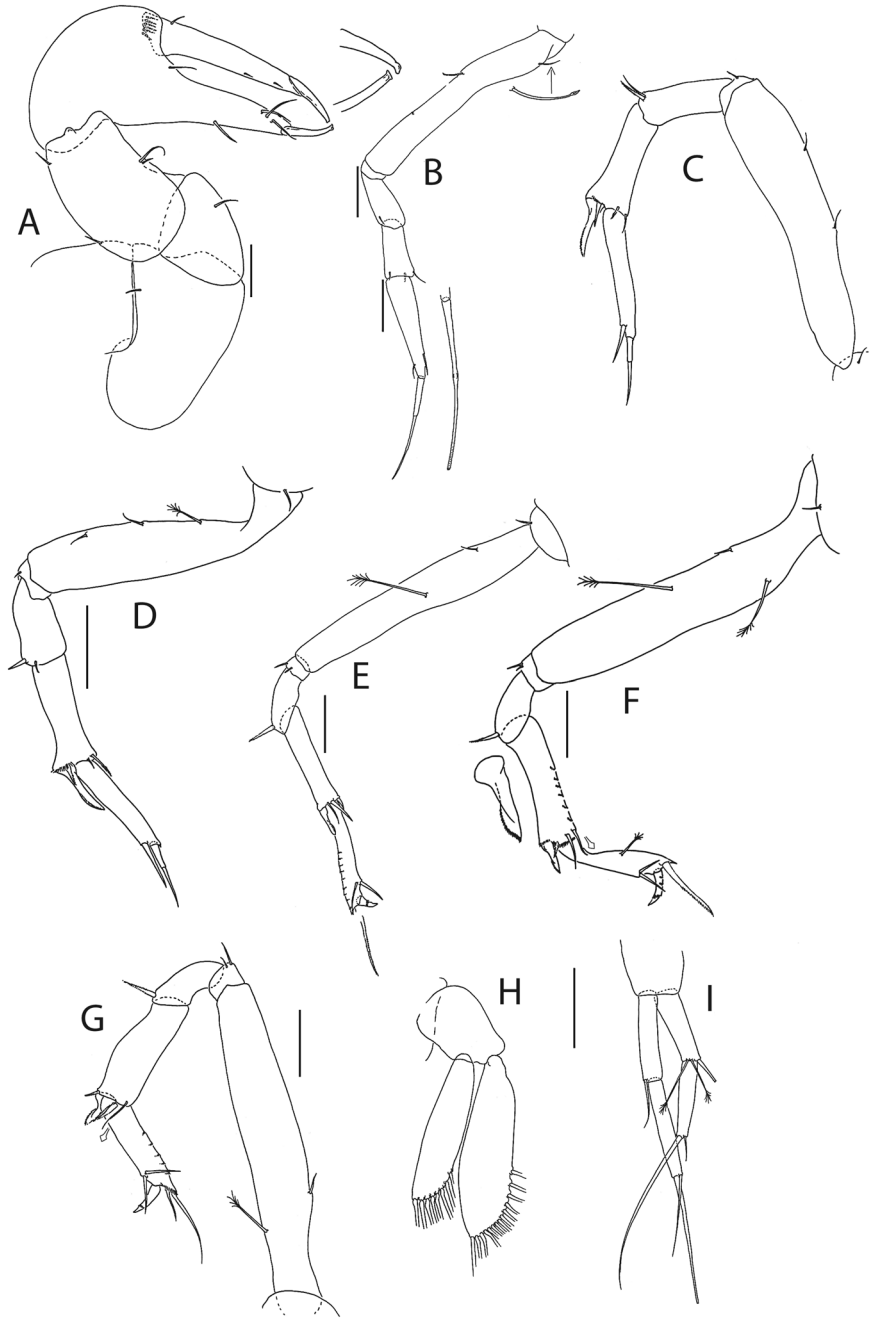

Figure 38. *Pseudotanais mariae* n. sp., ZMH K-56591, neuter. (**A**), cheliped; (**B**), pereopod-1; (**C**), pereopod-2; (**D**), pereopod-3; (**E**), pereopod-4; (**F**), pereopod-5; (**G**), pereopod-5; (**H**), pleopod; (**I**), uropod. Insets at (**F**,**G**) show detail of tip of the rod seta. Scale bar: 0.1 mm.

Paratypes: neutrum, BL = 1.4 mm, ZMH K-56590. St. 20, 11° 49.81′N 117° 0.28′W, 4093 m, 22 Mar 2015; neuter, BL = 2 mm, ZMH K-56591 (dissected). St. 81, 11° 3.97′N 119° 37.67′W, 4365 m, 1 Apr 2015; neuter, BL = 1.9 mm, ZMH K-56593. St. 99, 11° 2.61′N 119° 39.52′W, 4401 m, 4 Apr 2015.

Diagnosis: Mandible molar wide. Antenna articles 2–3 with seta. Pereopod-2 carpus blade-spine short. Uropod exopod slightly shorter than endopod.

Etymology: The species is dedicated to Maria Jakiel, the mother of the first author.

Description of neuter. BL 2.4 mm. Body robust (Fig. 36), 3.2 L:W. Carapace 0.8 L:W, 9.0x pereonite-1, 0.2x BL. Pereonites 0.6x BL, pereonites-1–6: 0.1, 0.2, 0.3, 0.4, 0.4 and 0.4 L:W, respectively. Pleon short, 0.2x BL. Pleonites 0.7 L:W.

Antennule (Fig. 37A) article-1 0.5x total length, 5.8 L:W, 2.6x article-2, with two simple and eight penicillate setae at mid-length and one simple and four penicillate setae distally; article-2 2.2 L:W, 0.9x article-3, one simple and one penicillate setae distally; article-3 3.5 L:W, with three simple and three bifurcate setae, and aestetasc distally.

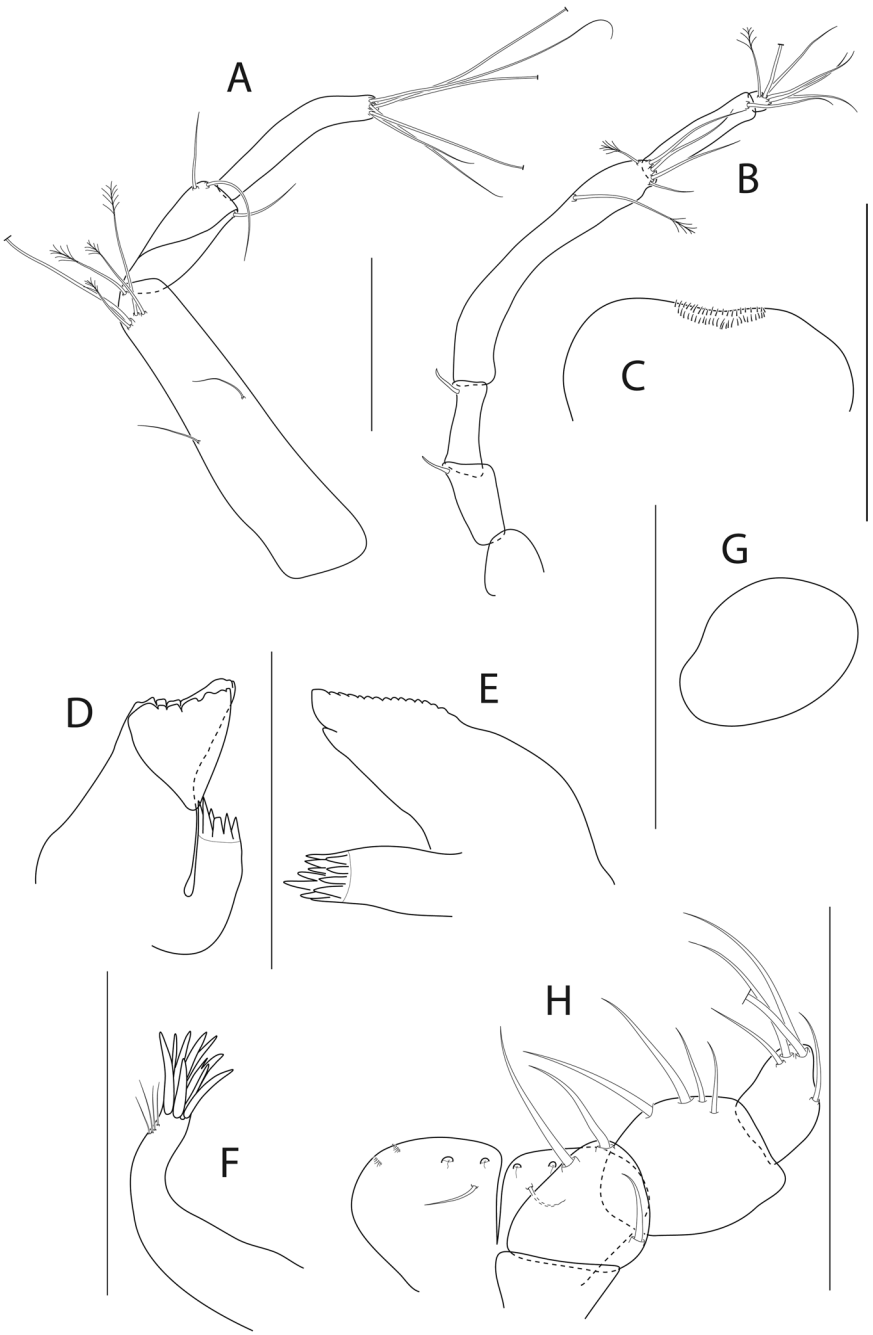

Figure 39. *Pseudotanais kobro* n. sp., ZMH K-56587, neuter. (**A**), antennule; (**B**), antenna; (**C**), labrum; (**D**), left mandible; (**E**), right mandible; (**F**), maxillula, (**G**), maxilla, (**H**), maxilliped. Scale bar: 0.1 mm.

Antenna (Fig. 37B) article-2 1.5 L:W; 0.9x article-3, with seta 0.4x article-2; article-3 1.6 L:W, 0.4x article-4, with seta 0.4x article-3; article-4 5.0 L:W, 1.8x article-5, with penicillate subdistal seta, three simple and three penicillate setae distally; article-5 4.9 L:W, 8.5x article-6, with distal seta; article-6 0.7 L:W, with five setae.

Mouthparts. Labrum (Fig. 37C) hood-shaped, naked. Left mandible (Fig. 37D) *lacinia mobilis* well developed and serrate distally, incisor distal margin serrate, molar wide, with spines distally. Right mandible (Fig. 37E) incisor distal margin serrate, *lacina mobilis* merged to a small process. Maxilliped (Fig. 37F) endites merged, with groove in the mid-length, distal margin with two tubercles (gustatory cusps) and seta; palp article-2 inner margin with three inner setae, outer margin with seta; article-3 with three inner setae; article-4 with five inner distal and subdistal setae and one outer seta. Epignath (Fig. 37G) distally rounded.

Cheliped (Fig. 38A) robust; basis 1.7 L:W, with distoproximal seta; merus with seta; carpus 1.6 L:W, with two ventral setae, one distal and one subproximal seta dorsally; chela non-forcipate, palm 1.1 L:W, with row of five setae on inner side; fixed finger with three ventral setae and three inner setae, cutting edge almost simple; dactylus 7.0 L:W, cutting edge with two spines, proximal seta present.

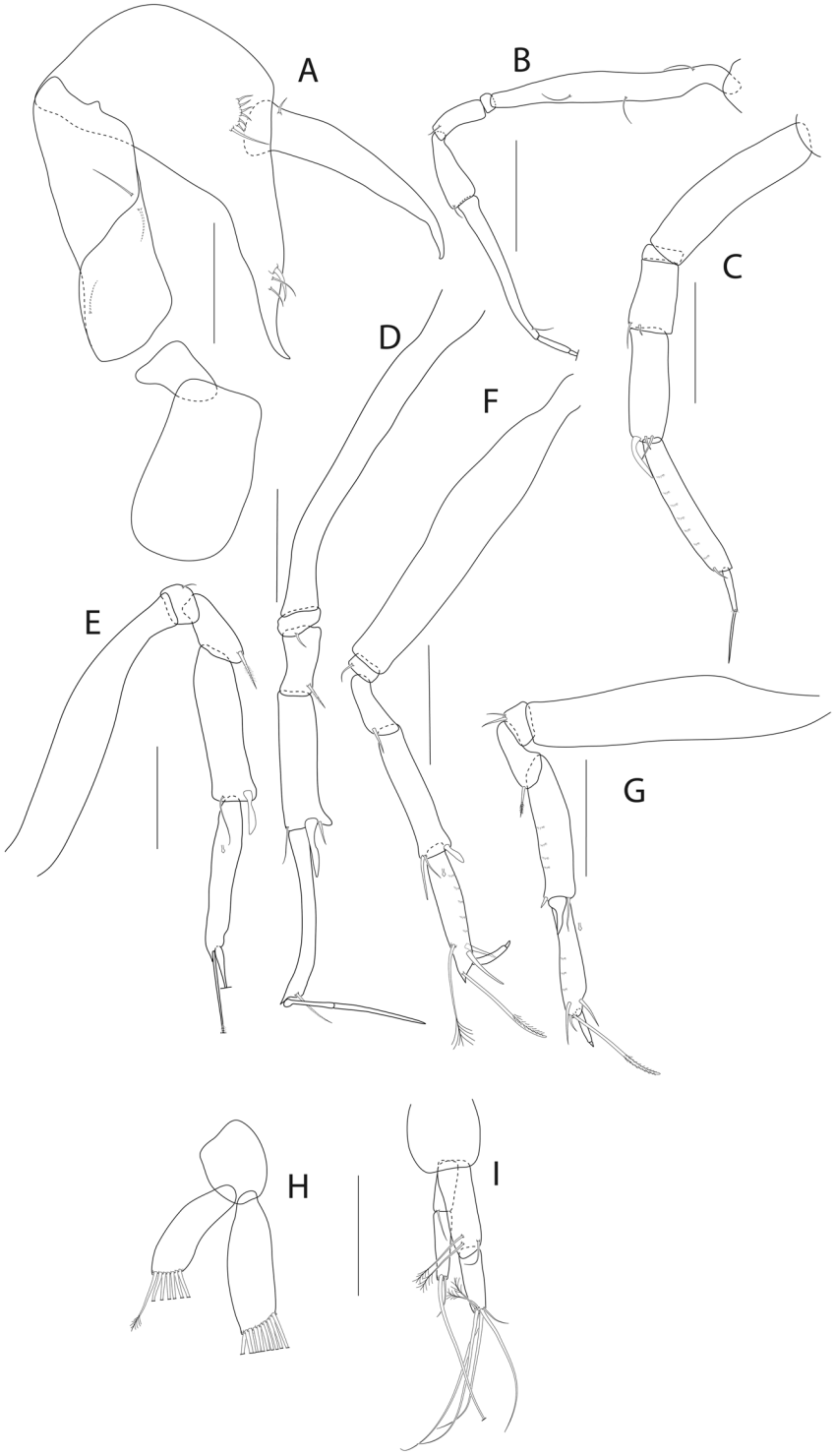

Figure 40. *Pseudotanais kobro* n. sp., ZMH K-56586 (D, E), ZMH K-56587 (**A**–**C**,**F**–**H**), neuter. (**A**), cheliped; (**B**), pereopod-1; (**C**), pereopod-2; (**D**), pereopod-3; (**E**), pereopod-4; (**F**), pereopod-5; (**G**), pereopod-6; (**H**), pleopod; (**I**), uropod. Insets at (**E**–**G**) show detail of tip of the rod seta. Scale bar: 0.1 mm.

Pereopod-1 (Fig. 38B) basis 7.3 L:W, with two simple ventral setae and sensory dorsal seta; merus 2.2 L:W and 0.9x carpus, with seta; carpus 2.4 L:W, 0.6x propodus, with three setae; propodus 4.0 L:W, 0.9x dactylus and unguis combined length, with two setae, dactylus 0.6x unguis.

Pereopod-2 (Fig. 38C) coxa with seta; basis 5 L:W, 3.5x merus, with two ventral seta; ischium with ventral seta; merus 2.4 L:W, 0.8x carpus, with two setae; carpus 3 L:W, 0.8x propodus, with two simple setae, one spine and one blade-like spine, 0.4x propodus; propodus 6.2 L:W, 2.1x dactylus and unguis combined length, with seta; dactylus 0.6x unguis.

Pereopod-3 (Fig. 38D) coxa with seta; basis 4.5 L:W, 3.2x merus, with two simple and one penicillate seta ventrally; ischium with two ventral setae; merus 2.1 L:W, 0.8x carpus, with two setae; carpus 3.1 L:W, with two simple setae, one spine and one blade-like spine, 0.5x propodus; propodus 5.7 L:W, 1.5x dactylus and unguis combined length, with seta; dactylus 0.7x unguis.

Pereopod-4 (Fig. 38E) basis 7.6 L:W, 4.4x merus, with penicillate ventral seta and simple dorsal seta; ischium with two ventral setae; merus 3 L:W, 0.6x carpus, with seta; carpus 4 L:W, 0.9x propodus, with one simple, one rod seta 0.3x propodus, one spine and one blade-like spine 0.3x propodus; propodus 5.2 L:W, 4.7x dactylus and unguis combined length, with two simple setae ventrally, one serrate seta dorsally 0.7x propodus and microtrichia on ventral margin; dactylus 3x unguis.

Pereopod-5 (Fig. 38F) basis 5.4 L:W, 7.7x merus, with one simple and one penicillate seta ventrally and with penicillate seta dorsally; ischium with two ventral seta; merus 5.2 L:W, 0.5x carpus, with seta; carpus 3.9 L:W, 1.3x propodus, one simple, one sensory 0.3x propodus, one spine and one blade-like spine, 0.3x propodus; propodus 4.0 L:W, 2.5x dactylus and unguis combined length, with two simple ventral seta and serrate dorsal seta 0.7x propodus; dactylus 0.1x unguis.

Pereopod-6 (Fig. 38G) basis 7.7 L:W, 4.9x merus, with simple seta ventrally and with penicillae seta dorsally; ischium with two ventral seta; merus 2.3 L:W, 0.6x carpus, with serrate seta; carpus 3.6 L:W, 1.2x propodus, with one simple, one sensory 0.3x propodus, one spine, and one blade-like spine 0.3x propodus; propodus 3.3 L:W, 2.5x dactylus and unguis combined length, with two setae on ventral margin and one serrate setae on dorsal margin 0.7x propodus and microtrichia on ventral margin; dactylus 3.0x unguis.

Pleopods (Fig. 38H) exopod with 8, endopod with 14 plumose setae.

Uropod (Fig. 38I) peduncle 0.8 L:W; exopod 0.6x as long as, with two articles; article-1 3.7 L:W, with one simple and two penicillate setae; article-2 five L:W, with two seta; endopod article-1 4.7 L:W, with one seta; article-2 6.7 L:W, with two setae.

Distribution: *P. mariae* n. sp. is known from the Belgium (GSR) and Interoceanmetal (IOM) licence areas of the Central Pacific.

Remarks: The presence of setae on antenna articles 2–3 distinguishes *P. mariae* from other members of the 'denticulatus + abathagastor' group (*P. abathagastor*, *P. corollatus*, *P. denticulatus*, *P. georgesandae*, *P. chopini*, *P. chaplini*, *P. oloughlini and Pseudotanais* sp. C), which have antenna articles 2–3 armed with spines.

'spicatus' group

Diagnosis: Mandible molar acuminate or wide. Antenna articles 2–3 armed with spine. Pereopod-1 basis with setae on ventral margin. Pereopod-1 merus and carpus distodorsal seta short. Pereopod-2 carpus blade-like spine short. Pereopod 5–6 carpus distodorsal seta short. Uropod slender, exopod slightly shorter or equal to endopod.

Species included: *Pseudotanais spicatus* Bird & Holdich, 1989; *P. tympanobaculum* Błażewicz-Paszkowycz, Bamber & Cunha, 2011; *P. kobro* n. sp.

Remarks: The presence of a very short blade-like spine on carpus of pereopod-2 allows to distinguish this group from other taxa.

***Pseudotanais kobro* n. sp.**

Figures 39 and 40.

Material examined: Holotype: neuter, BL = 1.3 mm, ZMH K-56589. St 117, 13° 52.39′N 123° 15.30′W, 4496 m, 7 Apr 2015.

Paratypes: neuter, BL = 1.4 mm, ZMH K-56585 (partly dissected). St 11° 3.97′N 119° 37.67′W, 4365 m, 1 Apr 2015; three neuters BL = 1.3–1.4 mm, ZMH K-56586 (dissected), ZMH K-56587 (dissected), ZMH K-56588. St 99, 11° 2.61′N 119° 39.52′W, 4401 m, 4 Apr 2015.

Diagnosis: Antenna articles 2–3 with a thin and long spine, unguis of pereopod 5–6 minute.

Etymology: The name of the species is dedicated to Katarzyna Kobro, a modern Polish sculptor.

Description. Antennule (Fig. 39A) article-1 0.5x total length, 4.2 L:W, 2.5x article-2, with two simple setae in mid-length, one simple and four penicillate setae distally; article-2 2.5 L:W, 0.8x article-3, with three setae; article-3 5.3 L:W, with six setae (three broken).

Antenna (Fig. 39B) article-2 2.1 L:W; article-2 0.9x article-3, with spine 0.3x article; article-3 2.8 L:W, 0.3x article-4, with spine, 0.3x article; article-4 6.2 L:W, 2.5x article-5, one penicillate seta in mid-length, four simple setae and one penicillate seta distally; article-5 5 L:W, 5x article-6, with distal seta; article-6 wide, one penicillate seta and 5 simple setae (one broken).

Mouthparts. Labrum (Fig. 39C) hood-shaped, setose. Left mandible (Fig. 39D) *lacinia mobilis* well developed and serrate distally, incisor distal margin serrate, molar wide. Right mandible (Fig. 39E) incisor distal margin serrate, *lacina mobilis* merged to a small process. Maxillule (Fig. 39F) with 8 simple and one bifurcate distal spine with four subdistal setae. Maxilla (Fig. 39G) oval. Maxilliped (Fig. 39H) endites merged, with groove in the mid-length, distal margin, with two tubercles and one seta; palp article-2 inner margin, with two setae, outer margin with seta; article-3 with four setae; article-4 with four inner distal and subdistal setae and one outer seta.

Cheliped (Fig. 40A) slender; basis 1.6 L:W; carpus 3 L:W, with two ventral setae, subproximal seta; chela non-forcipate; palm 1.2 L:W, row of 6 serrate setae on inner margin; fixed finger distal spine pointed, 1.4x palm, with three ventral setae; dactylus 7.5 L:W, cutting edge smooth, proximal seta present.

Pereopod-1 (Fig. 40B) basis 8.8 L:W, with one seta ventrally and two setae dorsally; merus 2.5 L:W and 0.8x carpus, with seta; carpus 2.6 L:W, 0.4x propodus, with seta; propodus 10 L:W, with seta.

Pereopod-2 (Fig. 40C) basis 4.5 L:W, 2.6x merus; merus 1.7 L:W, 0.6x carpus, with two setae; carpus 2.7 L:W, 0.8x propodus, with two simple setae and blade-like spine, 0.3x propodus; propodus 5.6 L:W, 1.5x dactylus and unguis combined length, with simple seta and microtrichia on ventral margin; dactylus 0.8x unguis.

Pereopod-3 (Fig. 40D) basis 7 L:W, 5.8x merus; ischium with simple seta; merus 2 L:W, 0.5x carpus, with one serrate setae; carpus 3.7 L:W, 0.7x propodus, with two simple setae and blade-like spine, 0.3x propodus; propodus 7 L:W, 1.3x dactylus and unguis combined length, with serrate seta; dactylus 0.5x unguis.

Pereopod-4 (Fig. 40E) basis 5.8 L:W, 3.9x merus; ischium with simple seta; merus 2.1 L:W, 0.5x carpus, with one serrate setae; carpus 3.7 L:W, 1x propodus, with one simple setae and blade-like spine, 0.3x propodus; propodus 6 L:W, with one serrate seta; unguis broken.

Pereopod-5 (Fig. 40F) basis 6.7 L:W, 5.6x merus; ischium with ventral seta; merus 3 L:W, 0.6x carpus, with one serrate seta; carpus 4.2 L:W, 0.9x propodus, one simple seta, one rod seta and one blade-like spine, 0.2x propodus, rod seta 0.4x propodus; propodus 5.7 L:W, 2.9x dactylus and unguis combined length, with two simple ventral setae and one dorsal serrate seta 0.7x propodus and microtrichia on ventral margin, dactylus 7x unguis.

Pereopod-6 (Fig. 40G) basis 5.8 L:W, 4.8x merus; merus 2.4 L:W, 0.5x carpus, with one serrate seta; carpus 4.2 L:W, 1.1x propodus, with one simple seta, one rod seta and one blade-like spine, 0.3x propodus, rod seta 0.3x propodus; propodus 5.7 L:W, 3.3x dactylus and unguis combined length, with two ventral and one serrate dorsal seta 0.9x propodus; dactylus 6x unguis.

Pleopods (Fig. 40H) exopod with seven and endopod with 10 plumose setae, respectively.

Uropod (Fig. 40I) peduncle 1.1 L:W, exopod with two articles; article-1 2.5 L:W, with seta; article-2 4.3 L:W, with two setae; endopod article-1 2.8 L:W, with one simple and two penicillate setae; article-2 3.7 L:W, with two penicillate and five simple setae. Exopod 0.8x endopod.

Distribution: *P. kobro* n. sp. is recorded from is known from the Belgium (GSR), German (BGR) and Interoceanmetal (IOM) licence areas of the Central Pacific.

Remarks: *Pseudotanais kobro* n. sp. can be distinguished from the other members of the 'spicatus' group by the presence of a thin, long spine on antenna article 2–3. Besides, the new species has wide mandible molar (being acuminate in *P. spicatus* and *P. tympanobaculum*) and it can be further distinguished from *P. spicatus* by having an endopod of uropod composed of two articles (one article in *P. spicatus*). Finally, *P. kobro* has a short, minute unguis on pereopod 5–6, differing it from the elongated unguis of *P. tympanobaculum*.

Identification keys to pseudotanaids found within the CCZ.

Key for Pseudotanaidae genera (modified from Bird & Holdich 1989 and McLelland 2008)

1. Pereopods 2 and 3 blade-like spine on carpus
   present (Fig. 16D)……2
   absent (see Larsen *et al.* (2012); Fig. 10C [34])……*Akanthinotanais*
2. Number of ventral setae on fixed finger (pollex) of chela
   one (Fig. 6A)……3
   two (see Bird & Holdich (1989); Fig. 23J [30])……*Parapseudotanais*
3. Inner margin of pollex (fixed finger)
   serrated (Fig. 6A)……4
   smooth (Fig. 16A)……*Pseudotanais*
4. Proportion of the length of pereonite-1 to 2 (S = < 0.4; L = > 0.75). Profile of the thick rod seta on antennular article-3, antennal article-6 and maxilliped palp article-4 (0 = absent; 1 = present)
   S-0-1-1 (see Jakiel *et al.* (2018); Fig. 5A,B,H [31])…… *Mystriocentrus*
   L-1-0-0 (Fig. 5A)…… *Beksitanais* n. gen.

Key for *Pseudotanais* morpho-groups

1. Forcipate chela
   present (Jakiel *et al.* (2015); Fig. 15A [35])……'forcipatus'
   absent (Fig. 16A)…….. 2
2. Uropod exopod
   short (≤½ endopod) (see Bird & Holdich (1989); Fig. 3H [30])……'colonus'
   long (>½ of endopod) (Fig. 16H)…… 3
3. Pereopod-1 merus seta
   long (≥½ of merus) (Fig. 16B)…….. 'affinis + longisetosus'
   short (≤½ of merus) (Fig. 35B)……4
4. Pereopod-5 and 6 unguis
   minute (Fig. 40F)…… 'spicatus' (*P. kobro* n. sp.)
   elongated (Fig. 30F)…… 'denticulatus + abathagastor'

Key to 'affinis + longisetosus' species

1. Pereopod-5 and 6 carpus dorsodistal seta
   short (0.3x propodus) (Fig. 25E)……2
   long (≥0.8x propodus) (Fig. 19E)…… 3
2. Pereopod-1 merus distal seta
   1x merus (Fig. 25B)…….. *P. geralti* n. sp.
   0.5x merus (Fig. 22B)…….. *P. yenneferae* n. sp.
3. Pereopod-1 basis
   few setae (1-3) (Fig. 11B)…… 4

many setae (5-6) (Fig. 16B) 5
4. Pereopod- 3 with blade-like spine
semilong (0.5x propodus) (Fig. 11D) ..... *P. uranos* n. sp.
long (≥0.6x propodus) (Fig. 13D) ..... *P. gaiea* n. sp.
5. Maxilliped endite
naked (Fig. 18F) ..... *P. romeo* n. sp.
with two tubercles (Fig. 15H) ..... *P. julietae* n. sp.

Key to 'denticulatus + abathagastor' species

1. Antenna article 2 and 3 with
spine (Fig. 34B) 2
seta (Fig. 37B) ..... *P. mariae* n. sp.
2. Uropod exopod length
≤1x endopod (Fig. 38I) 3
>1x endopod (Fig. 32H) 4
3. Mandible molar
wide (Fig. 26C) ..... *P. georgesande* n. sp.
acuminate (Fig. 29E) ..... *P. chopini* n. sp.
4. Pereopod-3 blade-like spine
short (0.3x propodus) (Fig. 32D) ..... *P. chaplini* n. sp.
long (0.6x propodus) (Fig. 35D) ..... *P. oloughlini* n. sp.

Discussion

The present study uncovered a significant diversity of pseudotanaids within the CCZ. A total of 15 new species are described here combining morphological and molecular data. Pseudotanaidae had been reported only once before from CCZ and without including any description[36]. This is also the first time pseudotanaids are studied using a DNA barcoding approach, with the only entry available in GenBank for this family being the histone 3 sequence from a *Pseudotanais* sp. collected in Crawl Key, Panama[27]. Another study on Pseudotanaidae from the North Atlantic reported a complex of cryptic species in four ecologically-diverse basins around Iceland[31], although the lack of genetic data prevented clear taxa delimitation. The wide geographic sampling carried out, combined with a reverse taxonomy approach, suggests that pseudotanaids might have comparatively narrow ranges (considering the entire study area), because most species were mainly limited to the closest stations. Potentially narrow ranges could also be inferred from the extensive tanaid collection made in Amundsen and Scotia Seas[29]. Deep-sea species are generally rare and sparsely distributed, so it is not surprising that each species in our study was represented by just a few individuals. The mechanisms maintaining the immense diversity but low abundances in the deep sea are hardly understood[29] and the low number of properly preserved individuals obtained, despite immense logistic efforts, hampers morphological and molecular studies of the abyssal fauna[37,38].

Resolving the presence of cryptic species is currently considered one of the main challenges for taxonomy[39–41]. Phenotypic plasticity and high sexual dimorphism may lead to misidentification of tanaidaceans[42,43] and lack of detailed morphological studies might obscure the real number of species and true diversity[44,45]. For example, dimorphic male and females of *Beksitanais apocalyptica* could be described for the first time here thanks to a DNA barcoding approach. *Beksitanais apocalyptica* is the only member of the genus described from the Pacific and the first for which molecular information is made available. The new genus is distinguished from the other Pseudotanaidae genera based on the following set of unique characters or character combination: Antennula article-3 with thickened rod seta; chela forcipate with serrate incisive margin, but propodus (palm) without small folds in distodorsal corner and pereopods 4-6 dactylus and unguis fused with a small hook on tip. Similarly, the separation of the known *Pseudotanais* species into the four groups proposed by Bird & Holdich[32] and Jakiel *et al*. namely, 'affinis', 'denticulatus', 'forcipatus' and 'longisetosus' was re-assessed here. Careful examination of the material from CCZ uncovered a close relationship between 'affinis' and 'longisetosus' and the presence of at least two more *Pseudotanais* species groups namely, 'abathagastor' and 'spicatus'. The recognition of these clades is supported by the setation pattern on pereopods 1, 5 and 6 and by the setal types on pereopods 2 and 3. The new 'spicatus' group can be characterized by very short blade-like spine in pereopod-2 and minute unguis in pereopods 5 and 6, whereas the 'abathagastor' group is distinguished by a combination of short setae on merus and carpus of pereopod 1, and by the presence of setae (not spines) on the antennal articles 2 and 3. The congruence observed for both morphological and molecular data suggests that *Pseudotanais* might in fact be formed by several complexes of cryptic species.

Discovering new taxa in a sample taken from any arbitrary chosen spot in the deep sea occurs quite frequently[46]. The deep-sea has traditionally been associated with a homogeneous environment, but state-of-the-art technologies proved that abyssal landscapes include different structures, such as seamounts, rises or fracture zones. This spatial heterogeneity is likely to impact the diversity and distribution of abyssal fauna, particularly for small epibenthic species[47]. The numerous asymmetric ridges, scarps, and elongate depressions at the Clarion facture zone can effectively limit dispersion and constitute geographical barriers, because none of the species collected from the APEI3 zone was found anywhere else. The Clarion Fracture Zone has been produced by seafloor spreading as the scar of transform faulting that began at least 80 million years ago and that is still continuing at present[48]. The patterns of magnetic intensity of the seafloor rocks in the studied area are displaced laterally, and rocks of the northern block are millions of years older than adjacent rocks south of the fracture zone[49]. Similarly, the elevated topography of the south-to-north ridge could be considered a remnant of an old east Pacific rise

(EPR), a sea-floor spreading center that was active approximately 30 mya. Our results suggest that physical barriers restrict the distribution of Pseudotanaidae species, promoting genetic differentiation and allopatric speciation. The sessile lifestyle of pseudotanaid females, which are generally found in self-constructed tubes, makes them particularly sensitive to geographic barriers[44].

Other environmental factors could explain the observed distribution of pseudotanaid taxa, and might be correlated with the CCZ deep sea landscape. There is mineralogical and chemical evidence for heterogenous sediment composition due to hydrothermal influence around the Clarion fracture zone between 113°W and 119°W. Similarly, nodules from pelagic clays found north of the Clarion fracture zone show higher Mn/Fe ratios[50]. Food availability might also affect the spatial distribution of diversity in the deep-sea[50], because only a small part of the particulate organic carbon (POC) from the euphotic zone will ever reach the ocean bottom[16]. Megafauna studies suggest higher abundance and diversity in the eastern part of CCZ, where POC availability is larger[37]. For example, Polychaeta family richness was found to be higher in the eastern IOM area than in the more western IFREMER region[43]. Nevertheless, the northernmost area studied here (APEI3) showed similar Pseudotanaidae abundances and species richness as the southeastern areas despite a gradual increase in POC flux. Finally, other factors such as the calcite compensation depth (CCD), which in the Pacific Ocean is about 4200–4500 metres, could also have an impact on the carapace-bearing crustaceans[16]. Further sampling within the CCZ would be essential to properly evaluate the relative importance of these factors on the observed distribution of deep-sea pseudotanaids.

The Clarion-Clipperton Zone remains the focus of international mining companies and faces a real danger of industrial exploitation, so recognizing its biological diversity and how it is structured are primary and critical steps preceding any potential anthropogenic activity[51,52]. A marginal understanding of deep-sea ecosystems utterly prevents an adequate assessment of the potential impact of mining operations on the marine environment[53]. Deep-sea expeditions are generally deprived of an opportunity for repeated sampling, being highly costly and burdened with logistic difficulties, so the large collection of pseudotanaids studied here is extremely valuable. The correlation observed between spatial features and species distribution has important implications for the establishment of protected areas, and the APEI3 area studied here would only protect one third of the total pseudotanaid species found in CCZ. It is possible that some species might have wider ranges than suggested by our current sampling, but this study represents an important first step in characterizing the diversity and distribution of pseudotanaids from the Tropical Eastern Pacific.

Material and Methods

Sampling. The European Joint Project Initiative – Oceans (JPI-O) 'Ecological Aspects of the Deep-Sea Mining' is a long-term intergovernmental initiative to assess the potential impact of deep sea mining using ecological and genetic techniques[54,55]. The marine expedition 'EcoResponse 2015' was organized to assess the genetic connectivity between populations from different CCZ areas. The biological material included in the present study was collected during SO-239 cruise, conducted on *RV Sonne*, from 10th March until 30th April 2015. Tanaidacean samples were taken from the Belgian, German and French license areas, but also from the APEI3 and Interoceanmetal (i.e. the consortium associating Bulgaria, Cuba, Czech Republic, Poland, Russian Federation and Slovakia). Thus, the areas surveyed include APEI3 (Areas of Particular Environmental Interest 3); BGR (Bundesanstalt fur Geowissenschalfen und Rofstoffe, Germany); IOM (Interoceanometal Joint Organisation); GSR (Global Sea Mineral Resources NV, Belgium) and IFREMER (France) (Table 1). An epibenthic sled (EBS) was used to collect material at each sampling site as in Brandt and Barthel[56]. Samples were sieved on board through a 300 µ mesh using cooled seawater and rapidly transferred to cold 96% EtOH. Fixed samples were stored at −20 °C until further processed. Detailed onboard and laboratory sample-processing procedures can be found in Rhiel[57].

Phylogenetic analyses. A single cheliped was taken using sterile needles as starting material for DNA extraction using the Chelex (InstaGene Matrix, Bio-Rad) method as in Palero *et al.*[58]. The COI gene was amplified using a 25 µL volume reaction containing 22 µL H_2O, 0.5 µL of each primer (10 pmol/µL) polyLCO and polyHCO[59,60] 1U of Illustra PuReTaq Ready−To−Go PCR Beads (GE Healthcare) and 2 µL of DNA template. The PCR protocol was 94 °C for 3 min, 40 cycles of 94 °C for 40 s, 42 °C for 30 s, 72 °C for 1 min, and a final elongation step of 72 °C for 10 min. A 2 µL aliquot of the PCR products was visualized in Midori Green-stained (Nippon Genetics) 1.5% agarose gels to verify PCR product quality and length. PCR purification and sequencing using forward and reverse primers was carried out by MACROGEN (Amsterdam, Netherlands). Consensus sequences were built using Geneious version 9.1.3 (www.geneious.com) and compared with the GenBank database using BLAST[61] to discard contamination from non-arthropod sources. Sequences were aligned using alignment option (L-INSi) of MAFFT[62] as implemented in Geneious. To improve reliability, we extracted conserved (ungapped) blocks of sequence from the alignment by using Gblocks server with default settings[63,64]. Selection of the best nucleotide substitution model was performed according to the BIC criterion as implemented in MEGA v7[58,65]. The aligned sequences and selected evolutionary model were used to estimate genetic distances and the corresponding Maximum Likelihood phylogenetic tree in MEGA. Initial trees for the heuristic search were obtained automatically by applying Neighbor-Join and BioNJ algorithms to a matrix of pairwise distances estimated using the Maximum Composite Likelihood (MCL) approach, and then selecting the topology with superior log likelihood value. Nodal support was assessed using 500 bootstrap replicates.

Spatial modelling and genetic gradients. A 3D-model of the deep sea landscape of the CCZ was built using the GeoElevationData function as implemented in the *Mathematica* v11.0 software package (Wolfram Inc., USA). GeoElevationData returns the elevation with respect to the geoid (=mean sea level) of a specified location. An array including the bathymetry for 12,231 different latitude longitude coordinates was built by uniformly

recording the mean sea level every 1/10th of a decimal degree in the rectangular area spanning from 11°N 116°W to 19°N 131°W. A contour-plot representing the array of mean sea level values and the location of the sampling sites was generated using the ListPlot and ListContourPlot functions in *Mathematica*. Names for particular structures, including fractures, seamounts and knolls, are taken from the General Bathymetric Chart of the Oceans (GEBCO) undersea feature Gazetteer (https://www.ngdc.noaa.gov/gazetteer/). The degree of association between geographic and genetic distances was measured using the Spearman rank correlation. This non-parametric correlation test was selected because it does not carry any assumptions about the distribution of the data. A standard isolation by distance (IBD) analysis was also carried out in *Mathematica* to further analyze the presence of a linear correlation between geographic and genetic distances.

Morphological analyses and species descriptions. Specimens were dissected with chemically-sharpened tungsten needles, and the dissected appendages slide-mounted using glycerine. Drawings were prepared using a light microscope (Nikon Eclipse 50*i*) equipped with a *camera lucida*. Digital drawings were obtained using a graphic tablet following Coleman[66]. Total body length (BL) was measured along the main axis of symmetry, from the frontal margin to the end of the telson. Body width (BW) was measured at the widest point along the main axis of symmetry. To simplify species descriptions, the expression '*N*x' replaces '*N* times as long as' and '*N* L:W' replaces '*N* times as long as wide'. The measurements were made with a camera connected to the microscope (Nikon Eclipse Ci-L) and NIS-Elements View software (www.nikoninstruments.com). The body width and the length of the carapace, pereonites, pleonites, and pleotelson were measured on whole specimens. The poor condition of individuals after DNA extraction or incompleteness even for well-preserved specimens, made the description of pereonite and pleonite setation not reliable. Therefore, this character was not included in the species description. The morphological terminology here follows Błażewicz-Paszkowycz *et al*. (2012)[67]. The unique blade-like spine of *Pseudotanais*, *Mystriocentrus* and *Parapseudotanais* species[67], is recognized as 'long' when is at least 0.6x propodus, 'semilong' when it is 0.5x propodus and 'short' when it is at most 0.3x the propodus. The type of sensory seta present on carpus of pereopod 4-6 is defined as rod seta (slightly inflated distally and with a pore) following[68] and[69]. This seta is recognized as 'long' when is at least 0.8x propodus, 'semilong' when it is 0.5x propodus and 'short when it is at most 0.25x propodus. Beside simple setae (=without ornamentation), at least four setae types are recognized here: (1) serrate – with serration or denticulation, (2) plumose – with any type of plumose or delicate setulae tufts distributed along the main axis, (3) penicillate – with a tuft of setules located distally and with a small knob on which a seta is fixed to the tegument and, (4) sensory – specified above.

Among the studied individuals: manca, neuter, and male stages were recognized. Specifically, the term 'manca' describes juveniles with or without buds of pereopod-6, respectively; 'mature (swimming) male'[30] refers to individuals with completely developed sexual dimorphic characters. 'Neuter' is retained for the stage developed from manca that cannot be classified as either female or juvenile male. The examined material will be deposited in "Senckenberg Research Institute and Natural History Museum" (Hamburg, Germany). Taxonomic descriptions and the corresponding identification key were prepared using the DELTA software (DEscription Language for TAxonomy)[44,66,70].

Received: 10 October 2018; Accepted: 1 October 2019;
Published online: 21 November 2019

References

1. Zeppilli, D., Pusceddu, A., Trincardi, F. & Danovaro, R. Seafloor heterogeneity influences the biodiversity-ecosystem functioning relationships in the deep sea. *Sci. Rep*., https://doi.org/10.1038/srep26352 (2016).
2. Kallimanis, A. S. *et al*. How does habitat diversity affect the species-area relationship? *Glob. Ecol. Biogeogr.* **17**, 532–538 (2008).
3. Buhl-Mortensen, L. *et al*. Biological structures as a source of habitat heterogeneity and biodiversity on the deep ocean margins. *Mar. Ecol.* **31**, 21–50 (2010).
4. Hessler, R. R. & Sanders, H. L. Faunal diversity in the deep-sea. *Deep Sea Res. Oceanogr. Abstr.* **14**, 65–78 (1967).
5. Smith, S. O. D. A. Evaluating stress in rocky shore and shallow reef habitats using the macrofauna of kelp holdfasts. *J. Aquat. Ecosyst. Stress Recover.* **7**, 259–272 (2000).
6. Pabis, K. & Sicinski, J. Polychaete fauna associated with holdfasts of the large brown alga *Himantothallus grandifolius* in Admiralty Bay, King George Island, Antarctic. *Polar Biol.* **33**, 1277–1288 (2010).
7. Tews, J. *et al*. Animal species diversity driven by habitat heterogeneity/diversity: The importance of keystone structures. *Journal of Biogeography* **31**, 79–92 (2004).
8. McClain, C. R., Nekola, J. C., Kuhnz, L. & Barry, J. P. Local-scale faunal turnover on the deep Pacific seafloor. *Mar. Ecol. Prog. Ser.* **422**, 193–200 (2011).
9. Mcclain, C. R. & Barry, J. P. Habitat heterogeneity, disturbance, and productivity work in concert to regulate biodiversity in deep submarine canyons. *Ecology* **91**, 964–976 (2010).
10. Durden, J. M., Bett, B. J., Jones, D. O. B., Huvenne, V. A. I. & Ruhl, H. A. Abyssal hills - hidden source of increased habitat heterogeneity, benthic megafaunal biomass and diversity in the deep sea. *Prog. Oceanogr.* **137**, 209–218 (2015).
11. Vanreusel, A., Hilario, A., Ribeiro, P. A., Menot, L. & Arbizu, P. M. Threatened by mining, polymetallic nodules are required to preserve abyssal epifauna. *Sci. Rep*. **6** (2016).
12. Uspenskaya, T. Y., Gorshkov, A. I. & Sivtsov, A. V. Mineralogy and Internal Structure of Fe-Mn Nodules from the Clarion-Clipperton Fracture Zone. *Int. Geol. Rev.* **29**, 363–371 (1987).
13. Duliu, O. G., Alexe, V., Moutte, J. & Szobotca, S. A. Major and trace element distributions in manganese nodules and micronodules as well as abyssal clay from the Clarion-Clipperton abyssal plain, Northeast Pacific. *Geo-Marine Lett.* **29**, 71–83 (2009).
14. Hein, J. R., Mizell, K., Koschinsky, A. & Conrad, T. A. Deep-ocean mineral deposits as a source of critical metals for high- and green-technology applications: Comparison with land-based resources. *Ore Geol. Rev.* **51**, 1–14 (2013).
15. Wedding, L. M. *et al*. Managing mining of the deep seabed. *Science (80-.).* **349**, 144–145 (2015).
16. Smith, C. R., De Leo, F. C., Bernardino, A. F., Sweetman, A. K. & Arbizu, P. M. Abyssal food limitation, ecosystem structure and climate change. *Trends Ecol. Evol.* **23**, 518–528 (2008).
17. Ramirez-Llodra, E. *et al*. Deep, diverse and definitely different: Unique attributes of the world's largest ecosystem. *Biogeosciences* **7**, 2851–2899 (2010).

18. Thiel, H. Evaluation of the environmental consequences of polymetallic nodule mining based on the results of the TUSCH Research Association. *Deep. Res. Part II Top. Stud. Oceanogr.* **48**, 3433–3452 (2001).
19. Vopel, K. & Thiel, H. Abyssal nematode assemblages in physically disturbed and adjacent sites of the eastern equatorial Pacific. *Deep. Res. Part II Top. Stud. Oceanogr.* **48**, 3795–3808 (2001).
20. De Smet, B. *et al*. The Community Structure of Deep-Sea Macrofauna Associated with Polymetallic Nodules in the Eastern Part of the Clarion-Clipperton Fracture Zone. *Front. Mar. Sci.* **4** (2017).
21. Appeltans, W. *et al*. The magnitude of global marine species diversity. *Curr. Biol.* **22**, 2189–2202 (2012).
22. Blazewicz-Paszkowycz, M., Bamber, R. & Anderson, G. Diversity of Tanaidacea (Crustacea: Peracarida) in the World's Oceans – How Far Have We Come? *PLoS One* **7**, e33068 (2012).
23. Bamber, R. N. The tanaidaceans (Arthropoda: Crustacea: Peracarida: Tanaidacea) of Esperance, Western Australia, Australia. in *In: Wells, F. E., Walker, D. I. & Kendrick, G. A. (eds) 2005. The Marine Flora and Fauna of Esperance, Western Australia. Western Australian Museum, Perth* (eds Wells, F. E., Walker, D. I. & Kendrick, G.) **1963**, 613–728 (Western Australian Museum, 2005).
24. Larsen, K. Morphological and molecular investigation of polymorphism and cryptic species in tanaid crustaceans: Implications for tanaid systematics and biodiversity estimates. *Zool. J. Linn. Soc.* **131**, 353–379 (2001).
25. Palero, F., Robainas-Barcia, A., Corbari, L. & Macpherson, E. Phylogeny and evolution of shallow-water squat lobsters (Decapoda, Galatheoidea) from the Indo-Pacific. *Zool. Scr.* **46**, 584–595 (2017).
26. Held, C. & Wägele, J. W. Cryptic speciation in the giant Antarctic isopod *Glyptonotus antarcticus* (Isopoda, Valvifera, Chaetiliidae). *Sci. Mar.* **69**, 175–181 (2008).
27. Drumm, D. T. Phylogenetic Relationships of Tanaidacea (Eumalacostraca: Peracarida) Inferred from Three Molecular Loci. *Journal of Crustacean Biology* **30**, 692–698 (2010).
28. Pabis, K., Jóźwiak, P., Lörz, A. N., Schnabel, K. & Błażewicz-Paszkowycz, M. First insights into the deep-sea tanaidacean fauna of the Ross Sea: species richness and composition across the shelf break, slope and abyss. *Polar Biol.* **38**, 1429–1437 (2015).
29. Pabis, K., Błażewicz-Paszkowycz, M., Jóźwiak, P. & Barnes, D. K. A. Tanaidacea of the Amundsen and Scotia seas: An unexplored diversity. *Antarct. Sci.* **27**, 19–30 (2014).
30. Bird, G. J. & Holdich, D. M. Tanaidacea (Crustacea) of the northeast Atlantic: the subfamily Pseudotanainae (Pseudotanaidae) and the family Nototanaidae. *Zool. J. Linn. Soc.* **97**, 233–298 (1989).
31. Jakiel, A., Stępień, A. & Błażewicz, M. A tip of the iceberg—Pseudotanaidae (Tanaidacea) diversity in the North Atlantic. *Mar. Biodivers.* **48**, 859–895 (2018).
32. Bird, G. J. & Holdich, D. M. Tanaidacea (Crustacea) of the north-east Atlantic: the subfamily Pseudotanainae (Pseudotanaidae) and the family Nototanaidae. *Zool. J. Linn. Soc.* **97**, 233–298 (1989).
33. Kudinova-Pasternak, R. K. Tanaidacea (Crustacea, Malacostraca) from the deep-sea trenches of the western part of the Pacific. *Tr. Instituta Okeanol. Akad. Nauk SSSR* **108**, 115–135 (1978).
34. Larsen, K., Nagaoka, R. & Froufe, E. Tanaidacea (Crustacea) from Macaronesia III. The shallow-water Tanaidomorpha from the Cape Verde archipelago. *Zootaxa* **3498**, 24–44 (2012).
35. Jakiel, A., Stępie ń, A., Jóźwiak, P., Serigstad, B. & Błażewicz-Paszkowycz, M. First record of tanaidacea (Crustacea) from a deep-sea coral reef in the Gulf of Guinea. *Zootaxa*, **3995**(1), 203–228, https://doi.org/10.11646/zootaxa.3995.1.18 (2015).
36. Wilson, G. D. F. Crustacean communities of the manganese nodule province (Domes Site A compared with Domes site C). *Rep. Natl. Ocanic.* **0030**, 1–43 (1987).
37. Woolley, S. N. C. *et al*. Deep-sea diversity patterns are shaped by energy availability. *Nature* **533**, 393–396 (2016).
38. Danovaro, R., Snelgrove, P. V. R. & Tyler, P. Challenging the paradigms of deep-sea ecology. *Trends Ecol. Evol.* **29**, 465–475 (2014).
39. Snelgrove, P. *Ecosystems of the Deep Oceans (Ecosystems of the World 28). Eos, Transactions American Geophysical Union* 84, (Elsevier, 2006).
40. Jennings, R. M., Brix, S., Bober, S., Svavarsson, J. & Driskell, A. More diverse than expected: distributional patterns of *Oecidiobranchus* Hessler, 1970 (Isopoda, Asellota) on the Greenland-Iceland-Faeroe Ridge based on molecular markers. *Mar. Biodivers.* **48**, 845–857 (2018).
41. Gubili, C. *et al*. Species diversity in the cryptic abyssal holothurian *Psychropotes longicauda* (Echinodermata). *Deep. Res. Part II Top. Stud. Oceanogr.* **137**, 288–296 (2017).
42. Havermans, C. *et al*. Genetic and Morphological Divergences in the Cosmopolitan Deep-Sea Amphipod *Eurythenes gryllus* Reveal a Diverse Abyss and a Bipolar Species. *PLoS One* **8** (2013).
43. Amon, D. J. *et al*. Insights into the abundance and diversity of abyssal megafauna in a polymetallic-nodule region in the eastern Clarion-Clipperton Zone. *Sci. Rep.* **6**, 1–12 (2016).
44. Błażewicz-Paszkowycz, M., Jennings, R. M., Jeskulke, K. & Brix, S. Discovery of swimming males of Paratanaoidea (Tanaidacea). *Polish Polar Res.* **35**, 415–453 (2014).
45. Vrijenhoek, R. C. Cryptic species, phenotypic plasticity, and complex life histories: Assessing deep-sea faunal diversity with molecular markers. *Deep. Res. Part II Top. Stud. Oceanogr.* **56**, 1713–1723 (2009).
46. Juan, C., Van Rooij, D. & De Bruycker, W. An assessment of bottom current controlled sedimentation in Pacific Ocean abyssal environments. *Mar. Geol.* **403**, 20–33 (2018).
47. Brandt, A. *et al*. Deep-sea isopod biodiversity, abundance, and endemism in the Atlantic sector of the Southern Ocean-Results from the ANDEEP I-III expeditions. *Deep. Res. Part II Top. Stud. Oceanogr.* **54**, 1760–1775 (2007).
48. Riehl, T., Lins, L. & Brandt, A. The effects of depth, distance, and the Mid-Atlantic Ridge on genetic differentiation of abyssal and hadal isopods (Macrostylidae). *Deep. Res. Part II Top. Stud. Oceanogr*, https://doi.org/10.1016/j.dsr2.2017.10.005 (2018).
49. Müller, R. D., Sdrolias, M., Gaina, C. & Roest, W. R. Age, spreading rates, and spreading asymmetry of the world's ocean crust. *Geochemistry, Geophys. Geosystems* **9**, Q04006 (2008).
50. Skornyakova, N. S. Zonal Regularities in Occurrence, Morphology and Chemistry of Manganese Nodules of the Pacific Ocean. in *Marine Geology and Oceanography of the Pacific Manganese Nodule Province* 699–727 (Springer US), https://doi.org/10.1007/978-1-4684-3518-4_21 (2012).
51. Błażewicz-Paszkowycz, M., Pabis, K. & Jóźwiak, P. Tanaidacean fauna of the Kuril-Kamchatka Trench and adjacent abyssal plain - abundance, diversity and rare species. *Deep. Res. Part II Top. Stud. Oceanogr.* **111**, 325–332 (2015).
52. Jamieson, A. J., Fujii, T., Mayor, D. J., Solan, M. & Priede, I. G. Hadal trenches: the ecology of the deepest places on Earth. *Trends in Ecology and Evolution* **25**, 190–197 (2010).
53. Beaulieu, S. E., Graedel, T. E. & Hannington, M. D. Should we mine the deep seafloor? *Earth's Futur.* **5**, 655–658 (2017).
54. Barbier, E. B. *et al*. Ecology: Protect the deep sea. *Nature* **505**, 475–477 (2014).
55. So-, R. V. S. C. Chief Scientist: Pedro Martínez Arbizu Captain: Lutz Mallon. (2015).
56. Brandt, A. & Barthel, D. An improved supra- and epibenthic sledge for catching peracarida (Crustacea, malacostraca). *Ophelia* **43**, 15–23 (1995).
57. Riehl, T. *et al*. Field and laboratory methods for DNA studies on deep-sea isopod crustaceans. *Polish Polar Res.* **35**, 203–224 (2014).
58. Palero, F., Guerao, G. & Abelló, P. Morphology of the final stage phyllosoma larva of *Scyllarus pygmaeus* (Crustacea: Decapoda: Scyllaridae), identified by DNA analysis. *J. Plankton Res.* **30**, 483–488 (2008).
59. Palero, F. *et al*. DNA extraction from formalin-fixed tissue: new light from the Deep-Sea. *Sci. Mar.* **74**, 465–470 (2010).
60. Carr, C. M., Hardy, S. M., Brown, T. M., Macdonald, T. A. & Hebert, P. D. N. A tri-oceanic perspective: DNA barcoding reveals geographic structure and cryptic diversity in Canadian polychaetes. *PLoS One* **6**, e22232 (2011).

61. Altschul, S. F., Gish, W., Miller, W., Myers, E. & Lipman, D. J. Basic local alignment search tool. *J. Mol. Biol.* **215**, 403–410 (1990).
62. Katoh, K. & Standley, D. M. MAFFT multiple sequence alignment software version 7: Improvements in performance and usability. *Mol. Biol. Evol.* **30**, 772–780 (2013).
63. Talavera, G. & Castresana, J. Improvement of phylogenies after removing divergent and ambiguously aligned blocks from protein sequence alignments. *Syst. Biol.* **56**, 564–577 (2007).
64. Castresana, J. Selection of conserved blocks from multiple alignments for their use in phylogenetic analysis. *Mol. Biol. Evol.* **17**, 540–552 (2000).
65. Kumar, S., Stecher, G. & Tamura, K. MEGA7: Molecular Evolutionary Genetics Analysis version 7.0 for bigger datasets. *Mol. Biol. Evol.* msw054, https://doi.org/10.1093/molbev/msw054 (2016).
66. Coleman, C. O. Digital inking: How to make perfect line drawings on computers. *Org. Divers. Evol.* **3**, 303–304 (2003).
67. Błażewicz-Paszkowycz, M. & Bamber, R. N. The Shallow-water Tanaidacea (Arthropoda: Malacostraca: Peracarida) of the Bass Strait, Victoria, Australia (other than the Tanaidae). *Mem. Museum Victoria* **69**, 1–235 (2012).
68. Thomas, W. J. The setae of *Austropotamobius pallipes* (Crustacea: Astacidae). *J. Zool.* **160**, 91–142 (1970).
69. Garm, A. Revising the definition of the crustacean seta and setal classification systems based on examinations of the mouthpart setae of seven species of decapods. *Zool. J. Linn. Soc.* **142**, 233–252 (2004).
70. M. J. Dallwitz, A Flexible Computer Program for Generating Identification Keys. *Systematic Biology* **23**(1), 50–57 (1974).

Acknowledgements

This study was conducted in the framework of the Joint Programming Initiative Healthy and Productive Seas and Oceans (JPI Oceans) project "Ecological Aspects of Deep-sea Mining" within a project 'EcoResponse Assessing the Ecology, Connectivity and Resilience of Polymetallic Nodule Field Systems'. The authors would like to express their thanks to Prof. Dr. Pedro Martínez Arbizu (Senckenberg, Germany) and all members of SO-239 cruise for great cooperation during and after the expedition, and for a help in collecting EBS samples. Special thanks are to Dr. Brigida (Brydzia) Wawrzyniak-Wydrowska (University of Szczecin, Poland), for her tireless help in sorting samples onboard and to Sahar Kodami (Senckenberg, Germany) for her assistance in DNA extractions during the cruise. This study was funded by the Polish National Science grant UMO-2016/13/B/NZ8/02495.

Author contributions

M.B. conceived the project; A.J. carried out the DNA lab work and completed species descriptions and drawings; F.P. analyzed the molecular and bathymetry data; A.J., M.B. and F.P. wrote the paper; and all the authors reviewed the manuscript.

Competing interests

The authors declare no competing interests.

Additional information

Correspondence and requests for materials should be addressed to F.P.

Reprints and permissions information is available at www.nature.com/reprints.

Publisher's note Springer Nature remains neutral with regard to jurisdictional claims in published maps and institutional affiliations.

5 January 2020

STATEMENT

In agreement with all co-authors of the publication entitled:

Deep ocean seascape and Pseudotanaidae (Crustacea: Tanaidacea) diversity at the Clarion-Clipperton Fracture Zone

published in *Scientific Report*

(2019) 9:17305. doi: https://doi.org/10.1038/s41598-019-51434-z

I declare that my contribution in this work is:

author	Contribution (%)	signature
Jakiel Aleksandra	40	
Ferran Palero	30	
Błażewicz Magdalena	30	

Chapter 4: Secrets from the deep: Pseudotanaidae (Crustacea: Tanaidacea) diversity from the Kuril–Kamchatka Trench

Contents lists available at ScienceDirect

Progress in Oceanography

journal homepage: http://ees.elsevier.com

Secrets from the deep: Pseudotanaidae (Crustacea: Tanaidacea) diversity from the Kuril–Kamchatka Trench☆

Aleksandra Jakiel [a,1], Ferran Palero [a,b,c,d,1,*], Magdalena Błażewicz [a]

[a] Department of Invertebrate Zoology and Hydrobiology, Faculty of Biology and Environmental Protection, University of Lodz, ul. Banacha 12/16, 90-237 Łódź, Poland
[b] Centre d'Estudis Avançats de Blanes (CEAB-CSIC), Carrer d'accés a la Cala Sant Francesc 14, 17300 Blanes, Spain
[c] Associate Researcher, Department of Life Sciences, The Natural History Museum, Cromwell Road, London SW7 5BD, UK
[d] Cavanilles Institute of Biodiversity and Evolutionary Biology, University of Valencia, Paterna, Spain

ARTICLE INFO

Keywords
Tanaidacea
DNA barcoding
Deep sea
Integrative taxonomy

ABSTRACT

A combination of morphological and genetic data (subunit I of the cytochrome *c* oxidase: COX1) was used to study the diversity and distribution of pseudotanaids in the Kuril-Kamchatka Trench and adjacent abyssal plain. Our results uncovered the presence of an undescribed species of *Mystriocentrus* (*M. hollandae*) and five new species of *Pseudotanais* (*P. chanelae, P. monroeae, P. curieae, P. szymborskae* and *P. locueloae*). The most abundant species was *P. curieae* (N = 182), followed by *P. monroeae* (N = 34), *P. szymborskae* (N = 31) and *P. chanelae* (N = 20). The number of individuals sampled was highest in shallower stations, but all four taxa could be found across the studied bathymetric range (4800–5500 m). Pseudotanaid abundance and bottom currents appear to be inversely related, which might be due to lower currents favouring sedimentation and, consequently, successful settlement of tanaids. Results are compared with previous studies on peracarid crustaceans from the Northwestern Pacific.

1. Introduction

In terms of small peracarid crustacea, the NW Pacific Ocean abyssal plain is one of the richest and more densely populated deep-sea regions of the world (Błażewicz-Paszkowycz et al., 2015; Brandt et al., 2019; Golovan et al., 2019). The Kuril-Kamchatka Trench (KKT) is a submarine ditch that belongs to the Ring of Fire or circum-Pacific belt, a nearly continuous series of oceanic trenches and volcanic arcs. Extending with NE-SW direction for ~3000 km, the KKT has a maximum depth of over 10,000 m and covers an area of 264,000 km^2 (Cadet et al., 1987). Sedimentation within this large area is determined by tectonic and volcanic processes, the peripheral position of the Kuril island arc, as well as the hydrographic regime and high biological productivity. The macrobenthos composition on the abyssal plain of the Northwest Pacific Basin adjacent to the KKT was intensively studied during the KuramBio expedition in 2012 (Kuril-Kamchatka Biodiversity Studies), with samples obtained at depths between 4830 and 5780 m (Brandt and Malyutina, 2015). Almost 2000 invertebrate taxa were collected, and this number is continuing to increase, as material from several taxa is still being processed. The diversity of tanaidaceans of the KKT studied by world-leading experts is high, particularly after the well-known R/V Vitjaz expedition (Kudinova-Pasternak, 1970), and the Japanese KH-01-2 expedition (Larsen and Shimomura, 2007). More tanaid species are known from Japan and KKT than have been recorded in the entire North Atlantic and, according to previous authors, trenches have yet to give up their last secrets (Larsen and Shimomura, 2007; Stępień et al., 2019).

The NW Pacific is a particularly interesting area for studying the Pseudotanaidae family, a frequent and diverse element of deep-sea benthic assemblages, only exceeded by polychaetes (Pabis et al., 2015, 2014). Pseudotanaids are inhabitants of abyssal plains, trenches (Kudinova-Pasternak, 1966), seamounts (Jakiel et al. 2015), shallow waters (Bamber et al., 2009) or caves (García-Herrero et al., 2019). The family comprises four genera (*Akanthinotanais* Sieg 1976, *Mystriocentrus* Bird & Holdich 1989, *Parapseudotanais* Bird & Holdich 1989 and *Pseudotanais* Sars 1882), and from ~70 pseudotanaid species described to date, eight are reported from NW Pacific waters. Six of those species seem to be restricted to the Kuril–Kamchatka area (i.e. *Pseudotanais abathogastor* Błażewicz-Paszkowycz et al., 2013; P. *inflatus* Kudinova-Pasternak, 1973; P. *intortus* Błażewicz-

☆ This article is registered in ZooBank under: **ZooBank number** urn:lsid:zoobank.org:pub:5699EBFA-7805-45E6-98CE-905107485033.

* Corresponding author at: Department of Invertebrate Zoology and Hydrobiology, Faculty of Biology and Environmental Protection, University of Lodz, ul. Banacha 12/16, 90-237 Łódź, Poland.
E-mail address: Ferran.Palero@nhm.ac.uk (F. Palero)

[1] Both authors contributed equally to this work.

https://doi.org/10.1016/j.pocean.2020.102288

Available online xxx
0079-6611/

Paszkowycz et al., 2013; P. *soja* Błażewicz-Paszkowycz et al., 2013; P. *nipponicus* McLelland, 2007; P. *vitjazi* Kudinova-Pasternak, 1966; see WoRMS 2018). Two other taxa were reported by Kudinova-Pasternak from the KKT area (*P. affinis* Hansen, 1887; *P. nordenskioldi* Sieg, 1977), but they are unlikely because these species originally described from the Atlantic Ocean. Within the KKT zone, half of the species are found in comparatively shallow waters, around 400–1300 m depth (*Pseudotanais abathogastor, P. intortus* and *P. soja*), and the other half are found below 3000 m (*P. nipponicus*, *P. vitjazi* and *P. inflatus*) (Błażewicz-Paszkowycz et al., 2013).

The present study was designed to characterize the diversity and distribution of pseudotanaids in the Kuril–Kamchatka region. The mitochondrial gene coding for the subunit I of the cytochrome *c* oxidase was selected to identify different taxonomical units. A combination of morphological and molecular genetic data uncovered the presence of five new species of *Pseudotanais* and a new species of *Mystriocentrus,* which is the first representative of this genus in the Pacific Ocean. The abundance, spatial and bathymetric distribution of pseudotanaids are compared against previous studies on peracarid crustaceans from the NW Pacific. Additionally, an identification key for *Pseudotanais* species present in the NW Pacific is included as well.

2. Material and methods

2.1. Sampling during the Kuril-Kamchatka Biodiversity studies

The tanaidacean materials for this study were collected on the KKT area during the German–Russian deep-sea expedition KuramBIO (Kuril-Kamchatka Biodiversity Studies), carried out from July to September of 2012 on board of RV *Sonne* (Brandt et al. 2015). Sampling stations were distributed along the abyssal plain next to the Kuril Islands archipelago between 4800 m and 5800 m depth (Fig. 1). An epibenthic sledge (EBS) was used to collect material at each sampling site as in Brandt and Barthel (1995). Additionally, environmental data (i.e. temperature, preassure, salinity, oxygen saturation and conductivity) were measured at each station using a CTD probe. Samples were washed with cold seawater on 300 μm mesh, fixed in pre-cooled 96% EtOH, and stored at −20 °C. Detailed on board and laboratory sample-processing procedures were described by Rhiel et al. (2014).

2.2. Phylogenetic and genetic distance analyses

A whole specimen was taken using sterile needles as starting material for DNA extraction using the Chelex (InstaGene Matrix, Bio-Rad) method as in Palero et al. (2010a). The cytochrome *c* oxidase I (COX1) gene was amplified using a 25 μL volume reaction containing 22 μL H_2O, 0.5 μL of each primer (10 pmol/μL) polyLCO and polyHCO (Carr et al., 2011), 1U of Illustra PuReTaq Ready – To – Go PCR Beads (GE Healthcare) and 2 μL of DNA template. The PCR protocol was 94 °C for 3 min, 40 cycles of 94 °C for 40 s, 42 °C for 30 s, 72 °C for 1 min, and a final elongation step of 72 °C for 10 min. A 2 μL aliquot of the PCR products was visualized in Midori Green-stained (Nippon Genetics) 1.5% agarose gels to verify PCR product quality and length. PCR purification and sequencing using forward and reverse primers was carried out by MACROGEN (Amsterdam, Netherlands). Consensus sequences were built using Geneious version 9.1.3 (www.geneious.com) and compared with the GenBank database using BLAST (Altschul et al., 1990) to discard contamination from non-arthropod sources. Sequences were aligned using MAFFT (Katoh and Standley, 2013) as implemented in Geneious. To improve reliability, we extracted conserved (ungapped) blocks of sequence from the alignment by using Gblocks server with default settings (Castresana, 2000; Talavera and Castresana, 2007). Selection of the best nucleotide substitution model was performed according to the AICc and BIC criteria as implemented in MEGA v7 (Kumar et al., 2016). The aligned se-

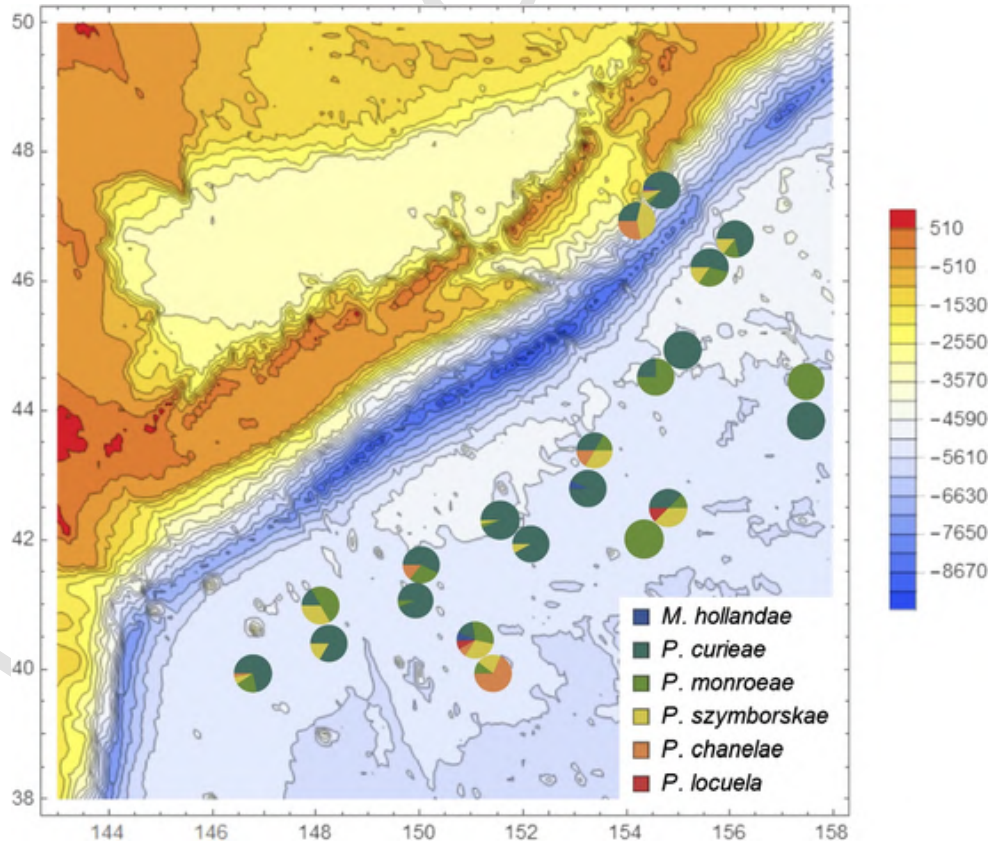

Fig. 1. Contour plot showing the bathymetry of the studied area and the spatial distribution of the newly described Pseudotanaidae.

quences and selected evolutionary model were used to estimate genetic distances and the corresponding Maximum Likelihood phylogenetic tree in RAxML v8.0.22 (Stamatakis, 2014). Nodal support was assessed using 500 bootstrap replicates. Patristic distances (i.e., sum of the length of all branches connecting two lineages in an evolutionary tree) were estimated using Geneious version 9.1.3 (www.geneious.com).

2.3. Morphological analyses and species description

All 273 individuals were morphologically identified using a microscope (Nikon Eclipse 50*i*). After distinguishing morphospecies, the best-preserved specimens were selected as holotypes and paratypes. Paratypes selected for drawing were dissected with chemically-sharpened tungsten needles, and dissected appendages were mounted on slides using glycerine. Drawings were prepared using a light microscope equipped with a *camera lucida*. Digital drawings were obtained using a graphic tablet following Coleman (2003). Total body length (BL) was measured along the main axis of symmetry, from frontal margin to end of telson. Body width (BW) was measured at the widest point along the main axis. To simplify species descriptions, the expression '*N*x' replaces '*N* times as long as' and '*N* L:W' replaces '*N* times as long as wide'. The measurements were made with a camera connected to the microscope (Nikon Eclipse Ci-L) and using the NIS-Elements View software (www.nikoninstruments.com). Body width and length of carapace, pereonites, pleonites, and pleotelson were measured on whole specimens. The length was measured along the axis of symmetry, whereas the width, perpendicular to the axis of symmetry, was measured at the widest point. The morphological terminology follows Bird and Holdich (1989), Błażewicz-Paszkowycz et al. (2013) and Błażewicz-Paszkowycz and Bamber (2012). The unique blade-like spine of *Pseudotanais* and *Parapseudotanais* is recognized as 'long' when it is at least 0.6x propodus, 'semilong' when it is 0.5x propodus and 'short' when it is at most 0.3x propodus. The sensory seta occurring on carpus of pereopod 4–6 is defined as "rod seta" following Thomas (1970) and Garm (2004) because it is a simple seta slightly inflated distally and with a pore. This rod seta is recognized here as 'long' when it is at least 0.8x propodus, 'semilong' when it is 0.5x propodus and 'short' when it is at most 0.25x propodus. Four setae types are recognized besides simple setae (=without ornamentation): (1) serrate – with serration or denticulation, (2) plumose – with any type of plumose or delicate setulae tufts distributed along the main axis, (3) penicillate – with a tuft of setules located distally and with a small knob on which a seta is fixed to the tegument and, (4) rod setae – slightly inflated distally and with a pore. Taxonomic descriptions and the corresponding identification key were prepared using Delta software (DEscription Language for TAxonomy) (Dallwitz et al., 1993). The examined material was deposited in Senckenberg Research Institute and Natural History Museum (Hamburg, Germany) with the museum codes presented in Table S1.

3. Results

3.1. Pseudotanaidae diversity and spatial and bathymetric distribution

A total of 273 individuals were used for molecular analyses, but only 68 provided positive DNA barcoding results, being assigned to eight distinct haplotypes (Table 1). These haplotypes correspond to two genera and six species in total, one *Mystriocentrus* and five *Pseudotanais* species. All of them are new to science and their description is given in the Appendix A. *Pseudotanais curieae* n. sp., with a total of 182 specimens, was the most abundant and widespread species and it was found at 86% of the surveyed stations (18 out of 21) (Table 1; Fig. 1). Other taxa, like *P. monroeae* n. sp. (N = 34), *P. szymborskae* n. sp. (N = 31) and *P. chanelae* n. sp. (N = 20) were less abundant, and found on 15, 13 and 7 stations respectively. The number of individuals was highest in shallower stations (Table 1; Fig. 2), but some taxa were most abundant below 5300 m. The four taxa were present across the bathymetric range studied (4800–5700 m), but the proportion of *Pseudotanais curieae* individuals decreased with increasing depth whereas *P. chanelae* became more frequent. Given their low abundances and therefore limited distribution, no clear pattern can be observed for *Mystriocentrus hollandae* n. sp. (N = 4) or. *Pseudotanais locueloae* n. sp. (N = 2)

3.2. Phylogenetic and genetic distance analyses

Eight different COX1 haplotypes were obtained, representing five *Pseudotanais* species and one *Mystriocentrus* species (Genbank accession numbers: XXXX-XXXX). The sequence alignment spanned 572 bp after running Gblocks. Haplotypes for *Pseudotanais monroeae, P. locueloae, P. curieae* and *P. chanelae* had 572 bp, while *P. szymborskae* (534 bp) and *Mystriocentrus hollandae* (529 bp) were slightly shorter. The General Time Reversible (GTR + *G* + *I*) model showed the lowest AICc (16282.62) and BIC (16775.88) scores and it is considered the best description of the substitution pattern. A larger proportion of transitions over transversions was observed (R = 1.64). Non-uniformity of evolutionary rates among sites was modelled using a Gamma distribution (+*G* = 1.23). The rate variation model allowed for some positions to be evolutionarily invariable (+*I* = 25.07% sites). The Maximum Likelihood tree with the highest log likelihood value (lnL = -8076.02) is shown in Fig. 3. Pseudotanaid species formed a well-supported clade, with all *Pseudotanais* species except *P. locueloae* grouping together. This clustering of COX1 sequences in the ML tree corresponds to the morphological identification of taxa (see comments on the morphology section below). Pairwise COX1 patristic distances between all the pseudotanaid specimens ranged between 0.035 and 1.416, while K2P distances between species ranged from 0.202 ± 0.023 to 0.587 ± 0.054 (Table S2). Net evolutionary divergences over sequence pairs were largest between *Mystriocentrus hollandae* and any *Pseudotanais* species. In agreement with the phylogenetic reconstruction result, *P. locueloae* showed the largest divergences within the *Pseudotanais* clade and is clearly distinct from the other species collected in the KKT area. Estimates of average evolutionary divergence over sequence pairs within *Pseudotanais* species showed comparatively high divergences (compared with other crustacean groups; see Discussion) and the lowest divergences were observed between *P. curieae* and *P. szymborskae* (0.202 ± 0.023). Finally, intraspecific genetic variation was very low, as expected given the limited sample size per species, and only *P. monroeae* showed several haplotypes.

3.3. Morphological analyses and species descriptions

A detailed morphological description of each new pseudotanaid taxon is presented in the Appendix A and only a short account of the morphology results is presented here. Within the material sampled during KuramBIO, the most abundant and diverse taxa belong to a single morphogroup. Four *Pseudotanais* species (*Pseudotanais curieae, P. szymborskae, P. chanelae* and *P. monroeae*) show a long or semilong blade-like spine on carpus of pereopods 2–3 or long rod seta on carpus of pereopods 5–6 and they can be assigned to the 'affinis + longisetosus' morphogroup. The fifth species (*P. locueloae*) can be distinguished from members of the 'affinis + longisetosus' clade by the slender cheliped, no seta on merus of pereopod-1, elongate propodus of pereopods 1–3 and short rod seta on pereopods 4–6, being classified in the 'denticulatus + abathagastor' morphogroup.

Key for NW Pacific *Pseudotanais* species (modified from Bird and Holdich (1989) and Jakiel et al. (2018)):

Table 1
Pseudotanaidae species abundance on the KuramBIO stations surveyed. N = Total number of specimens.

Station	Latitude	Longitude	Depth range	Trawling distance (m)	*Bottom current*	*M. hollandae*	*P. curieae*	*P. monroeae*	*P. szymborskae*	*P. chanelae*	*P. locueloae*	N
4–3	46°58.34′	154°33.03′	5681–5780	1574	3.5 ± 1.7	0	2	0	3	2	0	7
1–10	43°58.35′	157°18.23′	5418–5429	2222	7.4 ± 1.8	0	0	1	0	0	0	1
1–11	43°58.44′	157°18.29′	5412–5418	2161	4.3 ± 1.6	0	2	0	0	0	0	2
9–9	40°34.51′	150°59.92′	5399–5408	2315	3.3 ± 3.2	0	0	2	4	13	0	19
9–12	40°34.49′	150°59.85′	5392–5397	2377	2.3 ± 1.7	1	2	4	4	1	1	13
5–9	43°34.46′	153°58.13′	5376–5379	2469	3.1 ± 0.8	0	1	0	0	0	0	1
5–10	43°34.44′	153°58.06′	5375–5379	2624	3.8 ± 1.7	0	1	3	0	0	0	4
11–9	40°12.49′	148°05.40′	5362–5362	2408	12.4 ± 18.8	0	1	3	2	0	0	6
11–12	40°12.32′	148°05.73′	5348–5351	2346	11.2 ± 9.9	0	5	0	1	0	0	6
6–12	42°28.49′	153°59.54′	5291–5307	2562	4.4 ± 3.2	0	0	2	0	0	0	2
6–11	42°28.61′	153°59.68′	5291–5305	2624	6.2 ± 6.5	0	3	1	3	0	1	8
10–9	41°11.37′	150°05.63′	5248–5265	2778	5.5 ± 2.6	0	4	2	0	1	0	7
10–12	41°12.80′	150°6.162′	5249–5262	2778	3.7 ± 2	0	16	1	0	0	0	17
12–4	39°42.78′	147°09.55′	5215–5228	2716	5 ± 2.8	0	23	6	2	1	0	32
7–9	43°01.78′	152°58.61′	5216–5223	2994	2.3 ± 1.2	0	2	1	2	1	0	6
7–10	43°01.82′	152°58.55′	5218–5221	2624	4 ± 2.5	1	13	0	0	0	0	14
8–9	42°14.32′	151°42.68′	5125–5140	2840	3.3 ± 1.3	0	29	1	1	0	0	31
8–12	42°14.38′	151°43.12′	5115–5124	2408	2.6 ± 2	0	23	0	2	0	0	25
2–10	46°14.77′	155°32.79′	4859–4863	2932	8 ± 4.8	0	7	4	2	0	0	13
3–9	47°14.66′	154°42.88′	4859–4863	2840	2.1 ± 1.2	2	43	2	4	1	0	52
2–9	46°14.78′	155°32.63′	4830–4864	3117	5.9 ± 2.6	0	5	1	1	0	0	7

1. Chela shape	
a) forcipate	2.
b) non-forcipate (Fig. 9A)	3.
2. Mandible	
a) acuminated	*P. soja*
b) coronal	*P. inflatus*
3. Antenna article-2 with	
a) seta	4.
b) spine (Fig. 12C)	5.
3. Cephalothorax; antenna article-3; pereopod 2–3 carpus	
a) as long as pereonites 1–3; seta; short blade-like spine……	P. intortus
b) 0.75x pereonites 1–3; spine; long blade-like spine…….	P. abathagastor
4. Pereopods 5 –6 carpus rod seta	
a) short (< 0.3x propodus)	6.
b) long (≥0.8x propodus) (Fig. 9F)……	7.
5. Mandible; chela carpus; pereopods 4–6 merus:	
a) acuminate; as long as palm; with two spines and seta..…	*P. vitjazi*
b) coronal (Fig. 14D); 1.2x palm (Fig. 15A); with spine……	*P. locueloae* n. sp.

6. Pereopod-1 carpus seta	
a) short (≤½ of carpus) (Fig. 11B)…	8.
b) long (≥½ of carpus) (Fig. 9B)	9.
7. Cephalothorax; pereopod-1 merus seta	
a) 1.1x pereonites 1–3 (Fig. 12A); long (≥½ merus)……	*P. monroeae* n. sp.
b) 0.9x pereonites 1–3 (Fig. 10A); short (≤½ merus)…	*P. chanelae* n. sp.
8. Pereopod-1 basis	
a) few setae (1–4) (Fig. 7B)……	*P. curieae* n. sp.
b) many setae (6–7) (Fig. 9B)……	10.
9. Mandible; pereopods 4–6 merus	
a) acuminate; spine	*P. nipponicus*
b) coronal (Fig. 8D); spine and seta (Fig. 9G)…..…	*P. szymborskae* n. sp.

4. Discussion

The pseudotanaids collected in the KKT and adjacent waters during the KuramBIO expedition include six new species belonging to two genera. *Mystriocentrus* is collected from Pacific waters for the first time in this study, with the two species of the genus previously described being collected from North Atlantic waters (*Mystriocentrus biho* Jakiel et

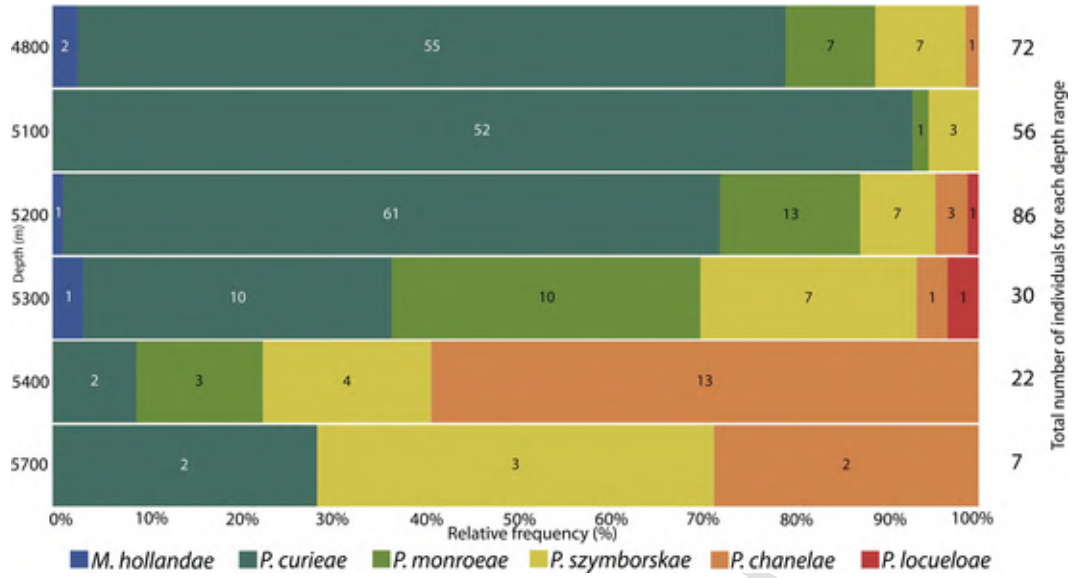

Fig. 2. Bathymetric distribution of Pseudotanaidae taxa collected during the KuramBIO expedition along the KKT zone and adjacent abyssal plain. Numbers on the right hand side of the plot indicate total number of individuals per bathymetric range.

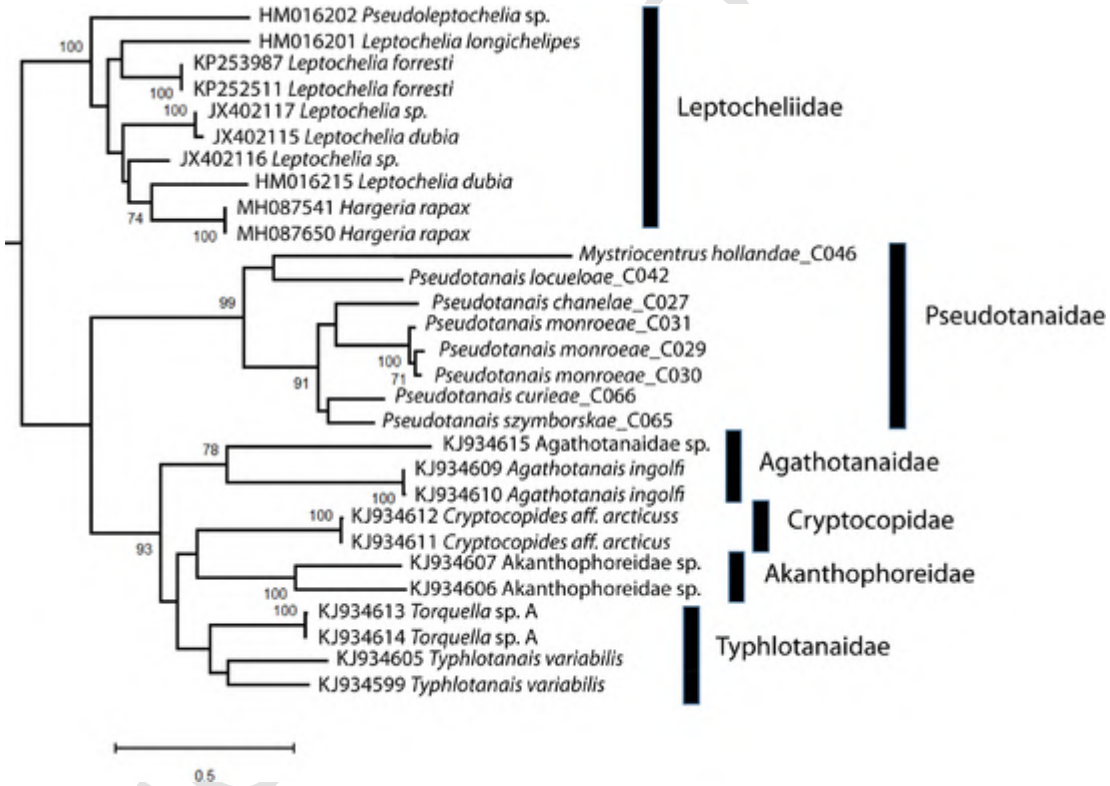

Fig. 3. Evolutionary relationships of Pseudotanaidae species inferred by using the COX1 sequences and the Maximum Likelihood method. The percentage of trees in which the associated taxa clustered together (bootstrap support) is shown next to the branches. Only values above 70% are shown.

al., 2018; *M. serratus* Bird & Holdich 1989). A thorough review of the published literature suggests that two individuals recorded by McLelland (2007) as *Pseudotanais* sp. may be in fact conspecific to *Mystriocentrus hollandae*, showing similar serrate margins on the chela and semi-long blade-like spines on the carpus of pereopods 2–3. The lack of a full description and detailed drawings of the appendages in McLelland (2007) excludes the possibility of further comparison among those individuals and *M. hollandae*. The present study increases our current knowledge on the diversity and distribution of Pseudotanaidae from the NW Pacific Ocean. Although some pseudotanaids are found in shallow waters (e.g. some species of *Akanthinotanais* or *Pseudotanais*), most of them are found in deep sea waters (e.g. Porcupine Seabight and North Biscay; Bird and Holdich (1989)). For example, *Pseudotanais* was the most abundant taxon in samples collected from SW Pacific waters, with relative abundance ranging between 12.5% and 72.7%, (Kaiser et al., 2018). Pseudotanaidae are particularly abundant and diverse in the Southern Ocean, being present in 73.6% and 94% of

all samples collected in Scotia and Amundsen Sea, respectively (Pabis et al., 2014).

Morphological identification of tanaidaceans is difficult because of their small size and sexual dimorphism, but reverse taxonomy (i.e. using sequencing techniques before thorough morphological analyses) can facilitate the identification of cryptic taxa (Held and Wägele, 2008; Palero et al. 2017). Intraspecific variation in NW Pacific pseudotanaids was low compared with values observed in an apseudomorph (*Mesokalliapseudes macsweenyi*) (Drumm and Kreiser, 2012), but they are in agreement with those observed in Pseudotanaidae from Central Pacific (Jakiel et al., 2019) or other deep sea peracarids (Riehl and Kaiser, 2012). Although results are based on a single gene (COX1) and should be considered preliminary, the main clades recovered are congruent with previous hypotheses based on morphology (Bird and Holdich, 1989; Jakiel et al., 2018). The phylogenetic tree obtained shows Paratanaoidea families to be monophyletic with high bootstrap support (except Typhlotanaidae). The reciprocal monophyly of the Pseudotanaidae and other deep-sea Paratanaoidea families is in agreement with the variation observed on the position and number of oostegites in Tanaidomorpha females (Larsen, 2005). Most Paratanaoidea families have a marsupium formed by four pairs of oostegites, but Pseudotanaidae females are unique in forming a marsupium from one pair of oostegites only. The reduced number of oostegites in pseudotanaids could be an adaptation for a more mobile lifestyle (Haupt and Richter, 2008).

Deep-sea crustaceans are generally considered to be rare, sparsely distributed, and to have restricted dispersial abilities (McClain and Hardy, 2010; Ramirez-Llodra et al., 2010). Nevertheless, studies from NW Atlantic and circum-Antarctic waters (Bird and Holdich, 1989; Brandt et al., 2012) and the combination of molecular and morphological data suggest that larger distributions and abundances are possible (see Results; Havermans et al., 2013; Jakiel et al., 2019). Pseudotanaid taxa represented in our samples by 20 individuals or more (i.e. *P. chanelae, P. monroeae, P. curieae* and *P. szymborskae*) show a particularly wide geographical distribution. This distribution pattern may be explained by the small spatial heterogeneity and high food availability of the abyssal plain adjacent to the KKT, a region with primary production of chemosynthetically derived organic matter (Mordukhovich et al., 2018). Geographical distance or geomorphology characteristics of the seabed, which are considered to be effective predictors of biological community composition, do not seem to be so determinant for pseudotanaids in the KKT area. The total number of pseudotanaid specimens found in the KKT is mostly correlated with depth (decreased in deeper stations), as expected due to lower food availability (Rex et al., 2006). Nevertheless, the relative frequency of some taxa increased with depth and distance from the KKT area (i.e. *P. chanelae*), so the general motto that genetic diversity is lower at increasing depths should be taken with caution (Palero et al., 2010b; Taylor and Roterman, 2017). High relative abundance of pseudotanaids has been observed at bathyal sites and at least five *Pseudotanais* species were found with overlapping depth ranges in the abyssal zone >4000 m (Bird and Holdich, 1989; Kaiser et al., 2018). Understanding the key factors driving the spatial distribution of deep sea fauna is of utmost importance for the efficient management and conservation of abyssal environments (Dunn et al., 2018; Van Dover et al., 2014), and our results suggest that using geomorphological features as the only tool to define seabed habitats and faunal composition may be misleading. Integrative taxonomy studies are still uncovering new pseudotanaid taxa and will continue to improve our understanding of the relative importance of ecological and environmental conditions on the distribution of deep-sea biodiversity.

Declaration of Competing Interest

The authors declare that they have no known competing financial interests or personal relationships that could have appeared to influence the work reported in this paper.

Acknowledgements

This study was funded by the Polish National Science grant UMO-2016/13/B/NZ8/02495.

Appendix A. Morphological analyses and species descriptions

Family: Pseudotanaidae Sieg, 1976

Genus: *Mystriocentrus* Bird & Holdich, 1989

Diagnosis: Antenna article-6 and maxilliped palp article-4 with thickened seta. Chela forcipate, cutting edge serrate.

Species included: *Mystriocentrus biho* Jakiel, Stępień & Błażewicz, 2018; *M. serratus* Bird & Holdich, 1989; *Mystriocentrus* sp. A McLelland, 2008; *Pseudotanais* sp. McLelland, 2007.

Mystriocentrus hollandae n. sp.

Figs. 4 and 5

Material examined. **Holotype:** neuter (partially dissected), BL = 1 mm (ZMH K-57039), St. 9–12, 40°34.49′N 150°59.85′E, 5392–5397 m, EBS, 24 Aug 2012.

Paratypes: Two neuters, St. 3–9. Neuter, St. 7–10.

Diagnosis: Pereopods 2–3 merus without spatulate setae; pereopods 2–3 carpus with blade-like spine 0.5x propodus. Pereopods 4–6 carpus without spatulate setae. Uropod exopod with one article, 0.5x endopod.

Etymology: The species is dedicated to Agnieszka Holland, Polish film director and screenwriter, one of Poland's most recognized filmmakers.

Description of neuter: BL = 1 mm. Body, lateral view (Fig. 4A).

Antennule (Fig. 4B) article-1 4.7 L:W, 3.1x article-2, with simple mid-length seta, two penicillate setae and two simple distal setae; article-2 1.9 L:W, 0.7x article-3, with two distal setae; article-3 5 L:W, with three simple setae, one bifurcate seta, two rod setae and one aesthetasc.

Antenna (Fig. 4C); article-2 0.9x article-3, with distodorsal seta (0.9x the article-2); article-3 1.2 L:W, 0.17x article-4, with distodorsal seta (0.6x the article-3); article-4 11.1 L:W, 3x article-5, with one simple and two penicillate setae subdistally, two simple and one penicillate setae distally; article-5 4.1 L:W, 8.2x article-6, with seta; article-6 0.7 L:W, with three simple and one thick seta.

Mouth parts. Labrum not observed. Left mandible (Fig. 4D) *lacinia mobilis* well developed, distally serrate, incisor distal margin serrate, molar acuminate, simple. Right mandible (Fig. 4E) incisor unequally bifid, distal margin serrate, molar acuminate, as in left mandible. Maxillule endite (Fig. 4F) with nine terminal spines and two fine subdistal setae. Maxilliped (Fig. 4G) basis and endites broken; palp article-2 inner margin with robust seta; article-3 with four setae (two long and two short); article-4 with five simple and one thick seta distally and subdistally.

Cheliped (Fig. 5A) slender; basis 1.4 L:W; merus with ventral seta; carpus 3.3 L:W, 1.5x palm, with midventral seta; chela forcipate; palm 1.6 L:W, with small folds (crenulation) in distodorsal corner and small ventral seta; fixed finger 6.1 L:W; 1.7x palm, cutting edge finely serrate with three setae; dactylus 11.7 L:W, cutting edge serrate.

Pereopod-1 (Fig. 5B) coxa with seta; basis 10 L:W, 0.8x merus with midventral seta; ischium with seta; merus 2.4 L:W, 0.6x carpus, naked; carpus 5.2 L:W, 0.7x propodus, with distal seta; propodus 6 L:W, 1.4x dactylus and unguis combined length, with one subdistal dorsal and distal ventral simple setae; dactylus 0.5x unguis.

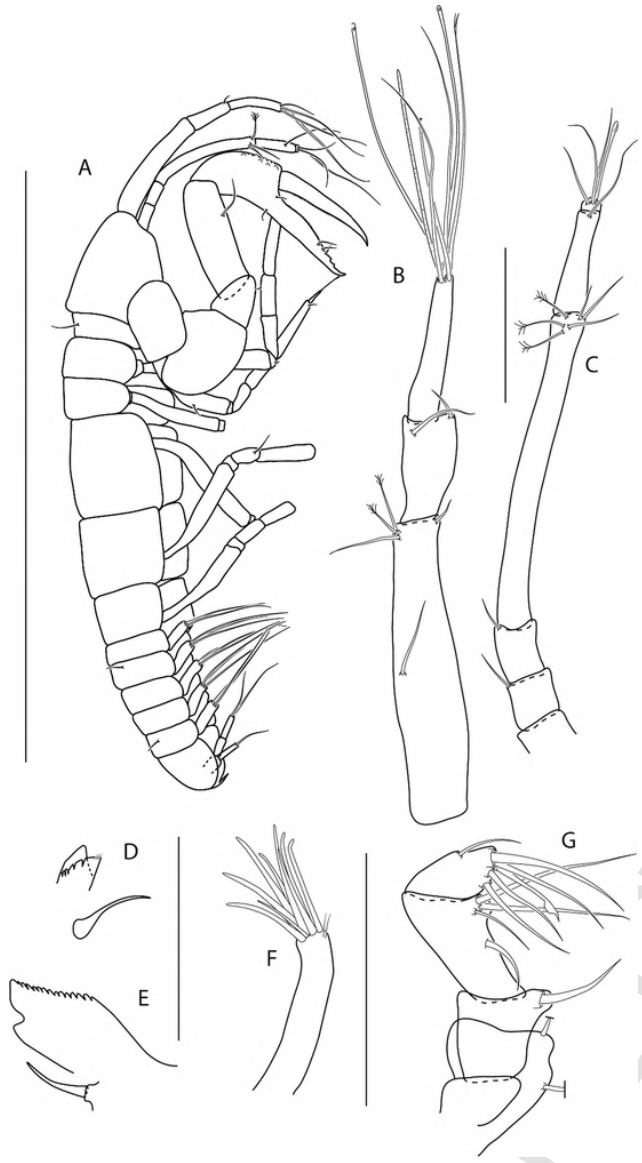

Fig. 4. *Mystriocentrus hollandae* **n. sp.,** neuter type. A, holotype (ZMH K-57039); B-G paratype (ZMH K-57038). A, lateral view; B, antennule; C, antenna; D, left mandible; E, right mandible; F, maxillule; G, maxilliped. Scale bars: A, 1 mm; B–G, 0.1 mm.

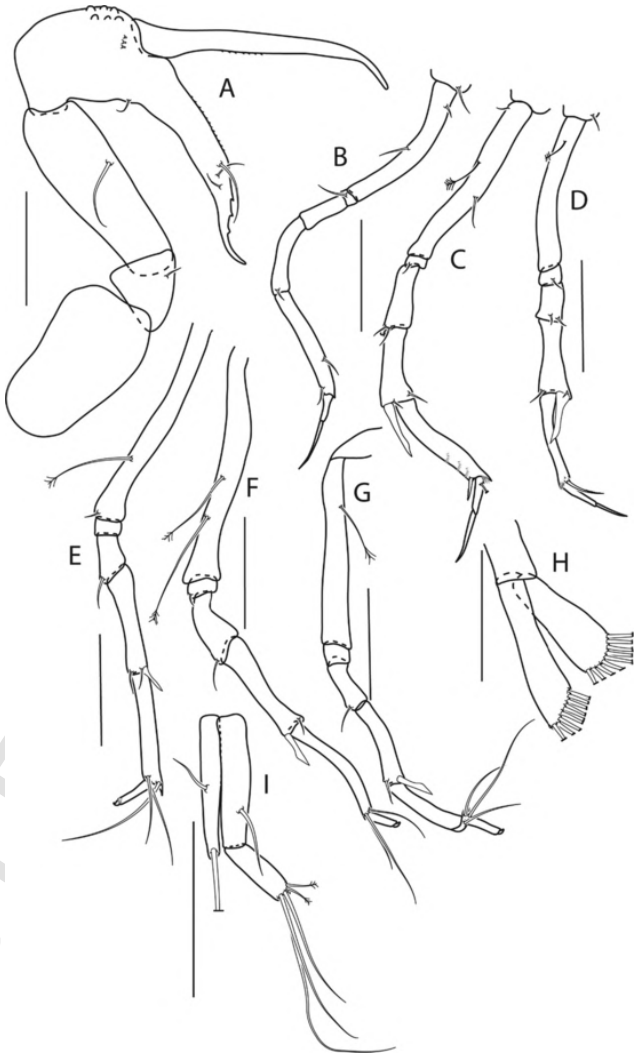

Fig. 5. *Mystriocentrus hollandae* **n. sp.**, neuter type (ZMH K-57038). A, cheliped; B, pereopod-1; C, pereopod-2; D, pereopod-3; E, pereopod-4; F, pereopod-5; G, pereopod-6; H, pleopod; I, uropod. Scale bar: 0.1 mm.

Pereopod-2 (Fig. 5C) larger than pereopod 1; basis 7.8 L:W, 2.9x merus, with one simple proximal seta, one simple and one penicillate midlelength seta; ischium with ventral seta; merus 2.7 L:W, 0.8x carpus, with two simple ventrodistal setae; carpus 2.8 L:W, as long as propodus, with two simple and blade-like spine (0.5x propodus); propodus 5.0 L:W, 1.4x dactylus and unguis combined length, with ventrodistal serrate seta shorter than dactylus; dactylus 0.8x unguis with subproximal seta.

Pereopod-3 (Fig. 5D) coxa with seta; basis 7.7 L:W, 4.6x merus; ischium with seta; merus 1.6 L:W, 0.5x carpus, with two simple setae; carpus 2.8 L:W, 0.8x propodus, with two simple setae and one blade-like spine (0.6x propodus); propodus 8.0 L:W, 1.3x dactylus and unguis combined length, with serrate seta as long as dactylus; dactylus 1.1x unguis.

Pereopod-4 (Fig. 5E) basis 11.4 L:W, 8.1x merus, with penicillate ventral seta and simple ventrodistal seta; merus 1.6 L:W, 0.4x carpus, with seta; carpus 4.5 L:W, 0.9x propodus, with two simple setae, and one blade-like spine (0.2x propodus); propodus-6 L:W, with two distoventral and one distodorsal setae; dactylus and unguis fused to a small hook.

Pereopod-5 (Fig. 5F) basis 7.7 L:W, 5.2x merus, with two penicillate ventral setae; ischium with seta; merus 2.5 L:W, 0.7x carpus, with seta; carpus 5 L:W, 0.9x propodus, with seta and blade-like spine (0.3x propodus); propodus 8.0 L:W, with two ventrodistal and one dorsodistal setae; dactylus and unguis fused to a small hook.

Pereopod-6 (Fig. 5G) basis 8.1 L:W, 4.7x merus, with penicillate seta; merus 2.4 L:W, 0.5x carpus, with seta; carpus 5.5 L:W, 1x propodus, with simple seta and blade-like spine (0.4x propodus); propodus 7.3 L:W, 1.6x dactylus and unguis combined length, with three setae; dactylus and unguis fused toa small hook.

Pleopods (Fig. 5H) exopod and endopod with nine distal plumose setae.

Uropod (Fig. 5I) peduncle broken; exopod with one article, 6.6 L:W, with one middle and one strong distal setae; endopod with two articles, article-1 4.3 L:W, with middle seta, article-2 3.3 L:W, with three simple and two penicillate setae. Exopod 0.7x endopod.

Distribution. Kuril-Kamchatka abyssal plain; depth range 4859–5397 m.

Remarks: *Mystriocentrus hollandae* n. sp. is assigned to *Mystriocentrus* because it has a thick seta on maxilliped palp article-4 and on antenna article-6. Furthermore, *M. hollandae,* with 1-article exopod of uro-

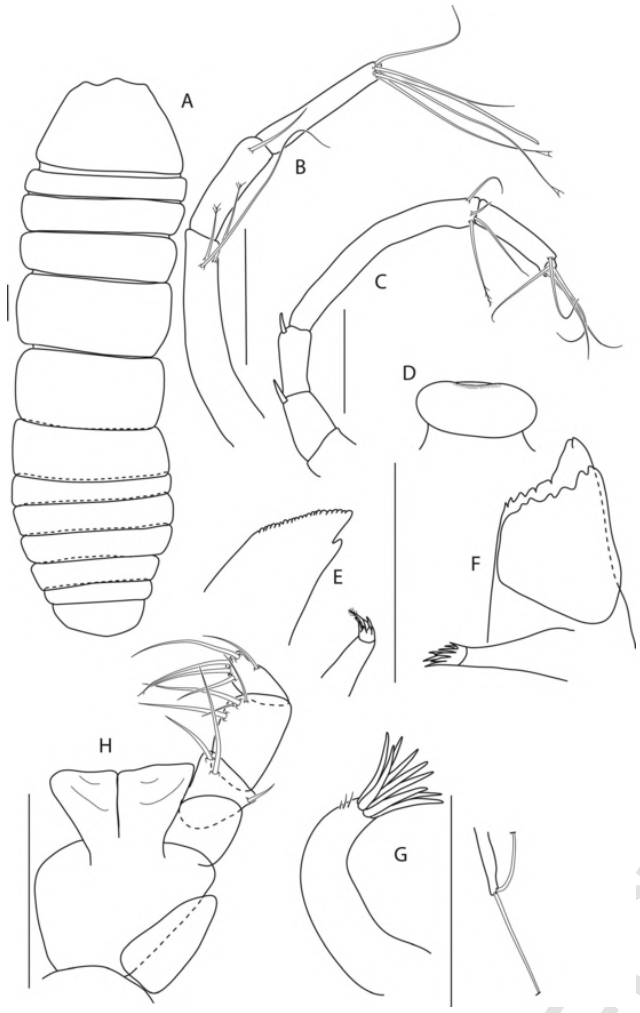

Fig. 6. *Pseudotanais curieae* **n. sp.,** neuter type. A, holotype (ZMH K-57133); B–H paratype (ZMH K-57127). A, dorsal view; B, antennule; C, antenna; D, labium; E, left mandible; F, right mandible; G, maxillule; G', endit; H, maxilliped. Scale bars: A, 1 mm; B–G, 0.1 mm.

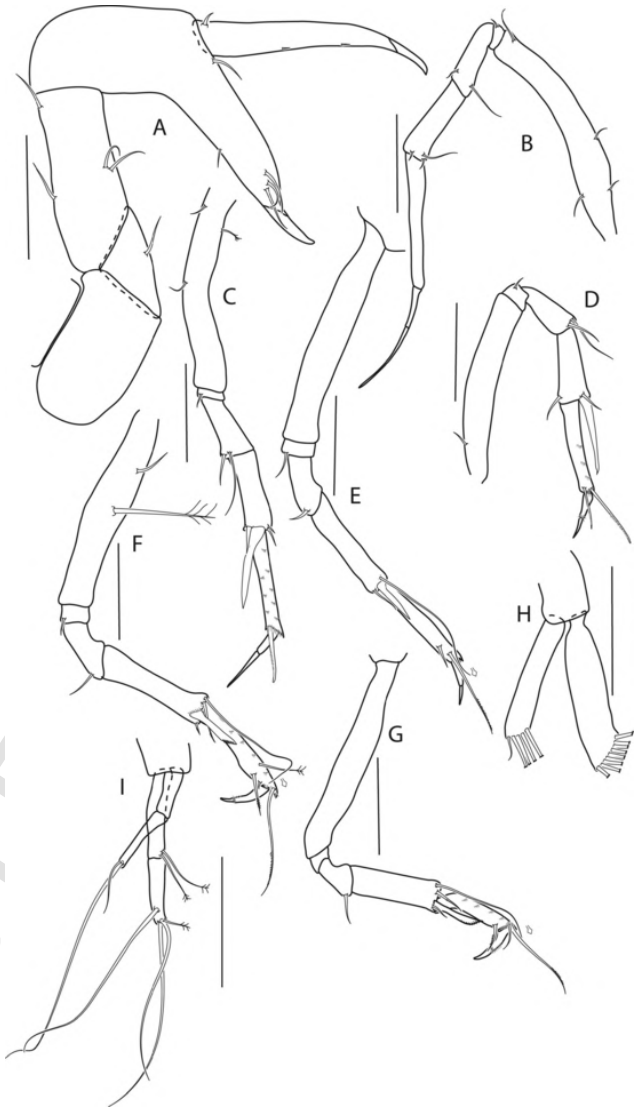

Fig. 7. *Pseudotanais curieae* **n. sp.,** neuter type (ZMH K-57127). A, cheliped; B, pereopod-1; C, pereopod-2; D, pereopod-3; E, pereopod-4; F, pereopod-5; G, pereopod-6; H, pleopod; I, uropod. Scale bar: 0.1 mm.

pod, can be distinguished from *M. biho* that has 2-article exopod. A blade-like spine on the pereopods 2–3 carpus, at least half as long as the propodus, makes *M. hollandae* different from its two congeners (*M. serratus* has this spine only 0.2x propodus and *Mystriocentrus* sp. A not longer than 0.3x propodus). Finally, the new species can be distinguished from *M. serratus* and *Mystriocentrus* sp. A. by the absence of spatulate setae on the pereopods 2–3 merus and pereopods 4–6 carpus. *M. hollandae* is the third species representing the genus, although *Pseudotanais* sp. recorded by McLelland (2008) from the North Pacific is considered conspecific to *M. hollandae,* sharing serrate margins of the chela, missing the spatulate setae on merus of pereopods 2–3 and carpus of pereopods 4–6 and semilong blade-like spines on the carpus pereopods 2–3. The individuals reported by McLelland (2008) were collected from a shallower depth range (3146–3272 m) than *M. hollandae* (4987–5399 m).

Genus: *Pseudotanais* G.O. Sars, 1882

Diagnosis (after Sieg (1976) and Bird and Holdich (1989), modified by Jakiel et al 2018): Antennule with three articles. Antenna with six articles. Maxilliped palp article-4 without rod (thickened) seta. Chela cutting edges smooth; fixed finger with one ventral seta. Pereopods 2–6 carpus with blade-like spine.

'affinis + longisetosus' group

Diagnosis: Antenna article 2–3 with spines. Mandible acuminate or wide. Chela non-forcipate. Pereopod-1 basis with few (0–3) or many (5–7) setae; merus with seta; carpus with or withour setae. Pereopod-2 carpus with long blade-like spine. Pereopods 5–6 carpus with short or long rod seta. Uropod slender, with exopod uropod about 0.75 of endopod, or equal to endopod.

Species included: *Pseudotanais affinis* Hansen, 1887; *P. gaiae* Jakiel, Palero & Błażewicz 2019; P. *geralti* Jakiel, Palero & Błażewicz, 2019; P. *julietae* Jakiel, Palero & Błażewicz, 2019; P. *longisetosus* Sieg, 1977; P. *longispinus* Bird & Holdich, 1989; P. *macrocheles* Sars, 1882; P. *nipponicus* McLelland, 2007; P. *nordenskioldi* Sieg, 1977; P. *romeo* Jakiel, Palero & Błażewicz, 2019; P. *spatula* Bird & Holdich, 1989; P. *scalpellum* Bird & Holdich, 1989; P. *svavarssoni* Jakiel, Stępień & Błażewicz, 2018; P. *uranos* Jakiel, Palero & Błażewicz, 2019; P. *vitjazi* Kudinova-Pasternak, 1966; P. *yenneferae* Jakiel, Palero & Błażewicz, 2019; *Pseudotanais* sp. O (see McLelland, 2008); *Pseudotanais* sp. P (see McLelland 2008); *P. curieae* n. sp., *P. szymborskae* n. sp., *P chanelae* n. sp., *P. monroeae* n. sp.

Pseudotanais curieae n. sp.

Figs. 6–7.

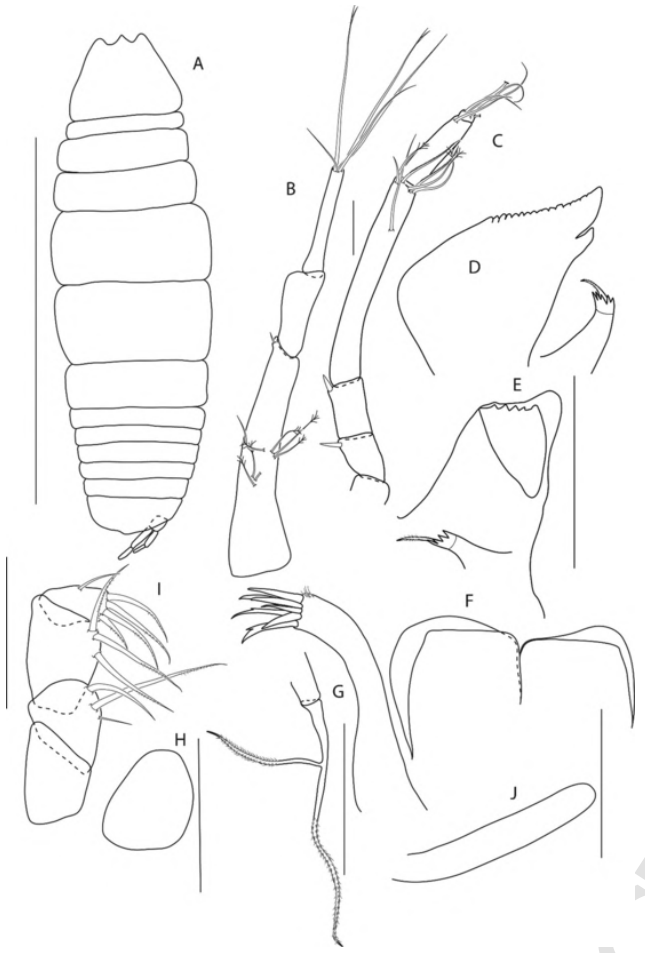

Fig. 8. *Pseudotanais szymborskae* **n. sp.,** neuter type. A, ZMH K-57272; B-H, ZMH K-57281. A, dorsal view; B, antennule; C, antenna; D, labium; E, left mandible; F, right mandible; G, maxillule; H, maxilliped. Scale bars: A, 1 mm; B–G, 0.1 mm.

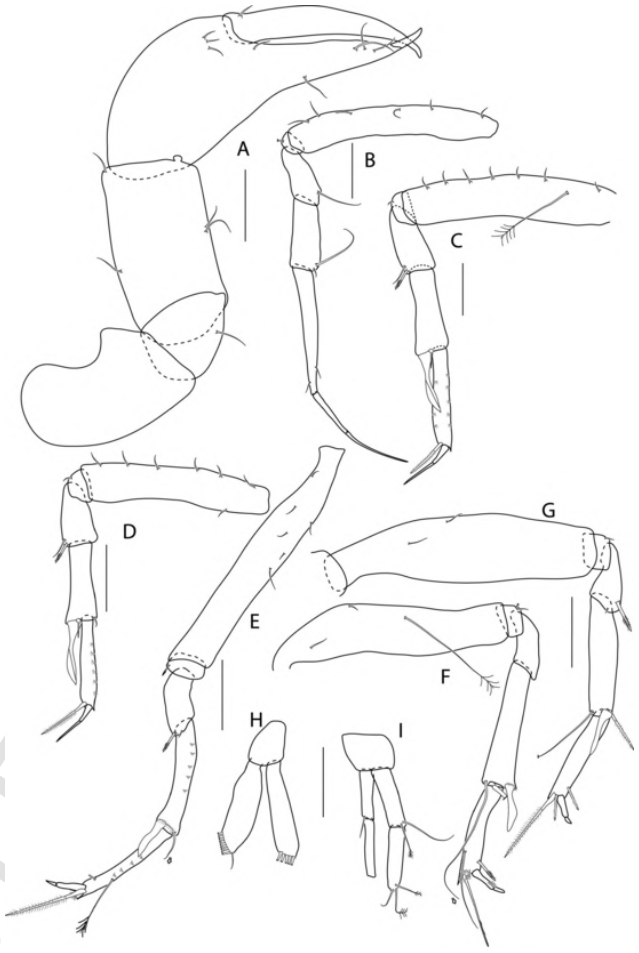

Fig. 9. *Pseudotanais szymborskae* **n. sp.,** neuter type (ZMH K-57276). A, cheliped; B, pereopod-1; C, pereopod-2; D, pereopod-3; E, pereopod-4; F, pereopod-5; G, pereopod-6; H, pleopod; I, uropod. Scale bar: 0.1 mm.

Material examined. Holotype: neuter, BL = 1.7 mm (ZMH K-57133), St. 7–10, 42°14.38′N 151°43.12′E, 5115–5124 m, EBS, 21 Aug 2012.

Paratypes: BL = 1.2–2 mm; two neuters, St. 1–11. Five neuters, St. 2–9. Seven neuters, St. 2–10. 43 neuters, St. 3–9. Two neuters, St. 4–3. Neuter, St. 5–9. Neuter, st 5–10. Three neuters, St. 6–11. Two neuters, St. 7–9. 13 neuters (dissected), St. 7–10. 29 neuters, St. 8–9. 23 neuters, St. 8–12. Two neuters, St. 9–12. Four neuters, St. 10–9. 15 neuters, St. 10–12. Neuter, St. 11–9. Five neuters, St. 11–12. 22 neuters, St. 12–4.

Diagnosis. Pereopod-1 basis with two simple setae; merus and carpus with long seta. Pereopods 2–3 merus with two setae; carpus with long blade-like spine. Pereopods 4–6 carpus with long seta.

Etymology. The species is dedicated to Maria Skłodowska-Curie, a Polish physicist and chemist; the first woman who was Nobel Prize Laureate in two categories.

Description of neuter. BL = 1.6 mm. Body slender (Fig. 6A), 3.6 L:W. Cephalothorax 1.6 L:W, as long as pereonites 1–3, 0.2x BL. Pereonites 0.5x BL, pereonites1–6: 0.1, 0.2, 0.3, 0.5, 0.5 and, 0.3x L:W, respectively. Pleon short, 0.3x BL. Pleonites 0.7x L:W. Pleotelson 0.5x pereonite-6.

Antennule (Fig. 6B) article-1 5.5 L:W, 1.7x article-2, with one simple (longer than article 2) and two penicillate setae; article-2 3.8 L:W, 0.8x article-3, with distal seta; article-3 6.7 L:W, with two simple setae, two trifurcated and one aesthetasc.

Antenna (Fig. 6C) 1.5 L:W, article-2 0.8x article-3, with distodorsal spine (0.6x the article-2); article-3 2.3 L:W, 0.3x article-4, with distodorsal spine (0.7x the article-3); article-4 8 L:W, 2.6x article-5, with three simple and one penicillate setae; article-5 3.5 L:W, 9.3x article-6, with distal seta; article-6 0.6 L:W, with four setae.

Mouth parts. Labrum (Fig. 6D) hood-shape, weakly setose. Left mandible (Fig. 6F) *lacinia mobilis* well developed and distally serrate, incisor distal margin irregularly serrate, molar coronal. Right mandible (Fig. 6E) incisor unequeally bifid distal margin serrate. Maxillule (Fig. 6G) with nine distal spines and three subdistal setae, endite with two distal setae. Maxilliped (Fig. 6H) basis 1.5 L:W, naked, endites partly fussed, distal margin naked (without gustatory cusps and without setae); palp article-2 inner margin with two setae, outer margin with one seta; article-3 with four inner setae; article-4 with five distal and subdistal setae.

Cheliped (Fig. 7A) slender; basis 1.7 L:W, naked; ischium with one seta; carpus 2.7 L:W; 1.2x palm, with two ventral setae, one subdistal and one subproximal setae; chela non-forcipate; palm 2.0x L:W, with one ventral seta; fixed finger distal spine pointed, regular size, 4.3x palm, with three setae on cutting margin; dactylus 7.4 L:W, cutting margin with two spines.

Pereopod-1 (Fig. 7B) basis 7.8 L:W, with three ventral and one dorsal setae; ischium with ventral seta; merus 3.6 L:W, 0.9x carpus, with two simple ventrodistal seta (short and long); carpus 3.2 L:W, 0.6x propodus, with three setae (two short one long); propodus 8 L:W, 1.1x dactylus and unguis combined length, naked; dactylus 0.5x unguis.

Pereopod-2 (Fig. 7C) basis 7.1 L:W, 3.3x merus, with dorsal seta; ischium with seta; merus 2.1 L:W, 0.8x carpus, with two ventrodis-

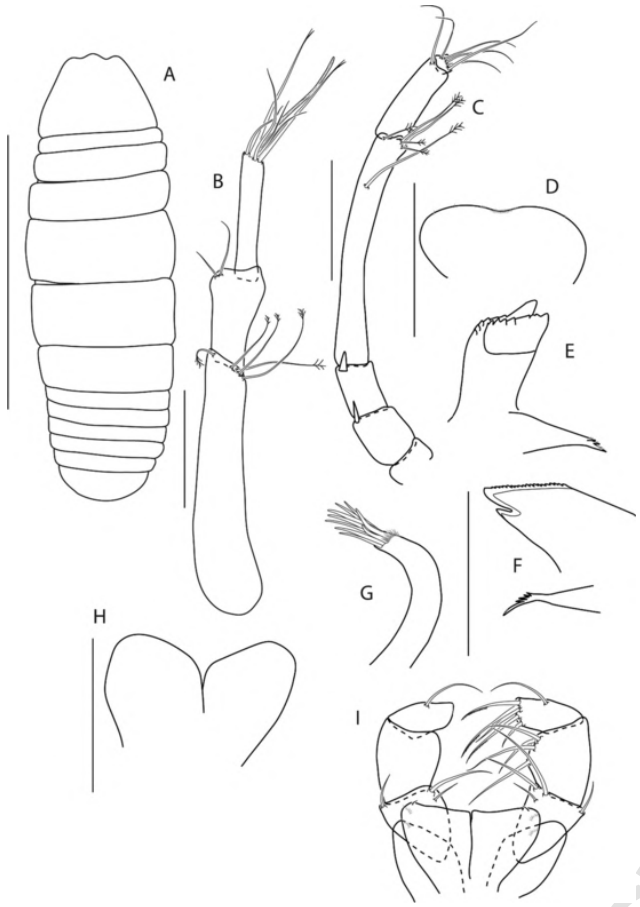

Fig. 10. *Pseudotanais chanelae* **n. sp.,** neuter type. A, ZMH K-57051; B-I, ZMH K-57042. A, dorsal view; B, antennule; C, antenna; D, labium; E, left mandible; F, right mandible; G, maxillule; H, Labrum; I, maxilliped. Scale bars: A, 1 mm; B–G, 0.1 mm.

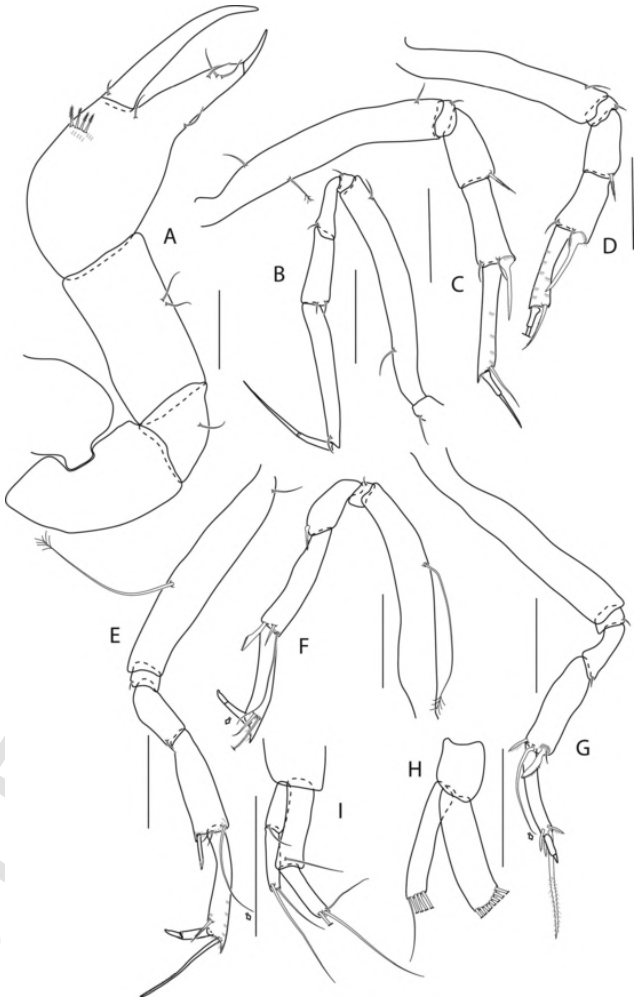

Fig. 11. *Pseudotanais chanelae* **n. sp.,** neuter type (ZMH K-57042). A, cheliped; B, pereopod-1; C, pereopod-2; D, pereopod-3; E, pereopod-4; F, pereopod-5; G, pereopod-6; H, pleopod; I, uropod. Scale bar: 0.1 mm.

tal setae (longer seta twice as long as shorter seta); carpus 2.6 L:W, 0.7x propodus, with two simple setae, one spine, and long blade-like spine (0.8x propodus); propodus 6.2 L:W, 1.4x dactylus and unguis combined length, with robust distoventral serrate seta and microtrichia; dactylus 0.6x unguis.

Pereopod-3 (Fig. 7D) basis 5.6x L:W, 3.2x merus, with dorsal seta; ischium with seta; merus 2.3 L:W, 0.8x carpus, with two setae (longer seta twice as long as shorter seta); carpus 2.8 L:W, 0.8x propodus, with two simple setae and long blade-like spine (0.8x propodus); propodus 5.5 L:W, 1.8x dactylus and unguis combined length, with two distal serrate setae and microtrichia on ventral margin; dactylus as long as unguis.

Pereopod-4 (Fig. 7E) basis 7 L:W, 3.7x merus; ischium with seta; merus 3 L:W, 0.6x carpus, with seta; carpus 5.2 L:W, as long as propodus, with one simple and one rod setae (1.2x propodus), and blade-like spine (0.4x propodus); propodus 6.5 L:W, 2.2x dactylus and unguis combined length, with one simple and one serrate setae (0.8x propodus); dactylus 1.2x unguis.

Pereopod-5 (Fig. 7F) basis 5.1 L:W, 1.3x merus, with one simple and one penicillate setae; ischium with seta; merus 2.3 L:W, with seta; carpus 4.7 L:W, 1.1 × propodus, with rod seta (1.3x propodus), two serrate setae and blade-like spine (0.5x propodus); propodus 6.5 L:W, 2.2x dactylus and unguis combined length, with one penicillate, one simple, two serrate setae (dorsal serrate seta 1.1x propodus), and microtrichia on ventral margin; dactylus 0.1 × unguis.

Pereopod-6 (Fig. 7G) 5.9x merus; ischium naked; merus 1.1 L:W, 0.4x carpus, with seta; carpus 3.1 L:W, 1.2x propodus, with one simple and one serrate seta, blade-like spine 0.7x propodus, and one rod seta (1.3x propodus); propodus 4.5 L:W, with one simple and two serrate setae (dorsal serrate seta 1.2x propodus), and microtrichia on ventral margin; dactylus 1.2x unguis.

Pleopods (Fig. 7H) basis 1.1 L:W; exopod with five plumose setae, endopod with eight plumose setae.

Uropod (Fig. 7I) basis naked, peduncle 0.9 L:W; exopod with two articles; article-1 3 L:W; article-2 5 L:W, with two setae; endopod article-1 5.5 L:W, with two penicillate setae; article-2 4 L:W, with one penicillate and three simple setae. Exopod 0.7x endopod.

Distribution. Kuril-Kamchatka abyssal plain; depth range 4830–5780 m.

Remarks. *Pseudotanais curieae* n. sp. that has a spine on antenna articles 2–3, long seta on pereopod 5–6, and uropod exopod at least 0.8 as long as endopod, is classified to 'longisetosus' morphogroup.

Currently nine species of 'affinis + longisetosus' morphogroup have long setae on pereopod 5–6 (*P. gaiae, P. julietae, P. longisetosus, P. longispinus, P. nipponicus, P. spatula*, *P. romeo*, *P. uranos,* and *Pseudotanais* sp. O.). The only species that has the same long seta on pereopod-4 as *P. curieae* is Antarctic *P. longisetosus* Sieg 1977. *P. curieae* can be distinguished from *P. longisetosus* by the presence of long and short distoventral setae on merus of pereopods 2–3 (longer seta twice as long as shorter seta). Moreover, the antennule article-3 is 6.7 L:W, while in *P. longisetosus* the article is 3.5 L:W. *P. curieae* cephalothorax is as long as pereonites 1–3 and it can be distinguished from *P. longisetosus*, with cephalothorax 1.5 as long as pereonites 1–

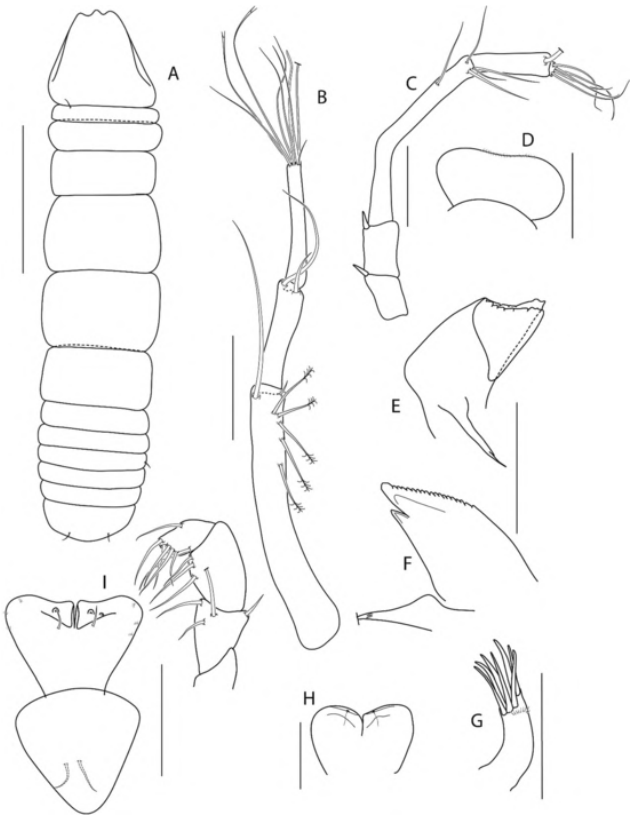

Fig. 12. *Pseudotanais monroeae* **n. sp.,** neuter type. A, holotype (ZMH K-57259); B–I, paratype (ZMH K-57254). A, dorsal view; B, antennule; C, antenna; D, labium; E, left mandible; F, right mandible; G, maxillule; H, Labrum; I, maxilliped. Scale bars: A, 1 mm; B–G, 0.1 mm.

3 combined length. The presence of few (3) setae on dorsal margin of pereopod-1 basis, distinghuishes the new species from *P. julietae, P. longispinus, P. nipponicus, P. romeo* and *P. spatula*, which have more setae (6, 6, 7, 5, 4, respectively). *P. curieae* with one seta on ischium of pereopods 4–6 is distinct from *P. longisetosus*, *P. longispinus*, *P. nipponicus* and *Pseudotanais* sp. O, which have two setae. Finally, the mandible coronal molar present in this new species distinguishes it from all other species mentioned above, with an acuminate molar.

Pseudotanais szymborskae n. sp.

Figs. 8–9

Material examined. Holotype: neuter (ZMH K-57283). BL = 1.4 mm, St. 11–12, 40°12.32′N 148°05.73′E, 5348–5351 m, EBS, 31 Aug 2012.

Paratypes: BL = 1.4–2.1 mm. Neuter, St. 2–9. Two neuters, St. 2–10. Four neuters, St. 3–9. Three neuters, St. 4–3. Three neuters, St. 6–11. Two neuters, St. 7–9. Neuter, St. 8–9. Two neuters, St. 8–12. Four neuters, St. 9–9. Four neuters (one dissected), St. 9–12. Two neuters (one dissected), St. 11–9. Two neuters, St. 12–4.

Diagnosis. Mandible molar coronal, with one longer spine. Pereopod-1 basis with six setae; merus and carpus with long setae (0.9x merus, 0.7x carpus, respectively). Pereopods 2–3 carpus with long (0.7x propodus) blade-like spine. Pereopod-6 carpus with long (1.4x propodus) rod seta.

Etymology. The species is dedicated to Wisława Szymborska, a Polish poet and essayist, a Nobel Prize Laureate in literature.

Description of neuter. BL = 1.4 mm. Body slender (Fig. 8A), 3.2 L:W. Cephalothorax 1.5 L:W, 0.8x pereonites 1–3, 0.2x BL. Pereonites 0.6x BL, pereonites-1–6: 0.1, 0.3, 0.3, 0.4, 0.6, and 0.3x L:W, respectively. Pleon short, 0.2x BL. Pleonites 0.7x L:W. Pleotelson 0.8x pereonite-6.

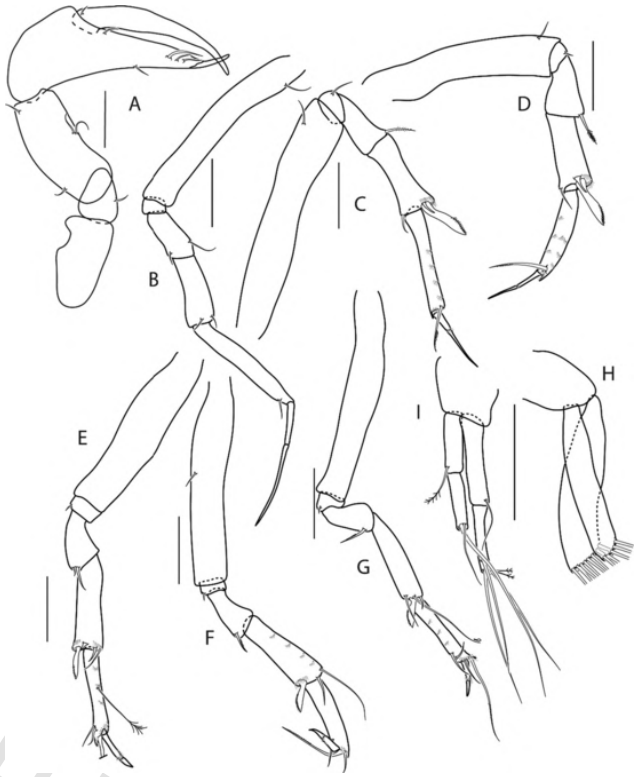

Fig. 13. *Pseudotanais monroeae* **n. sp.,** neuter type (ZMH K-57254). A, cheliped; B, pereopod-1; C, pereopod-2; D, pereopod-3; E, pereopod-4; F, pereopod-5; G, pereopod-6; H, pleopod; I, uropod. Scale bar: 0.1 mm.

Antennule (Fig. 8B) article-1 7.3 L:W, 2.7x article-2, with two groups of three and four penicillate setae, one simple midlength seta and one simple distal seta; article-2 2.7 L:W, 0.7x article-3, naked; article-3 8 L:W, with three simple and two bifurcate setae.

Antenna (Fig. 8C) article-1 1.3 L:W; article-2 0.8x article-3, with distodorsal spine (0.4x article-2); article-3 1.7 L:W, 0.3x article-4 with distodorsal spine (0.3x article-3); article-4 8.3 L:W, 2.6x article-5, with simple midlength seta, one simple, three penicillate and two serrate setae, distally; article-5 3.6 L:W, 9.7x article-6, with distal seta; article-6 0.6 L:W, with four setae.

Mouth parts. Labium not observed. Left mandible (Fig. 8E) *lacinia mobilis* well developed and distally serrate, incisor distal margin weakly serrate, molar wide with serrate distal spines. Right mandible (Fig. 8D) incisor unequal bifid, dorsal margin serrate. Labium (Fig. 8F) typical of genus. Maxillule (Fig. 8G) with seven distal spines (two bifurcate) and row of four fine setae; endite with two setae. Maxilla (Fig. 8H) oval. Maxilliped (Fig. 8I) basis lost during dissection; palp article-1 naked, article-2 with one simple and two serrate setae; article-3 with three inner setae, article-4 with four serrate distal and one simple subdistal setae. Epignath (Fig. 8J) sausage shape.

Cheliped (Fig. 9A) slender; basis 1.1 L:W; merus with seta; carpus 1.7 L:W, as long as palm, with two ventral setae, one distal and one subproximal setae dorsally; chela non-forcipate, palm 1.8 L:W, with simple seta near dactylus insertion; fixed finger distal spine pointed, regular size, cutting edge weakly chitinised, with three setae, ventral margin with seta, dactylus with dorsoproximal setae, cutting edge smooth.

Pereopod-1 (Fig. 9B) basis 7.1 L:W, with six ventral setae; ischium with ventral seta; merus 2 L:W; 0.7x carpus, with simple and long distodorsal seta; carpus 2.8 L:W, 0.5x propodus, with one long and one minute distodorsal setae; propodus 8.0 L:W, 1.1 × dactylus and unguis combined length, with two subdistal setae; dactylus 0.7x unguis, without proximal seta.

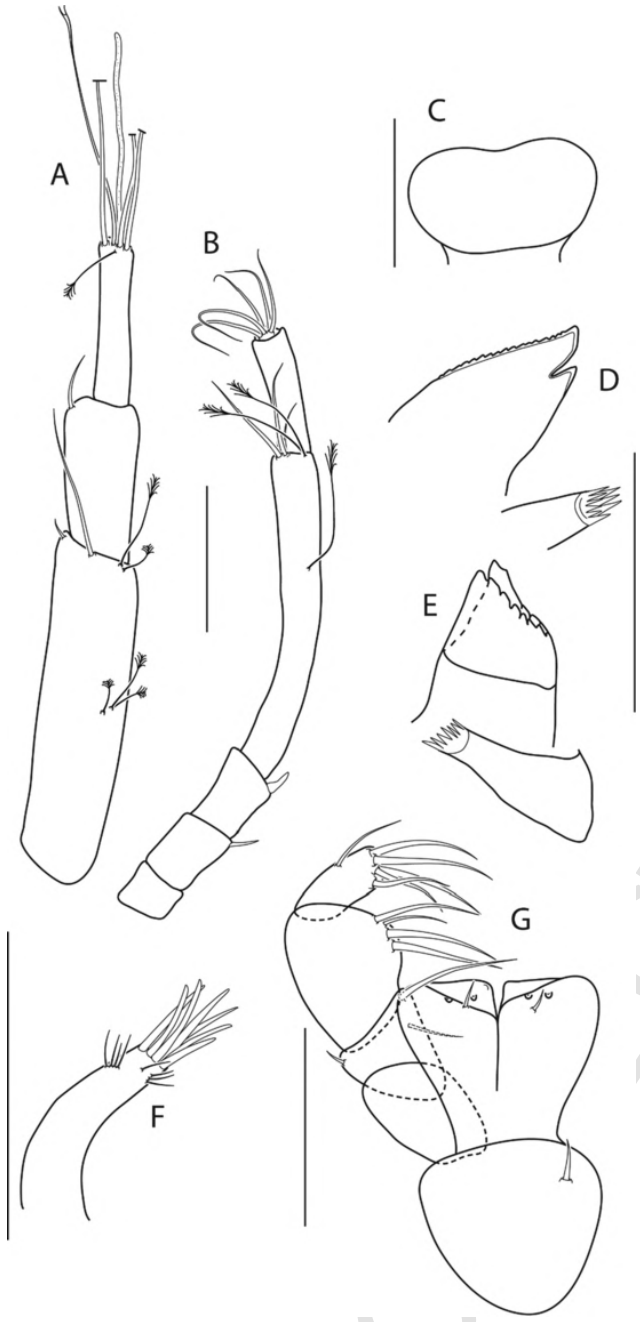

Fig. 14. *Pseudotanais locueloae* **n. sp.,** neuter type, holotype (ZMH K-57238). A, antennule; B antenna; C, labium; D, left mandible; E, right mandible; F, maxillule; G, maxilliped. Scale bars: A, 1 mm; B–G, 0.1 mm.

Pereopod-2 (Fig. 9C) basis 6.6 L:W, 3.4x merus, with seven simple and one penicillate ventral seta; ischium with ventral seta; merus 2.0 L:W, 0.7x carpus, with one simple and one serrate distoventral setae; carpus 3.4 L:W, 0.9x propodus, with one wide-base seta and one blade-like spine (0.6x propodus); propodus 5.8 L:W, 1.7x dactylus and unguis combined length, with serrate seta longer than dactylus, and microtrichia along the margin; dactylus 0.5x unguis.

Pereopod-3 (Fig. 9D) basis 10.2x L:W, 3.6x merus, with one ventral and five dorsal setae; ischium with seta; merus 4.7 L:W, 0.6x carpus, with ventral simple and serrate setae; carpus 3.7 L:W, 0.9x propodus, with distal simple seta and blade-like spine (0.7x propodus); propodus 6.2 L:W, 1.8x dactylus and unguis combined length, with seta as

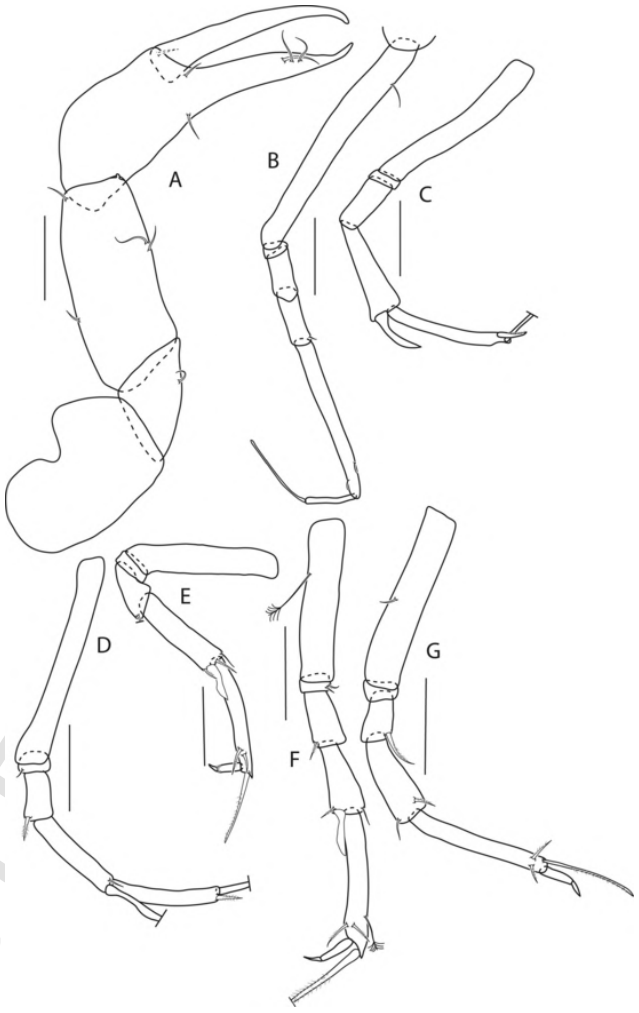

Fig. 15. *Pseudotanais locueloae* **n. sp.,** neuter type (ZMH K-572379). A, cheliped; B, pereopod-1; C, pereopod-2; D, pereopod-3; E, pereopod-4; F, pereopod-5; G, pereopod-6. Scale bar: 0.1 mm.

long as dactylus and unguis, and microtrichia along the margin; dactylus 0.5x unguis.

Pereopod-4 (Fig. 9E) basis 6.2 L:W, 4.1x merus, with three ventral and three dorsal setae; ischium with serrate ventral seta; merus 2.5 L:W, 0.6x carpus, with one simple and one serrate ventrodistal setae; carpus 4.5 L:W, 1.0x propodus, with one rod seta (0.3x propodus) and blade-like spine (0.7x propodus); propodus 8.7 L:W, 2.9x dactylus and unguis combined length, with one dorsal penicillate seta, one distoventral seta (broken), one long serrate distodorsal seta, and microtrichia on ventral margin; dactylus 2.7x unguis.

Pereopod-5 (Fig. 9F) basis 5.2 L:W, 4.1x merus, with dorsal seta and one simple and one penicillate setae ventrally; ischium with two setae; merus 2.8 L:W, 0.5x carpus, naked (seta/ae possibly lost); carpus 6 L:W, 1.2x propodus, with one simple, one rod seta (1.2x propodus) and blade-like spine (0.4x propodus); propodus 6.2 L:W, 2.7x dactylus and unguis combined length, with one distal and two subdistal setae; dactylus 2.7x unguis.

Pereopod-6 (Fig. 9G) basis 3.9 L:W, 3.9x merus, with two ventral setae; ischium with seta; merus 0.9 L:W, 0.5x carpus, with two (long and short) distoventral setae; carpus 3.0 L:W, 1.2x propodus, with one serrate seta, one rod seta (broken) and blade-like spine; propodus 5.2 L:W, 3.5x dactylus and unguis combined length, with two distoventral setae, one long serrate distodorsal seta; dactylus 3.5x unguis.

Pleopods (Fig. 9H) basis 0.8x L:W; exopod with five plumose setae, endopod with ten plumose setae.

Uropod (Fig. 9I) peduncle 0.8 L:W; exopod with two articles; article-1 3.7 L:W, with seta; article-2 7 L:W, seta broken; endopod article-1 1.4 L:W, with one simple and one penicillate setae; article-2 4 L:W, with one simple and two penicillate setae. Exopod 0.8x endopod.

Distribution. Kuril-Kamchatka abyssal plain; depth range 4830–5780 m.

Remarks. *Pseudotanais szymborskae* n. sp., has a spine on antenna articles 2–3, a long rod seta on pereopods 5–6, and an exopod at least 0.75x endopod, is assigned to the 'affinis + longisetosus' morphogroup. Its short distodorsal rod seta on the carpus of pereopod-4 distinguishes it from *P. curieae* and *P. longisetosus* which have a long seta. Additionaly, the new species has many seta (6) on dorsal margin of basis of pereopod-1 can be distinghuished from the mentioned species, which have fewer setae (3 and 2, respectively). A short rod seta on pereopod-4 is also present in: *P. gaiae, P. julietae*, *P. longispinus, P. nipponicus, P. spatula*, *P. romeo*, *P. uranos* and *Pseudotanais* sp. O. New species with cephalothorax 0.8x pereonites 1–3 is different from *P. julietae, P. longiestosus, P. longispinus, P. romeo, P. spatula, P. uranos* and *Pseudotanais* sp. O that have this proportion different (1.2x, 1.5x, 1.0x, 1.2x, 1.0x, 1.0x, 1.0x, respectively). Only *P. nipponicus* has the same length of the carapace as *P. szymborskae*, however two setae on merus of pereopods 4–6 in *P. nipponicus* differentiated from *P. szymborskae* that has a spine on this article. Finally, the coronal mandible molar of *P. szymborskae* distinguishes it from *P. gaiae, P. longispinus, P. nipponicus*, *P. spatula, P. uranos, Pseudotanais* sp. O, which have an acuminate mandible molar, albeit similarly spinose-tipped. Although coronal mandible molars have been observed in Atlantic species of the denticulatus morphogroup, *P. szymborskae* molar has a different number of terminal denticles. The uropod exopod, that is just shorter than the endopod, separates the new species from *P. julietae* and *P. romeo*, which have uropod exopod as long as endopod.

Pseudotanais chanelae n. sp.

Figs. 10–11

Material examined. Holotype: BL = 1.6 mm. (ZMH K-57047), St. 9–9, 40°34.51′N 150°59.92′E, 5399–5408 m, EBS, 23 Aug 2012.

Paratypes: BL = 1.3–1.8 mm. Neuter, St. 3–9. Two neuters, St. 4–3. Neuter, St. 7–9. 12 neuters (one dissected), St. 9–9. Neuter, St. 9–12. Neuter, St. 10–9. Neuter, St. 12–4.

Diagnosis. Mandible molar acuminate. Maxilliped endites without gustatory cusps and setae. Pereopod-1 merus and carpus with short seta. Pereopods 2–3 carpus blade-like spine long (0.6x and 0.7x propodus, respectively). Pereopods 4–6 carpus with long rod seta (0.8–1.0x propodus).

Etymology. The species is dedicated to Coco Chanel, the French fashion icon, founder of the Chanel brand.

Description of neuter. BL = 1.6 mm. Body robust (Fig. 10A), 2.9 L:W. Cephalothorax 0.7 L:W, 0.9x pereonites 1–3, 0.2x BL. Pereonites 0.6x BL; pereonites-1–6: 0.1, 0.2, 0.2, 0.4, 0.5, and 0.3x L:W, respectively. Pleon short, 0.2x BL. Pleonites 0.6x L:W.

Antennule (Fig. 10B) article-1 5.9 L:W, 2.9x article-2, with five penicillate setae; article-2 1.7 L:W, 0.7x article-3, with two setae; article-3 6.1 L:W, with four simple, two bifurcate setae and one aesthetasc.

Antenna (Fig. 10C) 1.2 L:W; article-2 1.1x article-3, with distodorsal spine (0.4x article-2); article-3 1.4 L:W, 0.2x article-4, with distodorsal spine (0.4x article-3); article-4 8.7 L:W, 2.5x article-5, with one subdistal and five distal penicillate setae; article-5 3.1 L:W, 9.3x article-6, with distal seta; article-6 0.5 L:W, with five setae.

Mouth parts. Labrum (Fig. 10D) hood-shape, setose. Left mandible (Fig. 10E) *lacinia mobilis* well developed, distally serrate, incisor distal margin serrate, molar acuminate, with a few distal spines. Right mandible (Fig. 10F) incisor unequally bifid, distal margin serrate. Maxillule (Fig. 10G) with nine terminal spines and a group of fine setae distally. Labium (Fig. 10H) margins smooth, naked and truncate. Maxilliped (Fig. 10I) endites separate, distal margin naked (without gustatory cusps and setae); palp article-1 naked; article-2 inner margin with three inner setae, outer margin with seta; article-3 with four inner setae; article-4 with six distal and subdistal setae.

Cheliped (Fig. 11A) slender; basis 1.9 L:W, naked; carpus 1.4 L:W, as long as palm, with two ventral setae; chela non-forcipate; palm 1.3 L:W, with inner row of four plumose setae; fixed finger distal spine pointed, 1.1x palm, with one ventral seta and three setae on cutting edge; dactylus 7.7 L:W, cutting edge smooth, proximal seta present.

Pereopod-1 (Fig. 11B) basis 7.7 L:W, with one ventral and one dorsal setae; ischium with ventral seta; merus 3.2 L:W, 0.7x carpus; with distoventral seta; carpus 3.1 L:W, 0.6x propodus, with two short dorsal setae; propodus 6.5 L:W, 1.2x dactylus and unguis combined length, with seta; dactylus 0.5x unguis.

Pereopod-2 (Fig. 11C) larger than pereopod-1, basis 6.4 L:W, 3.7x merus, with two subproximal and subdistal ventral setae and penicillate dorsal seta; ischium with seta; merus 1.7 L:W, 0.8x carpus, with ventrodistal seta; carpus 2.7 L:W, 0.8x propodus, with two simple setae and blade-like spine (0.6x propodus); propodus 7.5 L:W, 1.6x dactylus and unguis combined length, with distoventral seta longer than dactylus, and microtrichia on ventral margin; dactylus 0.7x unguis.

Pereopod-3 (Fig. 11D) basis 6.3x L:W, 3.3x merus, with ventral seta; ischium with seta; merus 3.3 L:W, 0.9x carpus, with ventral seta; carpus 2.2 L:W, 0.7x propodus, with two simple setae and blade-like spine (0.7x propodus); propodus 4.8 L:W, with distoventral seta longer than dactylus, and microtrichia on ventral margin; dactylus broken.

Pereopod-4 (Fig. 11E) basis 5.6 L:W, 3.1 x merus, with long penicillate ventral seta and proximal dorsal seta; ischium with seta; merus 2.8 L:W, 0.7x carpus, with ventral seta; carpus 3.2 L:W, 0.9x propodus, with simple seta, long rod seta (0.8x propodus) and blade-like spine (0.3x propodus); propodus 6 L:W, 2.5x dactylus and unguis combined length, with one ventral and one dorsodistal setae (as long as propodus), and microtrichia on ventral margin; dactylus 2.0x unguis.

Pereopod-5 (Fig. 11F) basis 6.8 L:W, 1.6x merus, with penicillate ventral seta; ischium with seta; merus 2.4 L:W, 0.6x carpus, with ventral seta; carpus 4.1 L:W, as long as propodus, with simple seta, rod seta (0.9x propodus) and blade-like spine 0.3x propodus; propodus 5.8 L:W, 2.4x dactylus and unguis combined length, with two setae; dactylus 2.0x unguis.

Pereopod-6 (Fig. 11G) basis 7.7 L:W, 4.4x merus; ischium with seta; merus 3.2 L:W, 0.5x carpus, with ventral seta; carpus 3.7 L:W, with simple seta, long rod seta (as long as propodus), serrate seta and blade-like spine (0.4x propodus); propodus 6.7 L:W, 3x dactylus and unguis combined length, with four serrate setae (dorsal seta 1.1x propodus); dactylus 3.0x unguis.

Pleopods (Fig. 11H) basis 0.7 L:W; exopod with five, endopod with eight plumose setae.

Uropod (Fig. 11I) basis naked, peduncle 0.7 L:W; exopod with two articles; article-1 2.6 L:W, with seta; article-2 4.5 L:W, with two setae; endopod article-1 3 L:W, with seta; article-2 4.2 L:W, with three setae. Exopod 0.7x endopod.

Distribution. Kuril-Kamchatka abyssal plain; depth range 4859–5780 m.

Remarks. *Pseudotanais chanelae* n. sp. with a spine on antenna articles 2–3, long rod seta on carpus of pereopod 5–6, exopod at least 0.7 as long as endopod, is assigned to 'affinis + longisetosus' morphogroup. *P. chanelae* is the third species that has long rod seta on pereopod-4. From *P. curieae* and *P. longisetosus*, which share this character with the new species, it can be distinguished by: presence of acuminate molar of mandible (coronal in *P. curieae*), short distodorsal setae on merus and carpus of the pereopod-1 (long in *P. curieae*), and by the presence of one seta on the ischium of pereopods 4–6 (two in *P. longisetosus*), and the proportion of the propodus of pereopod-1, that

is 1.2x dactylus and unguis combined length (0.8x in *P. longisetosus*). From the all species that have long rod seta on pereopods 5–6, *P. chanelae* can be distinghuished by the presence of spine and seta on merus of pereopods 5–6, while the congeners have a single spine (*P. curieae*, *P. gaiae*, *P. julietae*, *P. longisetosus, P. longispinus, P. spatula, P. szymborskae* and *Pseudtonais* sp. O) or two setae (*P. nipponicus* and *P. uranos*). The only species that share a spine and a seta on merus of pereopods 5–6 is *P. romeo,* both species can be separated by the proportion of the exopod to endopod in uropod, that is 0.7 in *P. chanelae* and 1.0 in *P. romeo*.

Pseudotanais monroeae n. sp.

Figs. 12 and 13

Material examined. Holotype: neuter. BL = 1.4 mm. (ZMH K-57259), St. 12–4, 39°42.78′N 147°09.55′E, 5215–5228 m, EBS, 31 Aug 2012.

Paratypes: BL = 1.2–1.9 mm. Neuter, St. 1–0. Neuter, St. 2–9. Four neuters, St. 2–10. Two neuters, St. 3–9. Three neuters (one dissected), St. 5–10. Neuter, St. 6–11. Two neuters, St. 6–12. Neuter, St. 7–9. Neuter, St. 8–9. Two neuters, St. 9–9. Four neuters (three partially dissected), St. 9–12. Two neuters, St. 10–9. Neuter, St. 10–12. Three neuters, St. 11–9. Five neuters, St. 12–4.

Diagnosis. Mandible molar acuminate. Maxilliped endites with two gustatory cusps and one seta. Pereopod-1 merus with long seta, carpus with short seta. Pereopods 2–3 carpus blade-like spines semilong (0.5x propodus). Pereopods 5–6 carpus rod seta long (0.9x and 1.0x propodus, respectively).

Etymology. The species is dedicated to Marilyn Monroe, an American actress, model, and singer who was perhaps the most famous sex symbols and iconic person in popular culture.

Description of neuter. BL = 3.6 mm. Body robust (Fig. 12A) 4.5 L:W. Cephalothorax 0.9 L:W, 1.1x pereonites 1–3, 0.2x BL. Pereonites 0.6x BL, pereonites-1–6: 0.1, 0.3, 0.4, 0.6, 0.6, and 0.5 L:W, respectively. Pleon short, 0.2x BL. Pleonites 0.9 L:W.

Antennule (Fig. 12B) article-1, 7.3 L:W, 2.3x article-2, with five penicillate subdistal setae and two simple distal setae; article-2 3.4 L:W, 0.9x article-3, with two setae (short and long); article-3 10 L:W, with six simple (one broken), two bifurcate setae and one aesthetasc.

Antenna (Fig. 12C) article-2 1.4 L:W, 0.8x article-3, with distodorsal spine (0.4x article-2); article-3 1.7 L:W, 0.3x article-4, with distodorsal spine (0.3x article-3); article-4 12.3 L:W, 2.5x article-5, with midlength seta and four distal setae; article-5 3.7 L:W, 15x article-6, with seta; article-6 0.3 L:W, with five setae.

Mouth parts. Labrum (Fig. 12D) hood-shape, naked. Left mandible (Fig. 12E) *lacinia mobilis* well developed, distally serrate, incisor distal margin irregularly serrate, molar acuminated, with two distal spines. Right mandible (Fig. 12F) incisor unequally bifid, distal margin regularly serrate. Maxillule (Fig. 12G) with eight terminal spines. Labium (Fig. 12H) distolateral corner of lobes naked. Maxilliped (Fig. 12I) basis 1 L:W, with two sub-posterior setae, endites partly fussed, distal margin with two gustatory cusps and seta; palp article-2 inner margin with three setae and outer margin with seta; article-3 with three inner setae; article-4 with six distal and subdistal setae.

Cheliped (Fig. 13A) slender, basis 1.7 L:W; carpus 1.9 L:W, 1.2x palm with two ventral and two dorsal setae (subproximal and subdistal); chela non-forcipate, palm 1.6 L:W, fixed finger distal spine pointed, with three setae on poorly calcified cutting edge, inner comb row setae not seen; dactylus 7 L:W, ventral margin smooth, proximal inner seta present.

Pereopod-1 (Fig. 13B) basis 3.2 L:W, with subproximal dorsal seta; merus 1.9 L:W; 0.8x carpus, with two setae (distodorsal longer than distoventral); carpus 2.4 L:W, 0.6x propodus, with two distal setae; propodus 6.8 L:W, 1.1x dactylus and unguis combined length, with distoventral seta; dactylus 0.5x unguis.

Pereopod-2 (Fig. 13C) basis 6 L:W, 4.1x merus; with ventral seta; ischium with seta; merus 2.3 L:W, 0.7x carpus, with distoventral seta; carpus 2.2 L:W, 0.7x propodus, with simple seta, wide-base seta and blade-like spine (0.5x propodus); propodus 6 L:W, 0.6x dactylus and unguis combined length, with distoventral serrate seta longer than dactylus, and microtrichia on ventral margin; dactylus 0.5x unguis.

Pereopod-3 (Fig. 13D) basis 5.4 L:W, 3.4x merus, with ventral seta; ischium with ventral seta; merus 1.6 L:W, 0.7x carpus, with serrate distoventral seta; carpus 2.3 L:W, 0.8x propodus, with simple seta, wide-base seta and blade-like spine (0.5x propodus); propodus 5.2 L:W, 0.6x dactylus and unguis combined length, with serrate distoventral seta longer than dactylus, and with microtrichia on ventral margin; dactylus 0.9x unguis.

Pereopod-4 (Fig. 13E) basis 5 L:W, 3.1x merus; ischium with ventral seta; merus 1.8 L:W, 0.6x carpus, with two setae; carpus 3.6 L:W, as long as propodus, with simple seta, rod seta short (0.3x propodus), spine and blade-like spine (0.4x propodus); propodus 6.2 L:W, 0.6x dactylus and unguis combined length, with midlength dorsal penicillate seta, simple distoventral seta, short simple seta and long serrate distodorsal seta (broken), and microtrichia on ventral margin; dactylus 2.5x unguis.

Pereopod-5 (Fig. 13F) basis 6 L:W, 1.1x merus, with ventral seta; ischium with seta; merus 1.9 L:W, 0.6x carpus, with serrate seta; carpus 2.8 L:W, 1.2x propodus, with simple seta, long rod seta (0.9x propodus) and blade-like spine (0.4x propodus); propodus 4.2 L:W, 0.4x dactylus and unguis combined length, with simple distoventral seta, short simple seta and long serrate distodorsal seta (0.9x propodus); dactylus 0.2x unguis.

Pereopod-6 (Fig. 13G) basis 6.3 L:W, 3.8x merus; ischium with ventral seta; merus 1.9 L:W, 0.6x carpus, with serrate seta; carpus 3.8 L:W, as long as propodus, with simple seta, long distodorsal rod seta (as long as propodus), one spine and one blade-like spine (0.4x propodus); propodus 5.5 L:W, 0.4x dactylus and unguis combined length, with two simple distoventral setae, one simple seta and one long serrate distodorsal seta (1.3 x propodus) and microtrichia on ventral margin; dactylus 1.5x unguis.

Pleopods (Fig. 13H) basis 0.9 L:W; exopod with five plumose setae, endopod with eight plumose setae.

Uropod (Fig. 13I) peduncle 0.6 L:W; exopod with two articles, article-1 3.4 L:W, with penicillate seta, article-2 4 L:W, with two setae (short and long); endopod article-1 5.2 L:W, with seta, article-2 5 L:W, with three simple and two penicillate setae; exopod 0.7x endopod.

Distribution. Kuril-Kamchatka abyssal plain; depth range 4830–5429 m.

Remarks. *Pseudotanais monroeae* n. sp. is classified within the 'affinis + longisetosus' morphogroup, because of a spine on antenna articles 2–3, a long distodorsal rod seta on the carpus of pereopod 5–6, and an uropod exopod at least 0.7x endopod. A short rod seta on carpus of the pereopod-4 make the new species similar to *P. gaiae, P. julietae*, *P. longispinus, P. nipponicus, P. spatula*, *P. romeo*, *P. uranos* and *Pseudotanais* sp. O. The only species that has short seta on the carpus of the pereopod-1 is *P. chanelae*, although it has also a short seta on the merus (long in P. *monroeae*), and the semilong blade-like spine on carpus of pereopod-3 (0.5x propodus); *P. chanelae* has blade-like spine on Pereopod-3 0.7x propodus. *P. monroeae* with short distal seta on the carpus on pereopod-1 is distinct from *P. gaiea, P. longisetosus*, *P. longispinus*, *P. nipponicus, P. spatula, P. uranos, P. curieae*, *P. szymborskae* and Pseudotanais sp. O, which have long seta on merus and carpus of pereopod-1. *P. monroeae* with two setae on ischium of pereopods 4–6 is different from *P. curieae, P. chanelae P. julieatae, P. spatula* and *P. uranos,* which have single seta. Finaly, the new species, with two setae on merus of pereopods 4–6, can be distighuished from *P. curieae, P. gaieae, P. julietae P. longisetosus, P. longispinus, P. spatula, P. szymborska* and *Pseudotanais* sp. O. with a spine on that position; *P. chanelae* and

P. romeo has a spine and a seta. The only two species that have two setae on pereopod 4–6 merus are *P. nipponicus* and *P. uranos,* but few seta (1) on basis of pereopod-1 can distinghuish *P. chanelae* from *P. niponicus* that has many setae (7). Additionally, a proportion of the cheliped carpus of *P. monroeae* (cheliped carpus 1.2x palm) separates it from *P. uranos*, with a carpus as long as palm.

'denticulatus + abathagastor' group

Diagnosis: article 2–3 with spines or setae. Mandible molar coronal. Pereopod-1 basis with few (1–3) setae, merus and carpus distodorsal seta short. Pereopod-2 with short, semilong or long blade-like spine on carpus. Pereopods 5–6 carpus distodorsal seta short. Uropod slender, exopod longer or slightly shorter than endopod.

Species included: *Pseudotanais corollatus* Bird & Holdich, 1984; *P. denticulatus* Bird & Holdich, 1989; P. *abathagastor* Błażewicz-Paszkowycz, Bamber & Jóźwiak, 2013; *Pseudotanais chopini* Jakiel, Palero & Błażewicz, 2019; *Pseudotanais georgesandae* Jakiel, Palero & Błażewicz, 2019*; Pseudotanais chaplini* Jakiel, Palero & Błażewicz, 2019; *Pseudotanais oloughlini* Jakiel, Palero & Błażewicz, 2019; P. *mariae* Jakiel, Palero & Błażewicz, 2019; *Pseudotanais* sp. C (McLelland 2008); *P. locueloae* n. sp.

Pseudotanais locueloae n. sp.

Figs. 14 and 15

Material examined: Holotype: Neuter (dissected), (ZMH K-57238), St. 6–11, 42°28.61′N 153°59.68′E, 5291–5305 m, EBS, 15 Aug 2012.

Paratype: Neuter (dissected), St. 9–12.

Diagnosis. Mandible molar wide. Pereopod-1 merus with short seta, carpus with short seta. Pereopods 2–3 carpus blade-like spines semilong (0.5x propodus).

Etymology. The species is dedicated to the second author closest friend Mevuelvo Locuelo, whom contributed significantly to enjoy the long hours used on the description part of this study.

Description of neuter.

Antennule (Fig. 14A) article-1, 3.7 L:W, 2.1x article-2, with three penicillate subdistal setae, two simple and two penicillate distal setae; article-2 2.1 L:W, 0.9x article-3, with simple seta; article-3 5.5 L:W, with one penicillate, one bifurcate setae, one aesthetasc and three setae (broken).

Antenna (Fig. 14B) article-1 0.8 L:W; article-2 1.3 L:W, 0.9x article-3, with distodorsal spine (0.4x article-2); article-3 1.5 L:W, 0.2x article-4, with broader distodorsal spine (0.3x article-3); article-4 9.3 L:W, 2.6x article-5, with midlength penicillate seta, three simple and two penicillate distal setae; article-5 4.2 L:W, 12.5x article-6; article-6 0.5 L:W, with five setae.

Mouth parts. Labrum (Fig. 14C) hood-shape, naked. Left mandible (Fig. 14D) *lacinia mobilis* well developed and distally serrate, incisor distal margin weakly serrate, molar narrowing distally, but not acute, with distal spines. Right mandible (Fig. 14E) incisor unequally bifid, dorsal margin serrate. Maxillule (Fig. 14F) with seven distal spines and two rows of four fine setae. Maxilliped (Fig. 14G) basis 0.9 L:W, with subdistal seta, endites partly fused, with groove in the midlength, distal margin with two gustatory cusps and seta; palp article-1 naked, article-2 two inner serrate setae and outer simple seta; article-3 with three inner setae, article-4 with six distal and subdistal setae.

Cheliped (Fig. 15A) slender, basis 1.4 L:W; carpus 2.3 L:W, 1.2x palm, with two ventral and two dorsal setae (subproximal and distal); chela non-forcipate, palm 1.8 L:W, fixed finger distal spine pointed, regular size, with three setae on poorly calcified cutting edge; dactylus 6.3 L:W, ventral margin smooth, inner proximal seta present.

Pereopod-1 (Fig. 15B) basis 9.2 L:W, with subproximal dorsal seta; merus 2.5 L:W; 0.9x carpus, naked; carpus 3.4 L:W, 0.4x propodus, with minute seta; propodus elongate and narrow, 11.7 L:W, 1.3x dactylus and unguis combined length, with two subdistal setae; dactylus 0.7x unguis.

Pereopod-2 (Fig. 15C) basis 8.3 L:W, 4.2x merus; ischium naked; merus 1.7 L:W, 0.4x carpus, distoventral spine and seta not observed; carpus 3.8 L:W, 0.8x propodus, with blade-like spine (0.6x propodus); propodus 8.7 L:W, with serrate distoventral seta shorter than dactylus; dactylus broken.

Pereopod-3 (Fig. 15D) basis 8.6 L:W, 4.6x merus; ischium with ventral seta; merus 1.6 L:W, 0.5x carpus, with serrate distoventral seta; carpus 6.7 L:W, 0.8x propodus, with simple seta and blade-like spine (0.6x propodus); propodus 8 L:W, with serrate seta; dactylus broken.

Pereopod-4 (Fig. 15E) basis 5 L:W, 1.4x merus, with ventral seta; ischium with seta; merus 2 L:W, 0.7x carpus, with serrate distoventral seta; carpus 2.6 L:W, 0.8x propodus, with short distodorsal rod seta, two serrate setae and blade-like spine (0.3x propodus); propodus 8.2 L:W, 4.0x dactylus and unguis combined length, with two serrate subdistal and long serrate distodorsal seta (0.6x propodus); dactylus 2.3x unguis.

Pereopod-5 (Fig. 15F) basis 4.0 L:W, 2.5x merus; ischium with two setae; merus 1.2 L:W, 0.4x carpus, with one broken distoventral seta; carpus 2.7 L:W, 0.5x propodus, with short distodorsal rod seta, one serrate seta and one blade-like spine (0.3x propodus); propodus 6.7 L:W, 3.1x dactylus and unguis combined length, with one dorsal penicillate seta, two serrate subdorsal setae and one long distodorsal seta (broken); dactylus 3.3x unguis.

Pereopod-6 (Fig. 15G) basis 5.1 L:W, 3.6x merus; merus 1.8 L:W, 0.5x carpus, with serrate distoventral seta; carpus 6.5 L:W, 0.65x propodus, with short distodorsal rod seta, one serrate seta, blade-like spine broken; propodus 10 L:W, 2.7x dactylus and unguis combined length, with two serrate subdistal setae and one long serrate distodorsal seta (0.7x propodus); dactylus 2.2x unguis.

Pleopods (not illustrated) exopod with seven plumose setae, endopod with ten plumose setae.

Uropod missing.

Distribution. Kuril-Kamchatka abyssal plain; depth range 5291–5397 m.

Remarks. *Pseudotanais locueloae* n. sp., with naked merus of pereopod-1 and no long rod distodorsal seta on carpus of pereopods 5–6, is the tenth species described of 'denticulatus + abathagastor' morphogroup. *P. locueloae* can be distinguished from other species of the group by the length and proportions of pereopod-1 propodus. The long propodus (11.7 L:W) distinguishes it from *P. chaplini, P. chopini, P. corollatus, P. denticualtus, P. georgesandae, P. oloughlini*, which have the propodus less than 6 L:W. *P. locueloae* has a spine on antenna article-2 and can be separated from *P. abathagastor* and *P. mariae*, which have a seta (not spine) at the article. The carpus/palm proportion of the cheliped is larger in *P. locueloae* (1.2x), while in *P. abathagastor, P. chaplini, P. chopini P. corollatus, P. denticulatus P. georgesandae, P. mariae, P. oloughlini* and *Pseudotanais* sp. C this proportion is smaller (1.0x, 1.0x, 1.1x, 0.9x, 1.0x, 1.1x, 1.1x, 1.1x, 1.0x, respectively). The spine on merus of pereopods 4–6 allows the new species to be separated from *P. abathagastor* (with seta)*, P. corollatus* and *P. mariae* (with two setae), *P. chopini, P. denticulatus, P. oloughlini* and *Pseudotanais* sp. C (with spine and seta); only *P. chaplini* and *P. georgesandae* have a spine, but the acuminate mandible molar in *P. chaplini,* and bifurcated teeth of *P. georgesandae,* separate them from *P. locueloae*, with a simple coronal molar (without additional denticles).

Appendix B. Supplementary material

Supplementary data to this article can be found online at https://doi.org/10.1016/j.pocean.2020.102288.

References

Altschul, S.F., Gish, W., Miller, W., Myers, E., Lipman, D.J., 1990. Basic local alignment search tool. J. Mol. Biol. 215, 403–410.

Bamber, R.N., Bird, G., Błażewicz-Paszkowycz, M., Galil, B., 2009. Tanaidaceans (Crustacea: Malacostraca: Peracarida) from soft-sediment habitats off Israel, Eastern Mediterranean. Zootaxa 2109, 1–44.

Bird, G.J., Holdich, D.M., 1989. Tanaidacea (Crustacea) of the north-east Atlantic: the subfamily Pseudotanainae (Pseudotanaidae) and the family Nototanaidae. Zool. J. Linn. Soc. 97, 233–298. doi:10.1111/j.1096-3642.1989.tb00548.x.

Błażewicz-Paszkowycz, M., Bamber, R.N., 2012. The Shallow-water Tanaidacea (Arthropoda: Malacostraca: Peracarida) of the Bass Strait, Victoria, Australia (other than the Tanaidae). Mem. Museum Victoria 69, 1–235. doi:10.24199/j.mmv.2012.69.01.

Błażewicz-Paszkowycz, M., Bamber, R.N., Jóźwiak, P., 2013. Tanaidaceans (Crustacea: Peracarida) from the SoJaBio joint expedition in slope and deeper waters in the Sea ofJapan. Deep. Res. Part II Top. Stud. Oceanogr. 86–87, 181–213. doi:10.1016/j.dsr2.2012.08.006.

Błażewicz-Paszkowycz, M., Pabis, K., Jóźwiak, P., 2015. Tanaidacean fauna of the Kuril-Kamchatka Trench and adjacent abyssal plain - abundance, diversity and rare species. Deep. Res. Part II Top. Stud. Oceanogr. 111, 325–332. doi:10.1016/j.dsr2.2014.08.021.

Brandt, A., Alalykina, I., Brix, S., Brenke, N., Błażewicz, M., Golovan, O.A., Johannsen, N., Hrinko, A.M., Jażdżewska, A.M., Jeskulke, K., Kamenev, G.M., Lavrenteva, A.V., Malyutina, M.V., Riehl, T., Lins, L., 2019. Depth zonation of Northwest Pacific deep-sea macrofauna. Prog. Oceanogr. 176, 102131. doi:10.1016/j.pocean.2019.102131.

Brandt, A., Barthel, D., 1995. An improved supra- and epibenthic sledge for catching peracarida (Crustacea, malacostraca). Ophelia 43, 15–23. doi:10.1080/00785326.1995.10430574.

Brandt, A., Błażewicz-Paszkowycz, M., Bamber, R.N., Mühlenhardt-Siegel, U., Malyutina, M.V., Kaiser, S., de Broyer, C., Havermans, C., 2012. Are there widespread peracarid species in the deep sea (crustacea: Malacostraca)? Polish Polar Res. 33, 139–162. doi:10.2478/v10183-012-0012-5.

Brandt, A., Elsner, N.O., Malyutina, M.V., Brenke, N., Golovan, O.A., Lavrenteva, A.V., Riehl, T., 2015. Abyssal macrofauna of the Kuril-Kamchatka Trench area (Northwest Pacific) collected by means of a camera-epibenthic sledge. Deep. Res. Part II Top. Stud. Oceanogr. 111, 175–187. doi:10.1016/j.dsr2.2014.11.002.

Brandt, A., Malyutina, M.V., 2015. The German-Russian deep-sea expedition KuramBio (Kurile Kamchatka biodiversity studies) on board of the RV Sonne in 2012 following the footsteps of the legendary expeditions with RV Vityaz. Deep. Res. Part II Top. Stud. Oceanogr. 111, 1–9. doi:10.1016/j.dsr2.2014.11.001.

Cadet, J.P., Kobayashi, K., Aubouin, J., Boulègue, J., Deplus, C., Dubois, J., von Huene, R., Jolivet, L., Kanazawa, T., Kasahara, J., Koizumi, K., Lallemand, S.E., Nakamura, Y., Pautot, G., Suyehiro, K., Tani, S., Tokuyama, H., Yamazaki, T., 1987. The Japan Trench and its juncture with the Kuril Trench: cruise results of the Kaiko project, Leg 3. Earth Planet. Sci. Lett. 83, 267–284. doi:10.1016/0012-821X(87)90071-9.

Carr, L.A., Boyer, K.E., Brooks, A.J., 2011. Spatial patterns of epifaunal communities in San Francisco Bay eelgrass (Zostera marina) beds. Mar. Ecol. 32, 88–103. doi:10.1111/j.1439-0485.2010.00411.x.

Castresana, J., 2000. Selection of conserved blocks from multiple alignments for their use in phylogenetic analysis. Mol. Biol. Evol. 17, 540–552.

Coleman, C.O., 2003. "Digital inking": How to make perfect line drawings on computers. Org. Divers. Evol. 3, 303–304. doi:10.1078/1439-6092-00081.

Dallwitz, M.J., Paine, T.A., Zucher, E.J., 1993. User's guide to the DELTA system: a general system for processing taxonomic descriptions. 4th edition. http://delta-intkey.com 117.

Drumm, D.T., Kreiser, B., 2012. Population genetic structure and phylogeography of Mesokalliapseudes macsweenyi (Crustacea: Tanaidacea) in the northwestern Atlantic and Gulf of Mexico. J. Exp. Mar. Bio. Ecol. 412, 58–65. doi:10.1016/j.jembe.2011.10.023.

Dunn, D.C., Van Dover, C.L., Etter, R.J., Smith, C.R., Levin, L.A., Morato, T., Colaço, A., Dale, A.C., Gebruk, A.V., Gjerde, K.M., Halpin, P.N., Howell, K.L., Johnson, D., Perez, J.A.A., Ribeiro, M.C., Stuckas, H., Weaver, P., 2018. A strategy for the conservation of biodiversity on mid-ocean ridges from deep-sea mining. Sci. Adv. 4, eaar4313. doi:10.1126/sciadv.aar4313.

García-Herrero, Á., Sánchez, N., García-Gómez, G., Pardos, F., Martínez, A., 2019. Two new stygophilic tanaidomorphs (Peracarida, Tanaidacea) from Canary Islands and southeastern Iberian Peninsula. Mar. Biodivers. 49, 107–130. doi:10.1007/s12526-017-0763-7.

Garm, A., 2004. Revising the definition of the crustacean seta and setal classification systems based on examinations of the mouthpart setae of seven species of decapods. Zool. J. Linn. Soc. 142, 233–252. doi:10.1111/j.1096-3642.2004.00132.x.

Golovan, O.A., Błażewicz, M., Brandt, A., Jażdżewska, A., Jóźwiak, P., Lavrenteva, A.V., Malyutina, M.V., Petryashov, V.V., Riehl, T., Sattarova, V.V., 2019. Diversity and distribution of peracarid crustaceans (Malacostraca) from the abyss adjacent to the Kuril-Kamchatka Trench. Mar. Biodivers. 49, 1343–1360. doi:10.1007/s12526-018-0908-3.

Haupt, C., Richter, S., 2008. Limb articulation in caridoid crustaceans revisited – New evidence from Euphausiacea (Malacostraca). Arth. Struct. Dev. 37, 221–233.

Havermans, C., Sonet, G., d'Udekem d'Acoz, C., Nagy, Z.T., Martin, P., Brix, S., Riehl, T., Agrawal, S., Held, C., 2013. Genetic and morphological divergences in the cosmopolitan deep-sea amphipod eurythenes gryllus reveal a diverse abyss and a bipolar species. PLoS One 8, e74218. doi:10.1371/journal.pone.0074218.

Held, C., Wägele, J.W., 2008. Cryptic speciation in the giant Antarctic isopod *Glyptonotus antarcticus* (Isopoda, Valvifera, Chaetiliidae). Sci. Mar. 69, 175–181. doi:10.3989/scimar.2005.69s2175.

Jakiel, A., Palero, F., Błażewicz, M., 2019. Deep ocean seascape and Pseudotanaidae (Crustacea: Tanaidacea) diversity at the Clarion-Clipperton Fractore Zone. Sci. Rep. doi:10.1038/s41598-019-51434-z.

Jakiel, A., Stępień, A., Błażewicz, M., 2018. A tip of the iceberg—Pseudotanaidae (Tanaidacea) diversity in the North Atlantic. Mar. Biodivers. 48, 859–895. doi:10.1007/s12526-018-0881-x.

Jakiel, A., Stępień, A., Jóźwiak, P., Serigstad, B., Błażewicz-Paszkowycz, M., 2015. First record of tanaidacea (Crustacea) from a deep-sea coral reef in the Gulf of Guinea. Zootaxa 3995, 203–228. doi:10.11646/zootaxa.3995.1.18.

Kaiser, S., Lörz, A.-N., Bird, G.J., Malyutina, M.V., Bowden, D.A., 2018. Benthic boundary layer macrofauna from the upper slope of the Chatham Rise (SW Pacific). Mar. Ecol. 39, e12521. doi:10.1111/maec.12521.

Katoh, K., Standley, D.M., 2013. MAFFT multiple sequence alignment software version 7: Improvements in performance and usability. Mol. Biol. Evol. 30, 772–780. doi:10.1093/molbev/mst010.

Kudinova-Pasternak, R.K., 1966. Tanaidacea of the Pacific ultra-abyssals. Crustaceana 45, 518–534.

Kudinova-Pasternak, R.K., 1970. Tanaidacea of the Kurile-Kamchatka Trench. Tr. Instituta Okeanol. Akad, Nauk SSSR.

Kudinova-Pasternak, R.K., 1973. Tanaidacea (Crustacea, Malacostraca) collected on the R/V "Vitjas" in regions of the Aleutian Trench and Alaska. Tr. Instituta Okeanol. Akad. Nauk SSSR 91, 141–168.

Kumar, S., Stecher, G., Tamura, K., 2016. MEGA7: Molecular Evolutionary Genetics Analysis Version 7.0 for Bigger Datasets. Mol. Biol. Evol. 33, 1870–1874. doi:10.1093/molbev/msw054.

Larsen, K., 2005. Deep-sea Tanaidacea (Peracarida) from the Gulf of. Crustaceana Monographs, Mexico.

Larsen, K., Shimomura, M., 2007. Foreword. Zootaxa 1599, 5–12.

McClain, C.R., Hardy, S.M., 2010. The dynamics of biogeographic ranges in the deep sea. Proc. R. Soc. Lond. B Biol. Sci. 277, 3533–3546.

McLelland, J.A., 2008. A systematic and taxonomic review of the family Pseudotanaidae (Crustacea: Peracarida: Tanaidacea) based primarily on morphometric cladistic analyses. Ph.D. 298, p.

McLelland, J.A., 2007. Family Pseudotanaidae Sieg, 1976. Zootaxa 1599, 87–99. doi:10.11646/zootaxa.1599.1.5.

Mordukhovich, V.V., Kiyashko, S.I., Kharlamenko, V.I., Fadeeva, N.P., 2018. Determination of food sources for nematodes in the Kuril Basin and eastern slope of the Kuril Islands by stable isotope and fatty acid analyses. Deep. Res. Part II Top. Stud. Oceanogr. 154, 365–373. doi:10.1016/j.dsr2.2018.01.003.

Pabis, K., Błażewicz-Paszkowycz, M., Jóźwiak, P., Barnes, D.K.A., 2014. Tanaidacea of the Amundsen and Scotia seas: An unexplored diversity. Antarct. Sci. 27, 19–30. doi:10.1017/S0954102014000303.

Pabis, K., Jóźwiak, P., Lörz, A.N., Schnabel, K., Błażewicz-Paszkowycz, M., 2015. First insights into the deep-sea tanaidacean fauna of the Ross Sea: species richness and composition across the shelf break, slope and abyss. Polar Biol. 38, 1429–1437. doi:10.1007/s00300-015-1706-z.

Palero, F., Hall, S., Clark, P.F., Johnston, D., MacKenzie-Dodds, J., Thatje, S., 2010. DNA extraction from formalin-fixed tissue: New light from the deep sea. Sci. Mar. 74, 465–470. doi:10.3989/scimar.2010.74n3465.

Palero, F., Matthee, C.A., Abelló, P., Pascual, M., Macpherson, E., 2010. Genetic Diversity Levels in Fishery-Exploited Spiny Lobsters of the Genus Palinurus (Decapoda: Achelata). J. Crustac. Biol. 30, 658–663. doi:10.1651/09-3192.1.

Palero, F., Robainas-Barcia, A., Corbari, L., Macpherson, E., 2017. Phylogeny and evolution of shallow-water squat lobsters (Decapoda, Galatheoidea) from the Indo-Pacific. Zool. Scr. 46, 584–595. doi:10.1111/zsc.12230.

Ramirez-Llodra, E., Brandt, A., Danovaro, R., De Mol, B., Escobar, E., German, C.R., Levin, L.A., Martinez-Arbizu, P., Buhl-Mortensen, P., Narayanaswamy, B.E., Smith, C.R., Tittensor, D.P., Tyler, P.A., Vanreusel, A., Vecchione, M., 2010. Deep, diverse and definitely different: unique attributes of the world's largest ecosystem. Biogeosciences. 7, 2851–2899. doi:10.5194/bg-7-2851-2010.

Rex, M.A., Etter, R.J., Morris, J.S., Crouse, J., McClain, C.R., Johnson, N.A., Stuart, C.T., Deming, J.W., Thies, R., Avery, R., 2006. Global bathymetric patterns of standing stock and body size in the deep-sea benthos. Mar. Ecol. Prog. Ser. 317, 1–8. doi:10.3354/meps317001.

Riehl, T., Kaiser, S., 2012. Conquered from the Deep Sea? A New Deep-Sea Isopod Species from the Antarctic Shelf Shows Pattern of Recent Colonization. PLoS One 7, e49354. doi:10.1371/journal.pone.0049354.

Sars, G.O., 1882. Revision af gruppen: Isopoda Chelifera med charakteristik af nye herhen hørende arter og slægter. Arch. Math. og Naturvidenskab 7, 1–54.

Sieg, J., 1977. Taxonomische Monographie der Familie Pseudotanaidae (Crustacea, Tanaidacea). Mitteilungen aus dem Museum für Naturkd. Berlin. Zool. Museum und Inst. für Spez. Zool. 53, 3–109. doi:10.1002/mmnz.4830530102.

Stamatakis, A., 2014. RAxML version 8: A tool for phylogenetic analysis and post-analysis of large phylogenies. Bioinformatics 30, 1312–1313. doi:10.1093/bioinformatics/btu033.

Stępień, A., Pabis, K., Błażewicz, M., 2019. Tanaidacean faunas of the Sea of Okhotsk and northern slope of the Kuril-Kamchatka Trench. Prog. Oceanogr. 178, 102196. doi:10.1016/J.POCEAN.2019.102196.

Talavera, G., Castresana, J., 2007. Improvement of phylogenies after removing divergent and ambiguously aligned blocks from protein sequence alignments. Syst. Biol. 56, 564–577. doi:10.1080/10635150701472164.

Taylor, M.L., Roterman, C.N., 2017. Invertebrate population genetics across Earth's largest habitat: The deep-sea floor. Mol. Ecol. 26, 4872–4896. doi:10.1111/mec.14237.

Thomas, W.J., 1970. The setae of Austropotamobius pallipes (Crustacea: Astacidae). J. Zool. 160, 91–142. doi:10.1111/j.1469-7998.1970.tb02899.x.

Van Dover, C.L., Aronson, J., Pendleton, L., Smith, S., Arnaud-Haond, S., Moreno-Mateos, D., Barbier, E., Billett, D., Bowers, K., Danovaro, R., Edwards, A., Kellert, S., Morato, T., Pollard, E., Rogers, A., Warner, R., 2014. Ecological restoration in the deep sea: Desiderata. Mar. Policy 44, 98–106. doi:10.1016/j.marpol.2013.07.006.

5 January 2020

STATEMENT

In agreement with all co-authors of the publication entitled:

Secrets from the deep: Pseudotanaidae (Crustacea: Tanaidacea) diversity from the Kuril–Kamchatka Trench
published in *Progress in Oceanography*

DOI: https://doi.org/10.1016/j.pocean.2020.102288

I declare that my contribution in this work is:

author	Contribution (%)	signature
Jakiel Aleksandra	45	
Ferran Palero	30	
Błażewicz Magdalena	25	

Chapter 5: General Discussion

Barriers in the deep sea and their role in limiting dispersal

The abyssal plain has been traditionally recognized as a homogeneous environment where zoogeographical ranges and potential dispersion of animals are unlimited. Pseudotanaidae is one of the most abundant and frequent families of Tanaidacea in these abyssal areas (Bamber and Błażewicz-Paszkowycz, 2013; Pabis et al., 2015), where it is an important component of deep-sea benthic assemblages (Bird and Holdich, 1989a, 1989b, 1988; Pabis et al., 2015, 2014). Before the first results of this dissertation were published in 2018 (Jakiel et al., 2018), this family only comprised two genera and 51 species (Figure 5.1) with the most substantial contributions resulting from Sieg (1977) and Bird and Holdich (1989), whom described eight and 11 new species, respectively.

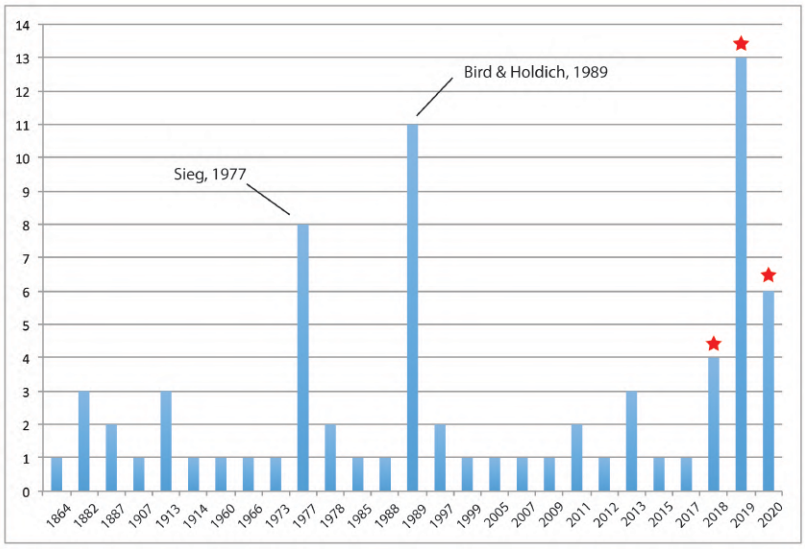

Figure 5.1. Number of Pseudotanaidae species sorted by the year of description, based on the literature data and information collected from World Register of Marine Species (WoRMS). Asterisks marked the species described in this thesis. List of all Pseudotanaidae species is given in Appendix 1.

Modern studies applying the most advanced technologies have shown that the ocean floor topography is highly diverse (Danovaro et al., 2014). Physical barriers, including underwater mountains, oceanic trenches or mid-oceanic ridges are widespread and represent important factors restricting distribution of organisms, similar to mountain chains, rivers or valleys on the land. Therefore, diverse deep sea topographies may harbour different levels of Pseudotanaidae species diversity. The research studies included in this dissertation span deep-sea collections of

Pseudotanaidae from several locations: North Atlantic, Central and Northwest Pacific (Fig. 5.2). The results presented here include as many as 23 new species of Pseudotanaidae (Chapters 2–4) increasing number the species diversity for that family an extra 45%. Additionally, one new genus – *Beksitanais* Jakiel, Palero and Błażewicz, 2019) was erected.

The North Atlantic was quite well studied in term of pseudotanaids before (Băcescu, 1960; Bamber, 2009, 2005; Bird, 1999; Bird and Holdich, 1989c, 1989b; Błażewicz-Paszkowycz et al., 2013, 2011a, 2011c; Bruce et al., 1963); [Dahl] in (Sieg, 1977) Sieg (1977); [Debouttevillе (1960), Debouttevillе et al. (1954)] in Sieg (1983); [Fee, Hatch] in Sieg (1977); (Dojiri and Sieg, 1997; Greve, 1965a, 1965b, 1965c; Holdich and Jones, 1983; Jakiel et al., 2015; Just, 1970) Kruuse, Ryder, Wandel in Hansen (1913); (Kudinova-Pasternak, 1978, 1975, 1973, 1966; Larsen, 2012) Kudinova-Paseternak (1978); Lilljeborg (1864;); [McLelland] in Larsen and (Eds, 2007); (García-Herrero et al., 2019; Sars, 1886, 1882; Shiino, 1978; Sieg, 1977, 1973; Sieg and Heard, 1988; Stephensen, 1937; Vanhoffen, 1907); [Vanhöffen, Kruuse, Ryder, Horring, Sars] in Hansen (1913); [Vanhöffen, R. Horring, H.J. Hansen, Sars, A.M. Norman, Stappers, Th. Scott] in Hansen (1913). The current dissertation complements the list of North Atlantic *Pseudotanais* (including Mediterranean Sea, Lusitanian area, Black Sea and Gulf of Mexico) with another 12 species, so now the Pseudotanaidae in the North Atlantic includes as many as 38 species.

The Kuril Kamchatka and CCZ regions were never studied or poorly known in terms of Pseudotanaidae. From the North-West Pacific six species were recorded before: *Pseudotanais abathagastor* Błażewicz-Paszkowycz, Bamber & Jóźwiak, 2013; *P. intortus* Błażewicz-Paszkowycz, Bamber & Jóźwiak, 2013; *P. soja* Błażewicz-Paszkowycz, Bamber & Jóźwiak, 2013; *P. inflatus* Kudinova-Pasternak, 1973; *P. nipponicus* McLelland, 2007 and *P. vitjazi* Kudinova-Pasternak, 1966. The first three were recorded from relatively shallow depths (from 400 to 1300 m) in the Sea of Japan, while three others were abyssal species. The *Pseudotanais* species in this region is now doubled thanks to the results presented here. Similarly, CCZ was never studied in terms of pseudotanaids, although Wilson (1987) mentioned the presence of this genus in the region. The first confirmation of the presence of Pseudotanaidae in

the region is included, with as many as 13 species newly described in this dissertation. A new genus, *Beksitanais*, is also erected and represents a relevant addition to the dissertation.

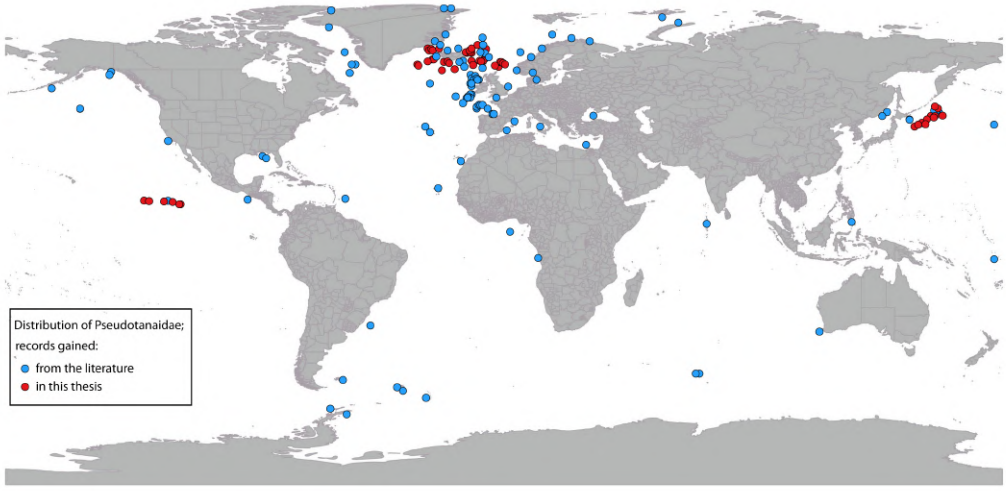

Fig. 5.2. Distribution of Pseudotanaidae based on literature records (see chapter 1) and current results (red dots).

Low mobility and lack of planktonic larvae make Pseudotanaidae a model group to study species distribution and population connectivity in the deep sea. Pseudotanaidae, with their low-mobility life-style (tube-builders) and breeding behaviour (brooders) are ideal model organisms for assessing the spatial distribution of the fauna and colonisation of new habitats. The diverse and complicated topography and hydrology of the studied locations, including Clarion-Clipperton Fracture Zone, Kurile Kamchatka Trench adjacent area and waters around Iceland, are ideal settings for studying diversity, distribution and population connectivity of pseudotanaids. Our results have brought a new insight on their distribution, diversity and dispersal potential.

Studies on pseudotanaids off Iceland collected during the expeditions IceAGE 1 and 2 revealed a great number (323) of individuals classified to four new species (Chapter 2). Three species *Pseudotanais sigrunis*, *Pseudotanais misericorde*, and *Mystriocentrus biho*, have a limited zoogeographical range restricted to only one well-defined basin and distinct bathymetric range. *Pseudotanais svavarssoni* was the most numerous tanaidacean species, and accounted for 57% of the specimens examined from that area. It was also the most widely distributed species (Chapter 2, Figure 7) present in a wide depth range (213.9 to 2746.4 m). Considering the low

mobility of the Tanaidacea and the presence of geographic and hydrographic barriers around Iceland, the wide distribution of this species was questioned. The morphometric analysis confirmed morphological differences between groups of individuals collected from different regions and depths, and revealed the presence of at least two (but possibly four) cryptic species. One of them is present at deeper stations (>1300 m), while the other one was collected from shallower waters (<800 m). The depth was pointed as important factor separating (Brix et al., 2014) and triggering speciation (Etter et al., 2005). Members of the isopod genus *Chelator* were continuously found in shallow waters on the southern coast of Iceland, but abyssal populations were inhabiting both sides of Reykjanes Ridge and were genetically distinct. In CCZ Pseudotanaidae are represented by 13 species in five studied areas (Chapter 3). Most species were sampled from only one of the five areas, separated by hundreds to thousands of kilometres, and just a few species were located in two closely located areas (IOM, BGR). The results obtained evidence low genetic connectivity between all five-studied areas. It is concluded that physical barriers such as deep sea mountain chains or fractures in CCZ restrict gene flow and promote allopatric speciation, although the presence of sympatric taxa suggests some sort of ecological niche adaptation. Furthermore, none of the pseudotanaids found off the northernmost located area designated for protection of the deep sea fauna (APEI-3) has been found on any other station. Similar was concluded for APEI-6. This means that only one-third of the diversity found in CCZ would be protected by the proposed APEI-3. Molecular analysis demonstrated that genetic distance decreased along with increased geographic distance (1500 km between the most distinct stations). Applying Spearman rank coefficient proved a significant correlation between genetic and geographic distances (Chapter 3: Fig. 9). Applying hydrodynamic model, it was demonstrated that propagules of demosponge *Plenaster craigi* released in the area are not transported to other regions of CCZ (Taboada et al., 2018). As so, APEI 6 can perform a conservation role for located in UK claim area, however limited genetic connectivity with the other CCZ areas questions it as an effective reservoir of biological diversity.

Research on scavenging amphipods revealed six widespread species among all claims area in CCZ (Patel et al., 2018). These amphipods are relatively large crustaceans, with adult body size exceeding 15 mm. They are highly mobile

crustaceans which determines their dispersal potential (Brandt et al., 2012). The results obtained here for other apparently less mobile Peracarida crustaceans, such as Tanaidacea, are very different. Błażewicz et al., (2019) indicated a similar distribution pattern as presented here for Pseudotanaidae. In that study only one species in the northernmost station (APEI-3) was shared with the remaining areas. These results allow us to conclude that Pseudotanaidae from the five studied areas of CCZ have limited zoogeographical ranges and restricted dispersion. Besides that, the geographic barriers, such as seamount chains and fractures, are influencing their limited occurrence. Presence of this kind of barriers promote allopatric speciation, where genetic connectivity inside population is reduced, and finally stopped at all (Johannsen et al., 2020).

Kuril Kamchatka Trench (KKT) has much lesser (limiting) effect for distribution of the Tanaidacea (Chapter 4) than oceanic Ridges in North Atlantic or fractures and seamount chains crossing the CCZ. In that area, Pseudotanaidae were represented by six species. Four of them species were found on both sides of the trench. Genetic results from this study confirmed the low intraspecific diversity, and five species (except *P. monroeae*) were represented by a single haplotype each. These observations question the relevance of the Kurile-Kamchatka Trench as a barrier for the dispersion of pseudotanaid species. Similar results were obtained by Bober J. et al. (2019), whom stated that Kuril-Kamchatka Trench is not an isolation barrier for abyssal ischnomesid isopods or preadating amphipods of genus *Rhachotropis* (Lörz et al., 2018). Bober S. et al. (2018) also showed higher intraspecific genetic variation between individuals of *Macrostylis sabinae* Macrostylidae (Isopoda) on both sides of KKT (0.5% p-distance, 4 mutations) than for haplotypes at the same side of KKT (0.3% p-distance). Further research with more data is needed to confirm robustness of those results because some haplotypes were represented by a few individuals only.

Factors and Processes Shaping Deep Sea Diversity Patterns

The vicinity of the Kurile-Kamchatka Trench is described as relatively homogenous in-depth and topography (Bogorov, 1973; Mikhailov, 1972). Besides, the total distance between the most distant stations sampled during the KuramBIO expedition, exceeds 1000 km. This allowed for testing to what extent geographical

distances influence population connectivity in deep sea taxa. The non-isolated abyssal plain of KKT comprises higher abundances and biodiversity comparing to an isolated basin of the Sea of Japan (Malyutina et al., 2015). More homogeneous topography may trigger easier dispersion, and geographic distance did not affect Pseudotanaidae species composition in the vicinity of KKT. Genetic diversity of pseudotanaids in the area showed that five out of six species were represented by a single haplotype, while *P. monroeae* had three haplotypes. It is concluded that molecular diversity in Pseudotanaidae was low.

Species-energy principle

CCZ is referred to as oligotrophic (Smith et al., 1992) in contrast to the eutrophic KKT (Mordasova, 1997), where the input of the organic matter to abyssal depth is delivered from the land. From this perspective, diversity in a eutrophic region like the area adjacent to the Kurile-Kamchatka Trench should be potentially higher than diversity in CCZ, especially given that the sampled area on KKT was three times bigger than the CCZ area (around 350 000 km^2 in KKT *versus* 115 000 km^2 in CCZ). Pseudotanaidae collected in KKT were four-time more abundant than in CCZ (273 to 67, respectively), but diversity was lower (six species and 13 species, respectively). These results demonstrate that the availability of organic matter in the sediments may influence pseudotanaid abundance. However, a relatively high number of species in the Central Pacific area can be promoted by big habitat heterogeneity. The high heterogeneity of habitats would result in an increasing number of potential ecological niches and rise the diversity of benthic fauna. In Central Pacific seamount chains and fracture zones might separate the abyssal plain. At the same time, the presence of these features may reduce dispersion.

Pseudotanaidae:

Bird and Holdich (1989) established two new genera (*Mystriocentrus* and *Parapseudotanais*) and proposed three morphological groups which could be considered as draw for erecting new genera in the future (Bird and Holdich, 1989c). The accurate and detailed morphological observations made here confirmed the overall patterns observed from the molecular analyses (Chapter 4; Fig. 1). Phylogenetic trees confirm the monophyly of deep-sea Pseudotanaidae with high

genetic support, as well as the paraphyletic origin of the genus *Pseudotanais* in relation to other deep-water subfamilies of Paratanaoidae (Chapter 4; Fig. 3).

The morphological diversity among genera is substantial. One of the most variable appendages is cheliped. According to different genera, chela can be crenulated on dorsal margin (*Mystriocentrus*) or not (*Akanthinotanais*, *Beksitanais*, *Parapseudotanais* and *Pseudotanaias*) (Fig. 5.3). Moreover, the cutting edge of dactylus and fixed finger can be serrated (*Beksitanais* and *Mystriocentrus*) or smooth (*Akanthinotanais*, *Parapseudotanais* and *Pseudotanaias*). Another important difference between genera is the presence of two setae on ventral margin of a fixed finger (*Parapseudotanais*), while all other members have a single seta here. The next most important and well-defined character is the presence of a blade-like spine. This character is present on the carpus of pereopods 2–6 in *Beksitanais*, *Mystriocentrus*, and *Pseudotanais*. This characteristic spine is lacking on *Akanthinotanais*, while *Parapseudotanais* has it only on the carpus of pereopods 2–3. The blade-like spine is an important character. Its relative length to the propodus, especially on the pereopods 2–3, is extremely useful for species discrimination. A large diversity is observed in pereopod–1; the proportion of particular articles, setation on basis, merus and carpus is used in defining species as well. Also, morphological variation was observed in the uropods, composed of exopod and endopod. Each of them can have one or two articles; additionally, the proportion between exopod and endopod is relevant.

Most pseudotanaid species belong to the genus *Pseudotanais*. It is the most species-rich and morphologically varied genus in Pseudotanaidae (57 taxa). Bird and Holdich (1989) propose three morphogroups: ‘affinis’, ‘denticulatus’ and ‘forcipatus’. In a later work of Pseudotanaidae from around Iceland, a fourth group (‘longisetosus’) was distinguished (Chapter 2). Newly obtained morphological and molecular data (Chapter 3) allowed the reconstruction of these groups by combining some (‘affinis+longiestosus’ or ‘denticulatus+abathagastor’) and creating a new (‘spicatus’). Subsequent studies of fauna from NW Pacific confirmed the validity of the proposed morphogroups. By analysing molecular data from the Central and NW Pacific, we have been able to confirm the monophyly of the whole family. In the same studies, the large morphological diversity of the genus *Pseudotanais* gives a reason to believe that it consists of at least two new genera (according to morphogroups).

However, due to the lack of sufficient molecular data from remaining morphogroups, this division is currently not performed.

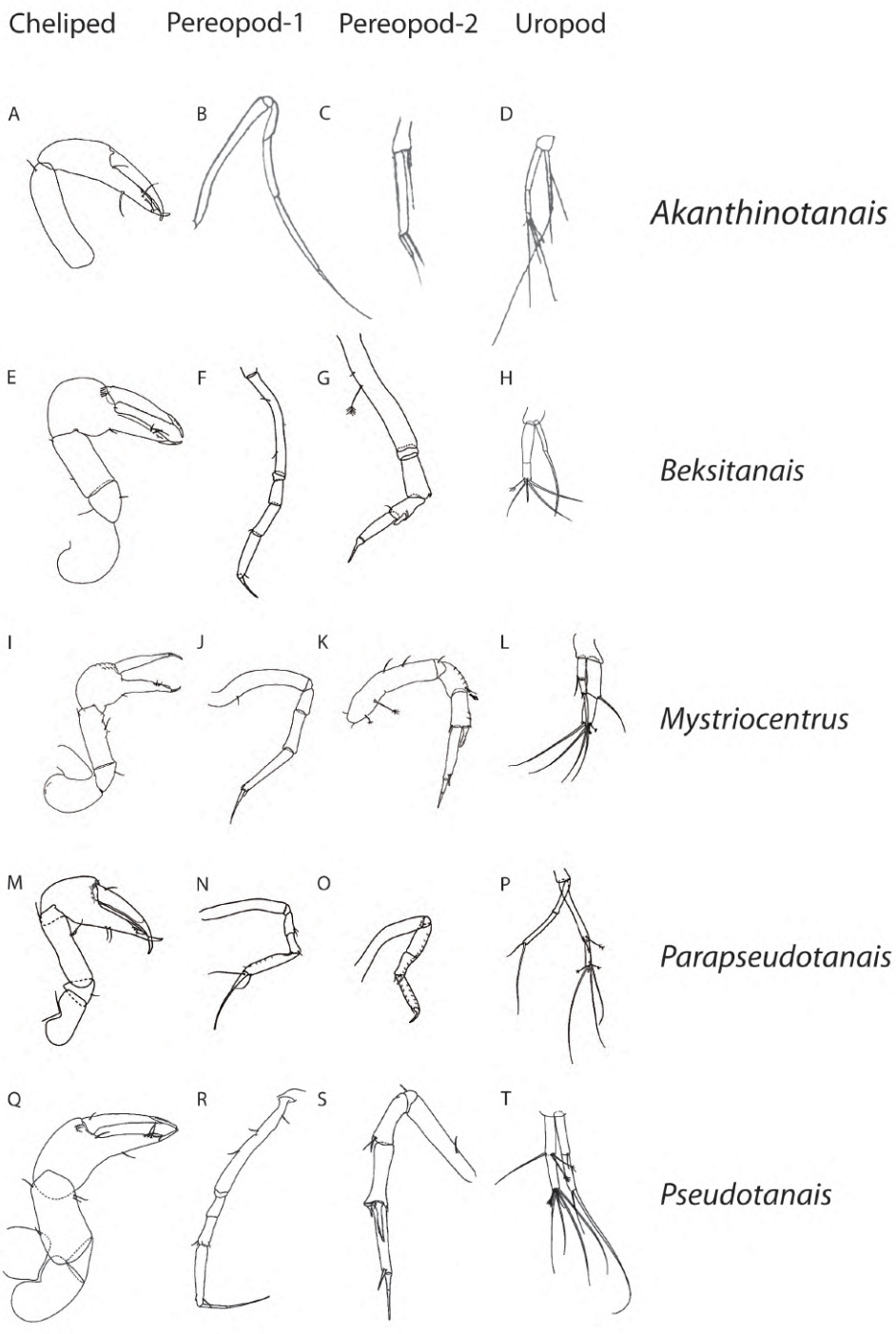

Figure 5.3. Morphological characters among genera in Pseudotanaidae. A–D *Akanthinotanais longipes* Hansen, 1913: A, cheliped; B, pereopod–1; C, pereopod–2; D, uropod. A Jakiel Stępień & Błażewicz, 2018, B–D Hansen 1913. E–H *Beksitanais apocalyptica* Jakiel, Palero & Błażewicz, 2019: E, cheliped; F, pereopod–1; G, pereopod–2; H, uropod. I–L *Mystriocentrus biho* Jakiel, Stępień & Błażewicz, 2018: I, cheliped; J, pereopod–1; K, pereopod–2; L, uropod. M–P *Parapseudotanais* Jakiel et al

unpublished: M, cheliped; N, pereopod–1; O, pereopod–2; P, uropod. Q–T *Pseudotanais oloughlini* Jakiel, Palero & Błażewicz, 2019: Q, cheliped; R, pereopod–1; S pereopod–2; T, uropod.

Molecular studies are an important part of integrative taxonomy. In the deep-sea, the probability of cryptic taxa is high, and molecular data are invaluable in defining species groups (MOTU molecular operational taxonomic units). For the first time, a true molecular approach for Pseudotanaidae is performed. So far Pseudotanaidae were basically missing from genetic studies. The only sequence available in a public database (GenBank) is a histone H3 single sequence obtained by Drumm (2010) from a shallow water species. Molecular data were obtained here for two Pacific collections (CCZ and KuramBIO). A total of 135 sequences were analysed, identifying 19 species from three genera (*Beksitanais*, *Mystriocentrus* and *Pseudotanais*) (Chapter 3 and 4). Intraspecific genetic divergence was low, and almost all the species were represented by single haplotype; only two species were more diverse (*P. mariae* from CCZ and *P. monroeae* from KuramBIO).

For the first time, traditional taxonomy of Pseudotanaidae is supported with genetic data. Morphological analyses of material from North Atlantic enabled the separation and description of four species new to science, belonging to two genera (*Mystriocentrus* and *Pseudotanais*). Research on the Pseudotanaidae fauna from the Central Pacific has found 13 new species, one of which is a representative of a new genus (*Beksitanais*). Finally the integrative taxonomy approach in NW Pacific unravels six new species belonging to two genera (*Mystriocentrus* and *Pseudotanais*).

Conclusions

This dissertation includes the first studies on Pseudotanaidae where studies on morphology are combined with molecular and zoogeographical analyses (integrative taxonomy). Distribution of pseudotanaids in three regions (North Atlantic, Central Pacific and NW Pacific) allows verifying three hypotheses.

- One genus (*Beksitanais*) and 23 new species were described in this PhD thesis. The total number of Pseudotanaidae increased for an extra 45% (from 51 to 74).
- Detailed taxonomic examination of *Pseudotanais* species allowed to define three morphological groups of phylogenetically closely-related species. The groupings were supported with molecular results.
- Mid-Atlantic Ridge hampers dispersion of Pseudotanaidae species. With a purely morphometric approach, the *Pseudotanais* collected around Iceland from different regions and different depths were confirmed to be a complex of at least two (but possibly four) cryptic species.
- Underwater mountain chains and fracture zones in CCZ restrict population connectivity. Most Pseudotanaidae species were present at only one of the five protected areas, separated by hundreds to thousands of kilometres, while only a few species were located in two closely located areas (IOM, BGR).
- Molecular analysis demonstrated that genetic distance increased along with increased geographic distance (1500 km between the most distinct stations). Applying Spearman rank coefficient was proved a significant correlation between genetic and geographic distances.
- Only one-third of the diversity found in CCZ would be protected by the APEI-3, thus the area proposed for a conservation role cannot preserve all biodiversity from deep-sea mining.
- Kurile-Kamchatka Trench does not restrict dispersion of Pseudotanaidae. Four out of six Pseudotanaidae species were recored on abyssal flor on both sides of the trench.
- Pseudotanaidae collected in KKT were four-times more abundant than in CCZ (273 to 67, respectively) but diversity was lower (six species and 13 species, respectively). These results suggest that the availability of

organic matter in the sediments influence abundance. However, a relatively high number of species in the Central Pacific area can be promoted also by habitat heterogeneity.

References

Băcescu, M., 1960. Bacescu (1960) Citeva animale, Marea Negra, Malacostracei. https://doi.org/10.1002/cne.20631

Bamber, R.N., 2009. Two new species of Shell-inhabiting tanaidaceans (Crustacea, Peracarida, Tanaidacea, Pagurapseudidae, Pagurapseudinae) from the shallow sublittoral off Vanuatu. Zoosystema 31, 407–418. https://doi.org/10.5252/z2009n3a1

Bamber, R.N., 2005. The tanaidaceans (Arthropoda: Crustacea: Peracarida: Tanaidacea) of Esperance, Western Australia, Australia. F.E. Wells, D.I. Walk. G.A. Kendrick 2005. Mar. Flora Fauna Esperance, West. Aust. West. Aust. Museum, Perth 1963, 613–728.

Bamber, R.N., Bird, G.J., Błażewicz-Paszkowycz, M., 2009. Tanaidaceans (Crustacea: Malacostraca: Peracarida) From Soft-Sediment Habitats Off Israel, Eastern Mediterranean Historical ecology of Lessepsian migration View project. Zootaxa 2109, 1–44. https://doi.org/10.5281/zenodo.187828

Bamber, R.N., Błażewicz-Paszkowycz, M., 2013. Another inordinate fondness†: Diversity of the tanaidacean fauna of Australia, with description of three new taxa. J. Nat. Hist. 47, 1767–1789. https://doi.org/10.1080/00222933.2012.742164

Bird, G.J., 1999. A new species of Pseudotanais (Crustacea, Tanaidacea) from cold seeps in the deep Caribbean, collected by the French submersible Nautile. Zoosystema 21, 445–451.

Bird, G.J., Holdich, D.M., 1989a. Deep-sea tanaidacea (Crustacea) of the North-East Atlantic: The genus Paranarthrura hansen. J. Nat. Hist. 23, 137–167. https://doi.org/10.1080/00222938900770091

Bird, G.J., Holdich, D.M., 1989b. Recolonisation of artificial sediments in the deep bay of biscay by tanaidaceans (crustacea: Peracarida), with a description of a new species of pseudotanais. J. Mar. Biol. Assoc. United Kingdom 69, 307–317. https://doi.org/10.1017/S0025315400029428

Bird, G.J., Holdich, D.M., 1989c. Tanaidacea (Crustacea) of the north−east Atlantic: the subfamily Pseudotanainae (Pseudotanaidae) and the family Nototanaidae. Zool. J. Linn. Soc. 97, 233–298. https://doi.org/10.1111/j.1096-3642.1989.tb00548.x

Bird, G.J., Holdich, D.M., 1988. Deep-sea tanaidacea (Crustacea) of the North-East Atlantic: The tribe Agathotanaini. J. Nat. Hist. 22, 1591–1621. https://doi.org/10.1080/00222938800771001

Błażewicz-Paszkowycz, M., Bamber, R.N., Cunha, M.R., 2011a. New tanaidomorph tanaidacea (Crustacea: Peracarida) from submarine mud-

volcanoes in the Gulf of Cadiz (North-east Atlantic). Zootaxa 2769, 1–53.

Błażewicz-Paszkowycz, M., Bamber, R.N., Cunha, M.R., 2011b. Apseudomorph tanaidaceans (Crustacea: Peracarida) from mud-volcanoes in the Gulf of Cadiz (North-east Atlantic). Zootaxa 2919, 1–36.

Błażewicz-Paszkowycz, M., Bamber, R.N., Jóźwiak, P., 2013. Tanaidaceans (Crustacea: Peracarida) from the SoJaBio joint expedition in slope and deeper waters in the Sea ofJapan. Deep. Res. Part II Top. Stud. Oceanogr. 86–87, 181–213. https://doi.org/10.1016/j.dsr2.2012.08.006

Błażewicz-Paszkowycz, M., Heard, R.W., Bamber, R.N., 2011c. A New Species of Shallow-water Metapseudid (Crustacea : Malacostraca : Peracarida : Tanaidacea) from Bermuda (Caribbean). Bull. Peabody Museum Nat. Hist. 52, 127–134.

Błażewicz, M., Jóźwiak, P., Jennings, R.M., Studzian, M., Frutos, I., 2019. Integrative systematics and ecology of a new deep-sea family of tanaidacean crustaceans. Sci. Rep. 9, 18720. https://doi.org/10.1038/s41598-019-53446-1

Bober, J., Brandt, A., Frutos, I., Schwentner, M., 2019. Diversity and distribution of Ischnomesidae (Crustacea: Isopoda: Asellota) along the Kuril-Kamchatka Trench – A genetic perspective. Prog. Oceanogr. 178. https://doi.org/10.1016/j.pocean.2019.102174

Bober, S., Brix, S., Riehl, T., Schwentner, M., Brandt, A., 2018. Does the Mid-Atlantic Ridge affect the distribution of abyssal benthic crustaceans across the Atlantic Ocean? Deep. Res. Part II Top. Stud. Oceanogr. 148, 91–104. https://doi.org/10.1016/j.dsr2.2018.02.007

Bogorov, V.G., 1973. Fauna of the Kurile–Kamchatka Trench and its environment. Acad. Sci. USSR. Proc. Inst. Ocean. 86.

Brandt, A., Błażewicz-Paszkowycz, M., Bamber, R.N., Mühlenhardt-Siegel, U., Malyutina, M. V, Kaiser, S., De Broyer, C., Havermans, C., 2012. Are there widespread peracarid species in the deep sea (Crustacea: Malacostraca)? Polish Polar Res. 33, 139–162. https://doi.org/10.2478/v10183-012-0012-5

Brix, S., Svavarsson, J., Leese, F., 2014. A multi−gene analysis reveals multiple highly divergent lineages of the isopod Chelator insignis (Hansen, 1916) south of Iceland. Polish Polar Res. 35, 225–242. https://doi.org/10.2478/popore−2014−0015

Bruce, J.R., Colman, J.S., Jones, N.S., 1963. Marine Fauna of the Isle of Man and its Surrounding Seas s. , Journal of the Marine Biological Association of the United Kingdom. Cambridge University Press (CUP). https://doi.org/10.1017/s0025315400024991

Danovaro, R., Snelgrove, P.V.R., Tyler, P.A., 2014. Challenging the paradigms of deep-sea ecology. Trends Ecol. Evol. https://doi.org/10.1016/j.tree.2014.06.002

Dojiri, M., Sieg, J., 1997. Taxonomic atlas of the soft-bottom benthic fauna of the Santa Maria Basin and Western Santa Barbara Channel, in: Taxonomica Atlas of the Soft-Bottom Benthic Fauna of the Santa Maria Basin and Western Santa Barbara Channel. pp. 181–268.

Etter, R.J., Rex, M.A., Chase, M.R., Quattro, J.M., 2005. Population differentiation decreases with depth in deep-sea bivalves. Evolution 59, 1479–91.

García-Herrero, Á., Sánchez, N., García-Gómez, G., Pardos, F., Martínez, A., 2019. Two new stygophilic tanaidomorphs (Peracarida, Tanaidacea) from Canary Islands and southeastern Iberian Peninsula. Mar. Biodivers. 49, 107–130. https://doi.org/10.1007/s12526-017-0763-7

Greve, L., 1965a. Tanaidacea from Trsndheimsfjorden. Der K. Nor. Vidensk. Selsk. Forhandliger 38, 140–143.

Greve, L., 1965b. The biology of some tanaidacea from raunefjorden, western norway. Sarsia 20, 43–54. https://doi.org/10.1080/00364827.1965.10409555

Greve, L., 1965c. New records of some Tanaidacea (Crustacea) from the vicinity of Tromso. Zool. Dep. Tromso Museum 27, 1–7.

Holdich, D.M., Jones, J.A., 1983. The distribution and ecology of british shallow-water tanaid crustaceans (Peracarida, tanaidacea). J. Nat. Hist. 17, 157–183. https://doi.org/10.1080/00222938300770141

Jakiel, A., Stępień, A., Błażewicz, M., 2018. A tip of the iceberg—Pseudotanaidae (Tanaidacea) diversity in the North Atlantic. Mar. Biodivers. 48, 859–895. https://doi.org/10.1007/s12526-018-0881-x

Jakiel, A., Stępień, A., Jóźwiak, P., Serigstad, B., Błażewicz-Paszkowycz, M., 2015. First record of tanaidacea (Crustacea) from a deep-sea coral reef in the Gulf of Guinea. Zootaxa 3995, 203–228. https://doi.org/10.11646/zootaxa.3995.1.18

Johannsen, N., Lins, L., Riehl, T., Brandt, A., 2020. Changes in species composition of Haploniscidae (Crustacea: Isopoda) across potential barriers to dispersal in the Northwest Pacific. Prog. Oceanogr. 180. https://doi.org/10.1016/j.pocean.2019.102233

Just, J., 1970. Decapoda, Mysidacea, Isopoda, and Tanaidacea from Jørgen Brønlund Fjord, North Greenland. C.A. Reitzel.

Kudinova-Pasternak, R.K., 1978. Tanaidacea (Crustacea, Malacostraca) from

the deep-sea trenches of the western part of the Pacific. Tr. Instituta Okeanol. Akad. Nauk SSSR 108, 115–135.

Kudinova-Pasternak, R.K., 1975. Tanaidacea, Atlantic sector, Antarctic and subantarctic. Akad. Nauk SSSR 103, 194–229.

Kudinova-Pasternak, R.K., 1973. Tanaidacea (Crustacea, Malacostraca) collected on the R/V “Vitjas” in regions of the Aleutian Trench and Alaska. Tr. Instituta Okeanol. Akad. Nauk SSSR 91, 141–168.

Kudinova-Pasternak, R.K., 1966. Tanaidacea of the Pacific ultra-abyssals. Crustaceana 45, 518–534.

Larsen, K., 2012. Tanaidacea (Peracarida) from macaronesia i. The deep-water fauna off the selvagen Islands, Portugal. Crustaceana 85, 571–589. https://doi.org/10.1163/156854012X633376

Larsen, K., Eds, M.S., 2007. Tanaidacea (Crustacea: Peracarida) from Japan III. the deep trenches; the Kurile-Kamchatka Trench and Japan Trench. Zootaxa 1599, 1–149.

Lilljeborg, W., 1864. Bidrag til kännedommen om de inom Sverige och Norrige förekommande Crustaceer af Isopodernas underordning och Tanaidernas familj. Inbjudningsskrift till Åhörande af Offentliga Föreläsninge 1865, 1–31.

Lörz, A.N., Jazdzewska, A.M., Brandt, A., 2018. A new predator connecting the abyssal with the hadal in the Kuril-Kamchatka Trench, NW Pacific. PeerJ 2018. https://doi.org/10.7717/peerj.4887

Malyutina, M. V, Brandt, A., Ivin, V. V, 2015. The Russian-German deep-sea expedition SokhoBio (Sea of Okhotsk Biodiversity Studies) to the Kurile Basin of the Sea of Okhotsk on board of the R/V Akademik MA Lavrentyev. 71st Cruise, July 6th-August 6th, 2015, The Cruise Report.

Mikhailov, O., 1972. Some new data on the bottom relief of the Kuril–Kamchatka Trench. Faunao f the Kurile–Kamchatka Trench and Its Environment 86, 75–79.

Mordasova, V.N., 1997. Some peculiarities of Chlorophyll distribution in the Sea of Okhotsk. Oceanology 37, 484–491.

Pabis, K., Błażewicz-Paszkowycz, M., Jóźwiak, P., Barnes, D.K.A., 2014. Tanaidacea of the Amundsen and Scotia seas: An unexplored diversity. Antarct. Sci. 27, 19–30. https://doi.org/10.1017/S0954102014000303

Pabis, K., Jóźwiak, P., Lörz, A.-N., Schnabel, K.E., Błażewicz-Paszkowycz, M., 2015. First insights into the deep-sea tanaidacean fauna of the Ross Sea: species richness and composition across the shelf break, slope and abyss. Polar Biol. 38, 1429–1437. https://doi.org/10.1007/s00300-015-

1706-z

Patel, T., Robert, H., D'Udekem D'Acoz, C., Martens, K., De Mesel, I., Degraer, S., Schön, I., 2018. Biogeography and community structure of abyssal scavenging Amphipoda (Crustacea) in the Pacific Ocean. Biogeosciences Discuss. 1–36. https://doi.org/10.5194/bg-2018-347

Sars, G.O., 1886. Crustacea. II. Nor. North Atl. Exped. 1876-1878 1–96.

Sars, G.O., 1882. Revision af gruppen: Isopoda Chelifera med charakteristik af nye herhen hørende arter og slægter. Arch. Math. og Naturvidenskab 7, 1–54.

Shiino, S.M., 1978. Tanaidacea collected by French Scientists on board the survey ship “Marion-Dufresne” in the regions around the Kerguelen Islands and other subantarctic islands in 1972, ’74, ’75, ’76. Sci. Rep. Shima Mar. 5, 1–122.

Sieg, J., 1977. Taxonomische Monographie der Familie Pseudotanaidae (Crustacea, Tanaidacea). Mitteilungen aus dem Museum für Naturkd. Berlin. Zool. Museum und Inst. für Spez. Zool. 53, 3–109. https://doi.org/10.1002/mmnz.4830530102

Sieg, J., 1973. Zum Problem Der Herstellung Von Dauerpraparaten Von Klein-Crustaceen, Insbesondere Von Typusexemplaren. Crustaceana 25, 222–224. https://doi.org/10.1163/156854073X00867

Sieg, J., Heard, R.W., 1988. Tanaidacea (Crustacea: Peracarida) of the Gulf of Mexico. V: The family Pseudotanaidae from less than 200 meters, with the description of Pseudotanais mexikolpos, n. sp. and a key to the known genera and species of the world. Proc. Biol. Soc. Washingt. 101, 39–59.

Smith, K.L., Baldwin, R.J., Williams, P.M., 1992. Reconciling particulate organic carbon flux and sediment community oxygen consumption in the deep North Pacific. Nature 359, 313–316. https://doi.org/10.1038/359313a0

Stephensen, K., 1937. Marine Isopoda and Tanaidacea. The Zoology of Iceland., in: Tmen, F. and S.L. (Ed.), The Zoology of Iceland III. PART 27. Copenhagen and Reykjavik . 1937, p. 26.

Taboada, S., Riesgo, A., Wiklund, H., Paterson, G.L.J., Koutsouveli, V., Santodomingo, N., Dale, A.C., Smith, C.R., Jones, D.O.B., Dahlgren, T.G., Glover, A.G., 2018. Implications of population connectivity studies for the design of marine protected areas in the deep sea: An example of a demosponge from the Clarion-Clipperton Zone. Mol. Ecol. https://doi.org/10.1111/mec.14888

Vanhoffen, E., 1907. Crustaceans from the small Karajak fjord in West

Greenland. universities zoological museum komenhavn, Krajak-fjord.

Wilson, G.D.F., 1987. Crustacean communities of the manganese nodule province (Domes Site A compared with Domes site C). Rep. Natl. Ocanic.... 0030, 1–43.

Appendix 1. List of current valid Pseudotanaidae species after this study. * described at this dissertation

Genus	Species	Region	Depth range [m]	References
Akanthinotanais	*A. breviaquas* Larsen, 2012	North Atlantic	0.5	Larsen, 2012
	A. gaussi Vanhöffen, 1914	Southern Ocean	170–385	Vanhöffen, 1914
	A. gerlachi Sieg, 1977	Central Pacific	5–32	Sieg, 1977
	A. guillei Shiino, 1978	Southern Ocean	62	Shiino, 1978
	A. kurchatovi Kudinova-Pasternak, 1978	Central Atlantic	480	Kudinova-Pasternak, 1978
	A. longipes Hansen, 1913	North Atlantic	90–1800	Hansen, 1913
	A. makrothrix Dojiri & Sieg, 1997	Central Pacific	393	Dojiri & Sieg, 1997
	A. malayensis Sieg, 1977	Central Pacific	35	Sieg, 1977
	A. mortenseni Sieg, 1977	North Atlantic	18–25	Sieg, 1977
	A. scrappi Bamber, 2005	North Atlantic	38	Bamber, 2005
	A. siegi Kudinova-Pasternak, 1985	North Atlantic	50	Kudinova-Pasternak, 1985
	A. similis Sieg, 1977	North Atlantic	20	Sieg, 1977
Beksitanais	*Beksitanais apocalyptica* Jakiel, Palero & Błażewicz, 2019 *	Central Pacific	4346	Jakiel, Palero & Błażewicz, 2019*
Mystriocentrus	*Mystriocentrus biho* Jakiel, Stępień & Błażewicz, 2018*	North Atlantic	913–2537	Jakiel, Stępień & Błażewicz, 2018*
	M. hollandae Jakiel, Palero & Błażewicz, 2020*	North Pacific	4800–5400	Jakiel, Palero & Błażewicz, 2020*
	M. serratus Bird & Holdich, 1989	North Atlantic	1378–4632	Bird & Holdich, 1989
Parapseudotanais	*Parapseudotanais abyssalis* Bird & Holdich, 1989	North Atlantic	4226–4327	Bird & Holdich, 1989
Pseudotanais	*Pseudotanais abathagastor*, Błażewicz-Paszkowycz, Bamber & Jóźwiak, 2013	North Pacific	400–600	Błażewicz-Paszkowycz, Bamber & Jóźwiak, 2013
	P. abyssi Hansen, 1913	North Atlantic	2500	Hansen, 1913
	P. affinis Hansen, 1913	North Atlantic	100–2200	Hansen, 1913
	P. artoo Błażewicz-Paszkowycz & Stępień, 2015	Central Atlantic	400	Jakiel et al., 2015
	P. baresnauti Bird, 1999	Central Atlantic	4900	Bird, 1999
	P. borceai Bacescu, 1960	North Atlantic	60–70	Bacescu, 1960
	P. californensis Dojiri & Sieg, 1997	Central Pacific	90–300	Dojiri & Sieg, 1997
	P. chanelae Jakiel, Palero & Błażewicz, 2020*	North Pacific	4800–5700	Jakiel, Palero & Błażewicz, 2020*
	P. chaplini Jakiel, Palero & Błażewicz, 2019*	Central Pacific	4100–5000	Jakiel, Palero & Błażewicz, 2019*
	P. chopini Jakiel, Palero & Błażewicz, 2019*	Central Pacific	4100–4400	Jakiel, Palero & Błażewicz, 2019*
	P. colonus Bird & Holdich, 1989	North Atlantic	2200	Bird & Holdich, 1989
	P. corollatus Bird & Holdich, 1989	North Atlantic	1000	Bird & Holdich, 1989
	P. crassicornis Hansen, 1887	North Atlantic	1200	Hansen, 1887
	P. curieae Jakiel, Palero & Błażewicz, 2020*	North Pacific	4800–5700	Jakiel, Palero & Błażewicz, 2020*
	P. denticulatus Bird & Holdich, 1989	North Atlantic	1100–4800	Bird & Holdich, 1989
	P. falcicula Bird & Holdich, 1989	North Atlantic	2800–4800	Bird & Holdich, 1989
	P. falcifer Błażewicz & Bamber, 2011	North Atlantic	700–1300	Błażewicz & Bamber, 2011
	P. forcipatus (Lilljeborg, 1864)	North Atlantic	10–200	Lilljeborg, 1864
	P. forcipatus Vanhöffen, 1907 (not Lilljeborg, 1864)	North Atlantic	80	Vanhöffen, 1907
	P. gaiea Jakiel, Palero & Błażewicz, 2019*	Central Pacific	4900	Jakiel, Palero & Błażewicz, 2019*
	P. georgesandae Jakiel, Palero & Błażewicz, 2019*	Central Pacific	4900	Jakiel, Palero & Błażewicz, 2019*
	P. geralti Jakiel, Palero & Błażewicz, 2019*	Central Pacific	4400	Jakiel, Palero & Błażewicz, 2019*
	P. inflatus Kudinova-Pasternak, 1973	North Pacific	3610	Kudinova-Pasternak, 1973
	P. intortus Błażewicz-Paszkowycz, Bamber & Jóźwiak, 2013	North Pacific	500–1000	Błażewicz-Paszkowycz, Bamber & Jóźwiak, 2013
	P. isabelae García-Herrero, Sánchez, García-Gómez, Pardos & Martínez, 2017	North Atlantic	8–30	Sánchez, García-Gómez, Pardos & Martínez, 2017
	P. jonesi Sieg, 1977	North Atlantic	100	Sieg, 1977

Pseudotanais	*P. julietae* Jakiel, Palero & Błażewicz, 2019*	Central Pacific	4500	Jakiel, Palero & Błażewicz, 2019*
	P. kobro Jakiel, Palero & Błażewicz, 2019*	Central Pacific	4300–4500	Jakiel, Palero & Błażewicz, 2019*
	P. lilljeborgi Sars, 1882	North Atlantic	10–200	Sars, 1882
	P. locueloae Jakiel, Palero & Błażewicz, 2020*	North Pacific	4800–5701	Jakiel, Palero & Błażewicz, 2020*
	P. longisetosus Sieg, 1977	Southern Ocean	1000–6100	Sieg, 1977
	P. longispinus Bird & Holdich, 1989	North Atlantic	2500–4800	Bird & Holdich, 1989
	P. macrocheles Sars, 1882	North Atlantic	100	Sars, 1882
	P. mariae Jakiel, Palero & Błażewicz, 2019*	Central Pacific	4100–4400	Jakiel, Palero & Błażewicz, 2019*
	P. mediterraneus Sars, 1882	North Atlantic	50	Sars, 1882
	P. mexikolpos Sieg & Heard, 1988	North Atlantic	72	Sieg & Heard, 1988
	P. misericorde Jakiel, Stepień & Błażewicz, 2018*	North Atlantic	1300–4600	Jakiel, Stępień & Błażewicz, 2018*
	P. monroeae Jakiel, Palero & Błażewicz, 2020*	North Pacific	4800–5400	Jakiel, Palero & Błażewicz, 2020*
	P. nipponicus McLelland, 2007	North Pacific	3100–3800	Larsen & Shimomura, 2007
	P. nordenskioldi Sieg, 1977	Southern Ocean	1000–6100	Sieg, 1977
	P. oculatus Hansen, 1913	North Atlantic	100	Hansen, 1913
	P. oloughlini Jakiel, Palero & Błażewicz, 2019*	Central Pacific	4900	Jakiel, Palero & Błażewicz, 2019*
	P. romeo Jakiel, Palero & Błażewicz, 2019*	Central Pacific	4100	Jakiel, Palero & Błażewicz, 2019*
	P. scalpellum Bird & Holdich, 1989	North Atlantic	2000–2600	Bird & Holdich, 1989
	P. sigrunis Jakiel, Stępień & Błażewicz, 2018*	North Atlantic	300–800	Jakiel, Stępień & Błażewicz, 2018*
	P. soja Błażewicz-Paszkowycz, Bamber & Jóźwiak, 2013	North Pacific	400–1300	Błażewicz-Paszkowycz, Bamber & Jóźwiak, 2013
	P. spatula Bird & Holdich, 1989	North Atlantic	1300–2200	Bird & Holdich, 1989
	P. spicatus Bird & Holdich, 1989	North Atlantic	2300–4800	Bird & Holdich, 1989
	P. stiletto Bamber, 2009	North Atlantic	28–60	Bamber, 2009
	P. svavarssoni Jakiel, Stępień & Błażewicz, 2018*	North Atlantic	2100–2400	Jakiel, Stępień & Błażewicz, 2018*
	P. szymborskae Jakiel, Palero & Błażewicz, 2020*	North Pacific	4800–5700	Jakiel, Palero & Błażewicz, 2020*
	P. tympanobaculum Błażewicz-Paszkowycz, Bamber & Cunha, 2011	North Atlantic	400–3000	Błażewicz-Paszkowycz, Bamber & Cunha, 2011
	P. unicus Sieg, 1977	North Atlantic	50	Sieg, 1977
	P. uranos Jakiel, Palero & Błażewicz, 2019*	Central Pacific	4800	Jakiel, Palero & Błażewicz, 2019*
	P. vitjazi Kudinova-Pasternak, 1966	North Pacific	4260–6065	Kudinova-Pasternak, 1966
	P. vulsella Bird & Holdich, 1989	North Atlantic	1000–1600	Bird & Holdich, 1989
	P. yenneferae Jakiel, Palero & Błażewicz, 2019*	Central Pacific	4800	Jakiel, Palero & Błażewicz, 2019*

Appendix 2. Localities and expedition of the stations from where Pseudotanaidae for the present dissertation were collected. RV – research vessel, N – number of individuals, EBS – epibenthic sledge, GKG – box corer, SG – Shipek grab, VV – Van Veen grab.

Location	Date	RV	Cruise	Station	Position		Depth	Gear	N
					latitude	longitude	(m)		
Atlantic Ocean									
Iceland Basin	28/08/2011	*Meteor*	IceAGE1	963	60°02.73' N	21°29.86' W	2746.4	EBS	2
Iceland Basin	30/08/2011	*Meteor*	IceAGE1	979	60°21.48' N	18°08.24' W	2567.6	EBS	1
Iceland Basin	02/09/2011	*Meteor*	IceAGE1	1010	62°33.10' N	20°23.71' W	1384.8	EBS	5
Iceland Basin	03/09/2011	*Meteor*	IceAGE1	1019	62°56.32' N	20°44.61' W	913.6	EBS	2
Irminger Basin	05/09/2011	*Meteor*	IceAGE1	1043	63°55.46' N	25°57.66' W	213.9	EBS	18
Irminger Basin	07/09/2011	*Meteor*	IceAGE1	1051	61°37.41' N	31°22.11' W	2538.9	GKG	1
Irminger Basin	07/09/2011	*Meteor*	IceAGE1	1054	61°36.19' N	31°22.60' W	2537.3	EBS	9
Irminger Basin	08/09/2011	*Meteor*	IceAGE1	1066	62°59.97' N	28°04.78' W	1621.8	GKG	1
Irminger Basin	08/09/2011	*Meteor*	IceAGE1	1072	63°00.46' N	28°04.09' W	1593.8	EBS	2
Irminger Basin	09/09/2011	*Meteor*	IceAGE1	1086	63°42.53' N	26°23.05' W	698.1	EBS	1
Denmark Strait	14/09/2011	*Meteor*	IceAGE1	1116	67°12.82' N	26°16.31' W	683.1	GKG	1
Denmark Strait	14/09/2011	*Meteor*	IceAGE1	1129	67°38.77' N	26°44.78' W	320.6	GKG	1
Denmark Strait	14/09/2011	*Meteor*	IceAGE1	1132	67°38.48' N	26°45.28' W	318.1	EBS	3
Denmark Strait	14/09/2011	*Meteor*	IceAGE1	1136	67°38.15' N	26°45.99' W	315.9	EBS	2
Denmark Strait	15/09/2011	*Meteor*	IceAGE1	1141	67°50.22' N	23°42.11' W	1241.6	GKG	1
Denmark Strait	15/09/2011	*Meteor*	IceAGE1	1148	67°50.79' N	23°41.76' W	1248.8	EBS	5
Norwegian Sea	17/09/2011	*Meteor*	IceAGE1	1152	69°05.60' N	09°56.01' W	2172.6	GKG	11
Norwegian Sea	17/09/2011	*Meteor*	IceAGE1	1155	69°06.89' N	09°54.72' W	2203.8	EBS	1
Norwegian Sea	17/09/2011	*Meteor*	IceAGE1	1159	69°06.66' N	09°55.02' W	2202.8	EBS	127
Norwegian Sea	19/09/2011	*Meteor*	IceAGE1	1166	67°35.28' N	06°57.47' W	2401.8	GKG	2
Norwegian Sea	19/09/2011	*Meteor*	IceAGE1	1168	67°36.38' N	07°00.08' W	2372.6	EBS	49
Norwegian Sea	20/09/2011	*Meteor*	IceAGE1	1178	67°38.71' N	12°10.10' W	1818.8	GKG	2

Norwegian Sea	20/09/2011	*Meteor*	IceAGE1	1184	67°38.63' N	12°09.72' W	1819.3	EBS	8
Norwegian Sea	21/09/2011	*Meteor*	IceAGE1	1188	67°04.32' N	13°00.89' W	1580.6	GKG	6
Norwegian Sea	22/09/2011	*Meteor*	IceAGE1	1212	66°32.63' N	12°52.48' W	317.2	EBS	13
Norwegian Sea	22/09/2011	*Meteor*	IceAGE1	1216	66°18.06' N	12°22.38' W	730.8	GKG	10
Norwegian Sea	22/09/2011	*Meteor*	IceAGE1	1219	66°17.34' N	12°20.82' W	579.1	EBS	7
Norwegian Channel	26/07/2013	*Poseidon*	IceAGE2	871-4	62°45.31' N	00°54.09' W	1562.7	GKG	2
Norwegian Channel	27/07/2013	*Poseidon*	IceAGE2	872-4	63°01.88' N	01°29.91' W	1858.3	EBS	3
Norwegian Channel	27/07/2013	*Poseidon*	IceAGE2	872-5	63°01.80' N	01°27.05' W	1842.0	GKG	1
Norwegian Channel	28/07/2013	*Poseidon*	IceAGE2	873-2	61°46.63' N	03°52.83' W	835.1	GKG	2
Norwegian Channel	28/07/2013	*Poseidon*	IceAGE2	873-6	61°46.52' N	03°52.38' W	833.7	EBS	1
Iceland-Faroe Ridge	31/07/2013	*Poseidon*	IceAGE2	879-2	63°06.02' N	08°35.14' W	505.9	SG	2
Iceland-Faroe Ridge	31/07/2013	*Poseidon*	IceAGE2	879-5	63°06.10' N	08°34.32' W	510.9	EBS	3
Iceland-Faroe Ridge	31/07/2013	*Poseidon*	IceAGE2	880-2	63°23.36' N	08°09.42' W	686.0	EBS	1
Iceland-Faroe Ridge	31/07/2013	*Poseidon*	IceAGE2	880-3	63°24.79' N	08°11.63' W	688.1	GKG	1
Iceland-Faroe Ridge	01/08/2013	*Poseidon*	IceAGE2	881-4	63°34.66' N	07°42.69' W	1043.6	EBS	1
Iceland-Faroe Ridge	01/08/2013	*Poseidon*	IceAGE2	881-6	63°38.50' N	07°47.03' W	1073.4	VV	1
Iceland-Faroe Ridge	02/08/2013	*Poseidon*	IceAGE2	882-2	63°25.01' N	10°58.80' W	441.4	VV	3
Iceland-Faroe Ridge	02/08/2013	*Poseidon*	IceAGE2	882-5	63°25.04' N	10°58.20' W	440.5	EBS	11
Pacific Ocean									
Clarion Clipperton Zone	21/03/2015	*Sonne*	JPIO	20	11º49.81' N	117º00.28' W	4093	EBS	7
Clarion Clipperton Zone	22/03/2015	*Sonne*	JPIO	24	11º51.52' N	117º01.19' W	4100	EBS	8
Clarion Clipperton Zone	27/03/2015	*Sonne*	JPIO	50	11º49.92' N	117º29.31' W	4330	EBS	3
Clarion Clipperton Zone	28/03/2015	*Sonne*	JPIO	59	11º48.55' N	117º29.03' W	4342	EBS	3
Clarion Clipperton Zone	01/04/2015	*Sonne*	JPIO	81	11º03.97' N	119º37.67' W	4365	EBS	8
Clarion Clipperton Zone	04/04/2015	*Sonne*	JPIO	99	11º02.28' N	119º40.89' W	4401	EBS	9

Clarion Clipperton Zone	07/04/2015	*Sonne*	JPIO	117	13º52.39' N	123º15.30' W	4496	EBS	3
Clarion Clipperton Zone	10/04/2015	*Sonne*	JPIO	133	13º50.98' N	123º15.07' W	4507	EBS	1
Clarion Clipperton Zone	15/04/2015	*Sonne*	JPIO	158	14º03.41' N	130º07.99' W	4946	EBS	1
Clarion Clipperton Zone	21/04/2015	*Sonne*	JPIO	192	18º44.81' N	128º21.87' W	4877	EBS	7
Clarion Clipperton Zone	22/04/2015	*Sonne*	JPIO	197	18º48.66' N	128º22.75' W	4805	EBS	17
Kuril-Kamchatka Trench	30/07/2012	*Sonne*	KuramBio	1-10	43º 58.35' N	157º18.23' E	5418–5429	EBS	1
Kuril-Kamchatka Trench	30/07/2012	*Sonne*	KuramBio	1-11	43º 58.44' N	154º18.29' E	5412–5418	EBS	2
Kuril-Kamchatka Trench	02/08/2012	*Sonne*	KuramBio	2-9	46º 14.78' N	155º32.63' E	4830–4864	EBS	7
Kuril-Kamchatka Trench	03/08/2012	*Sonne*	KuramBio	2-10	46º 14.77' N	155º32.79' E	4859–4863	EBS	13
Kuril-Kamchatka Trench	05/08/2012	*Sonne*	KuramBio	3-9	47º 14.66' N	154º42.88' E	4859–4863	EBS	52
Kuril-Kamchatka Trench	06/08/2012	*Sonne*	KuramBio	4-3	46º 58.34' N	154º33.03' E	5681–5780	EBS	7
Kuril-Kamchatka Trench	11/08/2012	*Sonne*	KuramBio	5-9	43º 34.46' N	153º58.13' E	5376–5379	EBS	1
Kuril-Kamchatka Trench	11/08/2012	*Sonne*	KuramBio	5-10	43º 34.44' N	153º58.06' E	5375–5379	EBS	4
Kuril-Kamchatka Trench	15/08/2012	*Sonne*	KuramBio	6-11	42º 28.61' N	153º59.68' E	5291–5305	EBS	8
Kuril-Kamchatka Trench	15/08/2012	*Sonne*	KuramBio	6-12	42º 28.49' N	153º59.54' E	5291–5307	EBS	2
Kuril-Kamchatka Trench	17/08/2012	*Sonne*	KuramBio	7-9	43º 01.78' N	152º58.61' E	5216–5223	EBS	6
Kuril-Kamchatka Trench	17/08/2012	*Sonne*	KuramBio	7-10	43º 01.82' N	152º58.55' E	5218–5221	EBS	14
Kuril-Kamchatka Trench	20/08/2012	*Sonne*	KuramBio	8-9	42º 14.32' N	151º42.68' E	5125–5140	EBS	31
Kuril-Kamchatka Trench	21/08/2012	*Sonne*	KuramBio	8-12	42º 14.38' N	151º43.12' E	5115–5124	EBS	25
Kuril-Kamchatka Trench	23/08/2012	*Sonne*	KuramBio	9-9	40º 34.51' N	150º59.92' E	5399–5408	EBS	19
Kuril-Kamchatka Trench	24/08/2012	*Sonne*	KuramBio	9-12	40º 34.49' N	150º59.85' E	5392–5397	EBS	13
Kuril-Kamchatka Trench	26/08/2012	*Sonne*	KuramBio	10-9	41º 11.37' N	150º05.63' E	5348–5265	EBS	7
Kuril-Kamchatka Trench	27/08/2012	*Sonne*	KuramBio	10-12	41º 12.80' N	150º06.16' E	5249–5262	EBS	17
Kuril-Kamchatka Trench	29/08/2012	*Sonne*	KuramBio	11-9	40º 12.49' N	148º05.40' E	5362–5362	EBS	6
Kuril-Kamchatka Trench	31/08/2012	*Sonne*	KuramBio	11-12	40º 12.32' N	148º05.73' E	5348–5351	EBS	6
Kuril-Kamchatka Trench	31/08/2012	*Sonne*	KuramBio	12-4	39º 42.78' N	147º09.55' E	5215–5228	EBS	32